UNIVERSITÀ
DEGLI STUDI
FIRENZE

DOTTORATO DI RICERCA IN
INGEGNERIA INDUSTRIALE

CICLO XXV

Design methods for modern electric and hybrid electric vehicles: concept design and context analysis

Settore Scientifico Disciplinare ING/IND 14

Candidato
Ing. Lorenzo Berzi

Tutori
Prof. Ing. Marco Pierini
Dott. Ing. Massimo Delogu

Coordinatore del Dottorato:
Prof. Ing. Marco Pierini

Anni 2010/2013

© Università degli Studi di Firenze – Faculty of Engineering
Via di Santa Marta, 3, 50139 Firenze, Italy

Tutti i diritti riservati. Nessuna parte del testo può essere riprodotta o trasmessa in qualsiasi forma o con qualsiasi mezzo, elettronico o meccanico, incluso le fotocopie, la trasmissione fac simile, la registrazione, il riadattamento o l’ uso di qualsiasi sistema di immagazzinamento e recupero di informazioni, senza il permesso scritto dell’ editore .

All rights reserved. No part of the publication may be reproduced in any form by print, photoprint, microfilm, electronic or any other means without written permission from the publisher.

ISBN XXX–XX–XXXX–XXX–X
D/XXXX/XXXX/XX

A Mariella

A Renzo

Summary

The main aim of the PhD activity here presented is the analysis and the proposal of methodologies that can be used for the integration of Computer Aided Engineering (CAE) tools starting from the early design phase of a vehicle. The topics described include the description of main factors pushing for the development of electric and hybrid electric vehicles, the description of model based engineering strategies through theory and examples, the proposal of guidelines for the definition of component models, the analysis of the use context of the city of Florence and the integration of such data on vehicle modelling environment. An application is then presented.

The first part defines the context of analysis, aiming to explain the relevance of transport activities on a world basis and the drivers pushing for innovation in the automotive field. The potential of EVs for environmental impact reduction in terms of GHG emissions is explained.

After that, a description of main explicit and emerging design goals and the potential related to the use of a structured approach for the integration of CAE tools in vehicle design process is proposed, thus defining a strategy for effective “concurrent engineering” activities during product development process. Literature data are collected and presented to support this section, from general modelling approach definition to the implementation in calculation tools having different capabilities and scopes, aiming to achieve a compromise between accuracy and simulation effort. The description include some notes about the low and high level communication methodologies between tools.

These topics are described in detail in chapter 3. The strategy offers guidelines for the description of mechatronic components inside simulation environment. Various example applications are proposed and models used in literature are described. The characteristics of the model to be used in each phase are therefore different depending on the accuracy needed (e.g. from primary vehicle sizing to detailed power, energy, efficiency sizing) or on the focus of the design step.

The description of model functionalities depending on simulation goal includes guidelines for the definition of model characteristics and of their input/output ports. The detail is on those powertrain components that are differentiating electric vehicles in comparison with conventional vehicles: battery, motors, inverters and converters.

Due to the fact that real world driving data are needed for the calculation of effective performances and energy consumption of electric vehicle, an introduction on driving cycle analysis and development is proposed. Chapter 4 offers a brief review of significant literature works and of known synthesis methodologies, while Chapter 5 describes the measurement activity performed by the Candidate. This phase includes measurements, analysis, treatment and then a procedure for data selection and driving cycle generation is proposed and implemented; the result is a set of driving cycle related to electric vehicles use in the context of the city of Florence. The procedure can also be applied for continuous generation of driving sequences interfacing with simulation models.

Chapter 6 describes the final application, including the modelling of an electric vehicle using a “range extender” (EREV) and the assessments of its performances within a complete use case, which is based on the data defined during the cycle synthesis activities.

Table of contents

Summary **7**

Table of contents **9**

List of figures **13**

List of tables **23**

Acronyms List **27**

Preface **29**

1. The electrification of road vehicles **31**

- 1.1. The environmental sustainability of transport systems 31
  - 1.1.1. Environmental impact assessment methods 34
  - 1.1.2. European regulation for air emissions containment 36
  - 1.1.3. Electric vehicles potential for environmental impact reduction 38
- 1.2. Emerging drivers for vehicle electrification 42
  - 1.2.1. The attitude of drivers towards innovative vehicles 42

2. The role of modelling activities in engineering **45**

- 2.1. General aims, scopes and potentialities of modelling activities 46
  - 2.1.1. The implications related to the extensive use of virtual simulation tools 46
  - 2.1.2. Increasing possibility of innovations: expectations 48
- 2.2. Integration of CAE tools on vehicle development process from preliminary design to late testing activities 49
  - 2.2.1. Integrated approach to development process: a case study 50
  - 2.2.2. Lesson learnt 52
  - 2.2.3. Scalable model for time–scale fitting 53

2.2.4. Integration of CAE tools in engineering process 55
2.3. Alignment strategies between different modelling tools 56
2.3.1. The design and the use of co–simulation tools 56
2.3.2. Meta–modelling approach 64
2.3.3. The design and the use of co–simulation tools 68
3. Mechanical and mechatronics systems modelling 73
3.1. The choice of modelling framework depending on design aim 74
3.1.1. Backward, Forward and test–bench models 78
3.1.2. A modelling framework 81
3.2. Case studies 89
3.2.1. Analysis and vehicle archetype confrontation 89
4. An introduction to driving cycles 101
4.1. The relevance of vehicle mission selection 101
4.1.1. Classification of driving cycles 103
4.2. Characterization of driving cycles 108
4.2.1. Parameters defining driving cycels 108
4.2.2. Performances distribution analysis 110
4.2.3. Clustering of driving sequences 113
4.3. A methodology for the definition of real–world driving cycles 123
4.3.1. Data collection methodologies 123
4.3.2. Pre–processing and preparation for analysis 125
4.3.3. Driving data processing 126
4.3.4. Methodologies for data synthesis 127
4.3.5. The extended use of “driving cycle datasets” 136
4.3.6. Notes about additional data 136
5. Real World Data acquisition and processing 139
5.1. Driving data acquisition: the case study of the city of Florence 139
5.1.1. Daily distance run: description of the users and comparison between Florence case study and literature data 140
5.1.2. Data analysis for driving sequences identification and clustering 149
5.2. Driving data processing: methods and results 159
5.2.1. Generation process of new driving cycles 159

5.2.2. Implementation of driving cycle synthesis methodology for dissemination 175
5.2.3. Additional results from on–road measurements 178

6. A simulation framework application 181

6.1. Context and motivation for the study 181
6.2. Modelling electric vehicle 183
6.2.1. Simulation environment 183
6.2.2. Vehicle Body Characteristics 184
6.2.3. Battery modelling 187
6.2.4. Supercapacitor system modelling 197
6.2.5. Electric motor modelling 198
6.2.6. Range extender modelling 200
6.2.7. Virtual driver model 203
6.2.8. Low voltage system, auxiliaries and comfort elements 203
6.2.9. Full model layout 204
6.2.10. Model representativeness verification 205
6.2.11. Calculations for all the driving data 208
6.3. Strategy definition for range extender vehicle 209
6.3.1. Strategies for range extender use 210
6.3.2. Range extender control depending on vehicle speed 215
6.3.3. Supercapacitors control strategy: active filtering 216
6.3.4. Model applications 217
6.4. Preparing use–case scenarios 222
6.4.1. A scenario for a Light Delivery Vehicle 222
6.4.2. A scenario for a Passenger Vehicle 224
6.5. Simulation results 228
6.5.1. Results for LDV scenario solution 229
6.5.2. Results for Passenger scenario solution 229

Conclusions and final remarks 233

Acknowledgements 237

Bibliography 239

List of figures

Figure 1 –Final energy demand by sector and future trend scenario to 2030 in Europe (source: EC, 2009). 32

Figure 2 – Final energy demand in transport: current value and trend to 2050 in Europe (source: EC, 2013). 32

Figure 3 – Trends in transport activity index and energy consumption in Europe (EC,2013). 32

Figure 4 – Final energy demand in transport by fuel type: current value and trend to 2050 in Europe (source: EC, 2013). 33

Figure 5 – Expected trend for transport activity on a world basis (source:WBCSD, 2004). ..33

Figure 6 – Expected trend for GHG emissions from transport on a world basis; colored areas represent the estimated GHG emissions reduction in case of technology shift (source:WBCSD, 2004). 33

Figure 7 – Global warming potential (left) and hazardous waste production (right) results of a full LCA analysis comparing different vehicle solutions (six alternatives for car body are considered, from Schmidt et al., 2004). For all case studies, “USE” phase is responsible of main impact. 35

Figure 8 – Most relevant energy conversion steps during the operation of a vehicle (from Guzzella, 2009). 36

Figure 9 – . Air pollution levels (NOx) in the city of Zurich in 1995 (left) and in 2002 (right). Source: Guzzella, 2009. 37

Figure 10 – Fleet average weight and CO_2 emissions in Europe by carmaker and comparison with EU target line. The size of each bubble represents the amount of CO_2 emission of total cars sold (source: TE, 2013). 38

Figure 11 – Emission factors for European Union Countries (source: Eurostat, 2013). 40

Figure 12 – Impact assessment on four different categories (GHG–GWP emissions, Abiotic Depletion Potential ADP, nonrenewable cumulated energy demand CED, Ecoindicator 99 H/A) of BEV and ICE vehicles considering all the use phases: road construction and maintenance, glider, battery and drivetrain production, use phase (operation and maintenance), vehicle End Of Life (EOL). Energy mix emissions calculated as EU average. Source: Notter et al., 2010. 41

Figure 13 – GWP impact of vehicle life (phase defined in the legend) and comparison of different alternatives: BEV using lithium nickel cobalt manganese cells (LiNCM), BEV using lithium iron phosphate cells ($LiFePO_4$), Diesel and Gasoline ICEV. BEV vehicle impact is calculated considering European Energy mix impact (Euro), Natural Gas (NG) electricity production impact, Coal (C) electricy production impact. Value 1.0 corresponds to the most impacting alternative. Source: Hawkins et al., 2012. 41

Figure 14 – Problem solving loop (Becker et al, 2005). 47
Figure 15 – Modified problem solving iteration, including abduction, induction and deduction (Becker et al., 2005)... 49
Figure 16 – Development process of complex system: structure and representation using SysML (Votintseva et al., 2011).. 51
Figure 17 – Equivalent circuit of ultracapacitors (source :Dougal et al., 2004). 53
Figure 18 – Comparison of the model predictions of impedance with the measurements. The simulation results are indicated by lines and the measurements are by squares and circles (source: Dougal et al., 2004). 53
Figure 19 – Supercapacitor equivalent circuit of the multi–stage ladder model: various alternatives (source: Wu and Dougal, 2005). 54
Figure 20 –Supercapacitor model alternatives depending on desired order; right: different model simulation results (lines) and comparison with measurements data (squares, stars). Source: Wu and Dougal, 2005. 55
Figure 21 – Heterogeneous discrete/continuous systems (on the left) and corresponding global execution model (on the right).. 58
Figure 22 – A flow for automatic generation of execution models (from Nicolescu et al., 2007). Continuous and Discrete model blocks are prepared through tools such as Simulink, Modelica, SystemC, while the “simulation library” block stores the elements defining simulation bus and simulation interfaces; both kind of elements are used for the automatic generation of execution models... 58
Figure 23 – Synchronization strategy between continuous and discrete models over the time axis (From Nicolescu et al., 2007).. 59
Figure 24 – Flowchart for the discrete domain interface (From Nicolescu et al., 2007). 60
Figure 25 – Flowchart for the continuos domain interface (From Nicolescu et al., 2007). ... 60
Figure 26 – The representation of a generic co–simulation model, including the detail of the elements to be included in a co–simulation library (from Nicolescu et al., 2007)...... 61
Figure 27 – Detection events from the discrete simulation model within Matlab/Simulink using a “triggered subsystem” submodel.. 63
Figure 28 – Simulink model including co–simulation interfaces (from Nicolescu et al., 2007). 64
Figure 29 – Meta model defining external models and their interconnections (from Siemers et al., 2009)... 66
Figure 30 – From external models definition (vehicle body in MSC.ADAMS, hub unit and bearings in BEAST) to the definition of their relation (interfaces points for mounting) and to final meta model, also including global simulation parameters (e.g. simulation start and end). Source: Siemers et al., 2009.. 66
Figure 31 – Simulation manager environment for external simulator tools (source: Siemers et al., 2009)... 68
Figure 32 – Networked Control System block layout (source: Quaglia et al., 2012). 69
Figure 33 – Co–simulation environment and available tools for each domain (plant and physical components, controllers, network). 69
Figure 34 – New entities in Matlab and SystemC environment and their relationships (from Quaglia et al., 2012). 70
Figure 35 – Layout of the NCS model including a command system (human side, O, and master controller C_m) and a robot operating on the environment (E) communicating over a network (slave controller C_s). Source: Quaglia et al., 2012. 71

Figure 36 – Errors on angular position at three different joints in case of uncongested (upper plots) and congested networks (lower plots). Source: Quaglia et al., 2012. 71
Figure 37 – Main powertrain schemes for ICE, HEV, and BEV vehicles (Chen et al, 2006). The Planetary gear unit is used, in many configuration, as mechanical coupling for different mechanical devices. Abbreviation used: ICE – Internal Combustion Engine; Bat: Battery; VSI: Voltage Source Inverter; EM: Electric Machine; Trans: Mechanical Transmission; HEV – Hybrid Electric Vehicle; BEV: Battery Electric Vehicle.........75
Figure 38 – Series HEV powertrain (Lhomme, 2004), graphical block scheme. 76
Figure 39 – Series HEV powertrain (Lhomme, 2004), functional block scheme. “Pipe” connection: fuel flux; Dot–dash line: mechanical link; continuous lines: electrical link. 77
Figure 40 – Series HEV powertrain (Lhomme, 2004), Energetic Macroscopic Representation (EMR), please refer to block scheme on Table 10. CS: Chemical Source (fuel); ES: Electrical Source (battery); SM: Mechanical Source (vehicle resistance). 77
Figure 41 – Series HEV powertrain (Lhomme, 2004), Energetic Macroscopic Representation (EMR), including control system. Sensors are represented as circles on other connections and their signals are represented by dashed lines. 77
Figure 42 – Series HEV powertrain (Lhomme, 2004), Matlab–Simulink implementation. ...78
Figure 43 – Backward model block diagram of HEV (Valera et al., 2009). 78
Figure 44 – Forward model (lateral and longitudinal dynamics) block diagram of vehicle (Valera et al., 2009)..79
Figure 45 – HEV test bench architecture and layout. The components on the right are physical elements of electrical powertrains (Valera et al., 2009). 81
Figure 46 – Distribution of battery requirements for PHEV designs selected by potential early market respondents and USABC, MIT, and EPRI (Axsen et al., 2010). 82
Figure 47 – Battery lumped parameters model presented in the model by He et al., 2012. ...83
Figure 48 – Lumped elements battery model (left) and battery SOC and SOH prediction (right) based on Current/Voltage observer(He et al., 2012). 83
Figure 49 – Non–uniformities in battery current production modeled through electrochemical FEM system (Pesaran, 2009). 84
Figure 50 – Sectioning of the cathode for the thermal imaging. Section 1 is near the core of the cylinder and section 5 is near the out edge of the cylinder. (b) Thermal maps of unaged and aged cathode samples for all the five sections (Nagpure et al., 2010). 86
Figure 51 – A summary of the steps of vehicle design process. From left to right, the steps determining the need for accuracy increase in the simulation, from abstraction to detailed modelling. From up to bottom, the three main actor of the design process: the boundary conditions (blue labels), the characteristics of the model to be used on that phase (green labels), the product of the activity (yellow labels). Each phase providing product alternatives needs a “validation” step in terms of performances, costs, functionality; it is therefore possible that in any moment it is needed to do a step backward (highlighted by empty arrows). The role of a CAE –based design strategy is to make available all the information and the tools needed at each phase. 88
Figure 52 – Fuel consumption as a function of car weight and engine size for gasoline cars (Duflu et. Al., 2009). 89
Figure 53 – Comparison of the amount of natural gas required during a 400 km travel for Battery EV compared to a fuel cell EV using electricity and hydrogen production technology expected in the 2010–2020 time period (source: Thomas, 2009). 90
Figure 54 – New European Driving Cycle as time–speed signal. 91

Figure 55 – Vehicle model scheme used in Doucette and McCulloch model. 91
Figure 56 – Equivalent circuit for battery model (left) and comparison of datasheet and simulated performances (voltage E over State of Charge SoC for different current values). 92
Figure 57 – Calculated CO2 emissions for the vehicles described in Table 13 considering USA electric energy generation data. 93
Figure 58 – Calculated CO2 emissions for the vehicles described in Table 13 considering France electric energy generation data. 94
Figure 59 – Calculated CO2 emissions for the vehicles described in Table 13 considering China electric energy generation data.. 94
Figure 60 – Efficiency data of conversion chain from primary source to vehicle (Campanari et al., 2009).. 95
Figure 61 – Powertrain model of Fuel Cell and Battery vehicles. 96
Figure 62 – European (ECE–EUDC) and United States (US06) driving cycles compared. .. 96
Figure 63 – Iteration procedure to be used for storage and conversion system sizing. 97
Figure 64 –Sizing of additional battery for fuel cell electric vehicle: the vehicle consumption can be expressed depending on the mass (weight) of the battery used. 97
Figure 65 – Tank to Wheel vehicle consumption for different configurations. 98
Figure 66 – Well to Tank CO_2 emissions of different vehicle configurations considering target range. Values corresponding to commercial vehicle (both ICE and HEV) are also indicated. 98
Figure 67 – The NEDC is composed by four repetition of low speed cycle (0–800s) and one high–speed cycle (800–1400s). It is the reference cycle for European N1 and M1 vehicles. Different alternatives are derived (e.g. the initial idle time is reduced). The total distance is about 11km. It is a “modal” cycle. An alternative cycle for the high speed phase is shown in Figure 68. 105
Figure 68 – The EUDC for low–powered vehicles is suitable for the analysis of extra–urban driving phase, considering that the maximum speed does not exceed 90 km/h........ 105
Figure 69 – The FTP–72 cycle is used for the emission estimation of light vehicles in United States. It is a legislative cycle, similarly to NEDC, but it is composed by transient signal segments. High speed segment is shown on Figure 70. 105
Figure 70 – The FTP–75 cycle is used for the emission estimation of light vehicles. It is a complementary to FTP–72 test phase, including high speed run. 106
Figure 71 – ETC is a legislative cycle constituted by transient speed signals. It is suitable for heavy transport vehicles. 106
Figure 72 – Orange County Bus Cycle, developed by West Virginia University, shows typical stop–and–go expected for bus service. 106
Figure 73 – Artemis common driving cycle, including urban, rural road and motorway phases. The distance of the full cycle is about 52 km... 107
Figure 74 – Speed and acceleration profile of WLTC version 5.3 (source: Tutuianu et al., 2013).. 107
Figure 75 – Vehicle speed distribution in different regions (source: Steven, 2013). 108
Figure 76 – Cumulative frequency of acceleration starting from speed equal to zero (source: Alessandrini et al., 2003).. 110
Figure 77 – Cumulative frequency of idle time (source: Alessandrini et al., 2003) 111
Figure 78 – Cumulative frequency of acceleration change (source: Alessandrini et al., 2003). 111

Figure 79 – Speed–acceleration duration shown as 3D bar plot for two different driving situation (from Andrè, 2004). In this case, the z–axis is on time units. 112
Figure 80 – Speed–acceleration relative frequency matrix shown as a 3D plot (from Hung et al., 2006). In this case, the z–axis is expressed on 0–100% units (relative frequency of each speed–acceleration class, used as probability). 112
Figure 81 – Speed acceleration 2D “bubbles” plot for different datasets; the diameter of each bubble is related to the numerosity of the class (source: Tutuianu et al., 2013)........113
Figure 82 – Examples of driving segment dot–plots on the basis of two kinematic parameters (source: acquired data). Each dot represent a different trip event. 114
Figure 83 – Visualization of main cycles as regards speed and acceleration (source: André et al., 2006). 116
Figure 84 – Dot plot representing driving sequences on a two–axis plane; the seven categories defined are those described in Table 17. The two arrows shows approximately the increasing direction of physical quantities such as Speed and Acceleration. Main axes are two of the five generated by a PCA applied on original 15 kinematic parameters...118
Figure 85 – Driving conditions clusters according to André, 2004, as defined in Table 19. Circle indicate the “center” of each class, while each dot represent a driving sample. 120
Figure 86 – Plot representing urban cycles according to speed and acceleration distribution, the clustering being done through factor analysis classification (André et al., 2006a). 121
Figure 87 – Partition of urban cycles in eight subclasses (each one being represented bu a coloured symbol), according to Table 21 and Figure 86. 122
Figure 88 – Box plot of the error on estimation of vehicle efficiency obtained with the same car during different days, using a constant time window (t=100 s) and different sampling rate for speed acquisition (source: Corti et al., 2012). 124
Figure 89 – Biweight smoothing kernel function used by Haan and Keller, 2001, for a duration of h=4s. 125
Figure 90 – SAPD for low–powered cars and high–powered cars over common acceleration classes. The third rows of the table shows the difference between the two classes. From André et al., 2006b. 127
Figure 91 – Chronology of traffic conditions for the selection of the driving sequences to develop a representative cycle; the numbers in the tables represent the probability to get from a driving condition on x–axis to a driving condition on y–axis (source: André, 2004). 128
Figure 92 – Flow chart for driving cycle definition according to Hung et al., 2007. 129
Figure 93 – Synthesis of real–world driving cycles using Markov chain (source: Lee and Filipi, 2011)...130
Figure 94 – Synthesis of real–world driving cycles using Markov chain – SAPD matrix data extraction (source: Lee and Filipi, 2011). 131
Figure 95 – Regenerative braking power depending on speed and acceleration for Nissan Leaf Vehicle (source: Lohse–Busch et al ., 2012)...137
Figure 96 – On road vehicle driving (Renault Twizy)...139
Figure 97 – Renault Kangoo vehicle (left) and Renault Twizy vehicles (right) during service. 141
Figure 98 – Peugeot iOn vehicle. 142

Figure 99 – Box plot representing the daily distances run by city freight delivery electric vehicles (Twizy and Kangoo ZE) and electric passenger vehicles (iOn); the plot also includes the data of a Conventional vehicle frequently used for highway runs........ 144
Figure 100 – Average daily travel distance (km) by day of the week and by country (source: Pasaoglu et al., 2013).. 145
Figure 101 –Box plot representing the trip distances run by city freight delivery electric vehicles (Twizy and Kangoo ZE) and electric passenger vehicles (iOn); the plot also includes the data of a conventional vehicle frequently used for highway runs (represented on a different scale for improved readability)..................................... 146
Figure 102 – Distribution of daily car trips by country (source: Pasaouglu et al., 2013).. .. 147
Figure 103 – Share of trips chains with a driven distance <50km by country (source: Pasaouglu et al., 2013).. 147
Figure 104 – Electric quadricycle, passenger GPS tracks (one week of use); missions include urban, suburban and rural transports. 148
Figure 105 – Light Delivery Vehicle GPS tracks (one day): missions usually include urban and suburban driving, but not highway trips. 149
Figure 106 – Upper plot: a portion of speed measurement for iOn passenger vehicle, showing a comparison between raw and filtered data. Lower plot: a detail coming from the same measurement... 151
Figure 107 – Power Spectral Density of vehicle speed before and after the application of the filter. 151
Figure 108 – SAPD matrix 3d plot (left) and contour plot (right) for all the road measurements. The value corresponding to zero speed and zero acceleration has been excluded to avoid distortions due to its dominance.. 154
Figure 109 – Number of identified mictrotrips for each cluster. 156
Figure 110 – Scatter plot representing distance and average speed for all cluster elements; centroids are indicated by numbers. 157
Figure 111 – Scatter plot representing average moving speed and mean positive acceleration for all cluster elements; centroids are indicated by numbers.................................. 157
Figure 112 – Scatter plot representing average positive and negative accelerations for all cluster elements; centroids are indicated by numbers... 158
Figure 113 – Scatter plot representing average positive and negative accelerations for all cluster elements; centroids are indicated by numbers... 158
Figure 114 – SAPD contour plot for the microtrip groups described in Table 30; the plots do not include the point corresponding to idle phases (zero speed and acceleration) to avoid distortions due to its predominance. 159
Figure 115 – Upper plot: “All long” cycle. Lower plot: comparison between original SAPD (left) and cycle SAPD (right)... 162
Figure 116 – Upper plot: “All mean” cycle. Lower plot: comparison between original SAPD (left) and cycle SAPD (right)... 163
Figure 117 – Upper plot: “Passenger long” cycle. Lower plot: comparison between original SAPD (left) and cycle SAPD (right). 164
Figure 118 – Upper plot: “Passenger mean” cycle. Lower plot: comparison between original SAPD (left) and cycle SAPD (right). 165
Figure 119 – Upper plot: “LDV long” cycle. Lower plot: comparison between original SAPD (left) and cycle SAPD (right)... 166
Figure 120 – Upper plot: “LDV mean” cycle. Lower plot: comparison between original SAPD (left) and cycle SAPD (right). 167

Figure 121 – Upper plot: “Quadricycle long” cycle. Lower plot: comparison between original SAPD (left) and cycle SAPD (right). 168
Figure 122 – Upper plot: “Quadricycle mean” cycle. Lower plot: comparison between original SAPD (left) and cycle SAPD (right). 169
Figure 123 – Upper plot: “Unsteady long” cycle. Lower plot: comparison between original SAPD (left) and cycle SAPD (right). 170
Figure 124 – Upper plot: “Unsteady mean” cycle. Lower plot: comparison between original SAPD (left) and cycle SAPD (right). 171
Figure 125 – Driving cycle “builder” tool: main GUI screenshot. 175
Figure 126 – Output from “builder” tool: cycle plot (left), cycle SAPD plot (right)....................176
Figure 127 – Driving cycle “binder” tool: main GUI screenshot. 177
Figure 128 – Typical output from “binder” tool. 177
Figure 129 – iMiev motor working points from CAN acquisition; different colours corresponds to different trips. 178
Figure 130 – Frequency of energy consumption for 12V system of Twizy during use. 179
Figure 131 – Simulated Ragone plots for constant power discharge for the battery cells (BU, black), capacitors cells (SC, red) and various combination of both (see n=16, n=4 and n=1 configurations, corresponding to different LiB–SC couples). Source: Cericola et al, 2010. 182
Figure 132 – Forces acting on vehicle body (Wong, 2001). 184
Figure 133 – Calculated traction force, traction power and coast down time from 130 km/h for data on Table 37; C1 refers to Eckstein et al., 2013 source and C2 refers to Becker et al., 2013 source 186
Figure 134 – Voltage drop for cells elements in Table 39 as a response of a current step. ..189
Figure 135 – Thermal section of the battery model. 191
Figure 136 – Battery open circuit voltage V_{oc} according to datasheet. 193
Figure 137 – Battery open circuit voltage V_{oc} using a normalized DOD value and calculated V_{oc} depending on the current couples used. 193
Figure 138 – Estimated resistance depending on the Current plot selected for estimation. The values at the edges (DOD=1 or DOD=0) need manual adjustment due to inaccuracy of the data available on the datasheet. The differences on the estimation depending on C–Rate are probably due to inaccuracy in the datasheet. A mean value has been used. 193
Figure 139 – Estimated resistance depending on temperature at constant current (50A). The values at the edges (DOD=1 or DOD=0) need manual adjustment due to inaccuracy of the data available on the datasheet. 194
Figure 140 – Coefficients for current emphasis for SOC calculation depending on current and on temperature. 194
Figure 141 – A comparison between datasheet and simulated voltage. 194
Figure 142 – Voltage “shift” between measured and simulated battery voltage depending on current (negative current corresponds to traction). The SOC is varying from 90% to 40%, while the total error on the supplied energy is 4.3%. 195
Figure 143 – Battery model layout. 196
Figure 144 – Capacitor and resistor network for supercapacitor simulation. 197
Figure 145 – Torque and Power of Leaf motor (left) and of iMiev motor (right). 198
Figure 146 – Efficiency map for Leaf motor (source: Burress and Campbell, 2013)....................198
Figure 147 – Adapted efficiency map for iMiev motor. 199
Figure 148 – Motor model blocks. 199

Figure 149 – Original ICE map (left) and adapted ICE map for specific consumption. 202
Figure 150 – Final performances of range extender assembly: power power of range extender unit depending on RPM. The first curve shows the points for which the efficiency is best for each RPM; the best point over all is highlighted. The second curve shows maximum power points; the maximum point over all is highlighted. 202
Figure 151 – Final performances of range extender assembly: specific fuel consumption depending on RPM. The first curve shows the points for which the consumption is lower is for each RPM. The second curve shows the consumption at maximum power points. 203
Figure 152 – "Virtual driver" block using two PI. Normal one: P=1.2; I=0.5. Anticipated one: 0.3. Anticipation value: 1s. 203
Figure 153 – Simplied model for auxiliaries. 204
Figure 154 – Full model layout. 205
Figure 155 – ECOTEST driving cycle (source: Geringer and Tober, 2012). 206
Figure 156 – Calculation of energy used and regeneration results for driving cycles included in the "binder" tool. 209
Figure 157 – An example cycle, comprehending an "unsteady" cycle, an highway sequence and a passenger cycle (upper plot). Bottom plot shows the total energy consumption expected and the energy consumption expected on next time portion both for "fixed" and "variable" time advance. 213
Figure 158 – The ratio between energy used and energy expected to be use during the simulation of the cycle described in the preceding plot. 214
Figure 159 – Upper plot: a comparison between the energy needed to run the cycle as estimated by the scheduling logic ("E next", with variable and fixed time windows) and the energy available on the vehicle (that is, the sum of remaining battery energy and the energy that the range extender can supply in that time windows). As soon as one of the needed energy overpasses the available energy, the range extended is activated at maximum power (bottom plot). The range extender is often operated at his best efficiency point due to the fact that the overall needed energy overpasses the energy of the battery. 214
Figure 160 – Traction power of vehicle depending on speed and power supplied by the range extender using a linear link function or 3rd degree polynomial link function. 215
Figure 161 – Various plots coming from the simulation of "unsteady–long" cycle for pure BEV (to emphasize the discharge, a small battery is used – 25% of original size). . 217
Figure 162 – Traction and battery power the simulation of "unsteady–long" cycle, pure BEV. 218
Figure 163 – Various plots coming from the simulation of "unsteady–long" cycle for BEV–supercapacitor (to emphasize the discharge, a small battery is used – 25% of original size). 218
Figure 164 – Traction, battery and SC power the simulation of "unsteady–long" cycle, BEV with supercapacitors. 219
Figure 165 – Traction, battery and SC power the simulation of "unsteady–long" cycle, BEV with supercapacitors (detail). 219
Figure 166 – Traction, battery and range extender power for the simulation of "unsteady–long" cycle, BEV with range extender used as support for higher power. 220
Figure 167 – Upper plot: desired speed and effective speed of the vehicle; in highway driving, since requested power exceeds range extender capability it is possible that the

battery SOC falls to low level, determining the occurrence of “safe” mode, highlighted by the distance between target and effective speed. 220
Figure 168 – Upper plot: desired speed and effective speed of the vehicle; bottom plot: corresponding battery SOC in case of application of “trip scheduling” strategy. 221
Figure 169 – The approach adopted for the simulation: the model receives boundary condition at input, which are varying according to their distribution over the year, and the output are calculated in terms of energy and fuel consumption as well as GHG emissions. The model is adapted on the input conditions depending on their influence on vehicle data (e.g. varying powertrain configuration varies mass and energy management strategy). 222
Figure 170 – Daily external temperature for the simulations of LDV scenarios. 224
Figure 171 – Trends in the average annual distance travelled by car (source: Enerdata/Odyssee consortium, 2012). 225
Figure 172 – Daily driven distance distribution from original source (Marker et al, 2013) and fitted function. 225
Figure 173 – Charging events per vehicle day driven (source: Smart et al., 2013). 226
Figure 174 – Boundary condition for each driving event temperature and battery initial SOC (here represented as a distribution). 227

List of tables

Table 1 – A comparison of CO_2 emissions for different versions of the same vehicle assuming fuel and energy consumption declared by the manufacturer. 39
Table 2 – Factor analysis for customers' HEV purchase motivation (adapted from Ozaki and Sevastyanova, 2011). 43
Table 3 – Time constant for supercapacitor model depending on network order and recommended time steps (source: Wu and Dougal, 2005). 54
Table 4 – Overview of the controls needed for integration of single simulators in a co–simulation tools; such functionalities have to be provided through appropriate APIs (adapted from Nicolescu et al., 2007). 62
Table 5 – a SystemC code for the implementation of the sensitivity at state events (et_mat0). Source: Nicolescu et al., 2007. 63
Table 6 – Main interface functions provided for the example implementation of a Simulink/SystemC co–simulation tool (adapted from Nicolescu et al., 2007). 64
Table 7 – Simulators considered for TLM co–simulation and proposal for possible implementation and interface plug in (source: Siemers et al., 2009). 67
Table 8 – Mechanical elements representation and equations. 73
Table 9 – Mechanical system modelling through equation system. 74
Table 10 – Elements used for Energetic Macroscopic Representation – their function and graphical block (Chen et al., 2008b). 77
Table 11 – Modelling detail depending on design phase for common BEV components, using electric machine as reference example. 87
Table 12 – Specifications of ICE models used as reference for modelling. 92
Table 13 – Calculated specification of BEV models, to be used for final comparison. 93
Table 14 – Calculated energy consumption for different vehicle models. 93
Table 15 – Full list of indicators usable to describe driving cycles. Their full definition is in Appendix 1. 109
Table 16 – Correlation matrix between kinematic parameters used for the analysis of driving cycles (source: André et al., 2006a..115
Table 17 – Sequence of clusters recognized over measured driving data (adapted from Borgarello et al., 2001)..117
Table 18 – 2 dimensional speed and acceleration distribution for the driving data, before (upper table)and after (bottom table) the introduction of an emphasis factor (Andrè et al , 2006a)...119
Table 19 – Driving conditions classes obtained by automatic clustering of speed profiles recorded on–boad vehicles (source: André, 2004). 119
Table 20 – Average characteristics of clusters of driving cycles (source: André, 2006)......121

Table 21 – Driving segment classifications within urban class cluster, according to André et al., 2006a. 122
Table 22 – Trip characteristics and distribution (in terms of total distance run) for two main classes of vehicles. Adapted from André et al., 2006b. 126
Table 23 – Kinematic parameters used for the validation of existing driving cycles (from Tong and Hung, 2009). 133
Table 24 – Summary of development methodologies for existing driving cycles (from Tong and Hung, 2009). The table continues in next page. 134
Table 25 – Questionnaire about electric quadricycle and users expectations. A group of four drivers responded; each one used the vehicle for at least one day. 143
Table 26 – Summary of daily driven distance for the vehicles under study in the city of Florence and for main literature sources. 144
Table 27 – Summary of trip distance descriptions for the vehicles under study in the city of Florence and for main literature source. 146
Table 28 – Parameters used for cycle characterization and grouping. The numerosity of elements on SAPD matrix used for plots is reduced for better readability. 153
Table 29 – Main parameters calculated for each data subset. 153
Table 30 – Summary of main descriptor parameters for each microtrip group. The name of the class and the notes in relation to the speed are assigned after the grouping and are not relevant for analysis. 156
Table 31 – Information summary for all generated cycles. 161
Table 32 – Main parameters regarding synthetical cycles selected after generation. 161
Table 33 – Characteristics of each group of microtrips used as input for cycle generation. 172
Table 34 – Parameters synthetized driving cycles. 173
Table 35 – Percentage difference between the parameters describing the input measurements and the corresponding synthetized driving cycles. 174
Table 36 – Adsorbed power for main Twizy 12V components. 179
Table 37 – Coast down results from literature for the Mitsubishi iMiev EV. 186
Table 38 – Equivalent mass calculation. 187
Table 39 – Equivalent networks alternatives for battery modelling and the related transfer function of order zero, one and two. The parameters suggested come from Einhorn et al., 2013. 188
Table 40 – Specifications of LEV50 lithium ion cell. 192
Table 41 – Main MAHLE ICE for range extender characteristics. 202
Table 42 – A comparison between reference data and simulated ones. 207
Table 43 – Power used by HVAC and auxiliaries depending on external temperature (adapted from Geringer and Tober, 2012). 207
Table 44 – Expected range for the vehicle depending on cycle and on temperature. 208
Table 45 – Energy supplied by the battery (in kWh) depending on cycle and on temperature; for this case, single driving cycles have been considered. 208
Table 46 – Calculation of energy used and regeneration results for a list of recent driving cycles. 209
Table 47 – Power disaggregation through transfer function (Trovão et al, 2013) and simplified dimensioning data for supercapacitor system. 216
Table 48 – Current supplied by the battery on three different configuration. 217
Table 49 – Configurations tested for “LDV” case study. 224
Table 50 – Configurations tested for “Passenger vehicle” case study. 228

Table 51 – Results for the simulation of LDV case study over a year of driving. Note for the vehicle configuration: “X” means “in use”. 231
Table 52 – Results for the simulation of a passenger vehicle in various configuration for a three–year period of use. Note for the vehicle configuration: “X” means “in use”…232

Acronyms List

ADAC: Allgemeiner Deutscher Automobil–Club (German automobile club)
BAB : Bundesautobahn (federal highway)
BEV: Battery Electric Vehicle
BMEP: Brake Mean Effective Pressure
CADC: Common Artemis Driving Cycle
CAE: Computer Aided Engineering
C-rate:Current rate
ECU: Electronic Control Unit
EREV: Range extender electric vehicle
EUDC: Extra Urban Driving Cycle
EV: Electric Vehicle (in the document, it includes BEVs, HEVs, PHEVs, EREVs etc.)
HEV: Hybrid Electric Vehicle
HVAC: Heating, Ventilation and Air Conditioning
ICE: Internal Combustion Engine
ICEV: Internal Combustion Engine Vehicle
NEDC : New European Driving Cycle
PHEV: Plug–in Hybrid Electric Vehicle
PID: Proportional–Integral–Derivative
PV: Performance Value
REX: Range Extender
SAPD: Speed Acceleration Probability Distribution
SC: SuperCapacitor
SOC: State Of Charge
SOH: State Of Health
SSD: Sum Square Distance
STD: Standard Deviation
WLTC: Worldwide harmonized Light vehicles Test Cycle
WLTP: Worldwide harmonized Light vehicles Test Procedures

Preface

It would be superfluous to highlight the relevance of Computer Aided Engineering tools within modern product design processes. Modelling and Simulation activities are an essential support and their potential is probably far beyond the mere substitution of physical experimentation.

A number of reasons are pushing towards the organization of design strategies in order to fully explicate the potential of existing and of future CAE. The possibility to consider a large number of design criteria in any design phase, in fact, enables the startup of a so–called “concurrent engineering” process. This leads to a reduction of the need for physical testing activities, with positive effect on the expected costs and on the overall total time–to–market; furthermore, a large number of different alternatives can be examined through preliminary simulations and this can promote the proposal of innovative solutions or the optimization of existing ones. Another advantage is the efficient data management, which has a primary relevance for the communication within different working teams. Vehicle concept characteristics can be controlled reducing the risk of non–compliance in terms of quality or performances. Nevertheless, since a large number of different CAE tools are available, guidelines are needed for the selection of model characteristics, for model implementation and for efficient simulation at each design step.

This work introduces the fundamentals of mechatronics system modelling, main focus being on automotive design activities. The aim is to describe different modelling approaches and also to provide a brief literature review. A study on driving cycle generation and an application on a full vehicle model is presented.

The more the field is under innovation, the more research tools are needed: it is therefore undoubted that due to new generation of electric and hybrid electric vehicles the automotive sector is under change. In addition, the methodologies for the evaluation of vehicle performances need to be updated together with the product: this has been the main motivation for the proposal of a new series of driving cycles that can be used for virtual or real world testing. The data and the method coming from such activity have been implemented in a procedure aimed at facilitating new vehicle development and validation through the use of “real world data”.

1. The electrification of road vehicles

Electric vehicles for road use have been proposed since the early years of automobile diffusion on mass market, but for more than a century vehicles using ICE as energy conversion and traction system have been the main solution both for passenger and freight transport. In the meanwhile, technological development made available at acceptable cost a number of technologies (e.g. semiconductors devices, calculation capabilities for control system, energy storage systems) that can be considered “critical” and “enabling” for the introduction on mass–market of vehicles whose traction system is partially or totally based on electric components. At the end of the ‘90s, HEVs have been introduced into world–market, while in very recent years BEVs capable of remarkable performances (e.g. range above 100–150km, up to about 400km) have also been developed. Due to such “vehicle electrification” phase, new models and different configurations (from hybrids to full electric, e.g. HEVs, BEVs, PHEVs, EREVs) have been introduced by different manufacturers, most time being promoted as a solution for the mitigation of environmental impact.

In this chapter a short review on the potential of EV technologies towards environmental sustainability will be explained, introducing the important role of assessments methods and models; these latter will be described in detail in the next chapters. An outlook on other factors pushing for vehicle electrification is also included in the present section.

1.1. The environmental sustainability of transport systems

The transport sector is responsible for a large amount of energy consumption on a continental basis (about 25–30% in Europe– see Figure 1); in particular, the data demonstrates that the use of road vehicles for passenger and freight transportation constitutes the dominant share of transport activity (see Figure 2). The growth previsions highlight the possibility of a constant increase of the activity within the European context (see EC report, 2013); however, Figure 3 shows that – in case of strong efficiency improvements in the sector – the energy consumption can be decoupled from the growth of transport service demand.

Considering that road transportation systems are based on the use of fossil fuels (see Figure 4), it is well known that transport activity implies a significant contribution to air pollution, to greenhouse gas emissions and to primary sources depletion; acoustic noise is also an issue. From a world point of view, the situation is similar: Figure 5 shows the expected transport activity increase on a world basis, while Figure 6 shows the related GHG emissions; also in this case, the “decoupling” between activity and emissions is hypothesized through a number of so–called “increments”: from technological improvement of vehicles (e.g. .hybrids, diesels, fuel cells) to primary source switch.

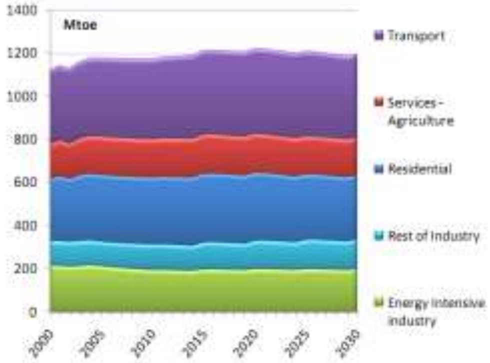

Figure 1 –Final energy demand by sector and future trend scenario to 2030 in Europe (source: EC, 2009).

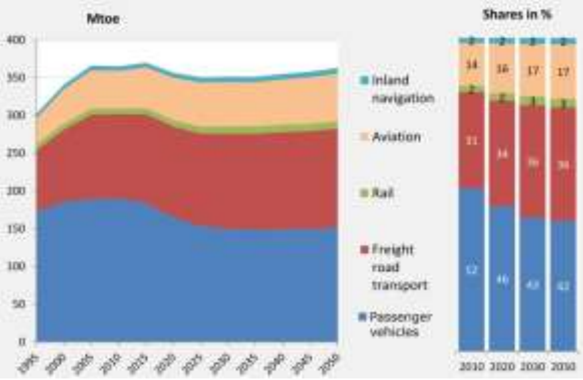

Figure 2 – Final energy demand in transport: current value and trend to 2050 in Europe (source: EC, 2013).

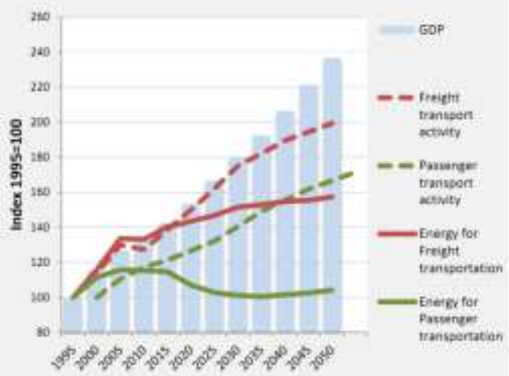

Figure 3 – Trends in transport activity index and energy consumption in Europe (EC,2013).

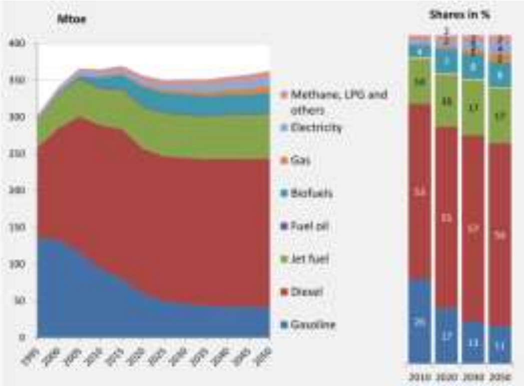

Figure 4 – Final energy demand in transport by fuel type: current value and trend to 2050 in Europe (source: EC, 2013).

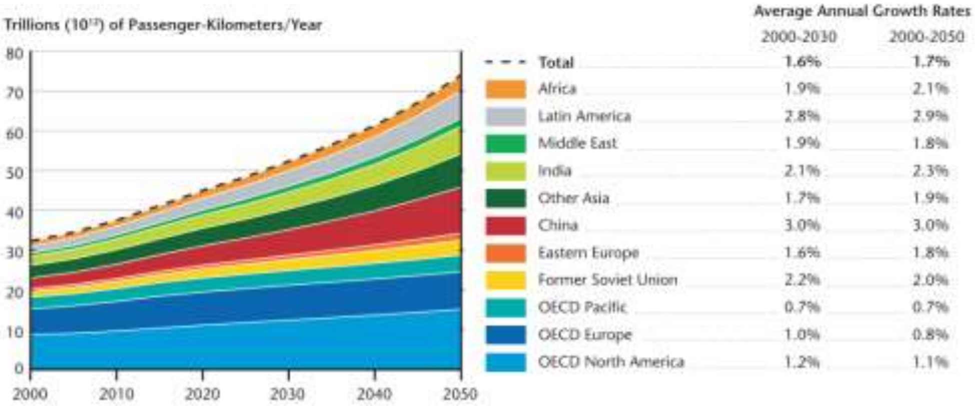

Figure 5 – Expected trend for transport activity on a world basis (source:WBCSD, 2004).

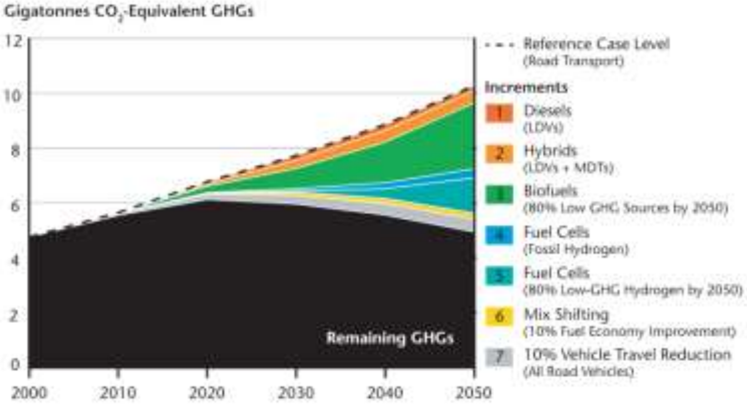

Figure 6 – Expected trend for GHG emissions from transport on a world basis; colored areas represent the estimated GHG emissions reduction in case of technology shift (source:WBCSD, 2004).

In the light of these facts, it can be said that the “sustainability” of road transports is uncertain. Even if the general meaning of the word “sustainability” is well known, it can be useful to define it in detail and to clarify how vehicle technology shift can help in reaching it. According to an early but still representative definition from the WCED, 1987, *sustainable development is development that meets the needs of the present without compromising the ability of future generations to meet their own needs*. Regarding the transport sector, seven reference goals have been suggested by the WBCSD, 2004:

(1). Ensure that the emissions of transport–related conventional pollutants do not constitute a significant public health concern anywhere in the world
(2). Limit transport–related GHG emissions to sustainable levels
(3). Significantly reduce the total number of road vehicle–related deaths and serious injuries from current levels in both the developed and the developing worlds
(4). Reduce transport–related noise
(5). Mitigate congestion
(6). Narrow the “mobility opportunity divides” that inhibit the inhabitants of the poorest countries and members of economically and socially disadvantaged groups within nearly all countries from achieving better lives for themselves and their families
(7). Preserve and enhance mobility opportunities for the general population of both developed and developing–world countries

It is clear that the electrification of road transport is an opportunity especially for the achievement of the goals number 1, 2 and 4 due to direct effects: efficiency increase, reduced air and acoustic emissions by the vehicles.

1.1.1. Environmental impact assessment methods

The technology of internal combustion engine is by large the most used for road transport vehicles. The proposal of different technologies for vehicles propulsion implies a number of modifications in the known industrial and social established habits. Changes could be needed in terms of production technologies, primary energy supply, material choice, while at the same moment also the support infrastructure has to be modified, in order to satisfy users’ expectations or to influence their acceptance. Before a deep change in the vehicle supply chain is started, a number of evaluations have to be performed to respond to question such as:

- what is the effective modification in terms of primary energy consumption for the deployment of a similar service using different vehicle technologies?
- what kind of performances are expected considering current state–of–the–art technologies?
- which technology is expected to have larger margins for improvement?
- what about the economical sustainability of the technology?
- what about the environmental sustainability of the technology?
- are there any possible future “bottlenecks” (e.g. resources having limited availability on national/continental/world scale) for the technology?

It is evident that in this kind of analysis the focus is not only on the vehicle itself but, in many case, on the general context where a fleet is going to operate; as a consequence, the expected result is related to general indicators such as primary energy consumption (e.g. MJ, or tons petroleum equivalent), resource consumption (renewable and not renewable) or to environmental impact indicators (e.g.: greenhouse gas emission – GHG; waste production; abiotic resource depletion potential; photochemical ozone creation potential; sometimes other indicators or a combination of them is also calculated). The build of so–called “Life Cycle Assessment” (LCA) is in many cases a suitable solution to offer a complete output for the analysis; the methodology is defined by the technical standard ISO 14040, which is aimed to reduce the arbitrariness and the uncertainties of the evaluation (although some authors highlight that such job can be difficult, e.g. see Ross et al., 2002). LCA approach is able to summarize in a small number of indicators the impact related to the use of primary resources, of energy vectors, of the use of the fleet, of the technology applied; in general, of all the material and energy flows related to a so called “functional unit”, that is the service or the product under examination. In case of a car, an example of functional unit definition is: *a European, compact–sized, five–door gasoline vehicle for 5 passengers including a luggage compartment, and all functions of the defined reference scenario with a mileage of 150,000 km over 12 years, complying with the same emission standards* (Schmidt et al., 2004).

Since full LCA studies have to take into account all the variables determining the impact of the vehicle on the environment, a very large amount of data are needed: material extraction, transport, production technology, component manufacturing, consumption during use phase, maintenance and end of life management are main examples. All of them are contributing to air/soil/water emission, to raw materials depletion and to any other relevant environmental impact that has to be taken into account. Similar general approach can be built also using economic indicators, thus defining the total cost of ownership through “Life Cycle Costing” (LCC) analysis. Considering that for vehicles (and, in general, for all durable goods) the use phase is by far the one producing the most relevant impact (see Figure 7), the analysis can be sometimes focused only on it.

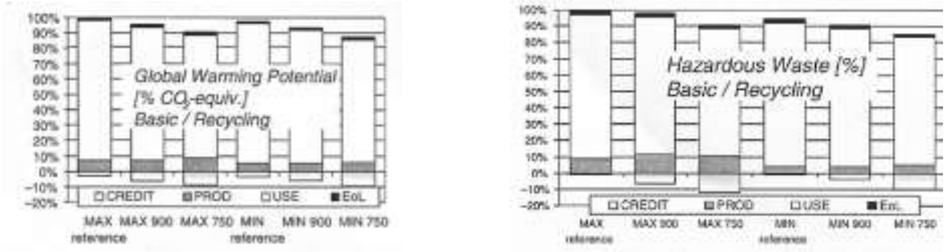

Figure 7 – Global warming potential (left) and hazardous waste production (right) results of a full LCA analysis comparing different vehicle solutions (six alternatives for car body are considered, from Schmidt et al., 2004). For all case studies, “USE” phase is responsible of main impact.

The analysis of the use phase (sometimes called “fuel cycle” or “energy cycle”) is therefore a very important step to evaluate the environmental impact of the vehicle and it can be focused on different sub–analysis, main being:

1. well to tank: it includes the analysis related to fuel production/extraction and delivery
2. tank to vehicle: it includes on–board energy conversion and is mainly related on vehicle powertrain characteristics
3. vehicle to miles: it includes vehicle energy consumption and is mainly related to the driving/duty cycle selected.

An analysis including point two and three of the above list is also said “tank to wheel”; a full use phase analysis (including point 1, 2 and 3) is said “well to wheel”. Figure 8 shows a simple scheme presenting such approach (from Guzzella, 2009).

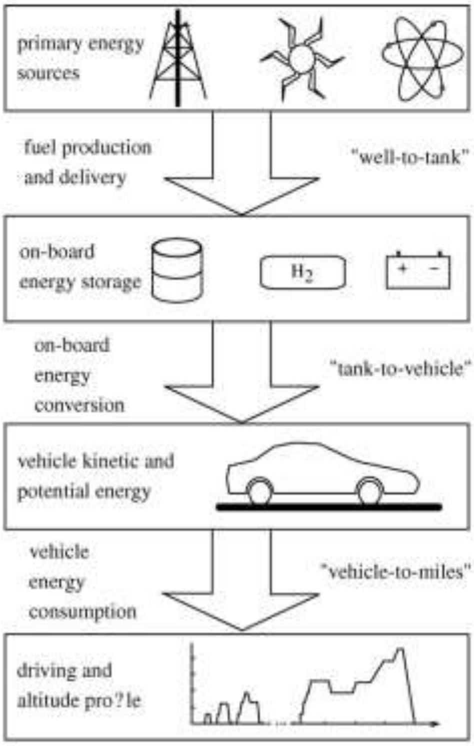
primary energy sources
fuel production and delivery
"well-to-tank"
on-board energy storage
H_2
+ -
on-board energy conversion
"tank-to-vehicle"
vehicle kinetic and potential energy
vehicle energy consumption
"vehicle-to-miles"
driving and altitude pro?le

Figure 8 – Most relevant energy conversion steps during the operation of a vehicle (from Guzzella, 2009).

Tank to wheel analysis is therefore very related to the knowledge of vehicle technology and of its performances: at least, a reference mission and a fuel/energy consumption model are needed. Since in many cases the value of the analysis relies on the comparison of different alternatives, the model should be able to calculate the variability of the output (e.g. efficiency, energy consumption) on given impact factors (e.g. mass variation) over different scenarios (e.g. different driving cycle).

1.1.2. European regulation for air emissions containment

Assuming a simplified point of view, the impact on atmosphere of vehicles can be measured using two main categories of emissions:

- air pollutants, substances capable of noxious or toxic effects on plants and/or animals
- GHG emissions, which provide their effect on a long time scale even if no harmful direct impact is related to their emission.

The first category includes the emissions of substances such as CO, NO_x, CH, PMX (fine particles); within Europe, the first regulation has been introduced in 1970 (Directive 70/220/EEC), then a number of updates with increased level of restriction (from EURO1 standard – Directive 91/441/EEC to EURO6 standard – Regulation 715/2007) came into force gradually, depending also on technical achievability. Even if it can't be said that the problem is solved, the regulations provided their effect in a noticeable way, as stated in the work by Guzzella (2009) and as shown in Figure 9.

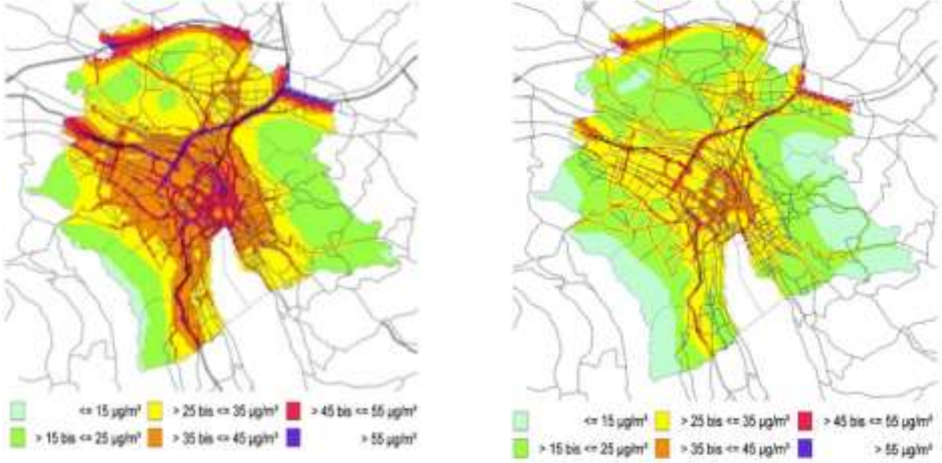

Figure 9 – . Air pollution levels (NOx) in the city of Zurich in 1995 (left) and in 2002 (right). Source: Guzzella, 2009.

Similar standards in other context (US, Japan) lead to similar improvements and results; on a world level, main achievements have been obtained through ICE engine technological improvements especially on combustion control and exhaust gas post–treatment. Fuel improvements (e.g. sulfur reduction) have also been applied.

The second category is related to the use of primary energy, thus it depends both on energy source and on overall vehicle efficiency. The Regulation 443/2009, in Europe, sets two steps for the CO_2 emissions of light vehicles:

- by 2012, the average new car fleet has to reach a target of 120gCO_2/km
  - the objective of 130 gCO_2/km has to be reached through improvements in vehicle motor technology
  - a further reduction of 10 gCO_2/km can be delivered by other improvements, including an increased used of biofuels
- from 2020 onward, the Regulation sets a target of 95gCO_2/km as average emission the new car fleet.

The target, however, is adjusted on vehicle mass using the following correction formula:

$$\mathit{Specific\ emission\ of}\ CO_2 = 130 + a * (M - M_0)$$

where M is the vehicle mass in kilograms (kg), M_0 is a value of 1372,0 kg and a is a constant value of 0.0457.

The introduction of such regulation introduces two innovative concept:

- considering constant emission factor for 1 liter of fuel, the vehicle consumption is limited
- the possibility of energy diversification, in this case introducing renewables such as biofuels.

According to Sullivan et al., 2004, an emission factor of 2650 gCO_2/l can be used for diesel fuel and 2360 gCO_2/l can be used for gasoline, thus limiting the consumption to about 4.9 l/100km for diesel vehicles and to about 5.5 l/100km for gasoline vehicles. The achievements status is shown in Figure 10, thus highlighting that the current target is quite challenging for manufacturers and that next target is expected to require significant improvements in comparison with current production.

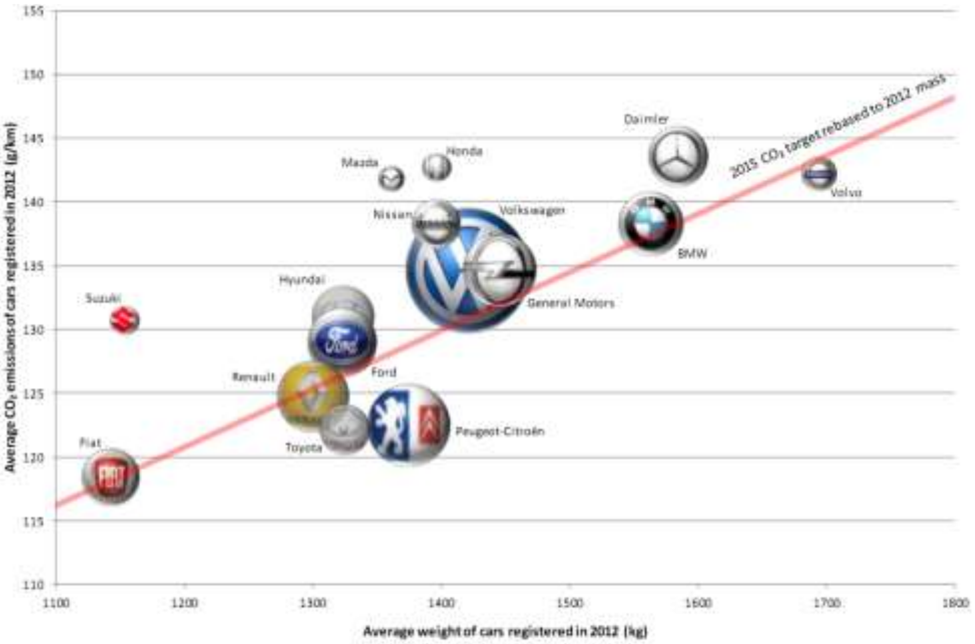

Figure 10 – Fleet average weight and CO_2 emissions in Europe by carmaker and comparison with EU target line. The size of each bubble represents the amount of CO_2 emission of total cars sold (source: TE, 2013).

1.1.3. Electric vehicles potential for environmental impact reduction

Both HEVs and BEVs (and all the related sub–categories) can contribute to the reduction of CO_2 emissions in comparison with equivalent ICE vehicles due to the high overall efficiency and to the high power regenerative braking capability, that can significantly improve total consumption. In case of pure BEVs or of PHEVs, the potential for GHG emissions reduction strongly depends on the “carbon” intensity of the primary energy source; t depends on the energy mix of the Country where the vehicle is used. In order to demonstrate the potential of EVs for impact reduction, Table 1 shows a comparison of final CO_2 emissions for different models of the same vehicle, that is a Renault Kangoo Express

LDV (below 3.5t). The Kangoo vehicle has been chosen due to the fact that different powertrains installed on the same body are available:

- conventional ICE, gasoline, atmospheric, 1.6 displacement
- conventional ICE, gasoline, turbocharged, 1.2 displacement (performances are comparable with 1.6 version)
- conventional ICE, diesel, turbocharged, 1.5 displacement, 55 kW version
- conventional ICE, diesel, turbocharged, 1.5 displacement, 80 kW version “Energy”
- electric traction (BEV), external excited synchronous motor, 44 kW version.

The emissions have been calculated assuming the fuel or energy consumption declared by the manufacturer (usually calculated over a NEDC test cycle). Regarding the emission factor for electric energy production, the value of 410.3 gCO2/kWh estimated for Italy (ISPRA, 2011) has been considered, that is also very similar to European average (see Figure 11). The GHG reduction is clear (at least –60%) in comparison with all the ICE versions. The lower part of Table 1 shows a comparison assuming different energy mix emission factor (in the range of 100–900 gCO_2/kWh), showing that the compliance with 2020 EU target can be obtained even in a worst–case condition. An absolutely favorable value of about 10–20 gCO_2/km is possible in case of low carbon sources (renewables, nuclear) able to contain the emission factor below 200 gCO_2/kWh. However, a limitation of the Regulation and of the proposed simplified analysis is that only the TTW efficiency is considered. In addition, regarding the full vehicle life, the production of the vehicle deals with the need of material extraction and manufacturing processes that are very different from ICE vehicles (e.g. lithium cells, rare–earths permanent magnet motors), so that new externalities and impacts could arise.

Renault Kangoo Express model		**Gasoline 1.6**	**Gasoline 1.2 TCe**	**Diesel – 1.5dCi**	**Diesel – 1.5dCi Energy**	**ZE –Electric**
Curb weight (kg)		1271	1245	1280	1280	1426
Vehicle Power (kW)		78	84	55	110	44
Declared consumption		8.2 l/100km	6.1 l/100km	4.6 l/100km	4.3 l/100km	115 Wh/km
Energy unit		l gasoline	l gasoline	l diesel fuel	l diesel fuel	kWh
km/energy unit		12.2	16.4	21.7	23.3	8.7
gCO_2/energy unit*		2360.0	2360.0	2650.0	2650.0	410.3
gCO_2/km		193.5	144.0	121.9	114.0	47.2
		GHG emission reduction in comparison with electric version				gCO_2/km
Electricity production emission	100 gCO_2/kWh	–94%	–92%	–91%	–90%	11.5
	200 gCO_2/kWh	–88%	–84%	–81%	–80%	23.0
	300 gCO_2/kWh	–82%	–76%	–72%	–70%	34.5
	400 gCO_2/kWh	–76%	–68%	–62%	–61%	46.0
	500 gCO_2/kWh	–70%	–60%	–53%	–51%	57.5
	600 gCO_2/kWh	–64%	–52%	–43%	–41%	69.0
	700 gCO_2/kWh	–58%	–44%	–34%	–31%	80.5
	800 gCO_2/kWh	–52%	–36%	–25%	–21%	92.0
	900 gCO_2/kWh	–47%	–28%	–15%	–11%	103.5
The value for electric energy production emission (gCO_2/kWh) refers to 2009 Italian mix, according to the report by ISPRA, 2011.						

Table 1 – A comparison of CO_2 emissions for different versions of the same vehicle assuming fuel and energy consumption declared by the manufacturer.

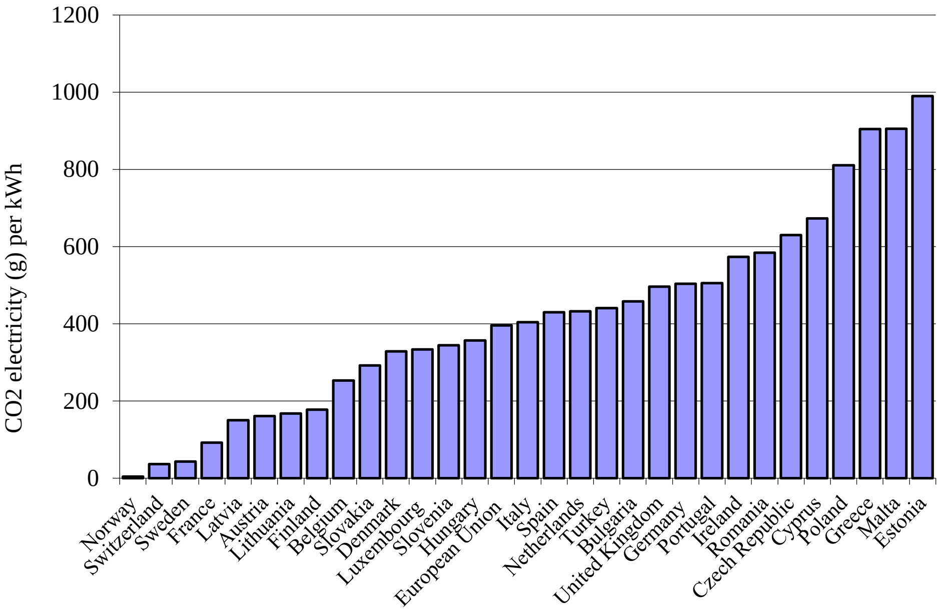

Figure 11 – Emission factors for European Union Countries (source: Eurostat, 2013).

Recent LCA researches show that the energy consumption share between phases is modified: production effort can be increased in comparison with Figure 7. As a consequence, there is no general agreement about expectations on total impact reduction in case of comparison between equivalent ICEVs and EVs. The work by Notter et al., 2010, estimates a significant reduction of the impact for all categories (including GHG and EI99 factor, that is an aggregated value calculated from all impact categories, see Figure 12). The work by Hawkins et al., 2012, estimates a potential for impact reduction, but a sensitivity analysis on main energy source used (from European mix, to natural gas–based energy production and coal–based energy production) demonstrates that BEVs could be *counterproductive in areas where electricity is primarily produced from lignite, coal, or even heavy oil combustion* (see Figure 13). Similar results are obtained also in the work by Doucette and McCulloch., 2011, where a sensitivity analysis compares CO_2 emissions on the basis of:

- varied vehicle size
- varied vehicle energy storage system capacity (determining different achievable range)
- varied primary energy source.

The cited work includes a vehicle physical model for consumption estimations and is described in detail in the next chapter.

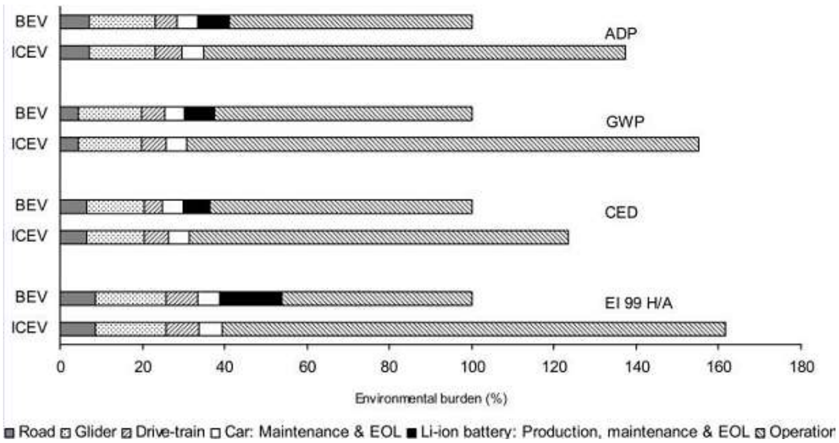

Figure 12 – Impact assessment on four different categories (GHG–GWP emissions, Abiotic Depletion Potential ADP, nonrenewable cumulated energy demand CED, Ecoindicator 99 H/A) of BEV and ICE vehicles considering all the use phases: road construction and maintenance, glider, battery and drivetrain production, use phase (operation and maintenance), vehicle End Of Life (EOL). Energy mix emissions calculated as EU average. Source: Notter et al., 2010.

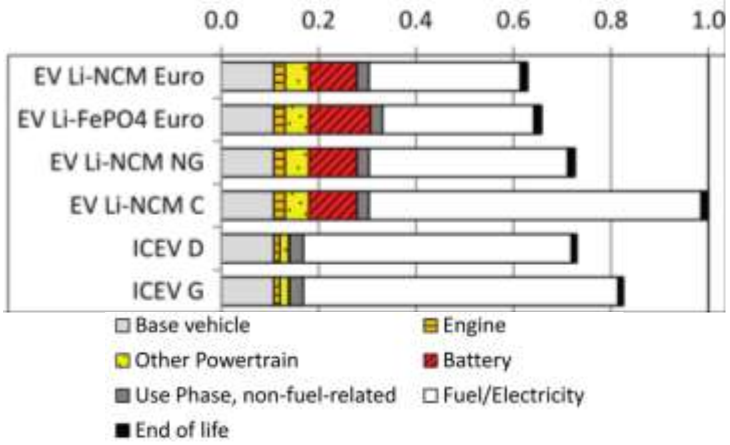

Figure 13 – GWP impact of vehicle life (phase defined in the legend) and comparison of different alternatives: BEV using lithium nickel cobalt manganese cells (LiNCM), BEV using lithium iron phosphate cells ($LiFePO_4$), Diesel and Gasoline ICEV. BEV vehicle impact is calculated considering European Energy mix impact (Euro), Natural Gas (NG) electricity production impact, Coal (C) electricy production impact. Value 1.0 corresponds to the most impacting alternative. Source: Hawkins et al., 2012.

As a conclusion, vehicle electrification is a feasible possibility for the reduction of transport impact, especially if non carbon–intensive energy sources are used. The need for environmental sustainability determined by Regulations can be considered an important driver pushing for the development and the mass production of EVs (both HEVs and BEVs).

1.2. Emerging drivers for vehicle electrification

The increase of efficiency and the reduction of overall environmental impact is probably the most relevant driver for HEV and EV diffusion; however, it is not the only one.

A relevant factor is that the existence of a large fleet availability of Electric Vehicles could represent an opportunity for electricity production and distribution industry; the use of Vehicle 2 Grid (V2G) solutions, in fact, could make available an energy storage network to be used for balancing and optimization of energy supply; similarly, EV fleets could be used for the integration and the efficient use of renewable energy systems, as an example through the compensation of their intermittency problems (Barkenbus, 2009), that is typical of photovoltaic (PV) plants. In other words, the large diffusion of EVs could also favorite the use of low–carbon, renewable sources. This factor is relevant for the reduction of environmental impact through energy diversification and efficiency improvements of anthropic activities.

Regarding the acceptance of EVs on the market, a number of literature researches analyze consumers' attitude towards new technologies, highlighting that multiple factors can determine future trends. Different approaches are needed to investigate the topic, and recent literature works include forecast analysis using structured models (the works by Propfe et al., 2013, shows an application of "VECTOR21" model for calculation of different scenarios in terms of EV fleet diffusion; the work by Tran et al., 201,3 also uses a Montecarlo based approach for the simulation of market behaviors) and investigation through surveys on experts (Zubaryeva et al., 2012) or on consumers' (Lieven et al., 2011) groups. Results from test panel that already experienced the use of latest generation EVs are also available (Cocron et al., 2011; Graham–Rowe et al., 2012; Smart et al., 2013).

1.2.1.The attitude of drivers towards innovative vehicles

In this paragraph, the contents of a few recent works are explained in detailed, in order to introduce the reader to the factors determining the demand for vehicle electrification; however, the aim is not to provide a full literature review on the topic.

The work by Ozaki and Sevastyanova, 2011, is particularly interesting since it analyses in detail common purchase motivations along a Prius owners' group; a survey has been sent to 4000 owners, and the results are coming from 1263 returned complete questionnaires – a quite large popultaion. The first research objective is to investigate the purchase behavior of hybrid buyers; for this reason, known motivational constructs coming from former studies are taken into account as reference. Motivational constructs usually fall into five main groups:

- financial benefits (e.g. reduction of total cost of ownership due to fuel efficiency)
- user "environmentalism", that includes environmental awareness, desire to reduce ecological footprint, possibility to show such aim to the community through the vehicle
- compliance with norms and values of the community
- attitude of the users to adopt new and/or innovative technologies
- possibility to achieve independence from oil producers through reduced petrol consumption.

The use of 21 different metrics (closed questions, expressed on a Likert–scores table) in the questionnaire and the application of Principal Component Analysis criteria provided an explanation of *interrelations between construct, identifying the common factors describing the greater part of the total variance* of the scores. The outcome is that about 65% of total variance in the results can be explained by the use of the above five factor, according to Table 2.

Factor	% of variance	cumulative %
1 – Perceived environmental benefits	22.11	22.11
2 – technological interest	16.04	38.15
3 – social orientation	12.60	50.75
4 – geopolitical and policy–related benefits	8.22	58.96
5 – financial benefits	5.88	64.84

Table 2 – Factor analysis for customers' HEV purchase motivation (adapted from Ozaki and Sevastyanova, 2011).

The study also includes an analysis of the "open comments" provided in the questionnaire, so that new motivations and factors can be identified directly from drivers impressions. The new factors highlighted by this second analysis are related to:

- comfort and ease of driving
- technological interest of the user
- social and personal identity, e.g. the use of the hybrid vehicle identify the user as a member of a distinct group
- manufacturers' good reputation
- style and fashion
- financial benefits from local transport policy (e.g. fee exemptions for those living in urban areas subjected to "congestion charge") –related also to economic benefit
- fuel economy – related to economic benefit
- environmental awareness
- smart consumption perception – related to economic benefit
- size of the car.

Most of this factors arise as a consequence of the fact the population under examination is experienced on the use of the vehicle; it can be also said that a clear limitation of the study is that such panel represents a group of "early adopters" of new technologies. Nevertheless, the study clearly demonstrates that "affective" dimensions (e.g. the driving pleasure, the interest in new technologies, the expression of self) strongly characterize consumers' perception and, therefore, that the reason for the introduction of EVs–HEVs can be found not only on "practical" needs (the reduction of carbon footprint), but also on the capability to satisfy emerging needs. In the case of Tesla motors – a brand currently producing high–end BEVs such as luxury and sport cars – high performances are a clear attribute.

Similar conclusions can be found in the very recent study by Schuitema et al., 2013, that is related to the evaluation of the behavioral response of consumers to technology innovations. According to the authors, car purchase and use are associated to three main categories of attributes:

- instrumental – referring to functionality or utility provided by the technology (e.g. cost, range, performance..)
- hedonic – referring to the emotional experience derived from using the technology (joy, pleasure)
- symbolic – referring to the sense of self or social identity related to the possession of the technology.

While *previous studies have tended to focus on the role of instrumental attributes when considering the potential adoption of EVs*, the results of this study confirm that instrumental attributes are important, but that their relevance is strongly related also on their influence on hedonic and symbolic attributes of EVs. The weight of such “indirect” effects is therefore comparable with that of “direct” effects. As an example, a comparative analysis *suggests that the perception of instrumental, hedonic and symbolic attributes of PHEVs are preferable to BEVs*; according to the study, the *negative perceptions of hedonic and symbolic attributes are explained by that people link limited instrumental attributes of BEVs* (e.g. reduced range) *to less joy and pleasure in owning and driving a BEV and a negative social identity.*

As a conclusion, it can be stated that the technology of HEV and EV can offer advantages not only on the basis of financial and environmental criteria. Even if environmental reasons and regulations are probably known as the most relevant drivers for vehicle electrification,. new technologies enable the possibility to obtain characteristics that are recognized and appreciated by the users: innovation (that is perceived as a value), comfort, ease of drive, quietness, compliance for social acceptance are a few examples. On the other hand, main instrumental attributes of the vehicle have to be satisfactory not only of the effective instrumental needs of the users, but also of the hedonic and symbolic attributes related to the ownership and the use of the vehicle.

2. The role of modelling activities in engineering

The applied research for innovation and for product development is a process that unavoidably takes the form of a process structured on different steps: from preliminary context analysis and "concepts" confrontation, to the definition of product technology and details; from the development of components and systems to the final testing and validation activities. If early concept phase are usually based on general requirements such as performances, the progress of the development phase implies the definition of component specifications, thus gradually shrinking the "design freedom" due to the consolidation of product configuration; iterations are often needed. In late development phases such as prototype preparation and real world testing, most part of the product is "frozen" and any variation determines an high cost. Information Technologies (IT) tools can support the engineer to in all these phases, but in order to effectively reduce time and cost their use has to fit with different exigencies: from the capability to explore the potential of a large number of alternatives in the early phase, to the accuracy of results in testing and validation activities. The use of software engineering tools enables the possibility to virtually design the system (modelling the product or the process under study) and to virtually test, through simulation, the operational performance of existing or potential design. The importance of IT tools in the engineering process has been constantly increasing in the last thirty years; during such period the whole approach to New Product Development (NPD) has been innovated. The purpose of this chapter is to explain the role of virtual simulation tools in new product development, that is a general topic; subsequent paragraphs of the present study will focus the attention on vehicle powertrain design process.

Main motivation for the preparation of this section has been the need of the author to identify the qualities that an "ideal" simulation environment should have and the characteristics to be considered during model creation in order to let it be used general and "upgradable" reference modelling framework for any application. The results have also been used the participation to the ASTERICS[1] project, which required the coordination of partners adopting different modelling environments through the definition of modelling guidelines.

---

[1] ASTERICS: Ageing and efficiency Simulation & TEsting under Real world conditions for Innovative electric vehicle Components and Systems, an international research project funded bu European Community within the 7th Framework Programme; www.asterics–project.eu

A short list of common terms used to describe vehicle powertrain modelling is needed to introduce the reader. The definitions used in the article by Gao et Al., 2007 are integrally presented:

1. System: The object or objects we wish to study[2].
2. Experiment: The act of obtaining information from a controllable and observable system by intelligently varying system inputs and observing system outputs.
3. Model: A surrogate for a real system upon which "experiments" can be conducted to gain insight about the real system. The types of experiments that can be validly applied to a given model are typically limited. Thus, different models are typically required for the same target system to conduct all of the experiments one wishes to conduct. Although there are various types of models (e.g., scale models used in wind tunnels), in this paper, we will mainly discuss about physics–based mathematical models.
4. In the following text, mathematical models are also described as "virtual" models; the same term is also used to describe tools, experiments and general activities.
5. Simulation: An experiment performed on a model.
6. Modelling: The act of creating a model that sufficiently represents a target system for the purpose of simulating that model with specific predetermined experiments.
7. Simulator: A computer program capable of performing a simulation. These programs often include functionality for the construction of models and can often be used in conjunction with advanced statistical engines to run trade studies, design of experiments, Monte Carlo routines, and other routines for robust design.

2.1. General aims, scopes and potentialities of modelling activities

The use of virtual simulation tools, at a first level, can act has a method to integrate or substitute physical experimentation. Virtual experimentation activities certainly offer the possibility to cut development time and cost in NDP: testing phase can be speeded up and the use of physical prototypes can often be reduced. As stated by some authors (Becker et al., 2005), this is only one of the advantages related to the extensive use of virtual simulation tools: the contribution of such tools can go well beyond the incremental improvement of the results obtained with physical experimentation, thus resulting in a general modification of design process and even in the organization of R/D centers. The cited analysis of Becker et al., 2005 will be extensively described in the following paragraphs.

2.1.1. The implications related to the extensive use of virtual simulation tools

The design phase, the whole NPD can be assimilated to a problem solving activity. Engineers can usually deal with such phase having as a support their "knowledge base" relying on two main sources:

- the known scientific background
- the experience in product and/or process applications.

---

[2] In case of Electric– Hybrid Vehicles powertrain, the object is mainly a mechanical/mechatronic system

The interaction of such competencies many times results in a cycle iteration (Figure 14), such as “theory building and testing”; both are needed for *advancing understanding*. Two different, but often complementary problem–solving strategies arise:

- Deduction: in this case, the knowledge is applied to specific case starting from general laws (e.g. physics), so that the problem can be solved producing “prediction” based on known boundary conditions.
- Induction: starting from examples, general concepts and laws can be formulated; e.g. empirical laws are an example of how to produce prediction on the evolution of a system even if the laws underlying there and the internal phenomena are (totally or in part) unknown.

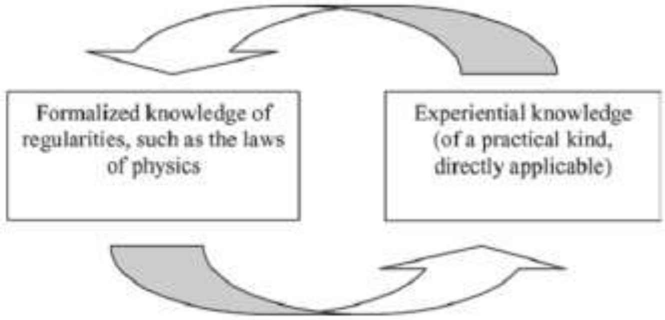
Formalized knowledge of regularities, such as the laws of physics
Experiential knowledge (of a practical kind, directly applicable)

Figure 14 – Problem solving loop (Becker et al, 2005).

The definition of the above strategies is useful to identify an important characteristic of virtual testing activities: a certain knowledge of the laws determining the phenomena is needed to build models and run them in simulation. As a consequence, pure *inductive* problem–solving through simulation is excluded; this simple evidence demonstrates that virtual simulation tools cannot be considered just an alternative to or an *upgrade* of physical simulation tools. Therefore substantial differences between the use of virtual and physical experiments arise and two of them should be highlighted:

- the fact that different prerequisites are needed, e.g. a different knowledge base, as stated above
- the new potential of simulations activities to enable non–conservative design due to multiple factors, including the possibility of various iterations of the same experiment.

The cited authors describe a significant impact of virtual simulation tools on R/D organization: the need for formalization of Procedures for Virtual Development (PVD), which are aimed to *effectively apply* virtual tools in product/process development and to maximize their benefits. The role PVD should be, amongst others:

- To enable collecting of all necessary data on how product/process as to be designed
    - Design norms
    - Former know–how
- To specify the whole flux of activities to be performed

  - Correct use the tools (how–to guides)
  - Simulation input–output analysis
  - Implementation in practice.

As a first consequence, in the described approach PVD can guide the whole design process, determining the interaction between components and the "incorporation" of all main data coming from company knowledge–base.

The build up of reliable virtual tools requires "calibration" through the comparison and the integration of data coming from physical experimentation; such phase can also include more than one iteration and is time–consuming.

Therefore, **as a second consequence**, PVD–based design process has an impact on the organization of the R/D team because of the need to coordinate different competencies and methodologies – namely formalized competencies, modelling and simulation capabilities, physical experimentation to get data for validation. It can be highlighted the opportunity to include people coming from different scientific and experiential background in the same team, thus unifying physical and virtual simulation in the same unit.

2.1.2. Increasing possibility of innovations: expectations

Describing problem solving activities two main steps can be usually identified:

- Starting from the problem, a preliminary set of possible solutions can be selected: such solutions constitute the *search space* for further activities. The selection is mainly based on the known methods, on any external/internal constraint, on current Best Available Techniques (BAT) and so on.
- An exploration is carried on within the space defined above; further selections are done through by testing, trial–and–error and any other suitable "sieve".

Since one of the major advantages of virtual testing tools is the possibility to speed up testing at – relative – low cost, an higher number of alternatives can be verified in a given time: this is an improvement on problem–solving activities, a primary effect of virtual testing.

At the same time, if PVD provide correct standardization of the procedures, a stable base–line can be defined: the importance of base–line result is that the effect of each parameter variation can be compared, enabling learning from experiment.

It is possible that a small amount of the results of such virtual experiments are somehow unexpected, *puzzling*: in such cases, a redefinition of the problem and of the search space can be proposed. The more the number of virtual test, the more the possibility to find unexpected results: as a consequence, such virtuous loop can enable a more frequent reformulation of the problem and the widening of the search space. In other words, a large number of virtual experiments also create opportunities for innovation: this is another effect of virtual testing application, a major improvement on problem–solving activities.

The creation of such opportunities has then to be finalized and guided, in order to get positive reflections acting from the virtual testing phase back to the search space. The role of efficient PVD in the organization is to make possible this process, that is *an organizational challenge* rather than a pure *technical issue*. Again, Becker et al., 2005, describe this approach in problem solving as a new strategy, *abduction* (cfr. Figure 15). The term describes the attitude to generate hypothesis on the basis of *background knowledge and implicit assumptions*, in order to give a possible explanation of *puzzling phenomena*.

Innovation possibilities are created since testing hypothesis can be formulated outside of the known premises.

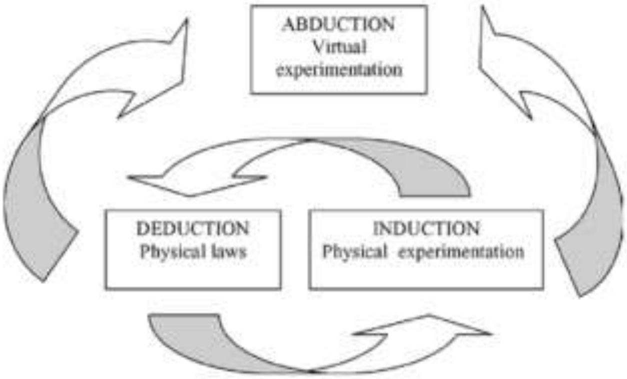

Figure 15 – Modified problem solving iteration, including abduction, induction and deduction (Becker et al., 2005).

The definition of abduction concept certainly goes beyond the scope of this document; however, the theory has been explained in order to highlight the important role of general modelling activities in the development phase. The goal of the research activity include the creation of a modelling framework for electric vehicle powertrain and the definition of the vehicle use context starting from users' needings: all this elements can be considered as part of a general PVD activity.

2.2. Integration of CAE tools on vehicle development process from preliminary design to late testing activities

The need for integration of different parts of a complex system (mechanical, electronic and software, that is the case of vehicle powertrain) is a strong driver to promote concurrent engineering of the system under study in early phase concept. It's a challenging issue for industry. Different experiences documented in literature will be explained in this paragraph, describing a path for integration of CAE tools in any product or process design phase.

According to the paper by Votintseva et al., 2011, mechatronic development process presents different critical issues, such as:

1. *In modern mechatronic systems, more and more functionalities are implemented in software, controlling mechanical and electrical components. This implies challenges in implementing different types of interfaces, semantics of communication, and concepts of hierarchical and modular development.*
2. *Integration aspects and complexity issues emerging through the interaction of the components in heterogeneous ways necessitate system simulation.*
3. *Non–functional aspects (like performance, safety, etc.) often refer to the whole system and are evaluated with specific tools (like timing analysis, fault–tree analysis, etc.) not integrated into other engineering tools.*

4. *One of the challenges in developing complex mechatronic systems is the heterogeneity of the backgrounds of developers working on different aspects. This also makes collaboration difficult.*

The review by Fotso et al.,2012 describes Model Based Design – MBD – and highlights the main advantages of such approach. It is described as the use of *graphical models to represent the system requirements and so identify issues early in the development process and reduce the time–to–market (TTM) of the system to develop*, but it differs from informal "functional modelling" approaches since it is formalized and supported with different modelling languages, so that the outputs are expected to be repeatable. A detailed examination of available tools and methods is presented. The article is very useful in introducing two kinds of tools that can be used for MBD:

- languages for mechatronic design: MBD often use graphical representations and interfaces to describe the system, so that a specific model language is needed (e.g. Modelica, Unified Modelling Language UML, System Modelling Language SysML)
- tool chains: language for modelling of complex system, such as Matlab/Simulink platform, their extension (for physical models) Simscape tool, CAMeL–View. LMS AMESim is not cited by the author, but it refers to this kind of tools.

Both languages and tools chains can be used for the general purpose of MBD application and model simulation, and it is important to note that the compatibility within these system is in most cases guaranteed both through direct import (e.g. Modelica implementation in LMS AMESim) or through common application interfaces (e.g. export/import of C compiled blocks).

A final advantage of *Model–Based Design is that such approach enables the reuse of existing design knowledge know in the Model–Based Design as "System reengineering". The problem in the functional modelling is that the archived design model can be used only for the same particular product model where in the Model–Based Design the archived design model can serve as basis to create, specify and explore product model*.

2.2.1. Integrated approach to development process: a case study

To describe the impact of modelling tools on system design let's consider again the development process (Votintseva et al., 2011). Main elements of the system are shown in Figure 16 and include:

- requirements data
- functional Architecture information
- logical Architecture information
- physical and software block
- product configurations containing instances of physical elements, software and product parameters

Each part interacts with other system parts. Cross phase activities establish relations between results from different phases and aspects:

- Test Cases & Environment, that can be performed at different levels of abstraction

- Allocation & Analysis for requirements tracing, function partition and any kind of analysis.

All this system, in the cited article, is modeled using SysML, a standardized general–purpose graphical modelling language.

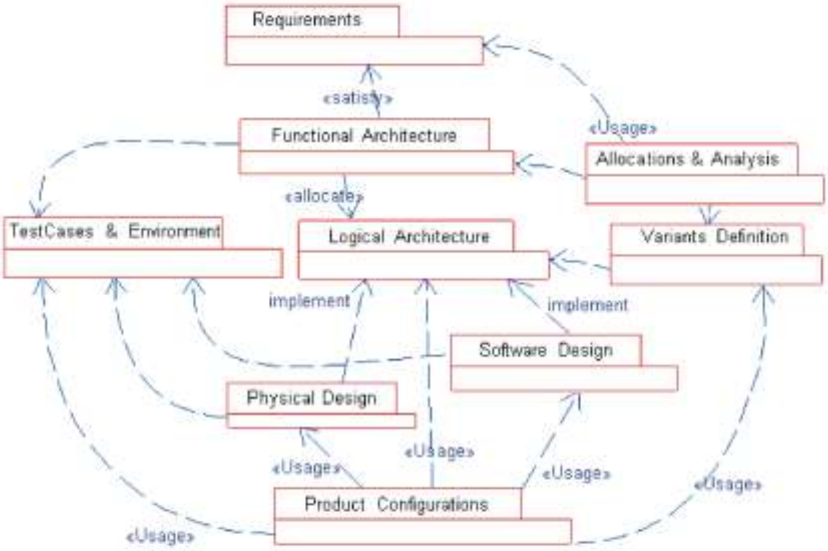
Requirements
«satisfy»
Functional Architecture
«Usage»
Allocations & Analysis
«allocate»
TestCases & Environment
Logical Architecture
Variants Definition
implement
implement
Software Design
Physical Design
«Usage»
«Usage»
«Usage»
«Usage»
Product Configurations
«Usage»

Figure 16 – Development process of complex system: structure and representation using SysML (Votintseva et al., 2011).

Therefore, in the presented case, a system representation becomes a CAE tool itself. After a generic model is prepared, each part of the system in fact is defined according to its nature. Simulation models are therefore associated to Physical Design and Test Cases & Environment, Production configurations block are defined as containers for mechanical and electrical properties and input signals, while in Software Design executable code are imported. This part represents a “transition from modelling to simulation”, so that large parts of the know–how needed for the process are imported in the SysML template.

The next step is to start up simulation: according to the methodology defined in precedent chapters, a low fidelity model can be used, focusing on the analysis of basic information and energy flow. During this phase, system simulations are tested and it is possible by the expert of each domain to verify if all relevant information are considered. An iteration is therefore established, and each component model is modified in order to include more details. Test Cases & Environment data are the source to define more and more system simulation, since new test inputs requirements arise.

In final design stage, hardware components testing becomes possible through HiL applications or, at least, generating test cases for other, offline test. In this case, SysML is used *as a central hub for keeping the various component and test revisions synchronized in the system simulation.*

A relevant advantage of the described approach is the possibility of “integration” on various levels:

- *"Input–output" exchange of data written by one component and used by another*
- *integration through a code, developed in one tool and invoked from another;*
- *Model transformation, providing automatic consistency of interfaces;*
- *Coordination between animation and simulation in different tools (additional settings for timing aspects).*

The buildup of an high–level manager for system development is however subjected to critical issues, most of them being related to the large number of variables to be considered:

- *Information distribution and collocation*: since a large number of information related to specific and different domain are included, in case of insufficient organization and separation most of such data should be unnecessary or, in other case, not transparent for component engineering team.
- *Multi–user, multi–domain and multi–level workflow*: since iteration is one of the basic principles for concurrent engineering design, there is an high risk of lack of capabilities of those models that have been built on early phases. The inconvenient can also imply the need to modify all the "surroundings" of the model or of the code that has been upgraded in order to implement the needing that were initially unknown.

2.2.2. **Lesson learnt**

In the former paragraph an option for mechatronic systems development workflow has been shown. The case study is particularly interesting since it highlights the role of a "central hub", a common language/platform to be used as reference knowledge base between different model/hardware of components. Other kind of data, such as testing methods, can be stored in the system, communicating with the other parts of the system. In case of a new MBD procedure development, the lessons learnt are that:

- interoperability between models has to be maintained at every modelling stage. For this reason, a common language should be used, meaning that both following alternatives are suitable:
    - a single software or programming language is used (Modelica, in the case study)
    - each model has to be able to communicate with other models through a common interface protocol, not depending on its source platform. A central "hub", however, is necessary (e.g. the solver platform)
- the system has to be easy upgradeable, that is hard to guarantee in case of iterative changes in a large design team
    - the solution should be to build using multiple interfaces or adopting interpreter for semi–automatic combination of models supporting the chosen set of interface detail.

Another requisite that has not been explicitly declared in the case study is that the detail of the model should be coherent with the time–scale for which the other submodels and test input have been designed. This guarantee that a single solver can obtain efficient and precise solution of the system; in alternative, different solvers should be used and interfaced through appropriate time–scaling methods (e.g. virtual sample–and–hold interfaces). An example of how this can be done is described on next paragraph.

2.2.3. Scalable model for time–scale fitting

Supercapacitors are electric components that can be suitable for EV, HEV of Fuel Cell Vehicles (FCV) for “power buffering”. Equivalent models of such components can be built on the basis of circuit schemes using basic electronic elements (capacitors and resistors networks) in order to represent the results obtained through advanced models or through impedance spectroscopic measurement (see Figure 18). The number of elements (a so called “ladder” of resistor–capacitor elements according to the work by Dougal et al., 2004) that are used determines the fidelity of the model and its capability to reproduce the impedance of the real component; a five order model is suitable for typical working frequency of switching power devices (e.g. 10kHz – 100μs timescale). Similar models and considerations apply also to electrochemical devices such as lithium cells (Einhorn et al., 2011).

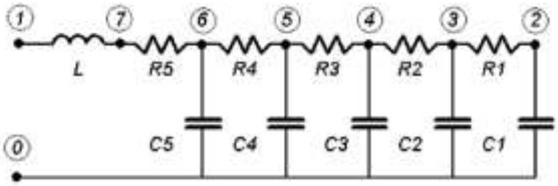

Figure 17 – Equivalent circuit of ultracapacitors (source :Dougal et al., 2004).

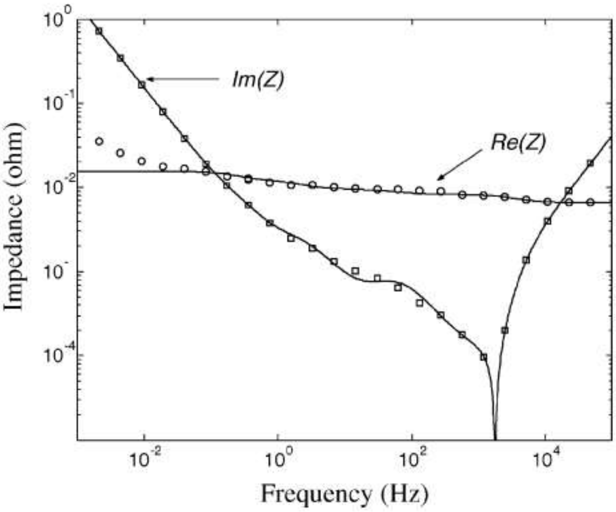

Figure 18 – Comparison of the model predictions of impedance with the measurements. The simulation results are indicated by lines and the measurements are by squares and circles (source: Dougal et al., 2004).

In every model, the integration time–step of the solver has to be calibrated on the minimum time constant arising from the model (Dougal et al., 2004); a suggestion is:

$$T_{ref} = \frac{1}{5} T_{smallest}$$

If such condition is not satisfied, numerical oscillation arise due to inappropriate time step choice. In case of ultracapacitor models, it is possible to reduce the order of the model in order to modify its time constant; if the model does not include any other component having similar time constant, in fact, simulation can run faster while the accuracy remain appropriate for the context of the whole model. Model order reduction (through the method proposed by Dougal et al., 2004) is shown in Figure 20; the effect of model order reduction on time constant and suitable time step are shown in Table 3.

According to the work by Wu et Dougal, 2005, model order variation is applied during simulation (so that a switch is possible in the same running experiment) using a criterion based on model output derivative as trigger to modify simulation time step and model order. The case study is therefore an example of advanced model control to guarantee accuracy as well as appropriate computational efforts, in a way that is "transparent" for the user.

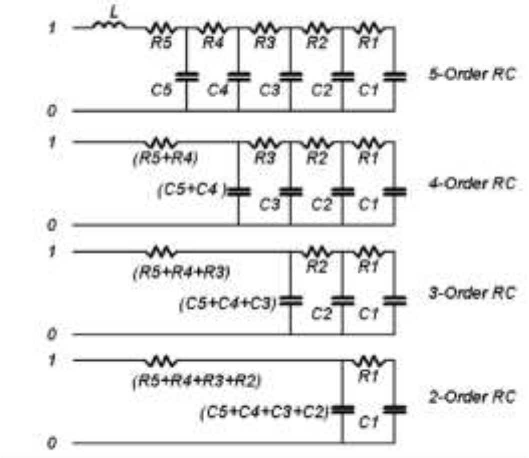

Figure 19 – Supercapacitor equivalent circuit of the multi–stage ladder model: various alternatives (source: Wu and Dougal, 2005).

Order network	**Time constant (s)**	**Recommended minimum simulation step (s)**
Five–order RC+L	9.8187E–6	1.964E–6
Four–order RC	0.002596	5.192E–4
Three–order RC	0.0688768	0.01378
Two–order RC	0.729579	0.145916

Table 3 – Time constant for supercapacitor model depending on network order and recommended time steps (source: Wu and Dougal, 2005).

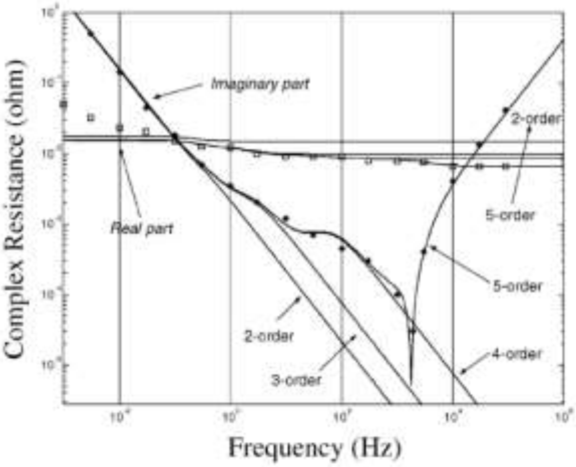

Figure 20 –Supercapacitor model alternatives depending on desired order; right: different model simulation results (lines) and comparison with measurements data (squares, stars). Source: Wu and Dougal, 2005.

2.2.4. Integration of CAE tools in engineering process

The examination of literature, of consolidated know–how and of selected case studies suggest that in order to maximally exploit the potential of model engineering it is needed to use a software language that can guarantee:

- the storage of different kind of data
- the dialogue between different models
- the dialogue between different environments.

To reach these goals, it is necessary to overcome the obstacle related to the different tools and the different signals that can be necessary at each design stage; some critical aspect are:

- the data exchange/storing protocol that is initially defined
    - over–dimensioning can be useful to let dataset expansion if needed (later engineering steps could require more detailed information than expected in early design stage)
    - data exchange/conversion interfaces should be prepared
- the difficulty related to the access of a large number of people to the data.

Finally, the choice of solver characteristics and of main time step has to be carefully evaluated, since inappropriate calculation efforts should hinder the use of models that are formally correct; to avoid such risk, models should be easily scalable, while the possibility to establish a dialogue between solver and model subsystem is an option to increase the rate of “automation” in submodels assembly.

2.3. Alignment strategies between different modelling tools

During the simulation of a complex mechatronic system it can be necessary to use submodels coming from different sources. The causes are both practical reasons and technical reasons.

Practical reasons can include a multitude of factors. It is possible that a model has been prepared using a specific software which cannot be shared within all the working group partners due to cost reasons, so that it is needed to export it to another simulation environment. Also, due the need for confidentiality on the detail of a determined model, a partner can choose not to communicate its full know–how on model definition (including typical parameters, equations and so on) but to share a compiled, not modifiable code, thus sharing only a particular routine or a setting of its model. Some authors (Siemers et al., 2009) highlight also the importance of re–using existing simulation models in different contexts in order to preserve the investment on them.

Technical reasons are related to the fact the different software can be best suited to model a determined model component, so that a co–simulation arrangement is needed: the typical case is the use of Matlab/Simulink for system control (e.g. because in this one advanced tools are available, such as subroutines for PID control tuning or for decision logic modelling – StateFlow) and other physical models (e.g. LMS AMEsim) for specific domain simulation. It is also possible that a model has been prepared using a very specific tool (e.g. FEM models for magnetic characterization of an electric machine, or multibody models for vehicle assembly), so that it has to be reduced or interfaced with more general simulation environment. In general, the need for co–simulation tools is related to the need of investigating several parts of a system simultaneously, not depending on the specific tools used for the most appropriate model creation. It has to be noted that also within the Matlab–Simulink environment, the physical components (e.g. Simscape Library elements) are included in Simulink generic layout, but their management is different from pure numeric blocks. A specific solver (also represented by a block) has to be used within the model and, in addiction, interface blocks have to be used to “convert” physical signals to numeric signals, so that the system usually looks like a co–simulation arrangement. One of the reason is related to the fact that Simscape uses “bidirectional” lines and “acausal” equation definition for the physical blocks, while Simulink lines are “unidirectional” and equations are explicity defined.

Physical models for submodels and systems can be prepared using Modelica language; component libraries (e.g. for mechanical, thermal, electrical domain) are available both as open source and commercial (e.g. Dymola–Smart electric vehicles) packages. Modelica–based subsystem can be solved using different compilers and solvers (e.c. freeware Coselica – within Scilab package – or Openmodelica, commercial Dymola) and can also be integrated in different simulation environment (e.g. LMS Amesim, or Matlab/Simulink if appropriate S–function based on C language can be exported from Modelica editor environment).

2.3.1. The design and the use of co–simulation tools

In this paragraph, a few literature examples about the constraints and the criteria to be considered during the design and the implementation of a co–simulation framework will be described. The descriptions and the methodology proposed are very general and can therefore be adapted to specific model issues.

The work by Nicolescu et al. (2007) describes the concept and the preliminary implementation of a methodology for efficient design of co–simulation tools including both continuous and discrete events models, that is a challenging issue in co–simulation tools. It is therefore worth to analyze the main elements of such reference work. The integration of continuous and discrete components in various engineering fields (defense, medical, communication, automotive) is increasingly needed for global validation of system models, enabling *joint simulation of existing heterogeneous components with different execution models*. The following definitions coming from the cited reference are useful to understand the problem:

- *in discrete–events models, time represents a global notion for the overall system and advances discretely when passing by time stamps of events*
- *in continuous models, the time is a global variable involved in data computation and it advances by integration steps that may be variable*
- *in discrete–events models, processes are sensitive to events*
- *in continuous models processes are executed at each integration step.*

The global validation of continuous/discrete systems requires simulation interfaces providing synchronization models for the accommodation of the heterogeneous aspects cited before. Validation tools able to generate automatically simulation interfaces for the global simulation of continuous/discrete systems are mandatory. According to the author, a generic system as represented in Figure 21 usually includes three main type of basic elements:

1) execution models representing the components of the heterogeneous system
    a) discrete
    b) continuous
2) simulation bus, its role being the interpretation of the interconnections between different components of the system
3) simulation interfaces, their role being:
    a) managing communication of components through the bus
    b) adapting continuous and discrete execution models
    c) adapting different simulators in the simulation bus.

The expression "simulation instance" is used to describe the implementation and simulation of an execution model in a given context. A co–simulation tool is therefore defined as an *instrument for the creation of simulation instances.* The simulation environment in which the co–simulation takes place has to *receive as input* an heterogeneous specification and to *generate automatically the simulation bus and the simulation interfaces required for the global execution of the system*.

Following this description, during the concept definition of a simulation environment it is necessary to define an *execution model* (simulation bus and interfaces architecture) and a *methodology* for the automatic generation of simulation instances; an example of a "flow" for automatic generation in execution models is shown in Figure 22.

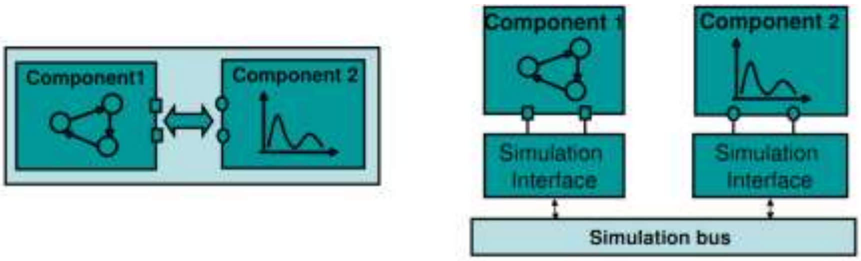
Component1
Component 2
Component 1
Component 2
Simulation Interface
Simulation Interface
Simulation bus

a) Heterogeneous system

b) Global execution model

Figure 21 – Heterogeneous discrete/continuous systems (on the left) and corresponding global execution model (on the right).

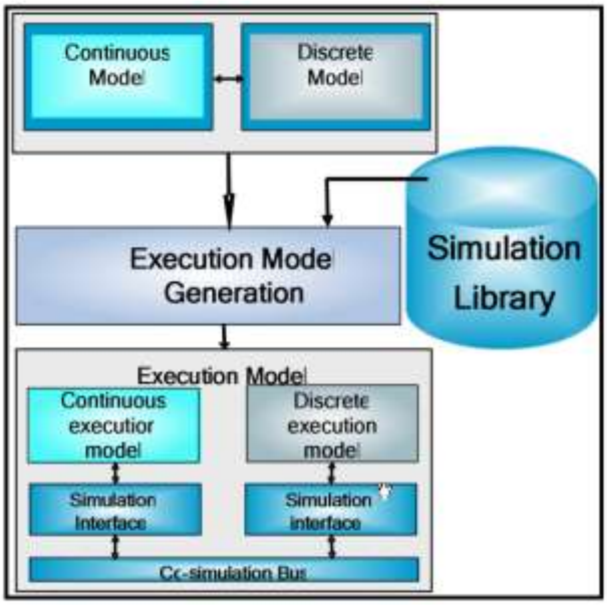
Continuous Model
Discrete Model
Execution Mode Generation
Simulation Library
Execution Model
Continuous execution model
Discrete execution model
Simulation Interface
Simulation interface
Co-simulation Bus

Figure 22 – A flow for automatic generation of execution models (from Nicolescu et al., 2007). Continuous and Discrete model blocks are prepared through tools such as Simulink, Modelica, SystemC, while the “simulation library” block stores the elements defining simulation bus and simulation interfaces; both kind of elements are used for the automatic generation of execution models.

The execution models should also comply with a few important specifications in order to *facilitate their automatic generation and to provide efficient global validation*, main being*:*

- flexibility, so that any modification on external environment (e.g. constraints), utilization mode (e.g. communication protocols) and technology variation (e.g. replacement of an internal simulator) can be tolerated
- modularity and scalability through independent handling of the different components in the system (e.g. including different solutions representing a given system, to add new components and functionalities, to validate the systems)

- accuracy
    - time validation (performances, respect of timing constraints)
    - functional validation (in terms of functionality, e.g. data transfers without taking into account the time for the transfer).

After the definition of the general architecture of a co–simulation environment, the cited authors also propose a methodology that can be used to design a continuous/discrete co–simulation tool. The definition is general so that it can apply to a conceptual framework, not depending on specific simulation tools. Six main steps are described.

Step one: operation semantics for synchronization in continuous–discrete global execution model

It is *a mathematical definition of communication/synchronization relation between continuous and the discrete simulators*, each one working on its domain. Considering the synchronization between continuous and discrete, it means that each simulator used has to accept the events coming from the external (*detection*) reaching accurately the time stamps of these events. These so called *time stamps* are synchronization and communication points such as clock events, time notified events, or events generated by "wait" functions; the continuous solver has to adjust the integration steps in order to detect time stamps events. Since continuous solvers can also generate state events at unpredictable time (e.g. zero crossing events, threshold overtaking events), it is necessary for the discrete solver to advance differently from its "normal" simulation step in order to fit the time step of the state events. Figure 23 shows how the steps can be adjusted, in both ways, in order to take into account external events.

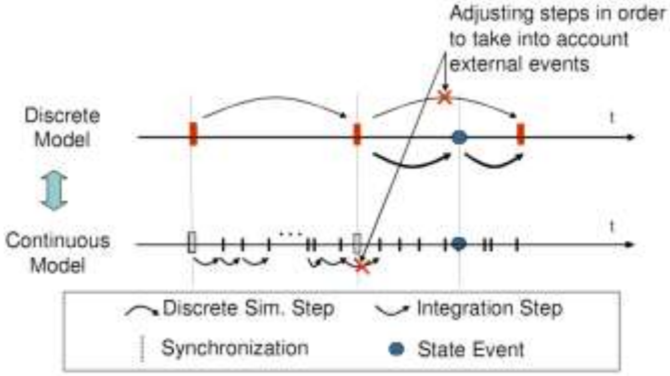

Figure 23 – Synchronization strategy between continuous and discrete models over the time axis (From Nicolescu et al., 2007).

Step two: distributing synchronization functionality to simulation interfaces

After that a synchronization strategy has been defined, its functionalities have to be distributed to each simulation interface. The processes occurring in the two simulation interfaces include:

- the data exchange (send–receive) between simulators in the simulation bus
- the time stamps of the next events

- the state events indication (from continuous to discrete) and consideration (within discrete)
- the context switch

The detailed flowcharts of main functionalities are shown in Figure 24 and Figure 25.

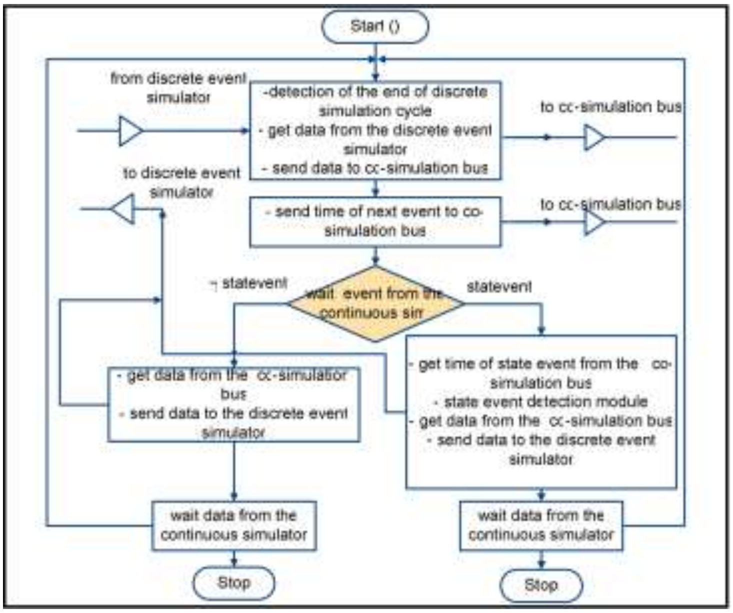
Start ()
from discrete event simulator
-detection of the end of discrete simulation cycle
- get data from the discrete event simulator
- send data to cc-simulation bus
to cc-simulation bus
to discrete event simulator
- send time of next event to co-simulation bus
to cc-simulation bus
¬ statevent
wait event from the continuous sim
statevent
- get data from the cc-simulator bus
- send data to the discrete event simulator
- get time of state event from the co-simulation bus
- state event detection module
- get data from the cc-simulation bus
- send data to the discrete event simulator
wait data from the continuous simulator
wait data from the continuous simulator
Stop
Stop

Figure 24 – Flowchart for the discrete domain interface (From Nicolescu et al., 2007).

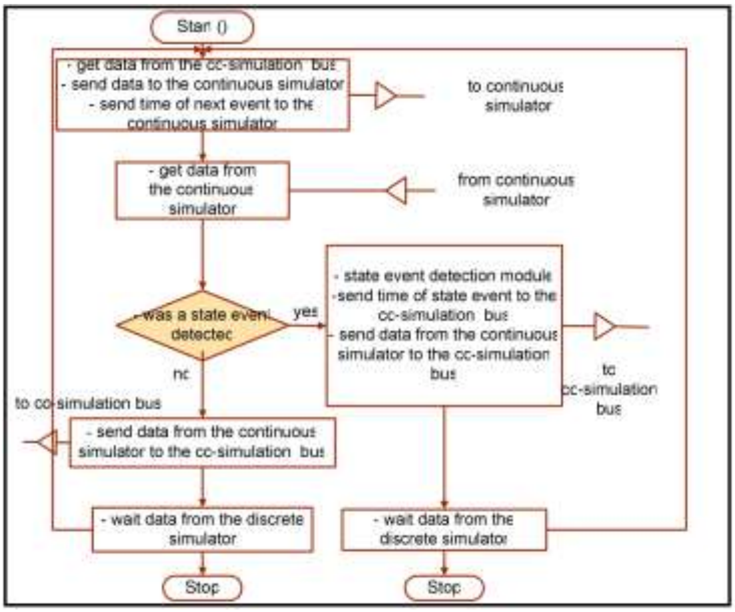
Start ()
- get data from the cc-simulation bus
- send data to the continuous simulator
- send time of next event to the continuous simulator
to continuous simulator
- get data from the continuous simulator
from continuous simulator
was a state event detected
yes
no
- state event detection module
-send time of state event to the cc-simulation bus
- send data from the continuous simulator to the cc-simulation bus
to cc-simulation bus
to co-simulation bus
- send data from the continuous simulator to the cc-simulation bus
- wait data from the discrete simulator
- wait data from the discrete simulator
Stop
Stop

Figure 25 – Flowchart for the continuos domain interface (From Nicolescu et al., 2007).

Step three: formalization and verification of simulation interfaces behavior

The verification of simulation interfaces behavior is needed to guarantee the respect of temporal logics and the expression of the changes in the state of the system when this one is evolving. The temporal logic that has to be used can include:

- *proposition that describe the states (e.g. elementary formulae)*
- *temporal operators that allow the expression of the state succession (called executions).*

The reference authors cite possible choice logics such as Linear Temporal Logic (LTL), Computation Tree Logic (CTL) and their extensions (Timed CTL – TCTL – and Metric Interval Temporal Logic – MITL). The descriptions of such formalism is a quite specialist topic and will not be part of this document.

The formalism has therefore to be validated through the verification of a broad range of properties characterizing the system. Key properties to be verified for continuous/discrete simulation interfaces are the *deadlock, the correct answer to a change in the behavior of one of the simulatos* and *the synchronization between the two interfaces (correctness in event detection).*

Step four: defining the library elements of the internal architecture of simulation interfaces for the co–simulation framework library

After former steps, a final architecture for the co–simulation framework has to be defined. Figure 26 shows a hierarchical representation of the global simulation approach described up to now.

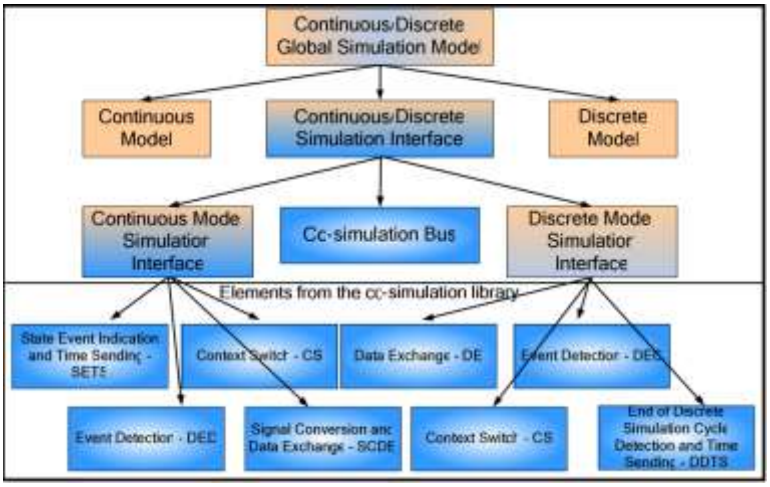
Continuous/Discrete Global Simulation Model
Continuous Model
Continuous/Discrete Simulation Interface
Discrete Model
Continuous Mode Simulatior Interface
Co-simulation Bus
Discrete Mode Simulatior Interface
Elements from the co-simulation library
State Event Indication and Time Sending - SETS
Context Switch - CS
Data Exchange - DE
Event Detection - DED
Event Detection - DED
Signal Conversion and Data Exchange - SCDE
Context Switch - CS
End of Discrete Simulation Cycle Detection and Time Sending - DDTS

Figure 26 – The representation of a generic co–simulation model, including the detail of the elements to be included in a co–simulation library (from Nicolescu et al., 2007).

- top level includes continues and discrete models and their simulation interfaces enabling global simulation;
- second level includes co–simulation bus, transferring data between different domain simulation interfaces

- third level includes the modules of each different domain specific simulation interfaces, thus representing the low–level functionalities defined in former steps such as synchronization, data exchange, model switch.

Step five: Simulation tool analysis for their integration in co–simulation framework

Former four step described the gradual formal definition of the simulation interfaces and the required library elements, which are independent on the different simulation tools and specification languages used. The next step is the integration and the analysis of the functionalities that have been defined; the integration of discrete and continuous simulation steps require different controls that have to be implemented in APIs (Application Programming Interface – see table Table 4 for details).

Controls needed to integrate continuous simulators in the co–simulation tool	**Controls needed to integrate discrete simulators in the co–simulation tool**
• Detection of state events • setting break points during differential equation solving • on–line update of the breakpoints settings • sending processing results and information for the synchronization (i.e. the time step of the state event) to the discrete simulator. This implies generally the possibility to integrate C–code and Inter–Process Communications (IPC).	• Detection of the end of the simulation cycle • insertion of new events (state events) in the scheduler’s queue. This must be done before the advancement of the simulator time • sending processing results and information for the synchronization to the continuous simulator (i.e. the time stap of its next discrete event)

Table 4 – Overview of the controls needed for integration of single simulators in a co–simulation tools; such functionalities have to be provided through appropriate APIs (adapted from Nicolescu et al., 2007).

The cited authors state that Simulink usually includes such kind of controls for continuous models (e.g. zero crossing detection in the simulator) and that other required functionalities can be added in generic library block, so that the environment supports the implementation of additional tools. For discrete models, SystemC is an illustrative example of an environment supporting the addition of the needed additional functionalities, but the implementation of a *simulation interface is more difficult in comparison with Simulink since the specifications in SystemC are textual and a code generator is required to facilitate the addition of simulation interfaces*.

Step six: Implementing library elements specific to different simulation tools

The reference article also provide a few examples of implementation of the logic and of the architecture of co–simulation systems within Simulink (for continuous) and SystemC (for discrete).

In the Simulink case a triggered subsystem (containing an S–function) is used in order to synchronize the execution of the Simulink model together with the other discrete solver, since this kind of subsystems let Simulink *adjust the integration steps to satisfy the criteria of resolution and to detect accurately the execution time of triggered signal.*

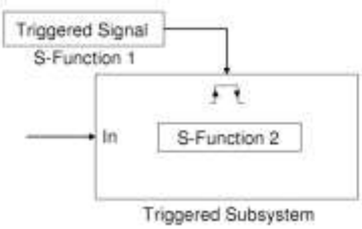

Figure 27 – Detection events from the discrete simulation model within Matlab/Simulink using a “triggered subsystem” submodel.

In the SystemC case, the “scheduler” of the software is modified through the creation of a set of events which can be notified by the scheduler in the case of state events presence. An example of a script which is sensitive to an externally generated event is presented in Table 5; the module is therefore called “Event Detection – DEC”.

```
#define et_matO
    sc_get_curr_sirricontext () –>et_mat [0]
/* this definition is in the file defining environment variables added for heterogeneous simulation */
My_module.h
/* ex. of module header file */
SC_CTOR(My_Module)
    {  //creation of et_matO event
    et_matO = new sc_event;
            //make My_Method sensitive to et_matO, //as consequence of state event
    SC_METHOD(My_Method);
            sensitive(et_matO); ... }
```

Table 5 – a SystemC code for the implementation of the sensitivity at state events (et_mat0). Source: Nicolescu et al., 2007.

Another needed functionality that has to be added in discrete model is the detection of the end of discrete cycle simulation, so that the discrete solver is sending data and simulation control to continuous solver *only after the stabilization of the discrete signal*. The module “End of Discrete Simulation Cycle Detection and Time Sending” (DDTS) integrates “wait” and “notify” functions.

The final example presented includes C++ programmed interfaces that are integrated in Simulink as S–Functions, so that they can be manipulated as well as any other Simulink library component, their input–output port being compatible with other model ports. SystemC interfaces are generated through a script generator and integrated in the main function “sc_main”. Figure 28 shows a generic Simulink model implementation (including library and co–simulation blocks), while main interfaces functionalities are described in Table 6.

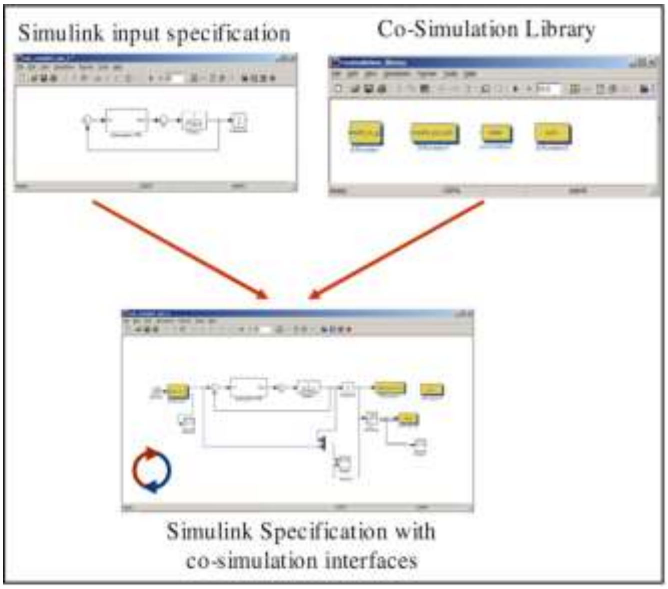

Figure 28 – Simulink model including co–simulation interfaces (from Nicolescu et al., 2007).

Interface	Domain	Function
Sim_inter_In	Simulink	provides the input communication function and synchronization with signals update events.
Sim_inter_Out	Simulink	implements the output communication function and provides synchronization with the sampling events sent by SystemC.
State	Simulink	implements synchronization functions used to send the state events once detected and to synchronize with SystemC. For the detection we use the Hit Crossing component from Simulink library.
Sync	Simulink	implements the synchronization function that creates break points which must be reached accurately by a solver (a variable step solver).
SC_inter_In	SystemC (sc_main)	implements the input communication function and ensures synchronization with input data and state events
SC_inter_Out	SystemC (sc_main)	implements the output communication function and provides synchronization with the sampling events sent by SystemC

Table 6 – Main interface functions provided for the example implementation of a Simulink/SystemC co–simulation tool (adapted from Nicolescu et al., 2007).

The work by Nicolescu et al., 2007, describes the problem of co–simulation tools definition starting from a very general point of view; furthermore, it focuses step–by–step on its design and implementation. The indications are valid in general for the set–up of any cosimulation application.

2.3.2.**Meta–modelling approach**

The approach presented by Siemers et al. (2009) is in large part comparable to the one already described.

In particular, the article focuses on the need for co–simulation tool in mechanical systems modelling, using vehicles as reference example. Different classes of models can and corresponding tools can be used, each optimized for a certain kind of analysis. Therefore, every tool can be seen as a black box handling a particular external model (e.g. a Modelica model, an MSC.ADAMS multibody model, a Simulink control system etc.), but since many of them are physically interdependent, it is needed to include them in an integrated one. This step is performed using meta–models, which is an entity defining the physical interconnections of various external models. In the example shown in Figure 29, the meta–model defines *the semantics of each external model and their interconnections within the structure.*

In general, the main information provided by meta–models include (adapted from Siemers et al., 2009):

- *A language representation with strict notation and grammar. This is used to represent and store the meta–model and to share meta–model information between different tools and people*
- *hierarchical modelling, where larger systems can be modelled using various sub–models. Sub–models are intermediate level nodes in the meta–model and define different hierarchical sub–levels, each of which might contain external models,connections between the external models, and other sub–models.*
- *model abstraction, where each external model is represented individually in a uniform and simulation tool independentway.*
- *a generic and uniform way to connect various simulation tools.*
- *platform independent models. No operating system, network, or other co–simulation platform dependent parameters are stored in the meta–model.*
- *graphical language elements for visual representations of the external models.*
- *entralised co–simulation control. A single meta–model simulator application can start the simulation tools and control the co–simulation based on the meta–model.*

Three main steps for the definition of a meta modelling process have also been defined:

- *External model design* in a specialised environment. Each external model in the co–simulation is modelled separately in its specific environment
- *Model integration* into the meta–modelling environment. First of all the external interfaces are defined in the externalmod els. Subsequently, all external models need to be encapsulated for integration into the meta–model. Startup methods,interface names, and possibly geometry data must be specified
- *Meta–model design* in a meta–model editor. The different external models are integrated into the meta–model and connect with each other. Global simulation parameters also need to be defined.

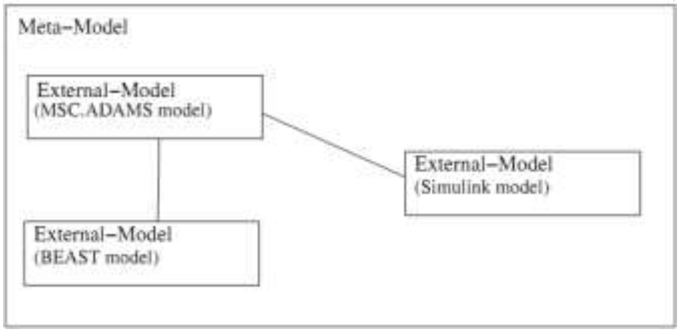
Meta–Model
External–Model
(MSC.ADAMS model)
External–Model
(Simulink model)
External–Model
(BEAST model)

Figure 29 – Meta model defining external models and their interconnections (from Siemers et al., 2009).

Again, these steps are coherent with the first steps already described in Nicolescu's approach. A meta–model example is shown in Figure 30.

Other requirements for a generic meta–model definitions are (from Fritzson et al., 2005):

- Meta–Models should be based on a standard language.
- A graphical model editor should be available for ease of use.

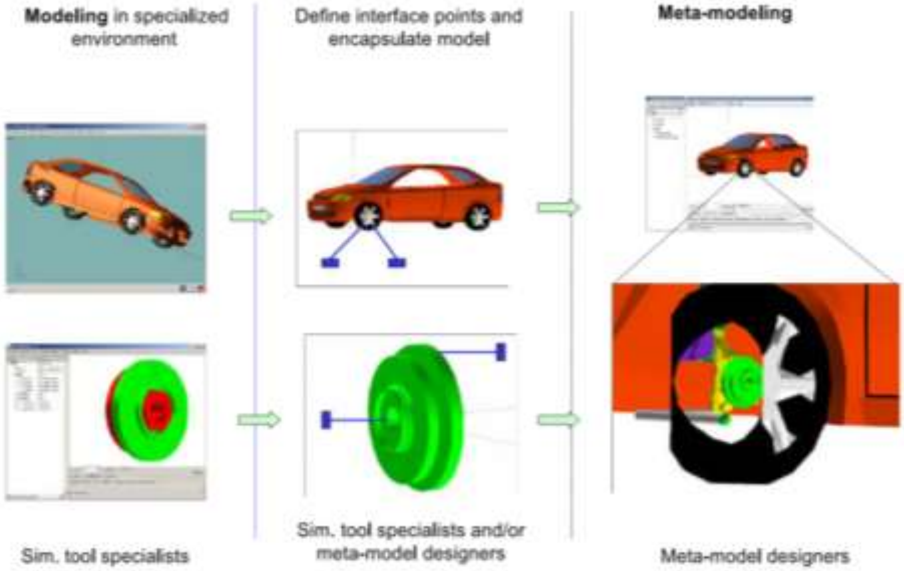
Modeling in specialized environment
Define interface points and encapsulate model
Meta-modeling
Sim. tool specialists
Sim. tool specialists and/or meta-model designers
Meta-model designers

Figure 30 – From external models definition (vehicle body in MSC.ADAMS, hub unit and bearings in BEAST) to the definition of their relation (interfaces points for mounting) and to final meta model, also including global simulation parameters (e.g. simulation start and end). Source: Siemers et al., 2009.

The presented example uses mechanical systems as reference; therefore the simulation framework is mainly a sub–case of the general framework presented by Nicolescu et al. A co–simulation framework in this domain thus requires:

- an external interface (for mechanical system it is a point on a mechanical object where position and velocity are calculated and reaction load are applied)
- a simulation manager, that is the central simulation engine starting each external model simulation and providing communication bridging between the running simulations
- an interface plug–in, that is exchanging data (signals, loads) with any external model; it is also in charge of handling coordinate system transformations between global and specific model inertial system
- an external model simulator, that is any simulation program incorporated as part of the model
    - an external interface for the control of simulation tools (e.g. simulation start, batch simulation mode, shutdown signals, position/orientation/speed/load data handling) programmed according to specific tool architecture also has to be provided, thus creating a "tool specific wrapper".

A deepening on the method used to enable interaction between dynamic models is presented. The method is called Transmission Line Modelling (TLM) and *uses physically motivated time delays to separate the components in time and enable efficient co–simulation*. TLM method gives numerical stability since through that it is possible to define a time delay that can be used to separate the simulation into several parts (each one solved with its own program) without introducing numerical errors. TLM is based on the definition of a "dimensional transmission line" (e.g., a one–dimensional elastic medium) in which any physical interaction has a finite propagation speed. A "parasitic element" (e.g. mass) is introduced, and the two simulation systems can be seen as decoupled by an appropriate time delay T_{TLM}; such delay can be used for efficient communication during co–simulation. For any other clarification on TLM method, please refer to specific reference works (John and O'Brien, 1980; Fritzson et al., 2007).

An example of common simulators to be used for co–simulation of mechanical system is presented in Table 7 while the layout of a simulation manager is shown in Figure 31.

Simulator	**Implementation**	**Interface**
BEAST (SKF in–house)	C++ implementation	TLM enabled control points (coordinate systems)
MSC.ADAMS	C wrapper DLL (dynamic link library)	General force with sub–routine call
Matlab–Simulink	C wrapper	S–function interface
Modelica	C or Fortran wrapper	External function interface
Simpack	Fortran wrapper	SIMPACK User routine

Table 7 – Simulators considered for TLM co–simulation and proposal for possible implementation and interface plug in (source: Siemers et al., 2009).

The characteristics of the presented co–simulation environment are:

- generality: many simulation tool can be integrated
- the implementation of a method for co–simulation based on meta–model definition
- the implementation of a method for external model execution using commands to execute external simulation tools involved

- the possibility of communication between different external models
- functionalities for data monitoring (analysis, post processing)
- implementation of controlled simulation termination for all external models (reduces errors possibility due to external problems or network failures).

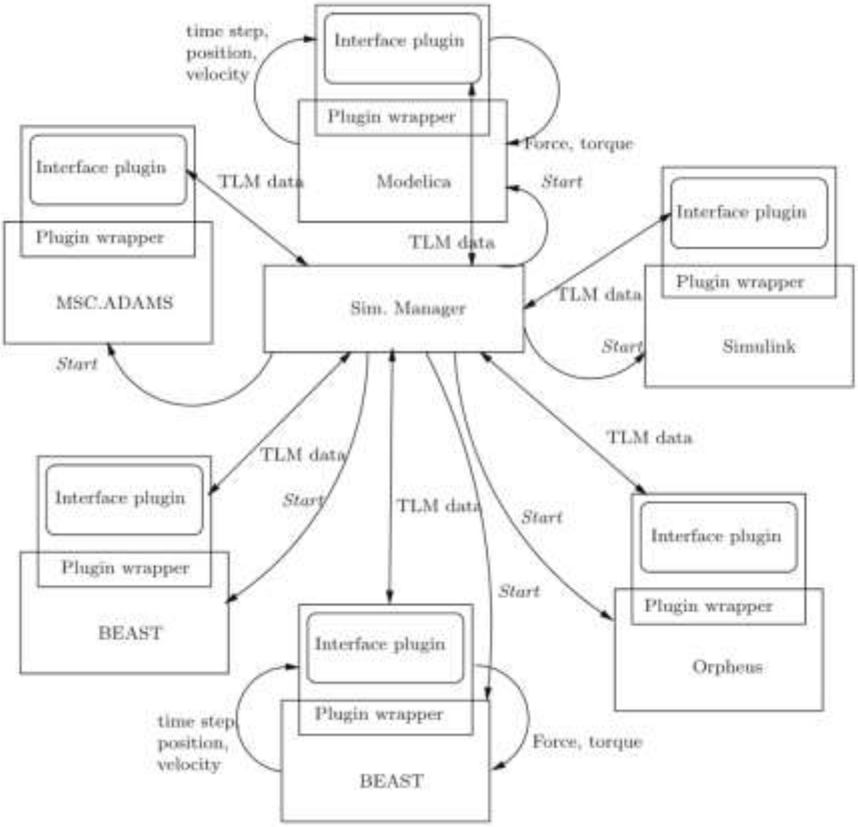
time step,
position,
velocity
Interface plugin
Plugin wrapper
Modelica
Force, torque
Start
TLM data
Interface plugin
Plugin wrapper
MSC.ADAMS
TLM data
Sim. Manager
Start
Interface plugin
Plugin wrapper
Simulink
TLM data
Start
TLM data
Start
TLM data
Start
Start
TLM data
Interface plugin
Plugin wrapper
BEAST
Interface plugin
Plugin wrapper
Orpheus
Interface plugin
Plugin wrapper
BEAST
time step,
position,
velocity
Force, torque

Figure 31 – Simulation manager environment for external simulator tools (source: Siemers et al., 2009).

2.3.3.**The design and the use of co–simulation tools**

The last point of the former paragraph is particularly relevant and it has also been object of specific research, as documented in literature. The work by Quaglia et al., 2012, is analyzing the problems related to feedback control systems in which the control loop is closed through a shared digital communication network rather than an ideal point–to–point connection. Co–simulation environment, therefore, are also an example of Networked Control System (NCS) and therefore are affected by two problems:

- communication delay
- packet loss.

This issues are, of course, of main interested also for Hardware in The Loop systems, for embedded and distributed system and for any other NCS in mechatronic and automotive applications (see Figure 32).

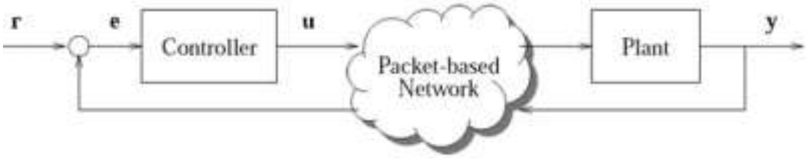

Figure 32 – Networked Control System block layout (source: Quaglia et al., 2012).

This reference work is therefore defining an integrated simulation environment including Matlab/Simulink and SystemC elements, the first one using a time–driven simulator and the second one using event–driven simulators, as already described. The generic co–simulation tool under examination is shown in Figure 33. The topic of the research is the proposal of synchronization modules between the elements involved, a very challenging topic which requires the definition of a co–simulation strategy and its validation.

According to Figure 34, the approach provides the definition of new entities both on Matlab and SystemC side. The modules are communicating using ports, each one having its unique identifier and a storage size to record data.

The new entity on Matlab/Simulink side is a “bridge”, called Matlab Wrapper, able to connect with scalar or vector input/output ports, each one having a given update frequency. The highest of these frequency is used for the execution of the block and for the calling of “packer” routines, that builds a message to be sent to SystemC side including time stamp and identification number of the port. A similar “unpacker” is also writing to Matlab the data coming from SystemC.

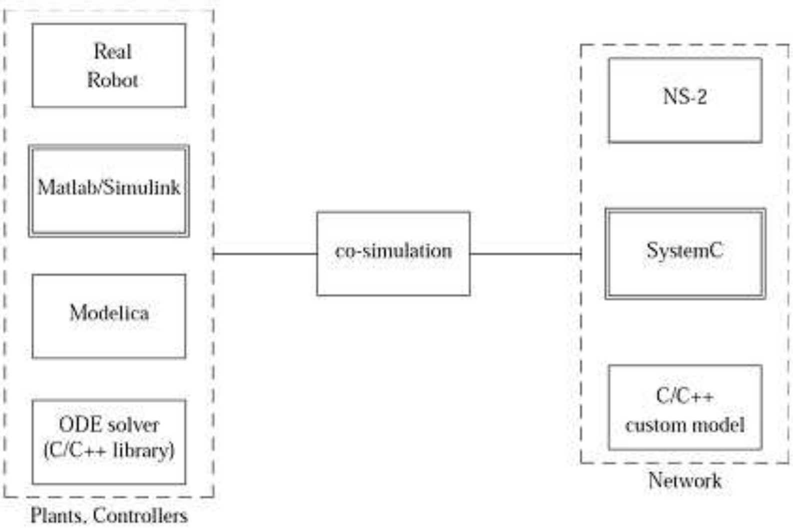

Figure 33 – Co–simulation environment and available tools for each domain (plant and physical components, controllers, network).

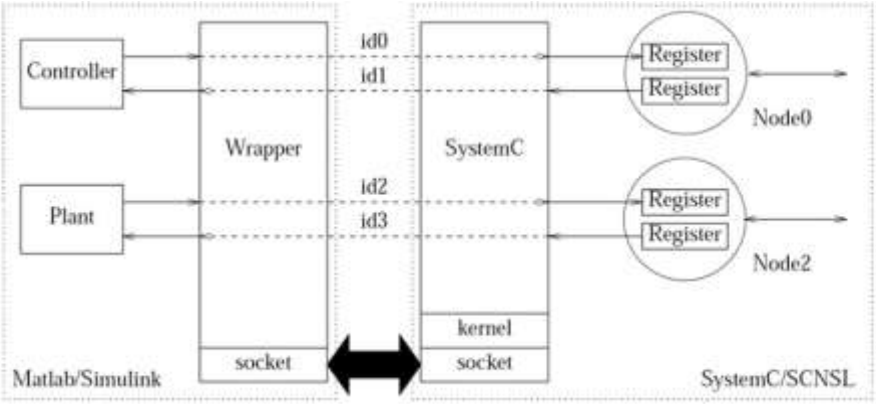

Figure 34 – New entities in Matlab and SystemC environment and their relationships (from Quaglia et al., 2012).

The new entity on SystemC side is a library able to exchange data packages with Matlab. In particular, whenever the SystemC kernel receives a message from Matlab, an event is generated for the destination port with the timestamp specified on the message, thus “waking up” the function related to that event. Data coming from SystemC are then processed and sent to Matlab.

Finally, the synchronization of the tools is the critical element of the networked communication system. The simplest approach is the “exact” timing one: *each simulator executes until a cosimulation event is to be scheduled; at this point it blocks itself and notifies its simulation time to the other simulator which is blocked on another cosimulation event; an hand–shake is performed in which the simulation times are compared and the simulator with the lower one is re–started.* Although this method guarantees alignment of simulation times, its disadvantage is that only one tool is running at each time.

More complex algorithm are needed in order to enable concurrent execution, thus improving calculation time and reducing the risks related to network delays of queues formation. Three main approach are compared in the reference work, the most advanced one being based on the definition of *synchronization checkpoints* starting from the timing of future events involving data exchange between co–simulation elements. The aim is to maximize the execution of each simulator in the system.

The details of such method are not part of the present document; but it is interesting to note that in the proposed work the co–simulation strategy has been validated on a detailed model, reproducing the possibility of congestion over the network. The proposed approach is able to maintain the communication and to let the simulation run also in case of phenomena such as increasing delay, packet loss and tracking errors. The result is a worsening in terms of the accuracy of the system control, thus resulting in larger control errors. The demonstration of such result is shown through the example in Figure 35, which leads to the increase of angular errors in joint position of a robot as shown in Figure 36.

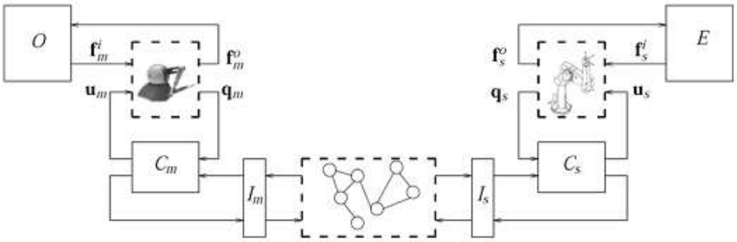
O
$\mathbf{f}_m^i$
$\mathbf{f}_m^o$
$\mathbf{u}_m$
$\mathbf{q}_m$
C_m
I_m
I_s
C_s
$\mathbf{f}_s^o$
$\mathbf{f}_s^i$
$\mathbf{q}_s$
$\mathbf{u}_s$
E

Figure 35 – Layout of the NCS model including a command system (human side, O, and master controller C_m) and a robot operating on the environment (E) communicating over a network (slave controller C_s). Source: Quaglia et al., 2012.

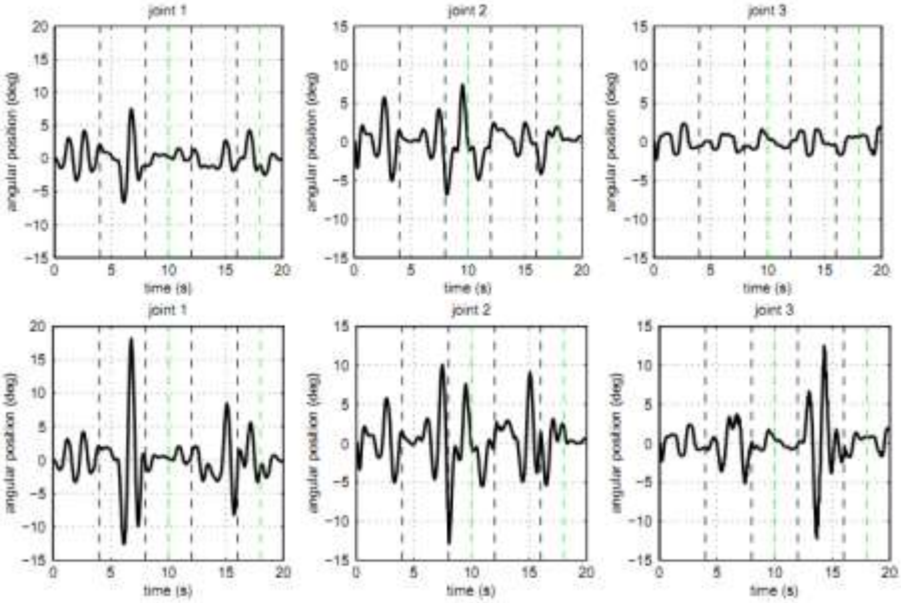

Figure 36 – Errors on angular position at three different joints in case of uncongested (upper plots) and congested networks (lower plots). Source: Quaglia et al., 2012.

3. Mechanical and mechatronics systems modelling

The modelling of any mechanical system is based on the definition of the physical laws defining the characteristics of the components and of the assembly in which these are arranged. As known, the mathematical model resulting is a system comprehending a number of equations; such mathematical definition includes both "physical equations" of the single components and "constraint equations" describing their relations (e.g. equivalence of physical quantities and states on those points where more components are acting). As a result, mathematical system can include just static (algebraic) equation or both static and differential equations.

After this definition phase, a "solver" is a software used to find out the solution of the mechanical system under given boundary conditions, e.g. through numerical integration of the Ordinary Differential Equations (ODE). Very simple examples of component equations for common mechanical elements are shown on Table 8, while Table 9 shows how, starting from simple elements, a two degrees of freedom mechanical system can be modeled. In this case, the system results in an ODE where the main equation is expressed using matrix formalism, that is the most appropriate in order to be solved through numerical calculation tools.

Component	**Representation**	**Equation**
Mass	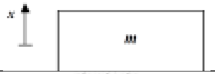	$F = m\ddot{x}$
Spring	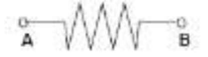	$F_{AB} = -k(x_A - x_B - x_0)$
Damper	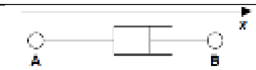	$F_{AB} = -c(\dot{x}_A - \dot{x}_B)$

Table 8 – Mechanical elements representation and equations.

Mechanical System	Mathematical model
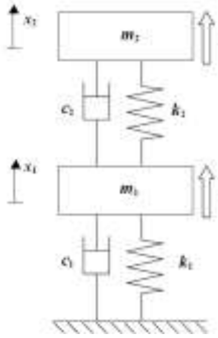 x_2 m_2 F_2 c_2 k_2 x_1 m_1 F_1 c_1 k_1	Equations system: $\begin{cases} m_1\ddot{x}_1 = -k_1x_1 - k_2(x_1 - x_2) - c_1\dot{x}_1 - c_2(\dot{x}_1 - \dot{x}_2) + F_1 \\ m_1\ddot{x}_2 = -k_2(x_1 - x_2) - c_2(\dot{x}_1 - \dot{x}_2) + F_2 \end{cases}$ Matrix definition: $x = \begin{bmatrix} x_1 \\ x_2 \end{bmatrix},$ $F = \begin{bmatrix} F_1 \\ F_2 \end{bmatrix},$ $M = \begin{bmatrix} m_1 & \\ & m_2 \end{bmatrix},$ $K = \begin{bmatrix} k_1 + k_2 & -k_2 \\ -k_2 & k_2 \end{bmatrix},$ $C = \begin{bmatrix} c_1 + c_2 & -c_2 \\ -c_2 & c_2 \end{bmatrix},$ $F = \begin{bmatrix} c_1 + c_2 & -c_2 \\ -c_2 & c_2 \end{bmatrix}$ Final matrix equation: $M\ddot{x} + C\dot{x} + Kx = F$

Table 9 – Mechanical system modelling through equation system.

The definition of basic equation of main mechatronic elements, the description of the methods used to build up equation systems and the analysis of numerical integration methods to solve such system is not a goal of this document, since they refer to basic engineering competencies. This chapter is mainly intended to offer an overview on how complex systems – including different physical domains such as mechanical, electrical and thermal – can be described depending on the target that is needed. The description will be focused on electric vehicle powertrain, aiming to describe how such modelling process can be assisted by CAE tools.

3.1. The choice of modelling framework depending on design aim

Vehicle system modelling can be used for the analysis of different vehicle performance, thus including (Gao et al., 2007):

- modelling for preliminary concept design/design exploration
- analysis of vibration, handling and noise (NVH)
- modelling of vehicle performances (acceleration, gradeability, maximum cruising speed)
- prediction, evaluation and optimization of fuel economy or, in general, of energy consumption
- modelling for safety and stability
- modelling for crashworthiness
- modelling of vehicle controls
- modelling for structural integrity
- modelling to facilitate component testing and validation
- modelling for cost and packaging
- modelling for the prediction of emissions.

It is evident that a tradeoff arise: in general, the more detailed results one needs, the longer the total time for model setup, simulation, and interpretation of results. The choice of the approach for model building as well as the detail that has to be reached is therefore done over a number of assumptions and hypothesis. A balance between the need for precise output and the data available at the selected engineering phase has to be found.

Usually, referring to vehicle powertrain, a “block” scheme can be used to define the main components involved in the system; each block contains all the equations needed to model the real function of the represented component. The lines connecting block can define physical interaction or information exchange. Such representation is very useful, since many different simulation environment software are using so called 1D–0D representation as graphical interface, in order to let the user build up the model through block creation and linking. It is important to note that, in general, the definition of 1D–looking system does not implicate the use of 1D models, since the degrees of freedom of the system depends only on the functions of the block used. After the definition of the block scheme, the software builds equation system and converts it in the form that can be used by solver for the calculation needed (e.g. matrix representation of ODE that can be used for eigenvalue analysis after linearization or for time–step solution).

The method used by software to solve the equations has to be taken into account by the user during block definition and block linking; as an example, some software environment only accept explicit equations (e.g. Simulink math blocks, AMESim), while in other cases it is possible to write acausal equations that are interpreted by the solver depending on the whole system built up (e.g. Modelica–based softwares, Simulink Physical libraries).

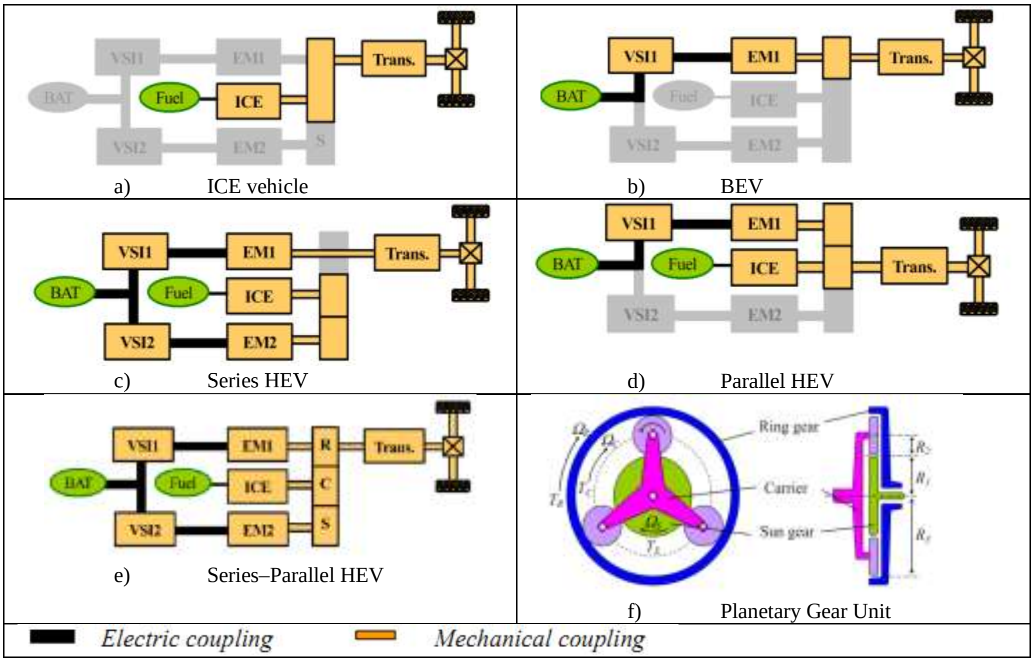

a) ICE vehicle

b) BEV

c) Series HEV

d) Parallel HEV

e) Series–Parallel HEV

f) Planetary Gear Unit

Figure 37 – Main powertrain schemes for ICE, HEV, and BEV vehicles (Chen et al, 2006). The Planetary gear unit is used, in many configuration, as mechanical coupling for different mechanical devices. Abbreviation used: ICE – Internal Combustion Engine; Bat: Battery; VSI: Voltage Source Inverter; EM: Electric Machine; Trans: Mechanical Transmission; HEV – Hybrid Electric Vehicle; BEV: Battery Electric Vehicle.

As a reference point, some example schemes of main vehicle powertrain (coming from the article by Chen et al., 2008) are showed in Figure 37. Such examples are useful to describe how, starting from system definition, a powertrain model can be described. In this case, a number of alternatives for vehicle powertrain (from ICE to BEV and various HEV configurations) are compared.

Let's take as example Figure 38, taken from the article by Lhomme et al., 2004. In this picture, main vehicle components are represented as graphical box. Figure 39 describes the same system, in this case using a convention to distinguish between mechanical, electrical and other physical links; in addiction, the graphical blocks are now exploded showing their internal components (e.g. battery block is represented as a voltage source, while chopper components are shown as power switches); the physical quantities defining interaction between components (Torque and Speed for mechanical shaft, Current and Voltage on electrical ports etc.) are also defined. This representation can be easily converted in a model, as soon as the equation of each block is defined. Figure 40, again, represents the same system in the form of Energetic Macroscopic Representation – EMR, that is *a synthetic graphical tool based on the principle of action and reaction between connected elements*. This representation immediately identifies the logical functions related to the block, referring to three main categories:

1. Source elements (green oval pictograms) produce state variables (outputs). They can be either generators or receptors. They are disturbed by reactions of other elements.
2. Conversion elements ensure energy conversion without energy storage. They have tuning inputs to define the con version between variables. Electrical conversions are depicted by orange square pictograms, electromechanical conversions by orange circular pictograms and mechanical conversions by orange triangular pictograms.
3. Accumulation elements (orange rectangular pictograms with an oblique bar) connect other elements, thanks to energy storage, which induces at least one state variable.

The EMR blocks are described in Table 10. Figure 41 is another step forward on the description of the system: in this case, the control system is added and all signal sources (e.g. current, voltage, speed measurements) are described.

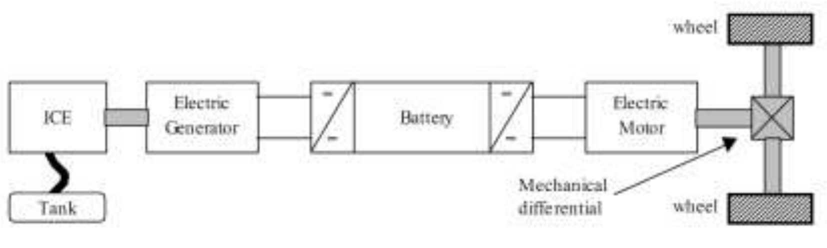

Figure 38 – Series HEV powertrain (Lhomme, 2004), graphical block scheme.

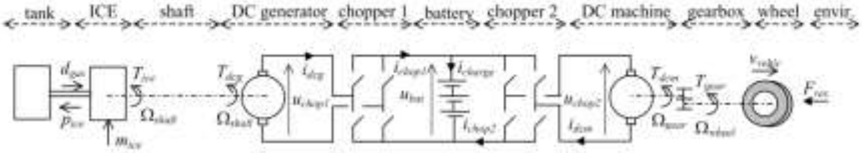
tank
ICE
shaft
DC generator
chopper 1
battery
chopper 2
DC machine
gearbox
wheel
envir.

Figure 39 – Series HEV powertrain (Lhomme, 2004), functional block scheme. "Pipe" connection: fuel flux; Dot–dash line: mechanical link; continuous lines: electrical link.

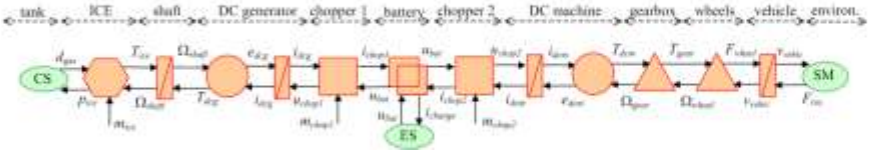
tank
ICE
shaft
DC generator
chopper 1
battery
chopper 2
DC machine
gearbox
wheels
vehicle
environ.
CS
ES
SM

Figure 40 – Series HEV powertrain (Lhomme, 2004), Energetic Macroscopic Representation (EMR), please refer to block scheme on Table 10. CS: Chemical Source (fuel); ES: Electrical Source (battery); SM: Mechanical Source (vehicle resistance).

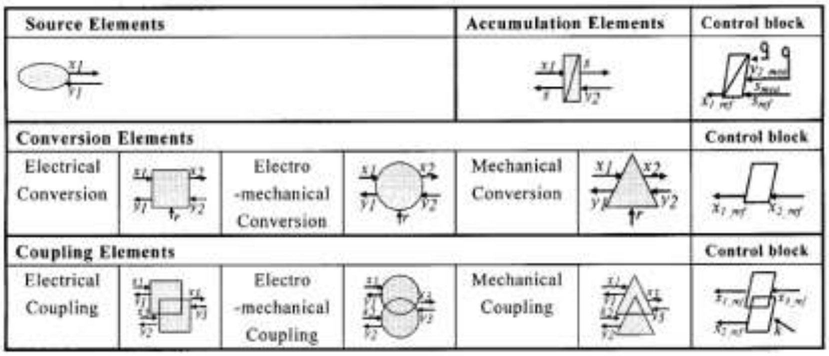

Source Elements				Accumulation Elements		Control block
Conversion Elements						**Control block**
Electrical Conversion		Electro -mechanical Conversion		Mechanical Conversion		
Coupling Elements						**Control block**
Electrical Coupling		Electro -mechanical Coupling		Mechanical Coupling		

Table 10 – Elements used for Energetic Macroscopic Representation – their function and graphical block (Chen et al., 2008b).

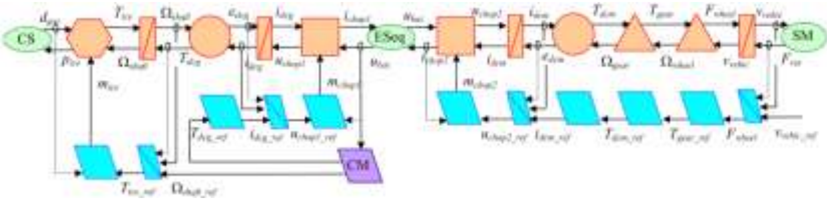
CS
ESeq
SM
CM

Figure 41 – Series HEV powertrain (Lhomme, 2004), Energetic Macroscopic Representation (EMR), including control system. Sensors are represented as circles on other connections and their signals are represented by dashed lines.

Figure 42 shows the resulting matlab–simulink model, in which each block corresponds to EMR blocks as they have been defined through the process described step–by–step by former pictures. Each block contains the equations related to its function. In this case, the EMR offered the opportunity to describe the system with a rigorous physical description and, in addition, it has been a guide for final model build up.

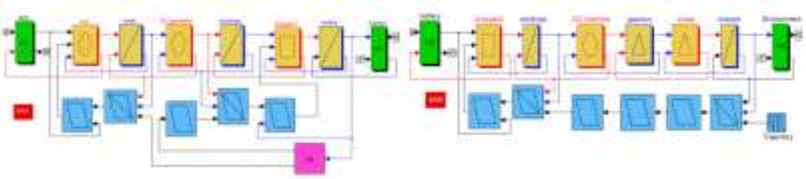

Figure 42 – Series HEV powertrain (Lhomme, 2004), Matlab–Simulink implementation.

3.1.1. **Backward, Forward and test–bench models**

The topology of a model has to be defined also on the basis of time simulation expectations.

The use of "backward–facing" topologies (as described by Valera et al., 2009) in numerical simulations means that the performance of each subsystem is calculated starting from a known input related to the state of the vehicle, that is its speed and acceleration signal. Using the "driving duty cycle" of the vehicle as direct input, only static equation can be used to calculate forces, torques, speeds (mechanical domain) as well as voltages, current, fuel consumption and so on. The model used can also be very simple (e.g. pure parametric equation for longitudinal forces, look–up tables for efficiency of motors etc.) but any dynamics of the system or of the subsystem cannot be exploited. Such models, therefore, are not suitable for detailed descriptions and for tuning of advanced control system; the main advantage is the possibility to speed up simulation, thus enabling the possibility to run "long time" simulation (e.g. to verify energy consumption on a "long" driving cycle on preliminary design stage) or a large number of iterations, that is the case of optimization loops. An example of such kind of model is shown in Figure 43: it is evident that main assumption, in this model, is that the vehicle is perfectly running the given time–speed signal, this one being the only input to the system. All other physical results are calculated in "backward" way.

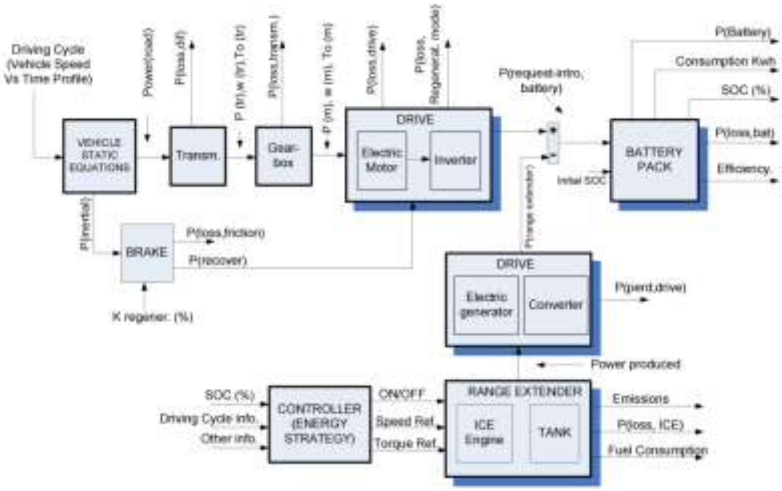
Driving Cycle (Vehicle Speed Vs Time Profile)
Power(road)
P(loss,dif)
P (tr),w (tr),To (tr)
P(loss,transm.)
P (m), w (m), To (m)
P(loss,drive)
P(loss, Regenerat. mode)
P(request-intro, battery)
P(Battery)
Consumption Kwh
SOC (%)
P(loss,bat)
Efficiency
VEHICLE STATIC EQUATIONS
Transm.
Gear-box
DRIVE
Electric Motor
Inverter
Initial SOC
BATTERY PACK
P(inertial)
BRAKE
P(loss,friction)
P(recover)
K regener. (%)
P(range extender)
DRIVE
Electric generator
Converter
P(perd,drive)
Power produced
SOC (%)
Driving Cycle info.
Other info.
CONTROLLER (ENERGY STRATEGY)
ON/OFF
Speed Ref.
Torque Ref.
RANGE EXTENDER
ICE Engine
TANK
Emissions
P(loss, ICE)
Fuel Consumption

Figure 43 – Backward model block diagram of HEV (Valera et al., 2009).

In forward dynamic simulation the inputs are provided in form of user command, such as throttle, brake, steering wheel positions, than the resulting acceleration and speed are calculated as outputs through the solution of dynamic equation of the system (powertrain and vehicle model, if needed including longitudinal and lateral dynamics). Reference maneuvers or cycles can be used as primary inputs while a “virtual driver” (e.g. a speed follower controller) calculates the needed secondary inputs (throttle etc., as described), thus acting in a manner that is quite similar to that of real driver; it is also possible to interface the model with real components or human drivers.

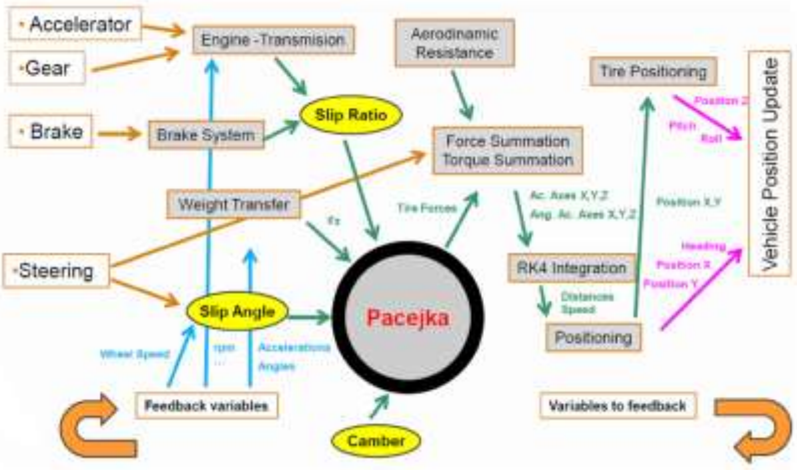

· Accelerator
·Gear
· Brake
·Steering
Engine -Transmision
Brake System
Weight Transfer
Aerodinamic Resistance
Slip Ratio
Force Summation Torque Summation
Tire Positioning
Vehicle Position Update
Position Z
Pitch
Roll
Fz
Tire Forces
Ac. Axes X,Y,Z
Ang. Ac. Axes X,Y,Z
Position X,Y
Heading
Position X
Position Y
RK4 Integration
Distances
Speed
Positioning
Slip Angle
Pacejka
Wheel Speed
rpm
...
Accelerations
Angles
Feedback variables
Variables to feedback
Camber

Figure 44 – Forward model (lateral and longitudinal dynamics) block diagram of vehicle (Valera et al., 2009).

Torque, power, speed, electrical parameters and all the internal parameters are calculated solving the given differential equations, so being an output of “virtual driver” inputs. Such solution is more accurate and limit conditions (e.g. maximum acceleration permitted by vehicle, adherence conditions and so on) can be verified; however, simulation time is longer than forward simulation cases, being about ten times more (Valera et al., 2009) for equivalent models and even more in other situations (e.g. power quality simulation of electric power switches).

The use of forward models also open the possibility to interface model components with real ones, thus being usable in “test bench” layouts. In order to verify some powertrain components, a full system in built using both virtual models and actuators and physical devices; the interfaces between the two are exchanging physical signals that are generated by the model (on the virtual side) and by sensors (on the physical side). According to Bringmann and Kramer, 2008, model–based testing technologies have a large potential in vehicle development, such as:

- allow the development of high–level models that can be used for simulation in very early stages of the development process
- improve communication within development teams, with customers, or between car manufacturers and suppliers
- reduce time to market through component re–use and reduces costs by validating systems and software designs up front prior to implementation

- provide a development process from requirements to code, ensuring that the implemented systems are complete and behave as expected
- allow segregation of concerns; technical aspects such as fixed–point scaling (i.e. the transformation of floating–point algorithms to fixed–point computations), calibration data management, and the representation of signals in memory are separated from the core algorithms thereby keeping the models as lean as possible.

Depending on the level integration, the model and its environment can run on a machine, on more than one machine, on dedicated hardware or physical devices; in some configuration, the synchronization between virtual and physical devices implies the need to run model on a real–time base, thus lean modelling fast solving has to be guaranteed in order to let the system run. Some distinctions on model–based testing can be provided (Bringmann and Krame, 2008):

- Model–in–the–Loop (MiL): The first integration level is based on the model of the system itself. Testing an embedded system on MiL level means that the model and its environment are simulated (interpreted) in the modelling framework without any physical hardware components.
- Software–in–the–Loop (SiL): Testing an embedded system on SiL level means that the embedded software is tested within a simulated environment model but without any hardware (i.e. no mechanical or hydraulic components, no sensors, actuators). Since the environment is virtual, a real–time environment is not necessary. Usually SiL tests are performed on Windows– or Linux–based desktop machines.
- Processor–in–the–Loop (PiL): Embedded controllers are integrated in embedded devices with proprietary hardware (ECU). Testing on PiL level is similar to SiL tests, but the embedded software runs on a target board with the target processor or on a target processor emulator.
- Hardware–in–the–Loop (HiL): When testing the embedded system on HiL level the software runs on the final ECU. However the environment around the ECU is still a simulated one. ECU and environment interact via the digital and analog electrical connectors of the ECU. The objective of testing on HiL level is to reveal faults in the low–level services of the ECU and in the I/O services.
- Test rig: Testing in a test rig means that the embedded software runs on the ECU. The environment consists of physical components (electrical, mechanical, or hydraulic).

In addition, the so called Human in the Loop (Huil) simulation approach is a configuration in which Human also interacts with virtual and physical system, thus providing its input.

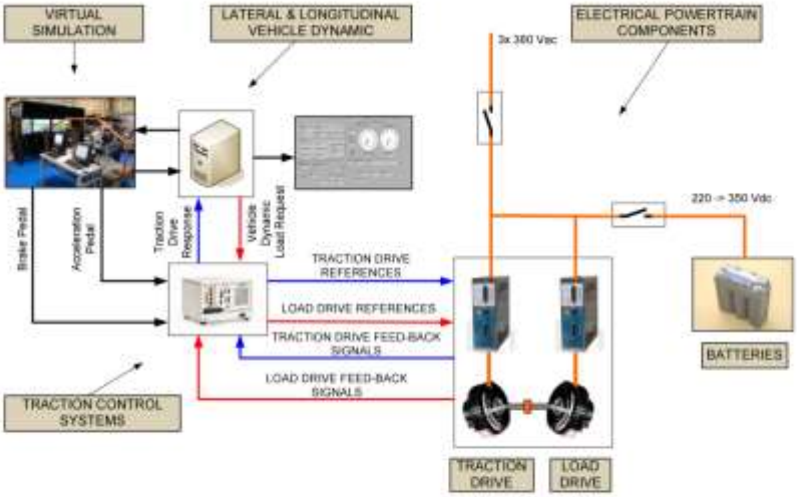
VIRTUAL SIMULATION
LATERAL & LONGITUDINAL VEHICLE DYNAMIC
ELECTRICAL POWERTRAIN COMPONENTS
3x 380 Vac
220 -> 350 Vdc
Brake Pedal
Acceleration Pedal
Traction Drive Response
Vehicle Dynamic Load Request
TRACTION DRIVE REFERENCES
LOAD DRIVE REFERENCES
TRACTION DRIVE FEED-BACK SIGNALS
LOAD DRIVE FEED-BACK SIGNALS
TRACTION CONTROL SYSTEMS
BATTERIES
TRACTION DRIVE
LOAD DRIVE

Figure 45 – HEV test bench architecture and layout. The components on the right are physical elements of electrical powertrains (Valera et al., 2009).

The need for physical accuracy, the capability to run on embedded device (sometimes having hardware limitation in comparison to desktop machines), the need for real–time capabilities implies that models for system development on test rig can be quite different from those designed for other engineering phase. Also, it can be highlighted that in order to simplify product and software engineering a requirement is asked to modelling environment: the capability to export models on common languages (e.g. C, C++ software) that can be directly used on embedded devices.

3.1.2. A modelling framework

Since the research activity is focused on BEV key elements (battery, motor, inverter), a short analysis on how such components can be modeled will be defined here, while detailed examples will be described in further paragraphs.

In the case of vehicles, the proposal of innovative powertrain architecture (e.g. EV, HEV; PHEV, EREV) has been widely investigated in the last fifteen years (e.g. Butler et al. article, presenting a matlab–based package in 1999). The main aim of such archetype analysis is to assess the overall performance in terms of energy consumption, acceleration, speed over reference maneuvers. The accuracy of the models in this phase is, in general, quite low, since the vehicle and its components are defined through simplified physical models or even through performance map coming from tailored simulation and/or measurements. Such simplified approach still enables the possibility to compare innovative architecture starting from the early design phase, while, at the same time, the effectuation of sensitiveness analysis can take advantage of generally low calculation efforts: batch procedures for virtual “design of experiment” can be easily applied even in case of “long” simulation timescale (e.g. timescale: minutes for most driving cycles, 10^{0}–10^{-2}s as typical simulation step). The approach can also be used to analyze the performance of vehicle components in the system before the technology is ready, thus defining the future requirements and the design priority. This is the case, as an example, of the battery requirement analysis performed by USCAR[3]: battery targets for technology breakthrough are showed on Ragone Plot on Figure 46.

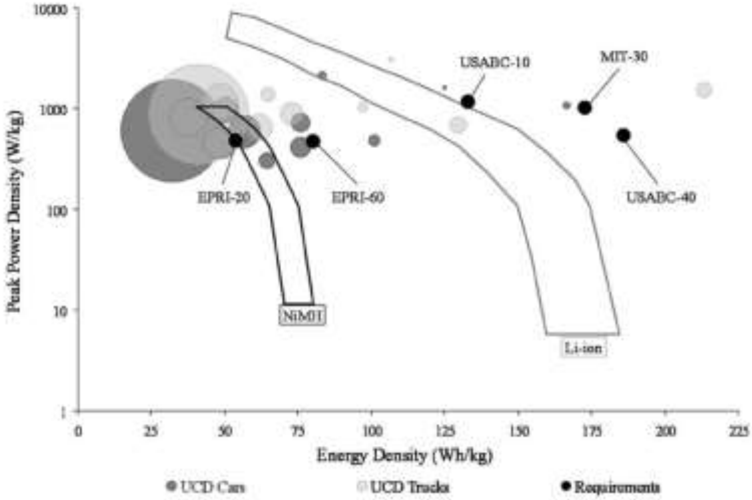

Figure 46 – Distribution of battery requirements for PHEV designs selected by potential early market respondents and USABC, MIT, and EPRI (Axsen et al., 2010).

In general, it is desirable to perform multi–domain simulation of mechanical, electric and thermal phenomena in the same environment, or, if needed, to coordinate different software (e.g. co–simulation of systems including control models and physical components, each one built in different modelling environment, see Dong–xu et al, 2009); it is therefore possible to verify the interaction of the components and the subsystems which are parts of a more complex system. Modelling environment such as AMESim, Matlab–Simulink, Modelica–based products offer a wide range of logical, control and physical libraries suitable for the set up of vehicle model. These environment can be used to build up so called 0D–1D models, but in some configurations multi dimension analysis (e.g. through multiple degrees of freedom vehicle body blocks) can also be performed. However, lumped parameters model for EV energy sources are currently widely used (Van Mierlo et al., 2004) sometimes including also thermal simulation (Forgez et al., 2010).

Multi–dimension software (e.g. multibody, 3D vehicle modelling environment) are suitable for detailed driveability, handling and comfort simulation, including detailed NVH analysis and the development of active safety device; in this latter case, input data have to include detailed vehicle mission and path characteristic with increased accuracy in comparison to 1D driving cycle (based on longitudinal speed definition): from lateral acceleration, to slope, up to the definition of road surface irregularities. Considering the case of BEVs, the low availability of on board energy implies the need for accurate energy management in order to precisely assess effective range considering also the consumption of auxiliaries, even the less relevant ones. Again, latest models should include any auxiliary part or subsystem (Roscher et al., 2012).

---

[3] www.uscar.org/

The increase of the physical details and the reduction of simulation timescale (typical simulation step of 10^{-6} for switching power electronics simulation, (Yoon et al., 20090) enhance the accuracy of the simulation and enables the use of such tools for the development of concept control algorithm, both at “high level” logic (e.g. energy flow management strategies in HEV) or “low level” logic (e.g. switching hardware control, electric motor phases control). The evaluation of small timescale phenomena (e.g. through electric power quality analysis) enables the detailed dimensioning of components and parts. The advanced use of models can therefore be used in the later design phase of the product to build up virtual (or partially virtual) test bed (MiL, SiL, HiL, HuiL as described), integrating them in mixed hardware/software system representing the full system under study.

Another important use of models is to define through them the expected response of real components, building up so–called observers. The application of observers include the possibility to control the system reducing the need for measurements or ensuring fault–tolerant working for the component (the case of sensorless control of BLDC motors is a typical example), identifying the state of the system in case that direct measurement is impossible (Tutunji et al., 2007); latest application in the field of EV are related to the development of diagnosis procedures able to identify component parameters (see a common lumped equivalent model used for batteries in Figure 47) for in–service evaluation of battery State Of Charge (SOC) and State Of Health (SOH), which still is a critical issue for the optimal use of the component (He et al., 2012); an example of “battery parameter observer” is described in Figure 48.

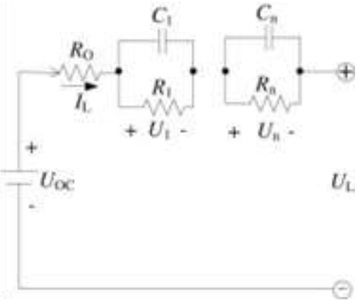
C_1
C_n
R_O
I_L
R_1
R_n
$+ \ U_1 \ -$
$+ \ U_n \ -$
$+$
U_{OC}
$-$
U_L

Figure 47 – Battery lumped parameters model presented in the model by He et al., 2012.

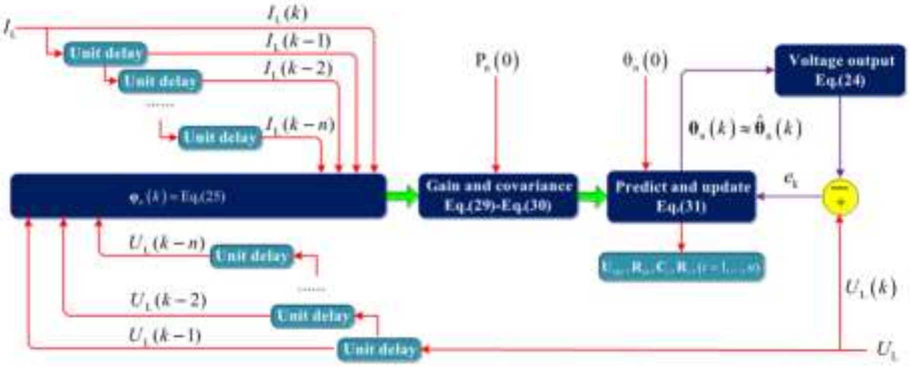
I_L
$I_L(k)$
$I_L(k-1)$
$I_L(k-2)$
$I_L(k-n)$
Unit delay
Unit delay
Unit delay
$P_n(0)$
$\theta_n(0)$
Voltage output Eq.(24)
$\theta_n(k)=\hat{\theta}_n(k)$
$\varphi_n(k)$=Eq.(25)
Gain and covariance Eq.(29)-Eq.(30)
Predict and update Eq.(31)
e_L
$U_L(k-n)$
Unit delay
$U_{oc}, R_0, C_i, R_i, (i=1,\dots,n)$
$U_L(k)$
$U_L(k-2)$
Unit delay
$U_L(k-1)$
Unit delay
U_L

Figure 48 – Lumped elements battery model (left) and battery SOC and SOH prediction (right) based on Current/Voltage observer(He et al., 2012).

The maximum detail can be obtained through advanced modelling of single component, e.g. through finite elements analysis of mechanical, thermal, electrical and magnetic phenomena, in some case using a multi–physical solver. This is especially the case of motor design and of battery cell advanced analysis (see Figure 49), but such approach usually is resource–consuming in comparison with detailed lumped elements models and, therefore, it is used mainly for advanced component design.

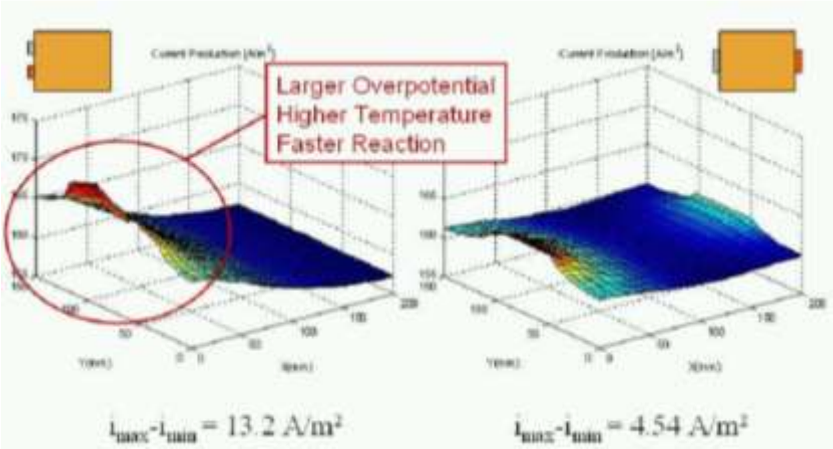

Figure 49 – Non–uniformities in battery current production modeled through electrochemical FEM system (Pesaran, 2009).

The literature review demonstrates that the tools needed to build various models with different detail level are already available, and that the choice depends on the aim of the engineering phase. Before we describe some case studies coming from literature, a general framework and guideline is presented.

Considering a common mechatronic component as an electric machine (motor/generator), we can identify at least five different levels at which it can be modeled:

1. The first step is to find out the main function of the machine: in this case, electric energy is converted to mechanical energy, and a thermal loss can be identified depending on efficiency.
2. For simple archetype confrontation, energy consumption evaluation and other general assessments, an efficiency map coming from experimental test or from detailed simulation can be used: this is case of many backward simulation approaches.
3. Very simple lumped elements model can be tuned to represent many different machine architecture and such model can provide the capabilities to find out dynamic response of the machine under electric/mechanical excitation.
    a. Lumped parameters model already allow the definition of performance modification depending on ageing, temperature and any external factors; time–varying parameters can be loaded on the model, if their describing equations are available (e.g. known empirical laws).
4. Detailed lumped parameters models: in this kind of models, each phase and switching controller is described. This approach offer the capabilities to examine in detail the performances of the whole motor drive, such as:

   a. time–varying voltage and current on each phase
   b. power quality analysis
   c. torque unevenness depending on rotor position (e.g. to identify excitation frequencies on driveline).
5. Detailed models using a large number of degrees of freedom, e.g. through flux modelling on discretized Finite Element Models (FEM). Such analysis allows to:
   a. model in detail machine performances, e.g. including copper losses
   b. rotor/stator shape optimization on the basis of flux/losses/torque performances
   c. evaluation of a reduced set of parameters to be used as calibration for more simple model (e.g. n°.3 and 4).

A general “overlap” between modelling approach can be found, so that, as an example, it is sometimes possible to find similar research using advanced lumped parameters model partly including FEM analysis (e.g. for co–simulation). In addition, it can be said that for electric machine (and also other kind of components) the more the model is detailed, the more innovation opportunities arise.

Detailed lumped models, as an example, can allow the research about low–level control, thus resulting in different performances of the machine and, in some cases, modifying the resulting efficiencies: a research on the component itself is allowed, while in simplified cases the machine is mostly used “as is” and only its known performances can be modeled.

Even in this case, however, ageing can be described only as parameter variation if such values are calculated using an external law. On the contrary, in case of detailed simulation it is sometimes possible to evaluate the influence of known deterioration factors and to evaluate the performances of the machine under this kind of stress; the model allows to describe the performance variation on the basis of physical principles, so that empirical experiences are used to tune the model on the basis of known causes, not just to describe the known effect. As an example, if temperature is modifying the performance of permanent magnets used in an electric machine, in a FEM model it is possible to identify the macro–variation of performances starting from material properties variation, even if the real entity of such variation under working conditions still has to be identified and calibrated. The example of battery cells in this case is even more clear: since electrochemical modelling of the cells surface can describe the ”current generation” by each small surface elements, the effect of temperature variation (modifying the reactivity of the chemical substances inside the cells) can be assessed through physical equations (e.g. Nerst equation, Yi et al., 2013) calculated on the points of the surface; ageing effect (producing surface degradation and modifying thermal diffusivity, see Figure 50) can also be calculated “a priori” modifying surface parameters. In this context, it is possible to perform a sensitiveness analysis using general parameter variation, exploring the search space, while real entity of such parameter variation will be lately identified.

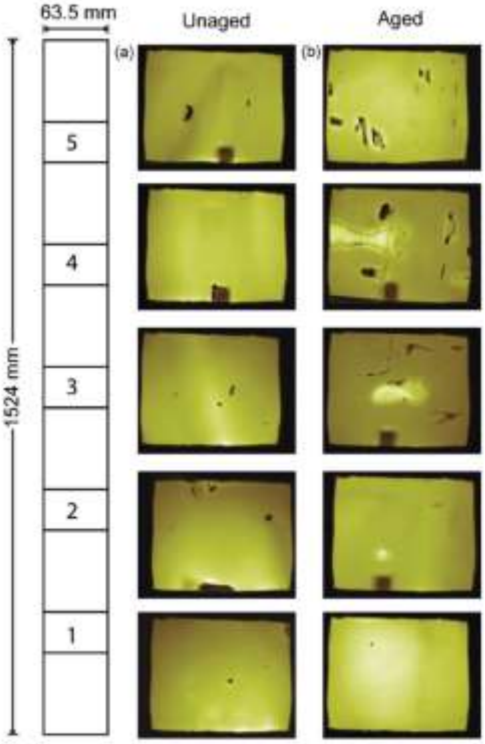

Figure 50 – Sectioning of the cathode for the thermal imaging. Section 1 is near the core of the cylinder and section 5 is near the out edge of the cylinder. (b) Thermal maps of unaged and aged cathode samples for all the five sections (Nagpure et al., 2010).

Table 11 describes common modelling approach for main EV components, again aiming to identify at least five different levels for component description. Figure 51 aims at summarizing the framework for system design based on CAE, highlighting the need for information and simulation integration at each design phase; any platform used should guarantee flexibility to make possible model re–use (e.g. for design “iterations” – see the empty arrows) both for detail “upgrading” and “downgrading.

	Function	**Element**	**Archetype confrontation**	**Early design dimensioning**	**Design and Testing**	**Component design**
Component	Energy conversion	Motor/ Generator	Efficiency table RPM/Torque performance	Simplified lumped parameters model	Component 0D–1D simulation through detailed lumped parameters models	Detailed FEM simulation
Example	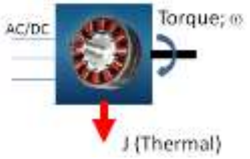		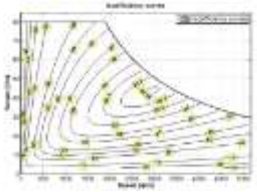	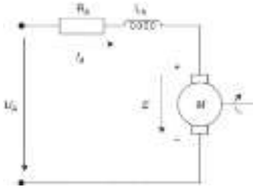	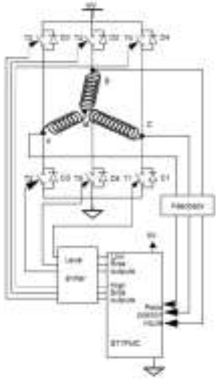	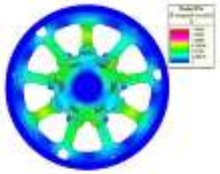
	$\begin{cases} VI = T\omega + J \\ T\omega = \eta VI \end{cases}$ case: motor		Source:Etel TMK0175–050 BLDC motor, from Monti, 2010.	$\begin{cases} L_A \frac{dI_A}{dt} + R_A I_A = U_A - E \\ T = k_1 I \\ E = k_2 \omega \end{cases}$	Source: STI– PWM management for 3–phase BLDC motor drives using ST7MC	Source: Moradi et al., 2011
	Vehicle energy source	Battery Fuel cell	Overall data kW/kg; kWh/kg; efficiency	Simplified model (e.g.source/resistor model)	Cells layout, thermal and electrical model	Detailed electrochemical simulation
	Power supply and control	Inverter/ Controller	Overall efficiency	Suitable technology selection and expected performance	Component simulation (0D–1D)	Detailed simulation (voltage, current, EMC)
	Energy transmission	Driveline components	Overall efficiency	Preliminary dimensioning, expected inertia, stiffness	Driveline simulation (lumped models) (0D–1D)	Detailed multibody/FEM simulation

Table 11 – Modelling detail depending on design phase for common BEV components, using electric machine as reference example.

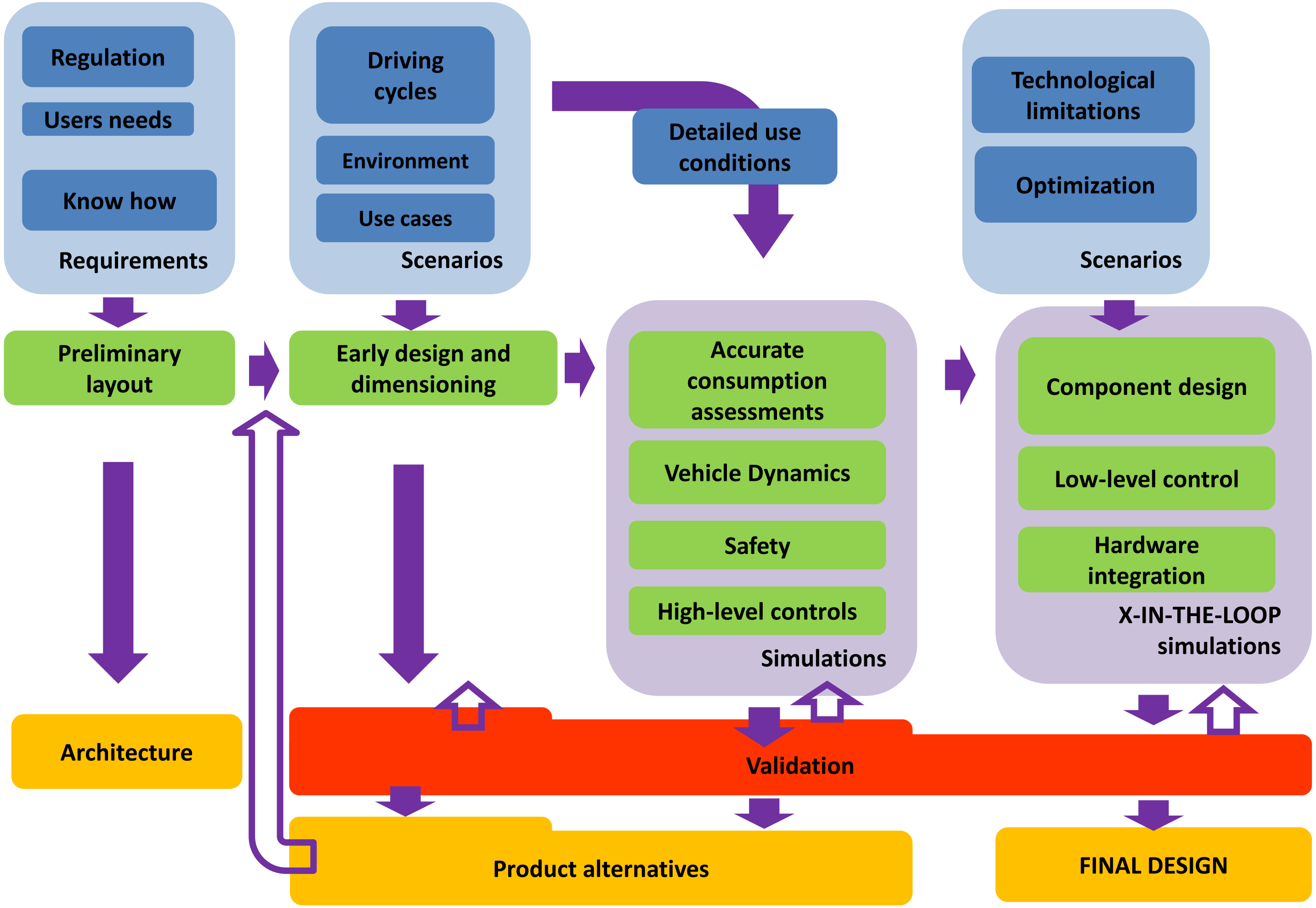
Regulation
Users needs
Know how
Requirements
Driving cycles
Environment
Use cases
Scenarios
Detailed use conditions
Technological limitations
Optimization
Scenarios
Preliminary layout
Early design and dimensioning
Accurate consumption assessments
Vehicle Dynamics
Safety
High-level controls
Simulations
Component design
Low-level control
Hardware integration
X-IN-THE-LOOP simulations
Architecture
Validation
Product alternatives
FINAL DESIGN

Figure 51 – A summary of the steps of vehicle design process. From left to right, the steps determining the need for accuracy increase in the simulation, from abstraction to detailed modelling. From up to bottom, the three main actor of the design process: the boundary conditions (blue labels), the characteristics of the model to be used on that phase (green labels), the product of the activity (yellow labels). Each phase providing product alternatives needs a "validation" step in terms of performances, costs, functionality; it is therefore possible that in any moment it is needed to do a step backward (highlighted by empty arrows). The role of a CAE –based design strategy is to make available all the information and the tools needed at each phase.

3.2. Case studies

In this section a short review of applications of simulation models will be presented. The aim is to define the elements described in this chapter, thus offering an overview of consolidated approaches. The description includes modelling activities which are not focused just on vehicle design but also include the analysis of the relation between environment and technology; in all the cases, the approach adopted is, in general, simplified; as an example, none of the cited works analyses vehicle dynamics (e.g. suspensions and body movements, cornering capabilities etc.) in detail.

3.2.1. **Analysis and vehicle archetype confrontation**

A short literature review of preliminary analysis shows that the tools used for similar calculation can be really different[4].

A very simple approach for the assessment of vehicle performances in terms of fuel consumption is presented in Figure 18. The analysis (Duflu et al., 2009) is focused on the effect of mass variation due the use of composite materials; a complete powertrain analysis of the vehicle is not prepared, but statistical data from vehicles on commerce are used. The fuel consumption is therefore estimated on the basis of a pure regression model from known data. The abstraction from the physics and the technology of the vehicle is complete and the model is even simpler than those presented in the first column on Table 4. The analysis is not able to describe alternative scenarios, e.g. including different powertrain technologies (hybrid/electric) having different sensitiveness to mass variation.

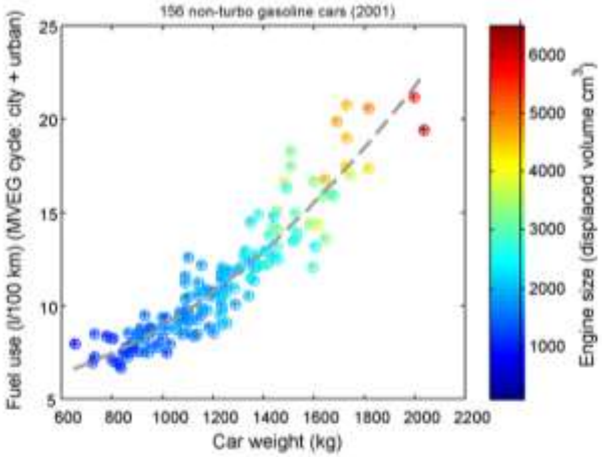

Figure 52 – Fuel consumption as a function of car weight and engine size for gasoline cars (Duflu et. Al., 2009).

---

[4] The order used to present the articles is not based on the publication year but on the model accuracy level, from “low technological detail” to “high technological detail”.

The example in Figure 53 shows a fuel/energy supply model (from generation to vehicle conversion) based on the expected efficiency of main systems involved. In this case, the technology of the vehicle is described through a very simplified model describing its powertrain, the main approximation being the use of average efficiency values. The model cannot take into account the variation of the efficiency depending on duty cycle (load, speed, traffic condition), but its definition is based on the powertrain technology of the vehicle. The model (Thomas, 2009) is based on energetic performances and can be easily improved through the use of efficiency map instead of fixed values.

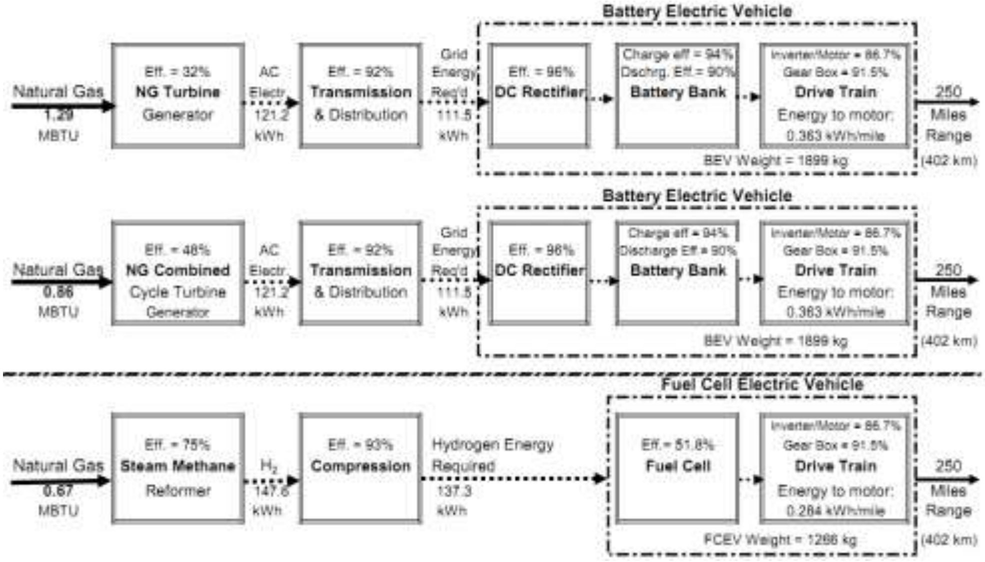
Battery Electric Vehicle
Natural Gas
1.29
MBTU
Eff. = 32%
NG Turbine
Generator
AC
Electr.
121.2
kWh
Eff. = 92%
Transmission
& Distribution
Grid
Energy
Req'd
111.5
kWh
Eff. = 96%
DC Rectifier
Charge eff = 94%
Dschrg. Eff. = 90%
Battery Bank
Inverter/Motor = 86.7%
Gear Box = 91.5%
Drive Train
Energy to motor:
0.363 kWh/mile
250
Miles
Range
(402 km)
BEV Weight = 1899 kg
Battery Electric Vehicle
Natural Gas
0.86
MBTU
Eff. = 48%
NG Combined
Cycle Turbine
Generator
AC
Electr.
121.2
kWh
Eff. = 92%
Transmission
& Distribution
Grid
Energy
Req'd
111.5
kWh
Eff. = 96%
DC Rectifier
Charge eff = 94%
Discharge Eff = 90%
Battery Bank
Inverter/Motor = 86.7%
Gear Box = 91.5%
Drive Train
Energy to motor:
0.363 kWh/mile
250
Miles
Range
(402 km)
BEV Weight = 1899 kg
Fuel Cell Electric Vehicle
Natural Gas
0.67
MBTU
Eff. = 75%
Steam Methane
Reformer
H2
147.6
kWh
Eff. = 93%
Compression
Hydrogen Energy
Required
137.3
kWh
Eff. = 51.8%
Fuel Cell
Inverter/Motor = 86.7%
Gear Box = 91.5%
Drive Train
Energy to motor:
0.284 kWh/mile
250
Miles
Range
(402 km)
FCEV Weight = 1266 kg

Figure 53 – Comparison of the amount of natural gas required during a 400 km travel for Battery EV compared to a fuel cell EV using electricity and hydrogen production technology expected in the 2010–2020 time period (source: Thomas, 2009).

The next model presented (Doucette and McCulloch, 2011) is also using an energy/efficiency powertrain model needed to compare final vehicle energy consumption depending on electric energy efficiency generation. In this case, the powertrain model is solved through a so called backward/forward [5]simulation approach: assuming the vehicle speed given by reference cycle (New European Driving Cycle, see Figure 54), simple physical equations are used to calculate torque and power needed, so that for working condition at given time for gearbox, motor and battery are calculated (see powertrain scheme in Figure 55 – Vehicle model scheme used in Doucette and McCulloch model.Figure 55).

---

[5] The backward–forward simulation approach was introduced by ADVISOR software, that is one Matlab–based simulation environment specifically designed for Battery electric and Hybrid Electric vehicles analysis (Wipke et al., 1999). It is mainly a backward simulation approach in which the available tractive force is compared to the one calculated using speed cycle, thus modifying vehicle speed if the required force is not physically attainable: in this way, *the computed vehicle speed never exceeds that possible given the torque and force available from the drivetrain or the speed that corresponds to any drivetrain component speed limits that might be active*. ADVISOR has been updated over the years and a large number of literature analysis are based on the use of it.

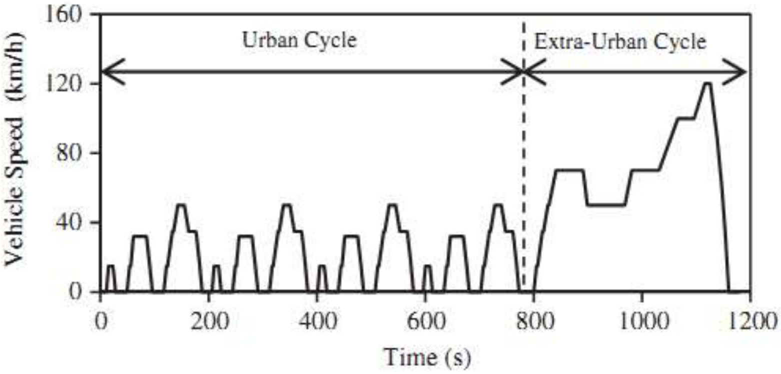

Figure 54 – New European Driving Cycle as time–speed signal.

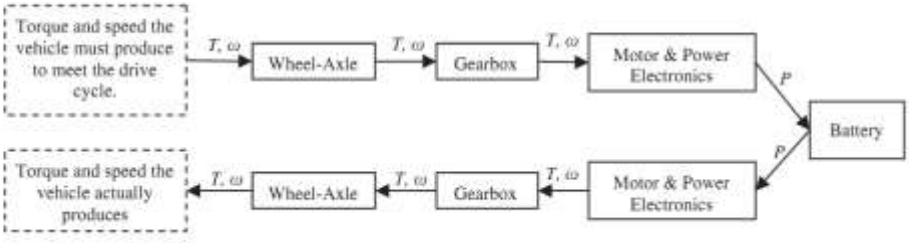
Torque and speed the vehicle must produce to meet the drive cycle.
T, ω
Wheel-Axle
T, ω
Gearbox
T, ω
Motor & Power Electronics
P
Battery
P
Torque and speed the vehicle actually produces
T, ω
Wheel-Axle
T, ω
Gearbox
T, ω
Motor & Power Electronics

Figure 55 – Vehicle model scheme used in Doucette and McCulloch model.

In this example, traction forces are calculated using known equations for vehicle longitudinal dynamics:

- aerodynamic drag force F_d:
  $F_d = \frac{1}{2}\rho A_f C_d v^2$
  (letters are indicating, respectively: air density; frontal area; drag coefficient; speed)
- rolling resistance force F_r:
  $F_r = \mu_r m g$
  (letters are indicating, respectively: rolling resistance coefficient; mass; g acceleration)
- inertial force F_A:
  $F_A = ma$
  (simbols are indicating, respectively: mass; longitudinal acceleration)

For the gearbox, efficiency is based on:

$$\eta = \frac{T_{in}\omega_{in}}{T_{in}\omega_{in} + k_{seal} i_G^2 T_{maxmotor}\omega_{in} + \left(k_{mesh} + k_{bearing}\right) T_{in}\omega_{in}}$$

T is the torque (input or max for engine), ω is shaft speed, i_g is the gear ratio and k coefficients are the values of losses due to seals, bearings and gear meshing.

For the motor, the efficiency is calculated together with power electronics using a producer–defined map.

For the battery, an equivalent model tuned on selected battery cells is used (Figure 56).

The model is therefore mainly based on the description of the powertrain but is still using black–box approach for some components (e.motor), so that an accurate evaluation of performances over specific interest point (e.g. selection of motor control strategy for optimal regenerative braking tuning) is not possible. However, the relation between energy consumption and mass can be fully exploited; in addiction, the total mass depending on vehicle range target can be described.

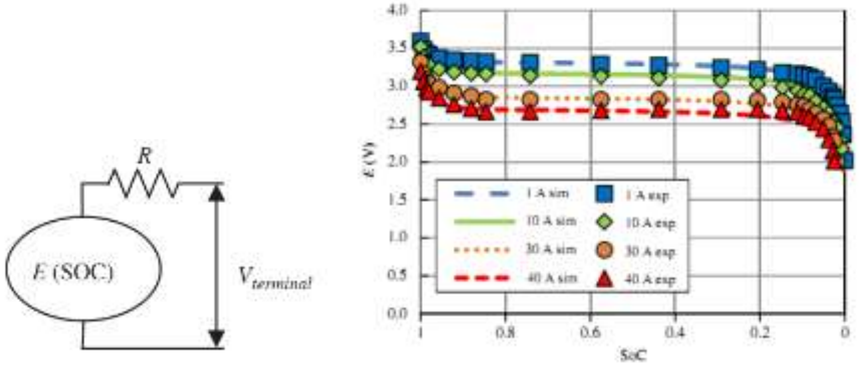

Figure 56 – Equivalent circuit for battery model (left) and comparison of datasheet and simulated performances (voltage E over State of Charge SoC for different current values).

The article, in fact, uses the known vehicle specifications (Table 12) to build up the hypothetical specifications of equivalent BEV models, declined in three versions having low, medium and high range battery (thus resulting in different mass, see Table 13). It is important to remember that battery mass increase and range increase have no linear relation due to the unavoidable increase of traction forces.

Vehicle	**C_d**	**A_f**	**f_r**	**Tire radius**	**ICE power**	**ICE mass**	**CO_2 emissions as an ICE–based vehicle**	**Curb mass as an ICE**
		m^2		(m)	(kW)	(kg)	(gC0$_2$/km)	(kg)
Two–wheeler	0.7	1.0	0.01	0.13	4.2	9.6	46	163
VW Polo BlueMotion	0.30	2.1	0.007	0.30	55	126	91	1225
Ford Mondeo	0.32	2.3	0.01	0.32	85	195	139	1582
Honda CR–V	0.30	2.8	0.01	0.36	112	257	173	1573

Table 12 – Specifications of ICE models used as reference for modelling.

Vehicle	**Battery pack mass (kg)**			**Battery energy capacity (MJ)**			**Curb mass as a BEV (kg)**		
	Low range	Medium range	High range	Low range	Medium range	High range	Low range	Medium range	High range
Two–wheeler	14	42	74	5	16	29	215	293	324
VW Polo BlueMotion	175	371	582	68	145	111	1321	1517	1728
Ford Mondeo	223	475	763	87	186	298	1645	1897	2185
Honda CR–V	224	483	111	87	189	303	1584	1843	2137

Table 13 – Calculated specification of BEV models, to be used for final comparison.

Vehicle	**BEV energy consumption (kJ/km)**		
	Low range	Medium range	High range
Two–wheeler	125	130	137
VW Polo BlueMotion	378	431	453
Ford Mondeo	519	554	594
Honda CR–V	525	562	604

Table 14 – Calculated energy consumption for different vehicle models.

The result of the calculation is the energy used on the given cycle (expressed in kJ/km) for each vehicle and for all the options; the final result is a comparison of CO2 emissions on the whole cycle (CO_2/kJ being known for each Country – see Figure 23 and following). The sensitiveness to the energy mix of the Country is, as expected, absolutely remarkable.

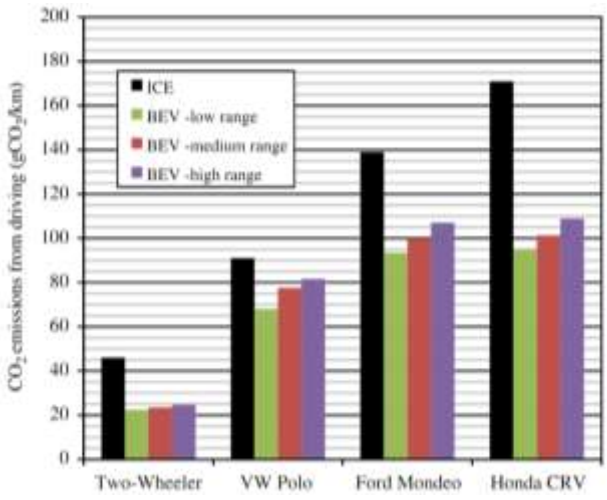

Figure 57 – Calculated CO2 emissions for the vehicles described in Table 13 considering USA electric energy generation data.

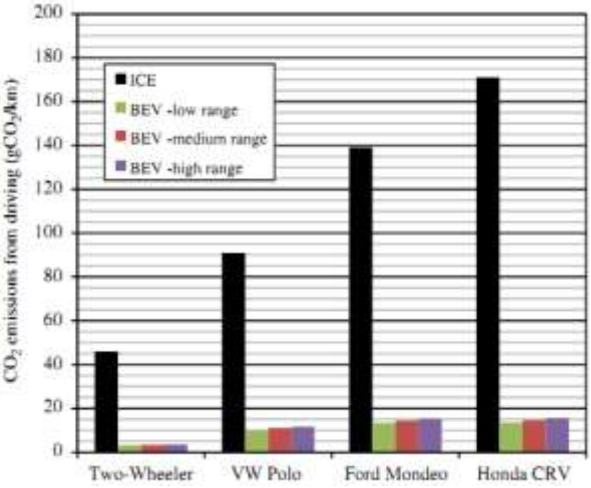

Figure 58 – Calculated CO2 emissions for the vehicles described in Table 13 considering France electric energy generation data.

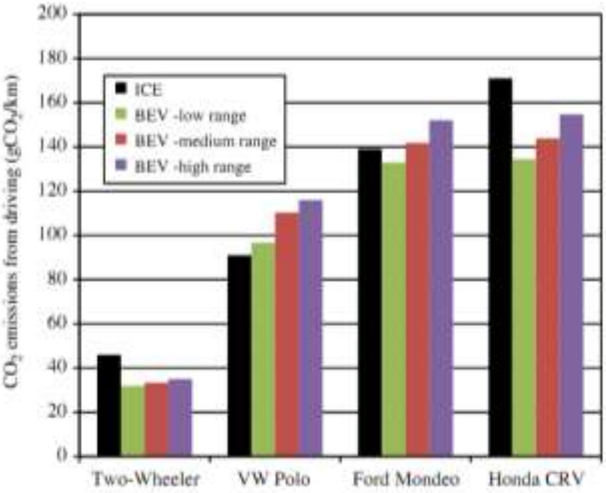

Figure 59 – Calculated CO2 emissions for the vehicles described in Table 13 considering China electric energy generation data.

Another similar analysis is performed in the work by Campanari et al., 2009. In this case, the aim is to compare three different vehicle technologies, each one using energy coming from different sources:

- Battery Electric Vehicle; electricity being produced from:
    - Renewables
    - Natural Gas
    - Coal
    - Italian source mix

- Fuel Cell Electric Vehicle using hydrogen being stored in two different ways (liquid and gaseous) produced from:
    - Renewables
    - Natural Gas
    - Coal
- Fuel Cell Electric Vehicle using fuels such as:
    - Gasoline
    - Ethanol
    - Methanol
    - Natural Gas.

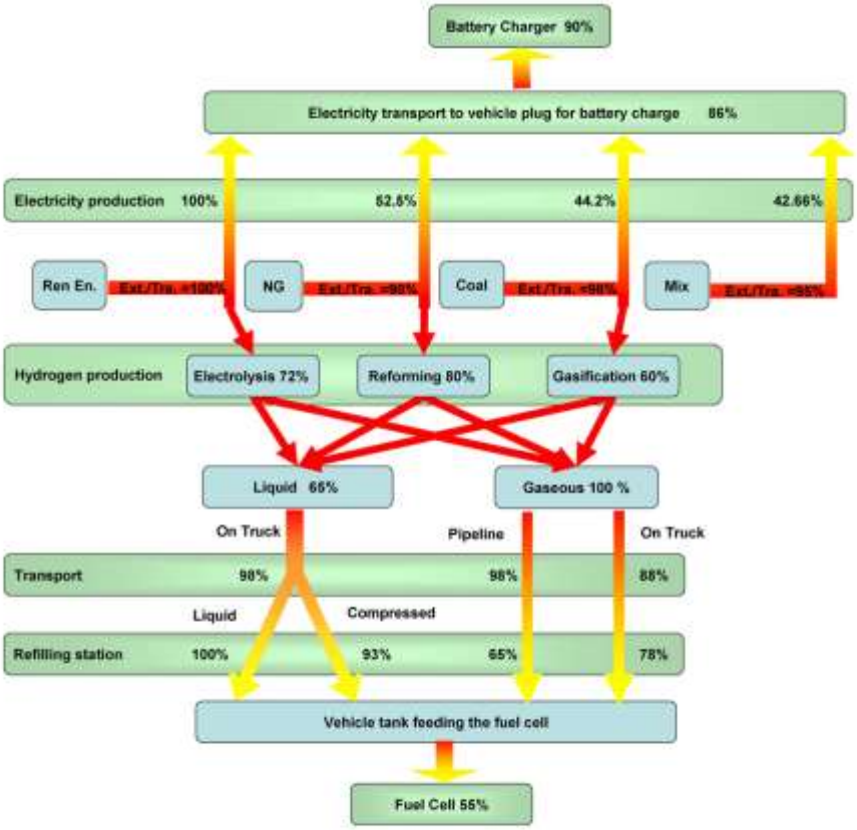
Battery Charger 90%
Electricity transport to vehicle plug for battery charge 86%
Electricity production 100%
52.5%
44.2%
42.66%
Ren En.
Ext./Tra. ≈100%
NG
Ext./Tra. ≈90%
Coal
Ext./Tra. ≈98%
Mix
Ext./Tra. ≈95%
Hydrogen production
Electrolysis 72%
Reforming 80%
Gasification 60%
Liquid 66%
Gaseous 100 %
On Truck
Pipeline
On Truck
Transport
98%
98%
88%
Liquid
Compressed
Refilling station
100%
93%
65%
78%
Vehicle tank feeding the fuel cell
Fuel Cell 55%

Figure 60 – Efficiency data of conversion chain from primary source to vehicle (Campanari et al., 2009).

The model includes the well to tank efficiency, using the data shown in Figure 60; the vehicle model is, again, very simple since it only includes static efficiency component models (see Figure 61).

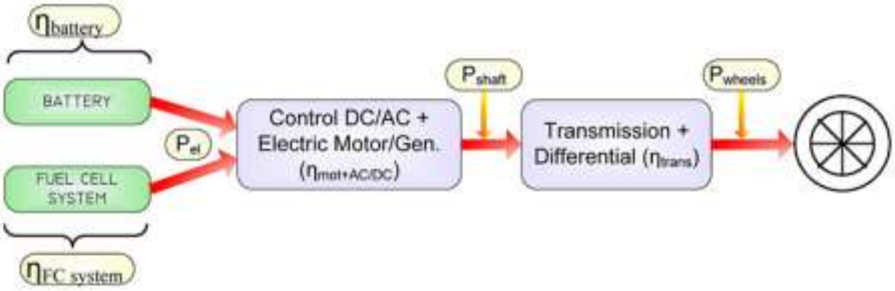
$\eta_{battery}$
BATTERY
FUEL CELL SYSTEM
$\eta_{FC\ system}$
P_{el}
Control DC/AC + Electric Motor/Gen. ($\eta_{mot+AC/DC}$)
P_{shaft}
Transmission + Differential (η_{trans})
P_{wheels}

Figure 61 – Powertrain model of Fuel Cell and Battery vehicles.

Despite of the simplified model assumed, the study demonstrates that even simplified approach can be used to assess primary design data. First of all, the power sizing is based on both European and United States “high power” cycle, the latter being more demanding than the first (see Figure 62). This is a first evaluation that the designer has to take into account to satisfy market expectations in terms of acceleration, achievable speed and so on.

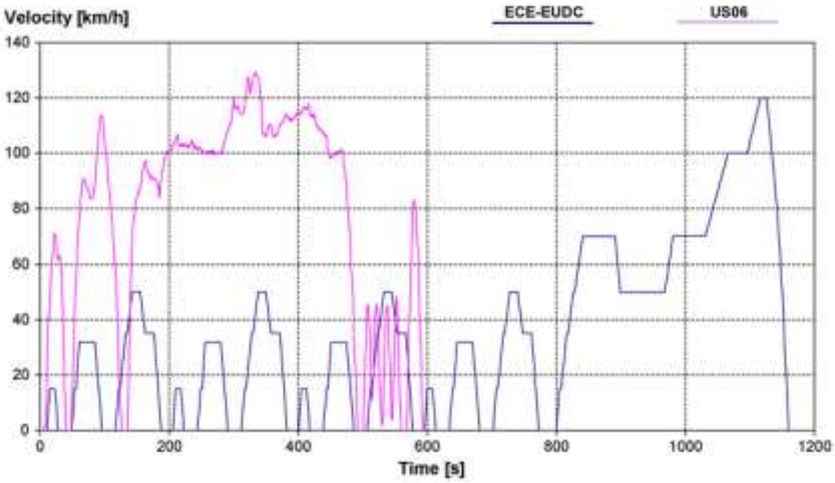

Figure 62 – European (ECE–EUDC) and United States (US06) driving cycles compared.

Furthermore, an iterative calculation method is presented to calculate the mass (Weight – W) of the vehicle considering the required target in terms of range and performances; such step (which was not explicitly presented in the work by Doucette and McCulloch, 2011) is necessary since the modification of one parameters (energy stored on the vehicle) is acting on the way that the mass is varied and, therefore, also range and performances are influenced. The procedure is based on the definition of a “guess” weight that is updated at each iteration, until the guess value fits the calculated one and also satisfy the requested performances.

Another interesting feature of the model is the possibility to calculate the effect of additional battery installation on Fuel Cell Electric Vehicles. Battery as additional component can be used to add regenerative braking capabilities (thus reducing global energy consumption), but its size influences weight and cost. Optimal value can be identified, assuming that EUDC cycle is used. Obviously, regenerative braking strategy is only approximated (again, because it is not possible to model exactly the “brake blending” that is tuned on real components), while the use of a different reference driving cycle could modify the result if the percentage and the characteristics of deceleration phases are different. However, a very small additional weight value (15 kg, that is less than 2% of vehicle mass) is estimated to reduce the overall consumption up to 9–10%, thus resulting surely advantageous.

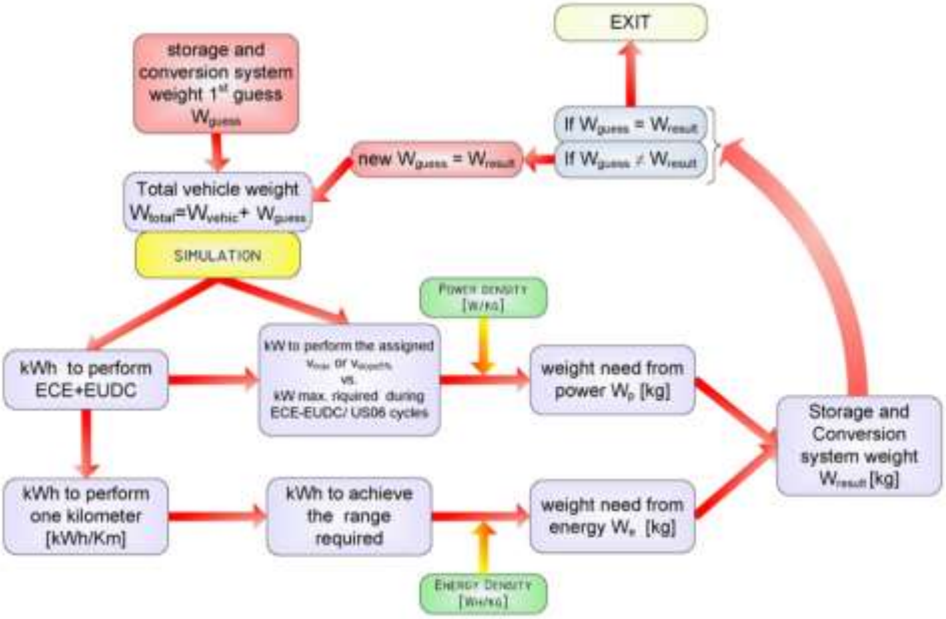
EXIT
storage and conversion system weight 1st guess W_guess
If W_guess = W_result
If W_guess ≠ W_result
new W_guess = W_result
Total vehicle weight W_total=W_vehic+ W_guess
SIMULATION
POWER DENSITY [W/KG]
kWh to perform ECE+EUDC
kW to perform the assigned V_max or V_slope% vs. kW max. riquired during ECE-EUDC/ US06 cycles
weight need from power W_p [kg]
Storage and Conversion system weight W_result [kg]
kWh to perform one kilometer [kWh/Km]
kWh to achieve the range required
weight need from energy W_e [kg]
ENERGY DENSITY [WH/KG]

Figure 63 – Iteration procedure to be used for storage and conversion system sizing.

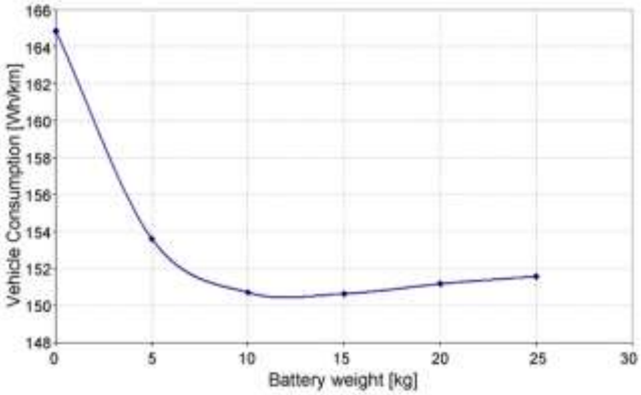

Figure 64 –Sizing of additional battery for fuel cell electric vehicle: the vehicle consumption can be expressed depending on the mass (weight) of the battery used.

The result of the calculation in terms of Tank to Wheel energy consumption is shown in Figure 65; it is evident that the sensitiveness of TTW consumption for battery vehicles depending on installed energy (expressed as achievable range) is much higher than Hydrogen vehicles due to the low energy density of batteries. It is remarkable to note that, currently, the threshold of 150–200km range has not been exceeded by last generation, mid–size electric vehicles (e.g. Mitsubishi I–MIEV, Nissan Leaf), while larger values (up to 300–400km) have been declared only for higher class vehicle (Tesla Model S).

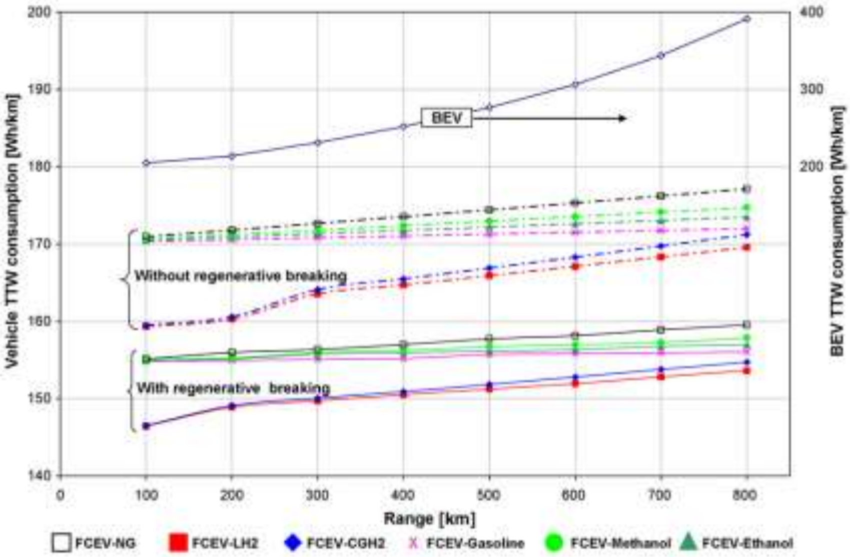

Figure 65 – Tank to Wheel vehicle consumption for different configurations.

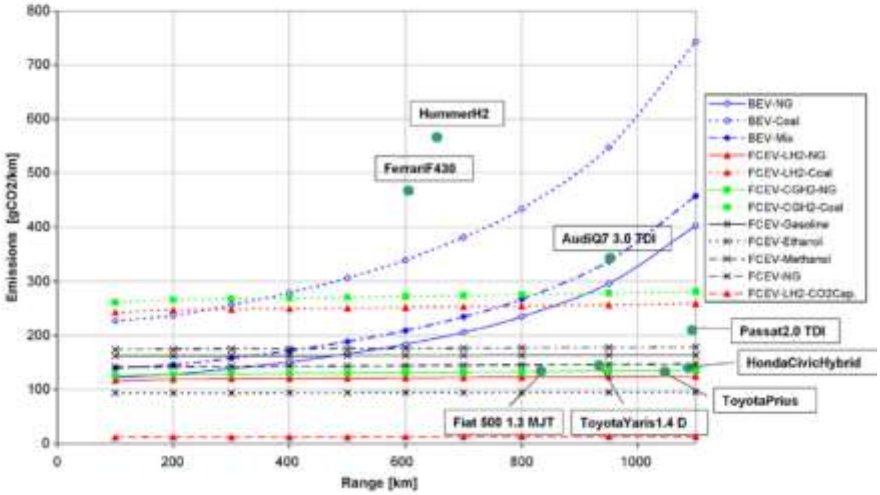

Figure 66 – Well to Tank CO_2 emissions of different vehicle configurations considering target range. Values corresponding to commercial vehicle (both ICE and HEV) are also indicated.

Figure 66 shows the final results of the comparison: coherently with other analysis, the environmental impact (expressed as CO_2 emissions) of electric vehicle is comparable with ICE powered ones, if primary sources are fossil fuels (including current Italian electric energy mix).

4. An introduction to driving cycles

Chapter 3 illustrated the main criteria that have to be considered for the estimation of vehicle performances, starting from preliminary sizing phases and archetype confrontation.

The capability to achieve a set of minimum performances (e.g. top speed, gradeability) is the first criterion used to define the very early attributes of the vehicle in terms of traction power and, as a consequence, of main powertrain characteristics. After that, the *power sizing* design phase needs the verification of vehicle ability to "follow" a pre–determined speed signal; in the Figure 54 example, a sequence of constant acceleration, constant speed and constant deceleration phases is used: such "trapezoidal" driving cycle is called "New European Driving Cycle" – NEDC. The NEDC is indicated as a reference test methodology for vehicle type approval in Europe: see Regulation (EC) No. 715/2007 and other related Directive and Regulations (e.g. former Directive 70/220/EEC, former Directive 80/1268/EEC, UNECE Regulation R101). The NEDC can be used also during the *energy sizing* design phase of the vehicle, so that the energy consumption of the vehicle can be expressed in terms of energy units over distance units (e.g. Wh/km). However, such data is influenced by the choice of the cycle: it can be easily verified that the use of different cycles could result in different results. Within this work, real–world driving data have been acquired and processed in order to build EV reference cycles.. A motivation for a depth study of driving cycles is the need for "tailored" cycle applicable to a local, specific context and to certain vehicle categories; this exigency has also been highlighted by the participation to the already cited ASTERICS project.

This chapter deals with the definition of driving cycles; it includes a brief literature review of main available driving cycles and the description of the methods used to describe, to classify and to build them.

4.1. The relevance of vehicle mission selection

In general, a large number of factors are acting on the energy consumption, including driver capabilities, driving context (city, countryside, highways), traffic conditions, ambient temperature etc.: such variability is the reason determining the need for extensive testing on the road of any kind of vehicle during its final development phase. In order to reduce the cost of such critical phase, virtual testing and testbed methodologies are used, and in this controlled contexts a "representative" driving cycle is needed as input. A driving cycle can be considered as a standardized procedure aimed to evaluate vehicle performance in a reproducible way under laboratory conditions, such as simulation environment, power–adsorbing chassis dynamometer and/or testbed. It has to include a time–vehicle speed signal as main input data, but a large set of boundary conditions can be also defined: dynamometer settings, gear shifting points, reference atmospherics conditions (wind, humidity, pressure, temperature,..), vehicle conditions (tyre pressure, lighting, oil viscosity..), “cold start” conditions (critical, for different reasons, both for ICE and EV vehicles) and any parameter influencing the performances of the application.

It is therefore clear that a single “driving cycle” cannot represent *all* the possible conditions on which the vehicle could be used during its life, but that some kind of compromises are needed. Despite of the fact that the research started in the early ‘70s, the definition of driving cycles is still a topic under development in scientific and technical literature. In the legislative context, acceptance test plans over standardized driving cycles are included in the type–approval procedures. The assessed parameters are mainly related to the evaluation of the environmental impact of the vehicle; in case of ICE, in fact, the attention has been focused on air pollutants and fuel consumption, which is related to GHG emissions. Currently a very large number of driving cycles are used worldwide: e.g. EU cycles, US cycles, Japanese cycles. They mainly differ on:

a) kind of vehicle (different vehicle class – e.g. light or heavy duty, low powered vehicle, motorcycles)
b) load patterns (entity of transient phases)
c) context of applicability (urban, extra urban, motorways)
d) expected vehicle mission (e.g. private use, freight delivery, bus service, etc...).

In most recent formulation, the performances of FEV and HEV can be also taken into account through the use of weighting formulae for electric energy consumption and fuel combined consumption (see UNECE Regulation R101 for further details). One important limitations that has to be taken into account is that the duration and/or the total length (in terms of run distance) of any driving cycles is limited by practical needs both during simulation and test–bed execution; typical duration are in the range of 500–1500s, while typical distances are in the range of 5–15 km.

EVs introduce new parameters for the evaluation of their performances and are affected by specific, new criticalities in comparison to conventional vehicles. A brief list of such new factors include:

- the possibility of energy recovery during braking, which could induce drivers to modify their style in order to optimize their energy consumption
- the limited range (about 150km on optimal conditions for most EVs currently on the market) that could induce drivers to particularly smooth, benign driving style. Some specific conditions (e.g. occasionally high daily distance driven, unavailability of charging points) are in particularly determining the so–called “range anxiety” phenomena
- a different “perception” of vehicle performances, due to different acoustic sensations, throttle feeling, and torque availability from the powertrain
- a different sensitiveness of the vehicle to the use of auxiliary systems.

In this section, the elements of a methodology for the build–up of representative cycles are presented using both literature information and data coming from authors’ experiences. Such methodology will the applied on selected case studies. The main aim of the whole activity is the definition of a subset of driving cycles for electric vehicles performance evaluation.

Driving cycle analysis and development has been widely described in literature. A wide review on the topic has been presented in the recent work by Tong and Hung (2010), that can be assumed as main reference document; therefore, it is not explicitly cited in the following paragraphs.

4.1.1. Classification of driving cycles

According to the work by Barlow et al., 2009, more than 250 driving cycles are currently available in literature. Driving cycles can be classified in different manner depending on their origin and on their suitable application field. Main distinctions are based on:

- legislative character: defines its main scope (regulation and/or research)
    - *legislative driving cycles* are used for type approval according to the jurisdictions of the considered States. Main examples are the NEDC driving cycle (including both ECE15 segment and EUDC segment) having legal value in Europe, the Japaneses 10–15 mode cycles, the US cycles such as FTP–72, FTP–75 and similar
    - *non–legislative driving cycles* are built for scientific or applied research and are used by carmakers, developers and researchers in order to investigate vehicle performances in detail. Cycles can be used for fuel consumption and exhaust emission estimation: sometimes the estimation has a wide range of representativeness, sometimes is focused on the analysis of specific case studies. The *Artemis* cycles (André, 2004), as an example, are designed to be representative of European driving conditions, one of the goal being the construction of a European emission inventory; the validity is wide, but a few main subset of data have also been proposed (urban, rural road and motorway being the main cycles). The work by Wang et al., 2008, presents different cycles each one being representative of a different city: in this case, the aim is to distinguish in detail the local patterns.
- signal source and related shape: depending on the data used as input, the synthetic cycles can be distinguished at a first “look” in two main categories
    - *modal* or *polygonal driving cycles are* composed by a sequence of steady state modes; there is a general agreement since early research years (see Lyons et al., 1986) that such kind of synthetic cycles do not accurately describe transient accelerations, therefore resulting in a loss of detail in terms of estimated output data (e.g. emissions). The NEDC is an example of polygonal driving cycle
    - *transient driving cycles* are developed starting from on road driving data, which are processed, divided in segments and assembled using suitable procedures. The ETC is an example of transient driving cycle. These cycles are also defined as “real world” derived. Usually, altitude variation is not part of driving cycles, even if it come from real–world data;
- vehicle class and/or power class: for any vehicle, the characteristics of typical accelerations and achievable speed depend on power/mass ratio, different typical use from users, specific limitations (e.g. top speed is limited to 80 km/h for heavy

vehicles in Europe). For this reason, for each driving cycle the field of applicability has to be clarified. Main classes are:
    - *motorcycles* (e.g. Saleh et al., 2009)
    - light vehicles
        - N1–M1 classes (e.g. ECE 15, EUDC, NEDC)
        - low–powered classes (e.g. low power EUDC)
    - heavy vehicles (e.g. ETC)
- cycle specific applicability: depending on the information from which the cycle has been developed, the applicability of the cycle can be almost general or specific for particular use. Some examples are:
    - *general suitability cycles*: the work by Lee and Filipi (2011) offers a few cycles suitable for a large area, due to the amplitude of data used as input; the aim is not to represent a specific pattern, but is an averaged results of the large input dataset
    - *service–specific cycles*: if the input data is related to a driving situation having strong peculiarities, its validity cannot be general, but the resulting cycle can be used for the analysis of specific situation
        - *delivery service cycles*: the delivery of small freights in a urban context is a particular service characterized by frequent stops, thus resulting in an overall high fuel consumption; the Artemis LDV_PVU cycles are representative of light van delivery typical services.
        - *buses services*: public transport vehicles are subjected to systematic stops, so that the cycle is determined both from casual factors (traffic) and from known factors (stop intervals); specific cycles, different from other heavy vehicles, have therefore been developed. The Manhattan bus cycle is an example of such driving cycle class.

A few examples of driving cycles are presented, in order to clarify main distinctions exposed above. Figure 67 and Figure 69 (which is also related to Figure 70) represent two cycles suitable for similar applications (light vehicle in general urban/extraurban use); the comparison between their appearance shows the differences related to the selection of polygonal shapes and real–world transient derived shapes. Note that an alternative high–speed cycle for low powered vehicles is presented in Figure 68.

Figure 71 and Figure 72 shows two examples of cycle applicable to heavy vehicles. The first is the ETC, so that it is a legislative cycle mainly developed for the evaluation of diesel engine emission. The second one is specific for bus services, so that its patterns shows main stops being separated by very similar distances. Figure 73 shows one of the results of ARTEMIS research project; in particular, this complete sequence includes urban, rural road and motorway sequence; its distance is about 52km. Since ARTEMIS project has taken into account the data coming from extensive vehicle testing, other cycles have been developed for other contexts and other categories. Furthermore, since driving cycle analysis has been mainly conceived as an emission assessment methods, strong research efforts have been concentrated on the correlation of driving data, ICE performances and air emission; this part is not included in the present study.

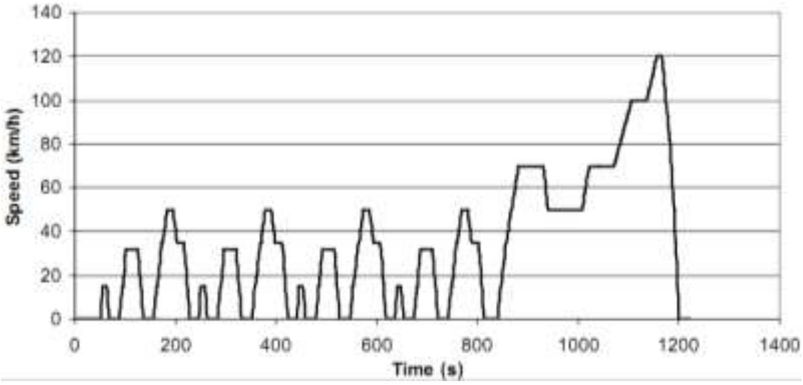

Figure 67 – The NEDC is composed by four repetition of low speed cycle (0–800s) and one high–speed cycle (800–1400s). It is the reference cycle for European N1 and M1 vehicles. Different alternatives are derived (e.g. the initial idle time is reduced). The total distance is about 11km. It is a "modal" cycle. An alternative cycle for the high speed phase is shown in Figure 68.

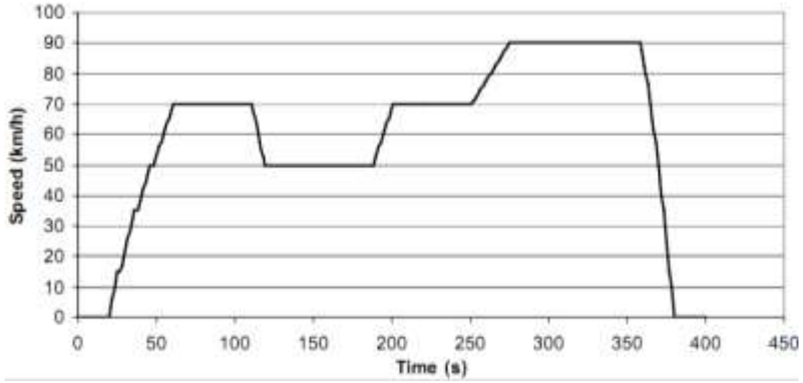

Figure 68 – The EUDC for low–powered vehicles is suitable for the analysis of extra–urban driving phase, considering that the maximum speed does not exceed 90 km/h.

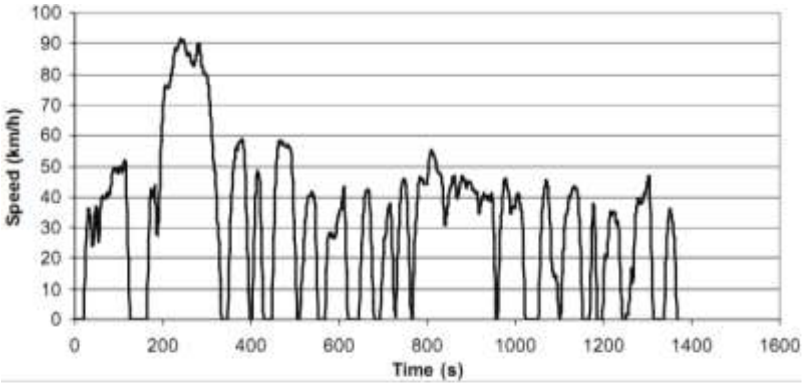

Figure 69 – The FTP–72 cycle is used for the emission estimation of light vehicles in United States. It is a legislative cycle, similarly to NEDC, but it is composed by transient signal segments. High speed segment is shown on Figure 70.

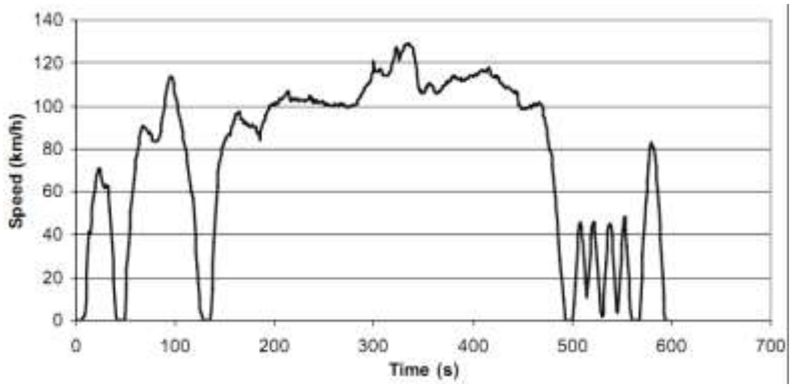

Figure 70 – The FTP–75 cycle is used for the emission estimation of light vehicles. It is a complementary to FTP–72 test phase, including high speed run.

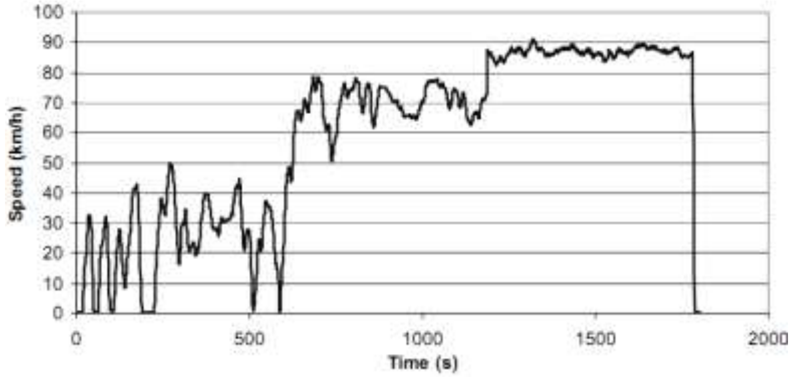

Figure 71 – ETC is a legislative cycle constituted by transient speed signals. It is suitable for heavy transport vehicles.

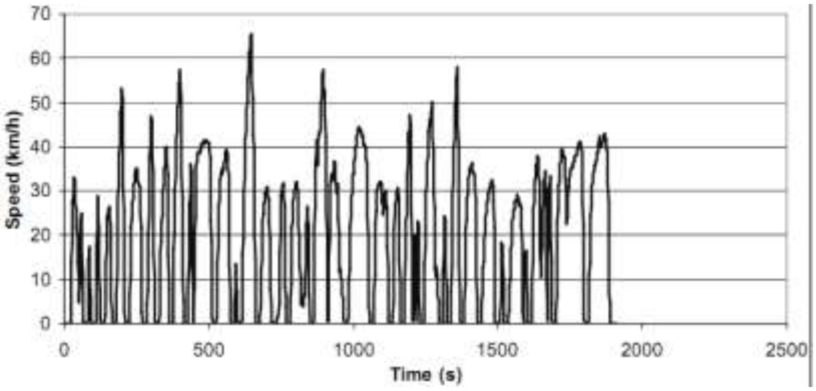

Figure 72 – Orange County Bus Cycle, developed by West Virginia University, shows typical stop–and–go expected for bus service.

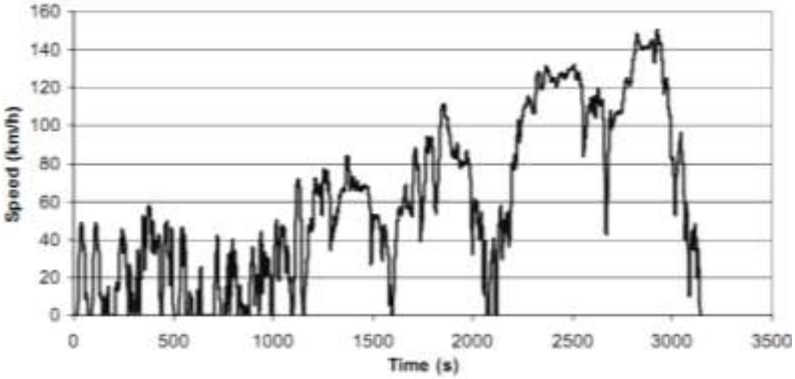

Figure 73 – Artemis common driving cycle, including urban, rural road and motorway phases. The distance of the full cycle is about 52 km.

An important note about legislative cycles is necessary. Late developments are pushing forward an harmonization of testing methodologies on a worldwide scale. The most recent initiative is the UNECE World Light duty Test Procedures (WLTP) development activity, which is still under development. As described by Weiss et al., 2011, WLTP establishes a complementary test procedure for the type approval of light–duty vehicles; due to an high randomization of the emission testing process, it is aimed to increase the reliability of emission estimation during testing for ICE vehicles, in particular during transient vehicle operation, high engine loads, low temperature phases (idling, low–load operation and so on). A large amount of information are available from the UNECE website (2013); Figure 75 shows a preliminary result of the study, that is the speed distribution for different countries and regions. Such distribution has an high information content and its use for cycle representation and classification will be described in next chapters. Figure 74 shows the most recent version of the proposed cycle (Worldwide Light Test cycle – WLTC), that comes from transient driving segment processing. The cycle, at the moment of the delivery of the present document, is still under modification; it will be delivered in different version (classes) to be adapted to local driving conditions, depending also on vehicles average power–to–mass ratio.

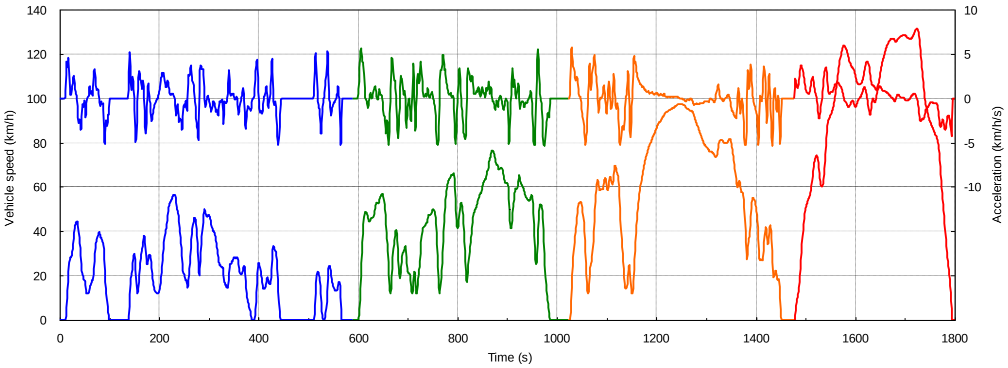

Figure 74 – Speed and acceleration profile of WLTC version 5.3 (source: Tutuianu et al., 2013).

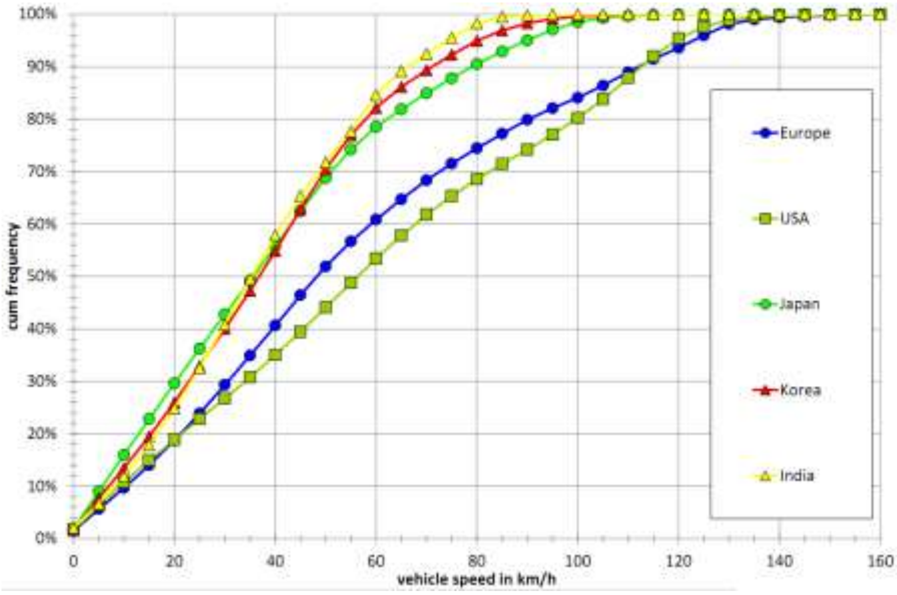

Figure 75 – Vehicle speed distribution in different regions (source: Steven, 2013).

4.2. Characterization of driving cycles

The analysis of driving cycle characteristics requires the definition and the evaluation of a set of numerical parameters to be calculated over the time–speed signal. This operation is in general needed for multiple reason, the main one being the ability to distinguish in a numerical way the different characteristics of a driving style and of a driving context: in a word, to enable the selection and the *clustering* of a signal or of its parts.

4.2.1.**Parameters defining driving cycels**

Numerical parameters are needed for the confrontation of signals coming from different measurements. Since synthetic driving cycle are coming from some kind of *compression* algorithm, the identification of numerical characteristics of input data and of output cycle also offers the possibility to validate the representativeness of the compressed cycles. In this paragraph, numerical parameters will be defined using a few reference articles, in order to define a large set of possible indicators. Most of them are included in the work by Barlow et al., 2009, which is also citing the art.kinema utility built up for former research activities on driving cycles (ARTEMIS project, see Andrè, 2006).

It is possible to distinguish six main categories of driving segment/cycles parameters depending on their physical dimension :

- distance
- time
- speed
- acceleration

- stop data (absence of speed)
- dynamics.

The full list of the parameters used within ARTEMIS is described in the work by Barlow et al., 2009; 40 parameters can be defined, and their list is provided in Table 15. In most research activities only a subset of such parameters has been considered; a few examples are the work by Hung et al., 2007, using 22 parameters; the work by Saleh et al, 2009, taking into account 12 parameters; the work by Kumar et al, using 13 parameters.

Group	**Parameter**	**Units**
Distance related	Total distance	m
Time related	Total time	s
	Driving time	s
	Cruising time	s
	Drive time spent accelerating	s
	Drive time spent decelerating	s
	Time spent braking	s
	Standing time	s
	% of time driving	%
	% of cruising	%
	% of time accelerating	%
	% of time decelerating	%
	% of time braking	%
	% of time standing	%
Speed related	Average trip speed	km/h
	Average driving speed	km/h
	Standard deviation of speed	km/h
	Speed: 75th – 25th percentile	km/h
	Maximum speed	km/h
Acceleration related	Average acceleration	m/s^2
	Average positive acceleration	m/s^2
	Average negative acceleration	m/s^2
	Standard deviation of acceleration	m/s^2
	Standard deviation of positive acceleration	m/s^2
	Acceleration: 75th – 25th percentile	m/s^2
	Number of acceleration per km	[null]/km
Stop related	Number of stops	[null]
	Number of stops per km	number/km
	Average stop duration	s
	Average distance between stops	m
Dynamics related	Relative positive acceleration (RPA)	m/s^3
	Positiv kinetic energy (PKE)	m/s^2
	Relative positive speed (RPS)	[null]
	Relative real speed (RRS)	[null]
	Relative square speed (RSS)	m/s
	Relative positive square speed (RRSS)	m/s
	Relative cubic speed (RCS)	m/s
	Relative positive cubic speed (RPCS)	m^2/s^2
	Relative real cubic speed (RRCS)	m^2/s^2
	Root mean square of acceleration (RMSA)	m^2/s^2

Table 15 – Full list of indicators usable to describe driving cycles. Their full definition is in Appendix 1.

In order to introduce the topic, it is also necessary to define the meaning of “trip” and “microtrip” words in driving cycle analysis context:

- “trip” is a sequence measured between a key–on and key–off event
- “microtrip” is a sequence measured between two stops events (e.g. from traffic light to traffic light). The number of microtrips in a trip, as an example, is therefore equal to the number of stops.

4.2.2. Performances distribution analysis

The numerical parameters above described offer an “aggregate” information of the final, average results of cycle analysis. The comparison of cycle on the basis of quantitative information needs to take into account a larger set of data describing the cycles: for this reason, the calculation of data distribution over a large range of values is usually performed in literature. Distribution can be calculated in terms of absolute indicators (e.g. time, distance) or in terms of relative frequencies (e.g. number of occurrence of an event over a class of events), and the confrontation can be built on the basis of 1–variable analysis of 2–variables analysis. The analysis, depending on the goal, can be also performed assuming that other factors are “free” or “conditioned”; it can also be based on “instantaneous” points or on “segment” data (e.g. taking into account average speed and average positive acceleration for specific microtrips, instead of the whole number of points in the signal).

Typical examples of 1–variable distribution are:

- speed–relative frequency analysis (see Figure 75), in this case expressed as cumulative curve
- acceleration distribution analysis; in Figure 76, the acceleration is shown assuming that the speed is equal to zero, thus the “speed” factor being conditioned
- idle time distribution analysis (see Figure 77)
- acceleration change (jerk) distribution analysis (see Figure 78).

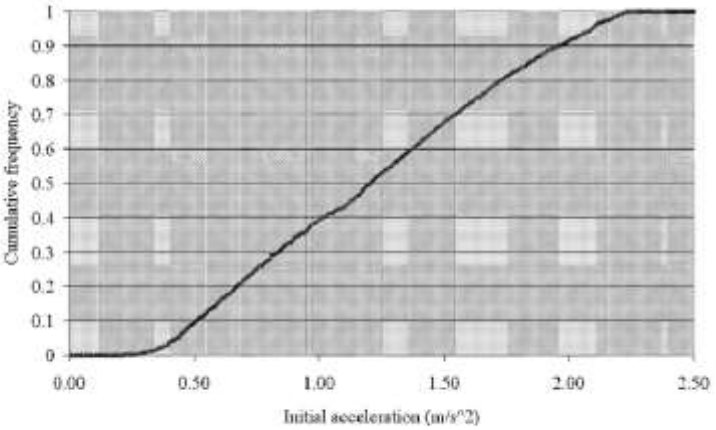

Figure 76 – Cumulative frequency of acceleration starting from speed equal to zero (source: Alessandrini et al., 2003)

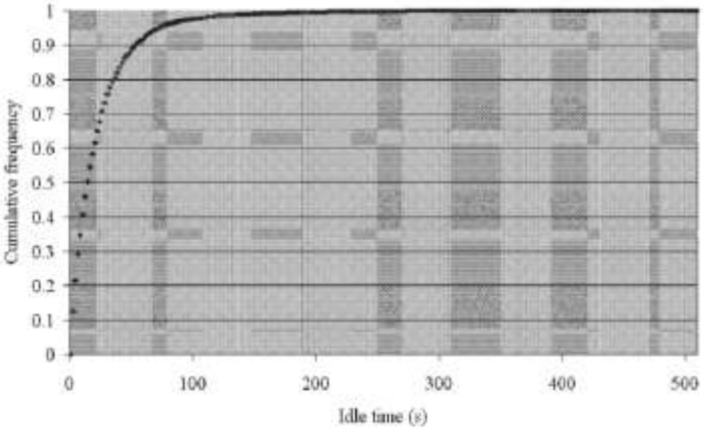

Figure 77 – Cumulative frequency of idle time (source: Alessandrini et al., 2003)

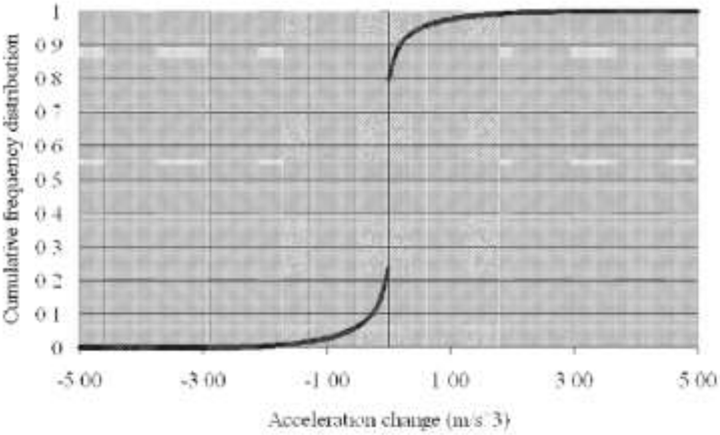

Figure 78 – Cumulative frequency of acceleration change (source: Alessandrini et al., 2003).

The scope of distribution analysis is both related data visual interpretation and for extended data processing; in particular, in case of creation of a new cycle using randomization methods, data distribution are used for the conditioned selection of sequences.

Regarding 2–variables distribution, a largely used method for cycle clustering and cycle build–up is based on the analysis of the distribution of elements falling in a determined class of speed–acceleration couples, expressed as relative frequency of occurrence or as total time. The data needs a comprehensible representation through a suitable 2D or 3D plot. Examples of plots for speed–acceleration distributions are shown in Figure 79, Figure 80 and Figure 81. In case of the use of such information for the extrapolation of a new cycle, the relative frequency assumes the meaning of "probability" of a determined occurrence; the definition used by some authors is therefore "SAPD" – Speed Acceleration Probability Distribution.

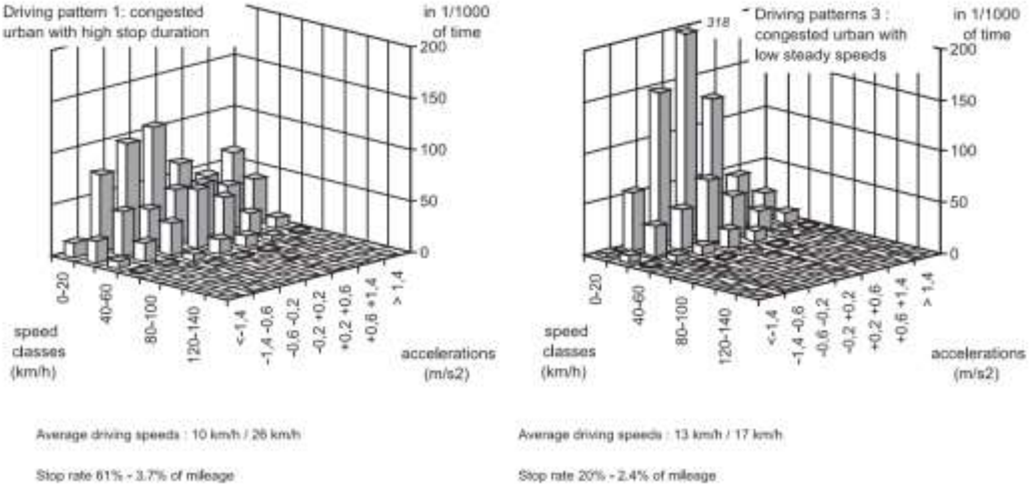

Average driving speeds : 10 km/h / 26 km/h

Stop rate 61% - 3.7% of mileage

Average driving speeds : 13 km/h / 17 km/h

Stop rate 20% - 2.4% of mileage

Figure 79 – Speed–acceleration duration shown as 3D bar plot for two different driving situation (from Andrè, 2004). In this case, the z–axis is on time units.

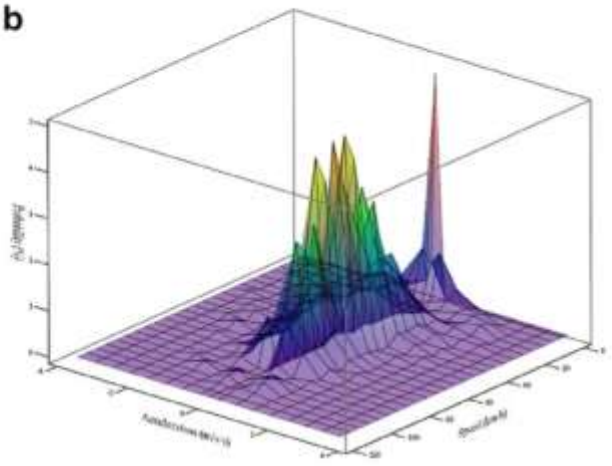

Figure 80 – Speed–acceleration relative frequency matrix shown as a 3D plot (from Hung et al., 2006). In this case, the z–axis is expressed on 0–100% units (relative frequency of each speed–acceleration class, used as probability).

	High	Ex-high
Unified distribution	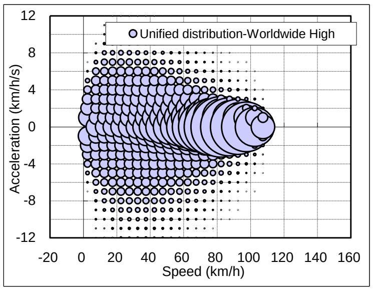	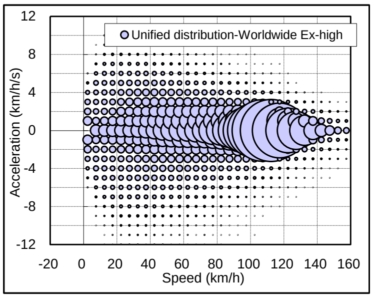
WLTC ver.1	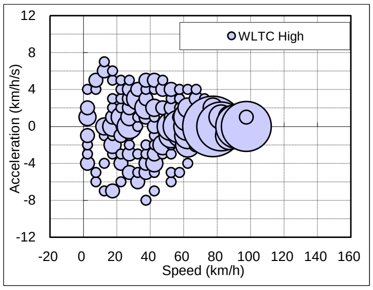	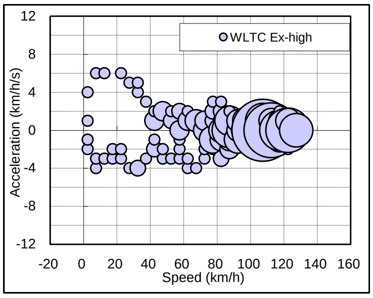

Figure 81 – Speed acceleration 2D "bubbles" plot for different datasets; the diameter of each bubble is related to the numerosity of the class (source: Tutuianu et al., 2013).

4.2.3. Clustering of driving sequences

The calculation of numerical indicators enables the possibility to build quantitative confrontation methods, in order to "stratify", to "cluster" road measurements, existing cycles as well as new cycle proposal. Main two goals therefore are:

- clustering through parameters for data pre–processing and selection
- validation of compressed cycles during post–processing, verifying their relation with original data.

The most simple analysis as described in the document by André et al., 2006, is based on the visualization of each driving segment as a function of 2 kinematic parameters; in this case, the results (e.g. a dot plot) can highlight the properties and the variability of the cycles through the visualization of clouds of different density. Suitable couples are:

- average speed/number of stops per km: as an example, urban–estimated trips (e.g. large number of stops, low speed) and extra–urban estimated trips (e.g. small number of stops, medium/high speed) tends to occupy different areas of the plot
- average speed/idle time: useful to identify the presence of urban, intense traffic
- trip duration/trip length: indicates the variability of trip distances and can identify user clusters (e.g. delivery services – short trips – in comparison to long–distance runners)

- positive/negative acceleration data: an useful plot to evaluate common couples, useful also for vehicle design (e.g. for regenerative braking tuning).

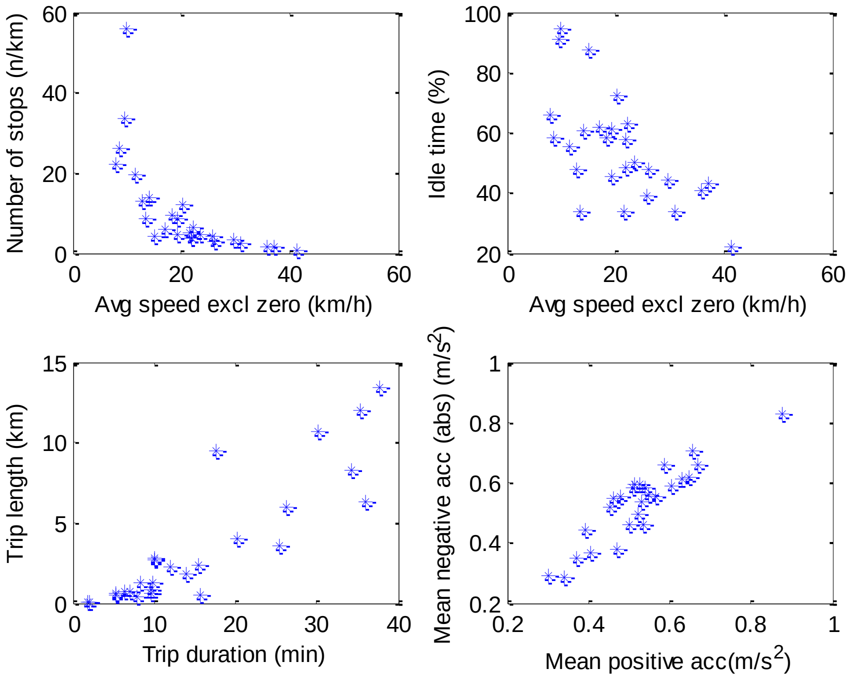

Figure 82 – Examples of driving segment dot–plots on the basis of two kinematic parameters (source: acquired data). Each dot represent a different trip event.

The main issue of this approach is the impossibility to efficiently separate clusters due the “overlap” between different but similar–looking situations (e.g. fluent traffic in urban context, slow traffic in extra–urban context). However, in order to compare data coming from known origins (e.g. urban segments and extraurban segments can be separated easily if a GPS information is available), they are still used. A question arise: which couple of parameter is preferable for useful representation in a plot?

Annex 2 shows the correlation matrix between specific parameters which is available in literature; a desirable combination is a couple of parameters having different dimension but strong correlation. According to the author of the table, “running speed” (excluding stops phases) compared with “positive acceleration” is a suitable one.

The application of the comparison criteria on existing cycles can highlight that analogous cycles (urban, rural road, motorways cycles) usually fall in similar speed/acceleration ranges. The plot in Figure 83 shows how cycles available in regulation and in technical literature fall in a large range of speed (0–140 km/h is considered) and positive acceleration (0.3–1.3 m/s^2 is considered).

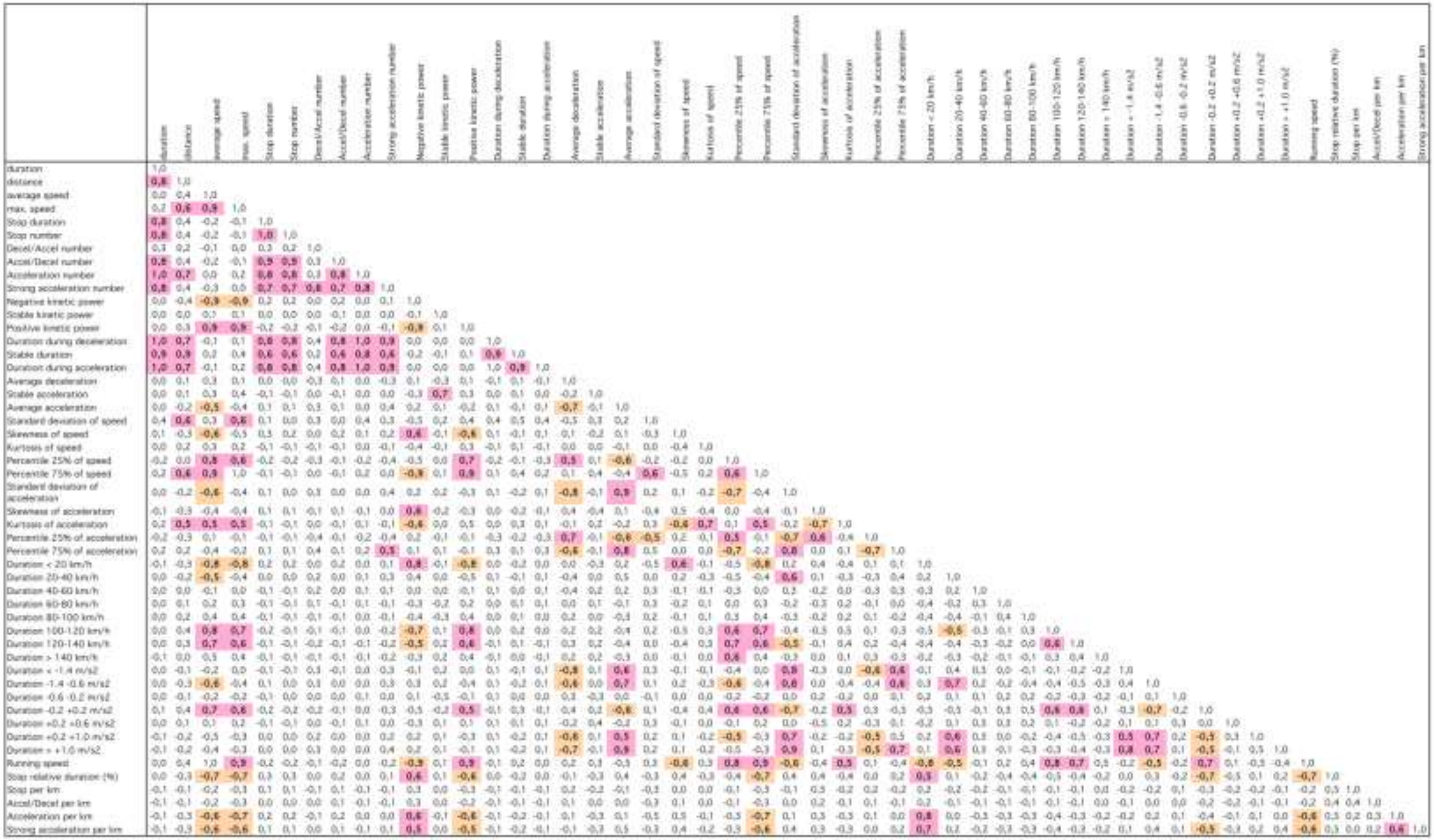

Table 16 – Correlation matrix between kinematic parameters used for the analysis of driving cycles (source: André et al., 2006a

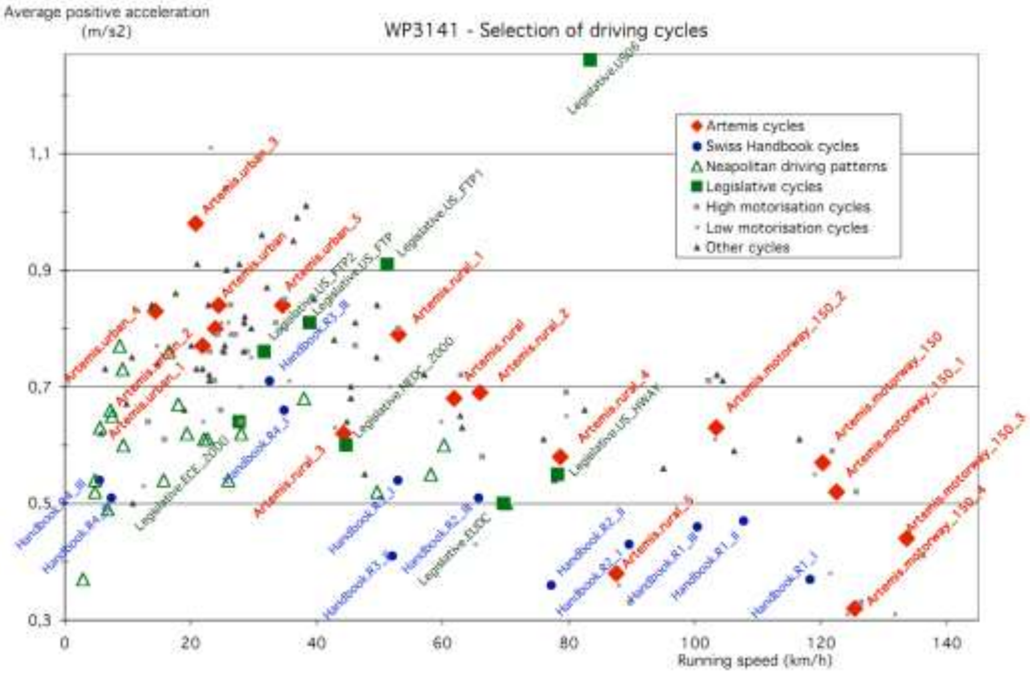

Figure 83 – Visualization of main cycles as regards speed and acceleration (source: André et al., 2006).

Other classification methods are documented in literature. The review by Tong and Hung, 2010, describes two main methods:

- the “factor analysis” of speed/acceleration patterns
    - used by Borgarello et al., 2001; used (in a different form) for ARTEMIS project and for related research activitied (André, 2004, André et al., 2006a)
- the “Fuzzy logic” analysis for the recognition of typical pattern
    - e.g. used by Liaw and Dubarry, 2007.

Our focus is on the first category of methods, which refer to the methods of multivariate data analysis; the description are adapted by the work from Jobson (1992) and Krzanowski (1988).

The first method described is the Principal Component Analysis – PCA. PCA is a multivariate technique for examining relationships within a set of quantitative variables. The methodology uses the correlation matrix to derive obtain a set of linear combinations of the input variables; such combination are called “principal components” and are orthogonal to each other. Principal components can represent the same information content of the original variables, but they can also be “ranked” on the basis of the “variance explained”. If needed, the dimension of the system using the components explaining the most part of the variance.

An application of PCA is described in the work by Borgarello et al., 2001. In this case, a number of sequences coming from measurements over the city of Bologna have been grouped through PCA. The grouping strategy was structured in the following steps:

- 15 kinematic indicators have been defined
  - stop duration
  - driving duration
  - mean on running speed, acceleration and deceleration (computed excluding the stop time)
  - standard deviation on running speed, acceleration and deceleration
  - 20% and 80% percentiles of speed distribution, acceleration and deceleration distribution
  - percentage of time with constant speed
- after outliers elimination, a PCA allowed to identify 5 new variables (linear combination of the previous variables) that explain 90% of the sequence sample variance; the two main axis explain 70% of the variance
- In the 5–dimensional space described above the sequences have been grouped in the following way
  - a non–hierarchical clustering procedure eliminated 11 multivariate outliers and grouped the other sequences in 40 pre–clusters
  - the pre–clusters have been aggregated in 12 clusters by a hierarchical procedure using the euclidean distance and the "average linkage" method
  - at the end 7 clusters have been obtained aggregating some small clusters (using indication of the average method).

The results of such grouping strategy is shown in Table 17, while the dot plot in Figure 84 shows the position of each main cycle over the two main axes.

Group Number	**Small description**	**Percentage of sequences in the group**	**Running speed mean (Km/h)**	**Stop duration mean (minutes)**	**Driving duration mean (minutes)**	**Acceleration mean (m/s^2)**	**Deceleration mean (m/s^2)**
1	Stop and go – quiet	0.23	8.40	0.20	0.30	0.54	0.52
2	Freeflow – quiet	0.24	26.00	0.30	1.30	0.45	0.58
3	Freeflow – accelerate	0.27	32.00	0.30	1.10	0.69	0.80
4	Stop and go – quiet	0.14	17.50	0.30	0.40	0.88	0.86
5	Long stops	0.03	21.00	0.90	0.70	0.67	0.75
6	Sport–short	0.04	27.00	0.30	0.40	1.15	1.30
7	Sport–long	0.04	45.00	0.50	1.10	0.90	1.11

Table 17 – Sequence of clusters recognized over measured driving data (adapted from Borgarello et al., 2001).

Within ARTEMIS activity, multivariate analysis methods have also been applied. In the case of the work of André, 2004, clustering is done on sequences having similar size (thus, resulting in different driven distance depending on their average speed) and grouped through Correspondence Analysis (based on chi–squared distance) and clustering tools, so that segments are defined according to speed–acceleration distribution. Similarly, in the case of the work performed by André et al., 2006a, the full information related to speed and acceleration distribution on considered sequences has been used. Considering 8 classes for speed and 7 classes for acceleration plus the stop duration information, 57 variables are defined, thus offering a detailed description of the speed profile. Due to the fact that the number of certain speed–acceleration couples on the whole range of possible values is very low or even zero, the authors also introduced an artificial correction on the acceleration values in order to reduce the occurrence of empty cells in the SAPD table: acceleration values are multiplied by a factor that increases linearly from 1 (at low speed) to 2 (at 140 km/h); the raw SAPD and the results after the application of such "emphasis" factor are shown in Table 18; the aim is to improve the description of the driving style especially at high speed range. A Binary Correspondance analysis method is then applied, in order to identify principal axes and to identify different classes.

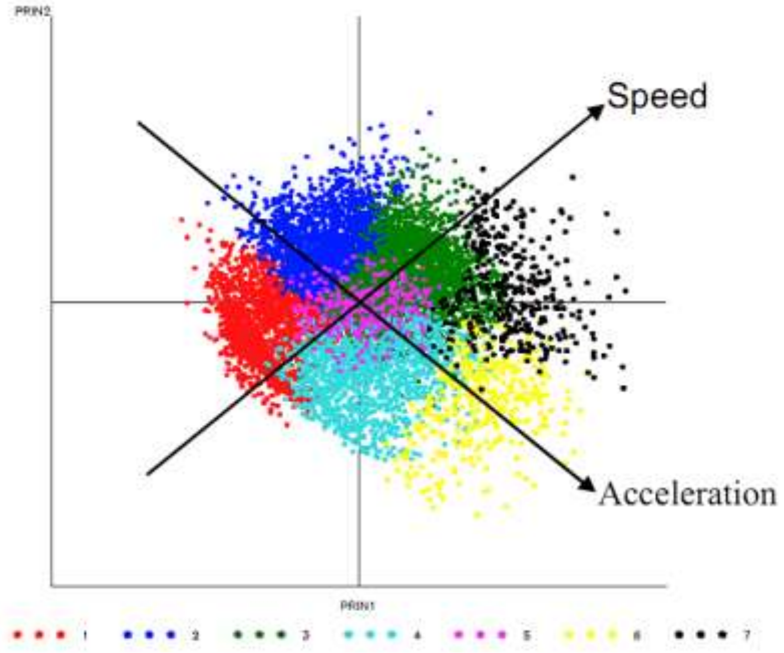

Figure 84 – Dot plot representing driving sequences on a two–axis plane; the seven categories defined are those described in Table 17. The two arrows shows approximately the increasing direction of physical quantities such as Speed and Acceleration. Main axes are two of the five generated by a PCA applied on original 15 kinematic parameters.

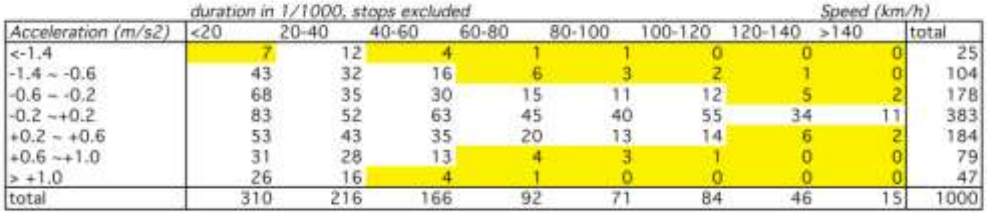

duration in 1/1000, stops excluded *Speed (km/h)*

Acceleration (m/s2)	<20	20-40	40-60	60-80	80-100	100-120	120-140	>140	total
<-1.4	7	12	4	1	1	0	0	0	25
-1.4 ~ -0.6	43	32	16	6	3	2	1	0	104
-0.6 ~ -0.2	68	35	30	15	11	12	5	2	178
-0.2 ~+0.2	83	52	63	45	40	55	34	11	383
+0.2 ~ +0.6	53	43	35	20	13	14	6	2	184
+0.6 ~+1.0	31	28	13	4	3	1	0	0	79
> +1.0	26	16	4	1	0	0	0	0	47
total	310	216	166	92	71	84	46	15	1000

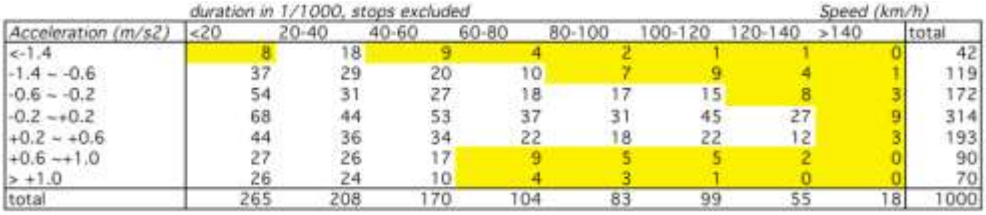

duration in 1/1000, stops excluded — Speed (km/h)

Acceleration (m/s2)	<20	20-40	40-60	60-80	80-100	100-120	120-140	>140	total
<-1.4	8	18	9	4	2	1	1	0	42
-1.4 ~ -0.6	37	29	20	10	7	9	4	1	119
-0.6 ~ -0.2	54	31	27	18	17	15	8	3	172
-0.2 ~+0.2	68	44	53	37	31	45	27	9	314
+0.2 ~ +0.6	44	36	34	22	18	22	12	3	193
+0.6 ~+1.0	27	26	17	9	5	5	2	0	90
> +1.0	26	24	10	4	3	1	0	0	70
total	265	208	170	104	83	99	55	18	1000

Table 18 – 2 dimensional speed and acceleration distribution for the driving data, before (upper table)and after (bottom table) the introduction of an emphasis factor (Andrè et al , 2006a).

The reference examples are shown: Table 19 describes the 12 classes defined within André, 2004 (in this case, each segment is a different measured trip).

Classes of driving conditions and their description			**Percentage Running of total speed mileage (km/h)**	**Running speed (km/h)**	**Average speed (km/h)**	**Stop duration (in %)**	**Stop rate (stop/km)**	**Average positive acceleration (m/s^2)**
1	Congested urban	high stop duration	3.7	25.9	10.2	60.8	3.90	0.87
2			5.9	23.6	15.9	32.7	3.00	0.81
3		low steady speeds	2.4	16.5	13.2	19.5	3.40	0.67
4	Free–flow urban		5.1	28.0	26.1	6.7	0.97	0.65
5		unsteady speeds	12.2	35.6	32.3	9.1	0.98	0.81
6	Secondary roads	unsteady speeds	10.8	52.2	48.8	6.6	0.41	0.75
7			8.8	45.5	43.8	3.7	0.39	0.63
8		steady speeds	7.2	65.0	64.0	1.5	0.15	0.55
9	Main road	unsteady speeds	11.8	75.0	72.5	3.3	0.15	0.67
0			6.2	86.1	85.7	0.4	0.04	0.48
1	Motorways	unsteady speeds	10.4	115.6	114.9	0.7	0.03	0.53
2			15.6	123.8	123.7	0.1	0.01	0.40

Table 19 – Driving conditions classes obtained by automatic clustering of speed profiles recorded on–boad vehicles (source: André, 2004).

Each sequence can therefore be associated to a cluster and visualized in simple dotplot, but adding in this case an additional information: Figure 85 (linked to Table 19) includes a color indication of the reference “cluster” for each dot.

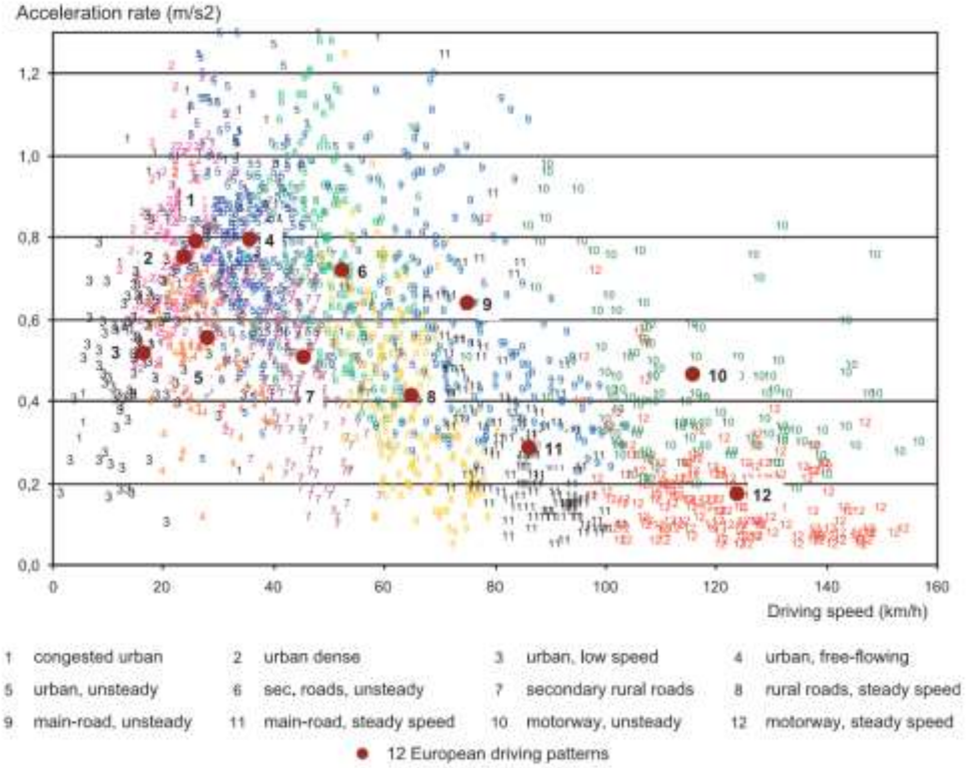

Figure 85 – Driving conditions clusters according to André, 2004, as defined in Table 19. Circle indicate the "center" of each class, while each dot represent a driving sample.

Table 20 shows another selection from the André et al., 2006a document; in this case, each examined segment is a different driving cycle. Four main classes for cycle grouping are identified. Figure 86 shows a subset of cycles dot plot, using a restricted speed range in comparison with Figure 83; all the points fall in the class of "urban cycles" according to Table 20.

Class	**Number of cycles or sub–cycles**	**Average speed (km/h)**	**Running speed (km/h)**	**Average positive acceleration (m/s^2)**	**Number of accelerations**	**Stop duration (%)**	**Number of stops/km**
1 – motorway cycles	14	121	122	0.41	0.4	0.3	0.02
2 – main roads (highways) cycles	21	92	94	0.60	1.1	1.5	0.07
3 – rural (and suburban) cycles	42	50	53	0.68	2.7	6.9	0.5
4 – urban cycles	74	15	21	0.73	8.1	29.8	5.8
All together	151	45	53	0.67	2.6	16.1	1.1

Table 20 – Average characteristics of clusters of driving cycles (source: André, 2006).

Further classification is possible. A deeper application of clustering method identifies, in the case of urban cycles, 8 different subclasses, which are described in Table 21. Figure 87 represents the urban cycles according to their secondary classification.

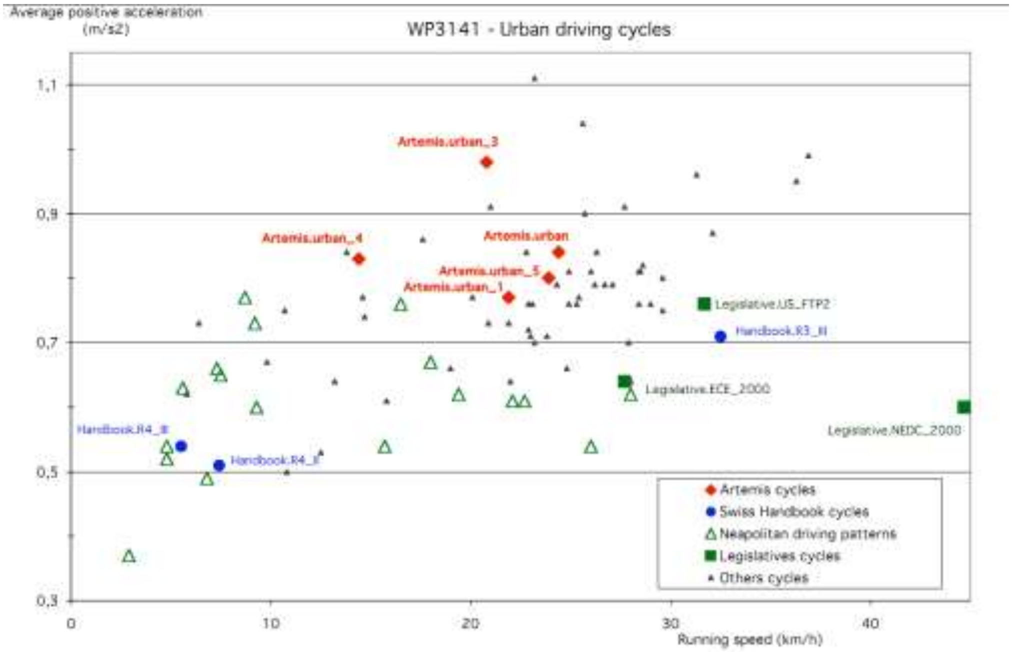

Figure 86 – Plot representing urban cycles according to speed and acceleration distribution, the clustering being done through factor analysis classification (André et al., 2006a).

Class and characteristics of the cycles	**Number of cycles or sub–cycles**	**Average speed (km/h)**	**Running speed (km/h)**	**Average positive acceleration (m/s2)**	**Number of accelerations /km**	**Stop duration (%)**	**Number of stops /km**
1 – speeds 60–80 km/h, high accelerations, high number of accelerations and strong accelerations	14	21,2	28,2	0,82	6,2	24,8	2,8
2 – speeds 40–60 km/h, low accelerations, few stops	7	25,5	29,3	0,68	4,7	13,2	2,0
3 – speeds 40 km/h, few stops, strong accelerations	14	18,2	23,6	0,75	7,4	22,9	3,3
4 – speeds 20–40 km/h, high number of accelerations and strong accelerations	13	14,8	19,0	0,72	11,5	22,2	5,3
5 – speeds 80–100 km/h and 40, strong accelerations, high speed and maximum speed	1	30,2	36,9	0,99	4,8	18,0	3,6
6 – high stop duration and number, low speed, average accelerations	10	4,6	12,5	0,73	8,7	63,6	30,0
7 – speeds 20 km/h, high number of low accelerations, low speed	2	5,2	6,2	0,52	14,5	16,1	7,7
8 – speeds 20 km/h, high stop duration and number, high number of acceleration and strong accelerations	13	5,6	8,6	0,65	21,5	35,5	26,5
All together	74	14,9	21,2	0,73	8,1	29,8	5,8

Table 21 – Driving segment classifications within urban class cluster, according to André et al., 2006a.

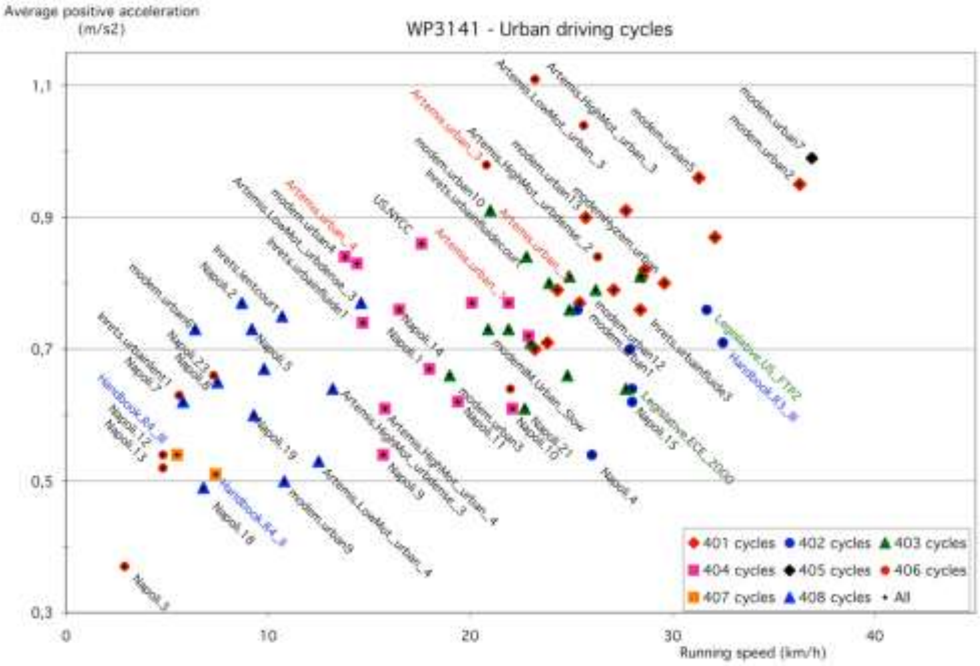

Figure 87 – Partition of urban cycles in eight subclasses (each one being represented bu a coloured symbol), according to Table 21 and Figure 86.

Similar applications are possible for each main class of cycles. In a few words, it is possible to distinguishing between events having similar general patterns (related to the context, and in particular with the average running speed); if remarkable differences can be recognized between them, sub–patterns can also be described. This data are related to driving attitudes of the driver or of the vehicle (e.g. a significantly different mean acceleration can be noticed) and to traffic conditions within the context (e.g. significantly different number of microtrips in a trip can be noticed).

4.3. A methodology for the definition of real–world driving cycles

This section is focused on the proposal of a methodology for the analysis of driving data coming from road measurements in order to develop new driving cycles. The process for the definition of a driving cycle is based on the following steps:

- road/vehicle data acquisition in a predefined context
- data pre– processing and preparation for analysis
    - outliers examination
    - filtering
- data processing
    - kinematic parameters evaluation
    - SAPD build–up
    - clustering
- cycle synthesis
    - boundary condition definition
    - data selection/randomization
    - verification
- additional data proposal
    - slope addiction
    - consumption of auxiliaries
    - environmental information

The discussion includes a step–by–step review of main literature references.

4.3.1. Data collection methodologies

The acquisition of data from vehicles usually can comprehend a large number of parameters, main categories being:

- signals coming from on board vehicle sensors
    - speed
    - acceleration (longitudinal, lateral, yaw etc.)
    - powertrain parameters (rpm, throttle position, engine parameters if ICE, battery/inverter/powertrain parameters if EV or HEV)
- signals coming from GPS sensors
- signals coming from emission measurement system (for ICE and HEV, see Alessandrini et al., 2009).

Within the case studies of this work, emission measurements will not be taken into account. GPS data will be used mainly for georeferencing and altitude recognition, since the speed assessment through that is subjected to approximation and unreliability, especially in urban context (due to so–called "tunneling" phenomena, that is signal alteration within obstacles such as buildings).

Regarding the selection of drivers and of their route, there are two main alternatives:

- on board measurement of vehicle/fleet monitoring
- "chase" car approach.

The reliability of the first method is related to the size and the characteristics of the monitored fleet itself. The more varied data are acquired (number of drivers, of vehicles, distance run), the more the acquired data are appropriate to fit the real characteristics of the fleet under study. A large data collection could be therefore necessary. The second method is widely used for the acquisition of data in order to represent the characteristics of the driving style on a specific area (e.g. to identify local driving patterns). Car chasing consists in following a varying "target" vehicle (randomly selected) with another vehicle; a trained driver is therefore needed, while the measurement is performed on the chasing vehicle even if the characterization is related to the "target" vehicle. The main advantage of the method is the possibility to acquire a large amount of data related to a population within its operating area, while the main disadvantage is the risk of data deformation: chased and chasing vehicle transient speed difference could occur, or chasing vehicles could interfere with chased vehicle, thus influencing the driving style.

The minimum data acquisition frequency should be at least 1Hz, that is also the value used for the signals defining most existing driving cycle. However, the work by Corti et al., 2012, showed that vehicle energy consumption and efficiency can be evaluated with acceptable results using low sample rates (0.2 – 1Hz) if a compensation technique is provided, but that higher sampling rate (from 2Hz to 10Hz) provide more accuracy and reliability for vehicle efficiency characterization due to the possibility to better describe vehicle dynamics.

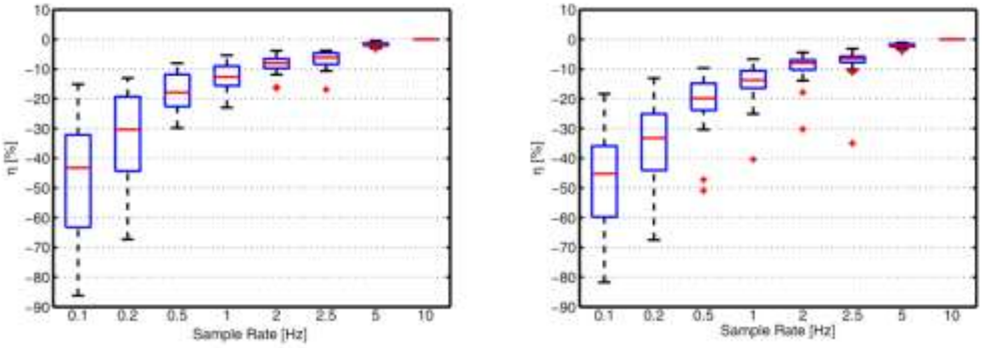

Figure 88 – Box plot of the error on estimation of vehicle efficiency obtained with the same car during different days, using a constant time window (t=100 s) and different sampling rate for speed acquisition (source: Corti et al., 2012).

A comparison of the effect of sampling rate for the determination of efficiency shows that, assuming 10Hz samples as reference values for the calculation of reference efficiency, 5Hz provide very good accuracy: the cited authors highlight that in this case the average error on a number of acquisition of 100s is –1.5% with a standard deviation if 0.812% (see Figure 88).

4.3.2. Pre–processing and preparation for analysis

During pre–processing of data, the first need is to verify the continuity of the information: data affected by strong cold–start uncertainties, large signal lack or similar should be rejected. GPS devices, however, sometimes include self–correction algorithm. Also, if a fleet is monitored on naturalistic conditions, some events should be excluded from driving patterns analysis (e.g. parking phases).

After that, the data signal should be analyzed and appropriately filtered. The work by Jun et al., 2006, describes advantages and disadvantages of main suitable filtering methodologies for GPS data:

- Piecewise polynomial regression model
- Kernel–based smoothing methods
- Discrete Kalman filter
- Modified Kalman filter

Other experiences (Alessandrini et al., 2006) use filtering techniques set at fixed cutting frequency (0.5Hz).

Haan and Keller (2001) used an arithmetic filter expressed as:

$$v_{smoothed}(t) = \frac{1}{h}\sum_{-h}^{h} s\,K\left(\frac{s}{h}\right) v(t+s)$$

The function *K(x)* is a weight for the measured velocity before and after the time t, while h is the amplitude of the filter data over the time. The shape of such “biweight” kernel function is shown in Figure 89.

$$K(x) = \begin{cases} \frac{15}{16}(1-x^2)^2\ (x^2<1) \\ 0 \quad otherwise \end{cases}$$

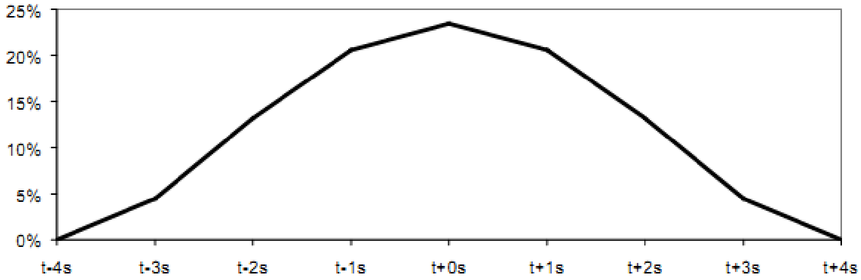

Figure 89 – Biweight smoothing kernel function used by Haan and Keller, 2001, for a duration of h=4s.

4.3.3. Driving data processing

The processing of driving sequences comprehends the evaluation of kinematic parameters, the build–up of SAPD matrices and, finally, the separation in clusters, as it has been already described in chapter 2.

Depending on the method applied for cycle compression, grouping of trips and microtrips can be a critical phase, since the selection of appropriate class–related segments for context (urban, rural, motorway) and for vehicle power determines the results of all subsequent activities. The work by André et al., 2006b, shows the results in terms of average distance run at each trip class (see Table 22) and the different acceleration distribution between two categories of vehicles, here described as “low powered” and “high powered” (see Figure 90). Therefore, the addiction of this a–priori classification has two main consequences:

- during cycle synthesis, different SAPD are used if target vehicles have a significant difference in mass–to–power ratio
- the length of each subphase of a cycle (urban/rural/motorway) can be set according to the “typical” mission expected during the life of that kind of vehicle.

Vehicles	**Trip class**	**% of distance**	**Running speed (km/h)**	**Average speed (km/h)**
High–powered cars	Motorway	35.0	98.0	94.0
	Rural	42.0	55.0	48.0
	Urban	24.0	31.0	23.0
	All	100.0	53.2	44.0
Low–powered cars	Motorway	20.0	96.0	91.0
	Rural	48.0	53.0	47.0
	Urban	33.0	31.0	22.0
	All	100.0	46.2	37.2

Table 22 – Trip characteristics and distribution (in terms of total distance run) for two main classes of vehicles. Adapted from André et al., 2006b.

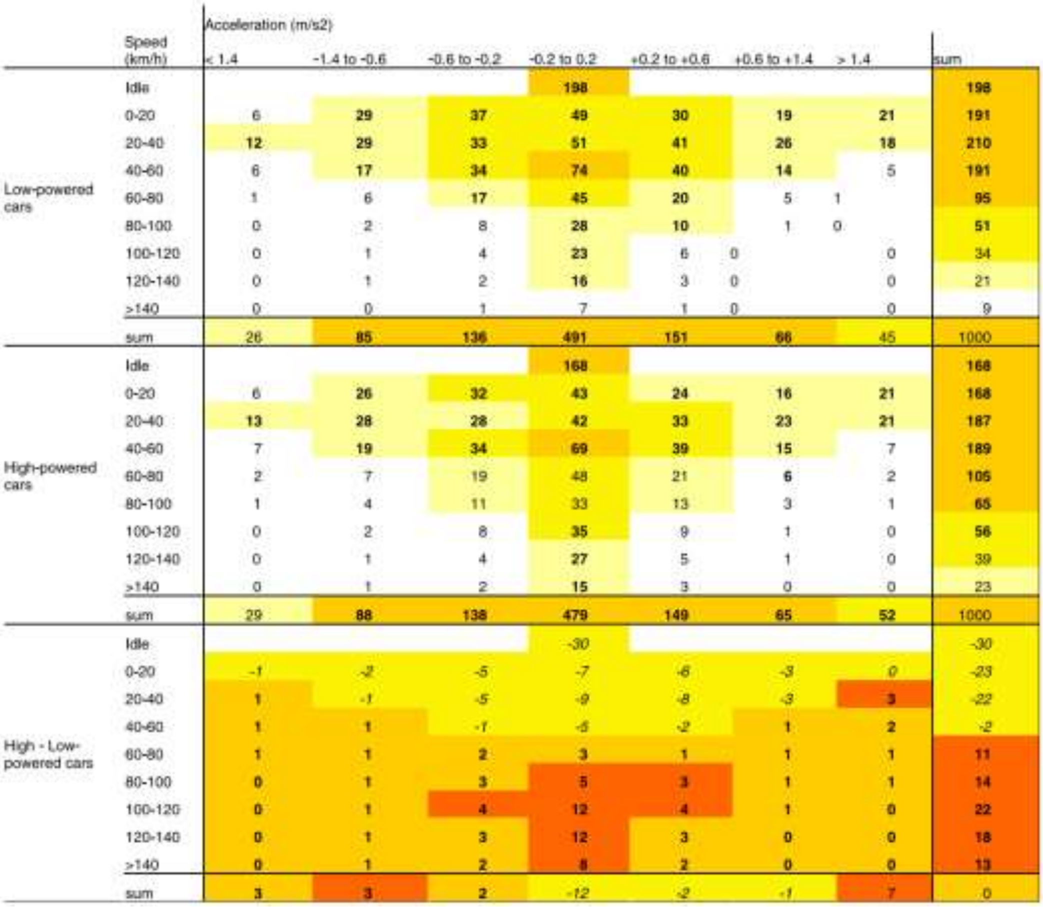

	Speed (km/h)	Acceleration (m/s2)							
		< 1.4	-1.4 to -0.6	-0.6 to -0.2	-0.2 to 0.2	+0.2 to +0.6	+0.6 to +1.4	> 1.4	sum
Low-powered cars	Idle				198				198
	0-20	6	29	37	49	30	19	21	191
	20-40	12	29	33	51	41	26	18	210
	40-60	6	17	34	74	40	14	5	191
	60-80	1	6	17	45	20	5	1	95
	80-100	0	2	8	28	10	1	0	51
	100-120	0	1	4	23	6	0	0	34
	120-140	0	1	2	16	3	0	0	21
	>140	0	0	1	7	1	0	0	9
	sum	26	85	136	491	151	66	45	1000
High-powered cars	Idle				168				168
	0-20	6	26	32	43	24	16	21	168
	20-40	13	28	28	42	33	23	21	187
	40-60	7	19	34	69	39	15	7	189
	60-80	2	7	19	48	21	6	2	105
	80-100	1	4	11	33	13	3	1	65
	100-120	0	2	8	35	9	1	0	56
	120-140	0	1	4	27	5	1	0	39
	>140	0	1	2	15	3	0	0	23
	sum	29	88	138	479	149	65	52	1000
High - Low-powered cars	Idle				-30				-30
	0-20	-1	-2	-5	-7	-6	-3	0	-23
	20-40	1	-1	-5	-9	-8	-3	3	-22
	40-60	1	1	-1	-5	-2	1	2	-2
	60-80	1	1	2	3	1	1	1	11
	80-100	0	1	3	5	3	1	1	14
	100-120	0	1	4	12	4	1	0	22
	120-140	0	1	3	12	3	0	0	18
	>140	0	1	2	8	2	0	0	13
	sum	3	3	2	-12	-2	-1	7	0

Figure 90 – SAPD for low–powered cars and high–powered cars over common acceleration classes. The third rows of the table shows the difference between the two classes. From André et al., 2006b.

4.3.4.Methodologies for data synthesis

According to the early work by Lyons et al., 1986, in general *a time–speed history of "real" driving is selected from the assembled data in such a way that it matches the overall summary characteristics of the data set. This can be a contiguous sequence or part sequence of driving along a particular route, a selectively reduced longer trip along a particular route or a composite of randomly mixed and matched microtrips from the survey data, usually involving some trial and error to achieve the correct statistical characteristics. Such cycles contain many of the transient events characteristic of real driving and the second–by–second speed values are usually specified to 0.1 km/h*. From such early work, a large number of applications of similar methods has been proposed. A synthesis method usually is composed by three main phases:

- using the available database of driving sequences and of the associated of kinematic parameters (see former paragraph), a number of microtrips or segment is randomly selected according to the desired characteristics of the cycles (representativeness of proportion for each class)

- sequences are “glued” according to “matching” criteria
  - a reference order for the sequence of classes can be imposed (e.g. see Figure 91)
  - coherence in terms of final speed of the preceding segment to the speed of its next segment; in case of microtrips linking, speed is zero, so that a duration for stop phase is needed together with an acceleration value
- once that the target duration has been reached, a verification of the representativeness of the cycle is performed.

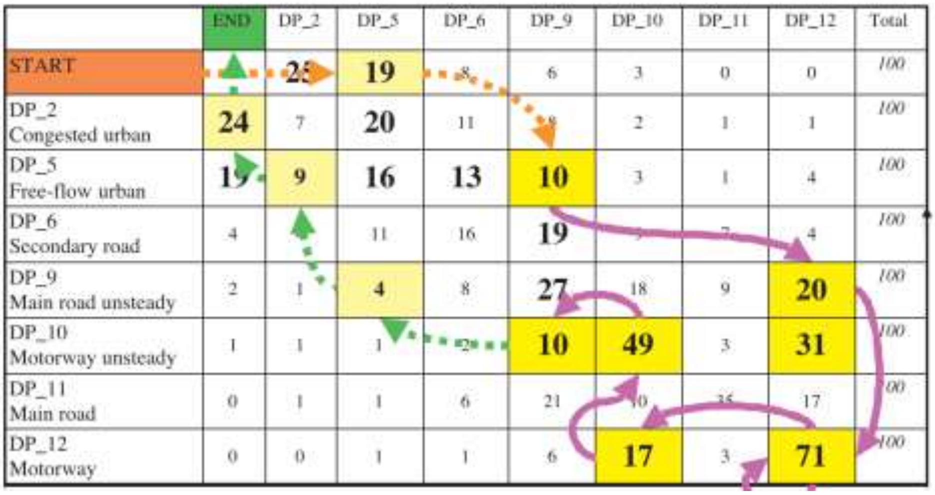

	END	DP_2	DP_5	DP_6	DP_9	DP_10	DP_11	DP_12	Total
START		25	19	8	6	3	0	0	*100*
DP_2 Congested urban	24	7	20	11	9	2	1	1	*100*
DP_5 Free-flow urban	19	9	16	13	10	3	1	4	*100*
DP_6 Secondary road	4		11	16	19	5	7	4	*100*
DP_9 Main road unsteady	2	1	4	8	27	18	9	20	*100*
DP_10 Motorway unsteady	1	1	1	2	10	49	3	31	*100*
DP_11 Main road	0	1	1	6	21	10	35	17	*100*
DP_12 Motorway	0	0	1	1	6	17	3	71	*100*

Figure 91 – Chronology of traffic conditions for the selection of the driving sequences to develop a representative cycle; the numbers in the tables represent the probability to get from a driving condition on x–axis to a driving condition on y–axis (source: André, 2004).

A few examples of existing procedures will be presented. The flowchart on Figure 92 can be assumed as a general methodology common to many approaches; the boxed section includes the main phases of cycle synthesis:

- selection of segments (microtrips) to form a cycle and “gluing” of them
- process data to get kinematic parameters, here represented by the symbol $\underline{\vartheta}_i$, that is the vector of a set of kinematic parameters (according to Table 15) for the obtained dataset (average)
- the vector $\underline{\vartheta}_i$ is compared with vector $\underline{\vartheta}_t$, that includes kinematic parameters for the starting dataset
  - if the tolerance is within the desired error (e.g. 5% is a common value), the cycle is accepted.

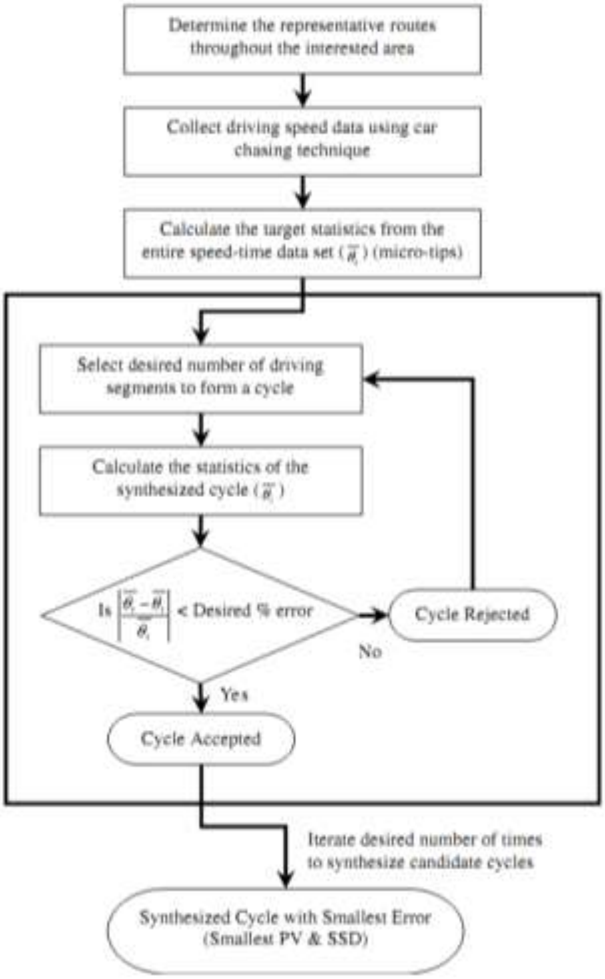
Determine the representative routes throughout the interested area
Collect driving speed data using car chasing technique
Calculate the target statistics from the entire speed-time data set ( ) (micro-tips)
Select desired number of driving segments to form a cycle
Calculate the statistics of the synthesized cycle ( )
Is < Desired % error
Cycle Rejected
No
Yes
Cycle Accepted
Iterate desired number of times to synthesize candidate cycles
Synthesized Cycle with Smallest Error (Smallest PV & SSD)

Figure 92 – Flow chart for driving cycle definition according to Hung et al., 2007.

An example of detailed description of sequence selection comes from Lee and Filipi, 2011. The cycle is built using Markov chain approach, assuming that future states depend only on the present state and independent from the past states. In other terms, *a Markov chain is a sequence of random variable* X_1, X_2, *X3,.. with the Markov property expressed as:*

$$P\left(X_{n+1}=x_{(n+1)}|X_1=x_1,X_2=x_2,..,X_n=x_n\right)=P\left(X_{n+1}=x_{(n+1)}|X_n=x_n\right)$$

The set of possible values that the random variables X_n can take is called the state space of the chain. The conditional probabilities

$$p_{ij}:=P(X_{n+1}=j|X_n=1)$$

are called transition probabilities. In this study, we used time–independent transition probability (or time–homogeneous Markov chain) while synthetizing cycles. The sum of all probabilities leaving a state must satisfy

$$\sum_j p_{ij} = \sum_j P(X_{n+1} = j | X_n = 1) = 1$$

Considering that the dynamics of the vehicle can be represented by its speed and acceleration, these two are selected as representative of the state–space of the chain; the SAPD is the matrix used for the selection of the sequences within the chain.

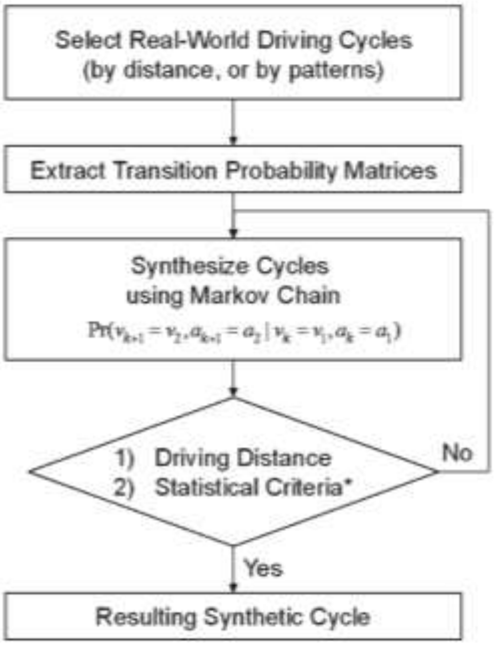
Select Real-World Driving Cycles
(by distance, or by patterns)
Extract Transition Probability Matrices
Synthesize Cycles
using Markov Chain
$\Pr(v_{k+1} = v_2, a_{k+1} = a_2 | v_k = v_1, a_k = a_1)$
1) Driving Distance
2) Statistical Criteria*
No
Yes
Resulting Synthetic Cycle

Figure 93 – Synthesis of real–world driving cycles using Markov chain (source: Lee and Filipi, 2011).

In this case, the transition matrix is used to build completely new microtrips, since the glued sequences do not include zero–to–zero speed segments. The work by Alessandrini et al., 2004, uses a similar methodologies but an additional condition is used: for each new segment, the acceleration value is generated according to the statistical distribution of acceleration variation (jerk), that is calculated from the preceding speed–acceleration couple.

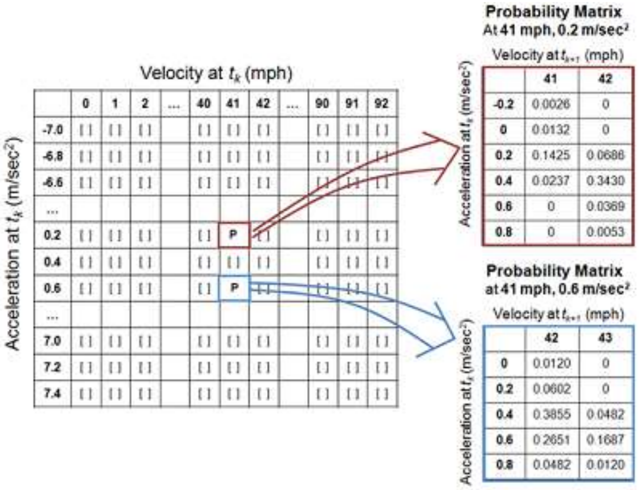
Velocity at t_k (mph)
Acceleration at t_k (m/sec^2)
0 1 2 ... 40 41 42 ... 90 91 92
-7.0 -6.8 -6.6 ... 0.2 0.4 0.6 ... 7.0 7.2 7.4
P
Probability Matrix
At 41 mph, 0.2 m/sec²
Velocity at t_{k+1} (mph)
41 42
-0.2 0.0026 0
0 0.0132 0
0.2 0.1425 0.0686
0.4 0.0237 0.3430
0.6 0 0.0369
0.8 0 0.0053
Probability Matrix
at 41 mph, 0.6 m/sec²
Velocity at t_{k+1} (mph)
42 43
0 0.0120 0
0.2 0.0602 0
0.4 0.3855 0.0482
0.6 0.2651 0.1687
0.8 0.0482 0.0120

Figure 94 – Synthesis of real–world driving cycles using Markov chain – SAPD matrix data extraction (source: Lee and Filipi, 2011).

In general, such procedure is iterated several times to obtain the satisfaction of basic matching condition. The general indication to be respected (using the already described vector $\underline{\vartheta}_t$ and a proper threshold) is:

$$\forall \vartheta_t \in \bar{\vartheta}_t, \left[\frac{\vartheta_t - \vartheta_i}{\vartheta_t}\right] < threshold$$

The choice of the parameters to be included in the vector $\underline{\vartheta}_t$ can vary from an author to another; Lee and Filipi, 2011, validated their proposal for eight parameters using a simulation model to calculate the correspondence of a large set of indicators on vehicle consumption, resulting in:

1. Standard deviation of velocity (mph)
2. Mean positive acceleration (m/s^2)
3. Standard deviation of acceleration (m/s^2)
4. Percentage of driving time under positive acceleration (%)
5. Percentage of driving time under negative acceleration (%)
6. Mean positive velocity (mph)
7. Percentage of idle time (%)
8. Number of stops/mile (1/mile).

Table 23 shows a summary of the parameters using for the validation of existing driving cycles. After that a number of possible candidate cycles are defined, additional confrontation parameters can be calculated, in order to let the user select the one having most favorable (usually, smaller) indicators:

- Performance Value – PV, that is the scalar product of the difference vector with a weight

$$PV = \left|\overline{\vartheta}_t - \overline{\vartheta}_\iota\right| \cdot W^T$$

- Lin and Neimeier, 2008, proposed the following expression:

$$PV = |\Delta\bar{v}| + |\Delta\bar{a}| + |\Delta v_{max}| \times 0.1 + |\Delta v_{min}| + |\Delta a_{max}| + |\Delta a_{min}| + |\Delta\%_{idle}| + |\Delta\bar{P}_d| + |\Delta v_{95}| + |\Delta a_{95}| + |\Delta P_{95}|$$

- Sum Square Difference – SSD – of SAPDs, that is the summary of quadratic product of the probability of each class of speed (N_s) and acceleration (N_a) for the source data (p_{ij}) and the candidate cycle (q_{ij}):

$$SSD = \sum_{i=1}^{N_S} \sum_{j=1}^{N_a} \left(p_{ij} - q_{ij}\right)^2$$

It is evident that a large number of alternatives are possible for the execution of the driving cycle development. Table 24 summarizes literature data, indicating the methodology used for existing driving cycles definition.

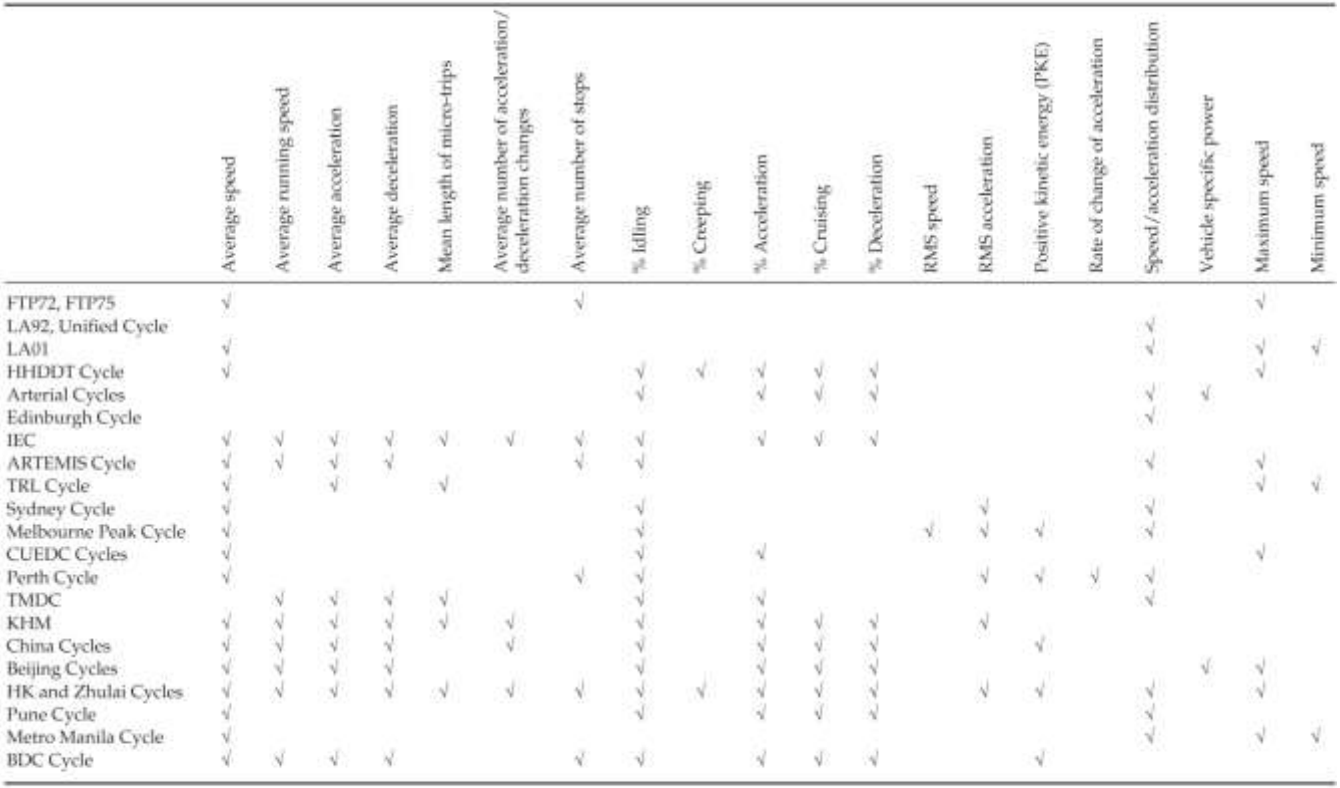

	Average speed	Average running speed	Average acceleration	Average deceleration	Mean length of micro-trips	Average number of acceleration/ deceleration changes	Average number of stops	% Idling	% Creeping	% Acceleration	% Cruising	% Deceleration	RMS speed	RMS acceleration	Positive kinetic energy (PKE)	Rate of change of acceleration	Speed/acceleration distribution	Vehicle specific power	Maximum speed	Minimum speed
FTP72, FTP75	√						√												√	
LA92, Unified Cycle																	√			
LA01	√																√		√	√
HHDDT Cycle	√							√	√	√	√	√							√	
Arterial Cycles								√		√	√	√					√	√		
Edinburgh Cycle																	√			
IEC	√	√	√	√	√	√	√	√		√	√	√								
ARTEMIS Cycle	√	√	√	√			√	√									√		√	
TRL Cycle	√		√		√														√	√
Sydney Cycle	√							√						√			√			
Melbourne Peak Cycle	√							√					√	√	√		√			
CUEDC Cycles	√							√		√									√	
Perth Cycle	√						√	√						√	√	√	√			
TMDC		√	√	√	√			√		√							√			
KHM	√	√	√	√	√	√		√		√	√	√		√						
China Cycles	√	√	√	√		√		√		√	√	√			√					
Beijing Cycles	√	√	√	√				√		√	√	√						√	√	
HK and Zhulai Cycles	√	√	√	√	√	√	√	√	√	√	√	√		√	√		√		√	
Pune Cycle	√							√		√	√	√					√			
Metro Manila Cycle	√																√		√	√
BDC Cycle	√	√	√	√			√	√		√	√	√			√					

Table 23 – Kinematic parameters used for the validation of existing driving cycles (from Tong and Hung, 2009).

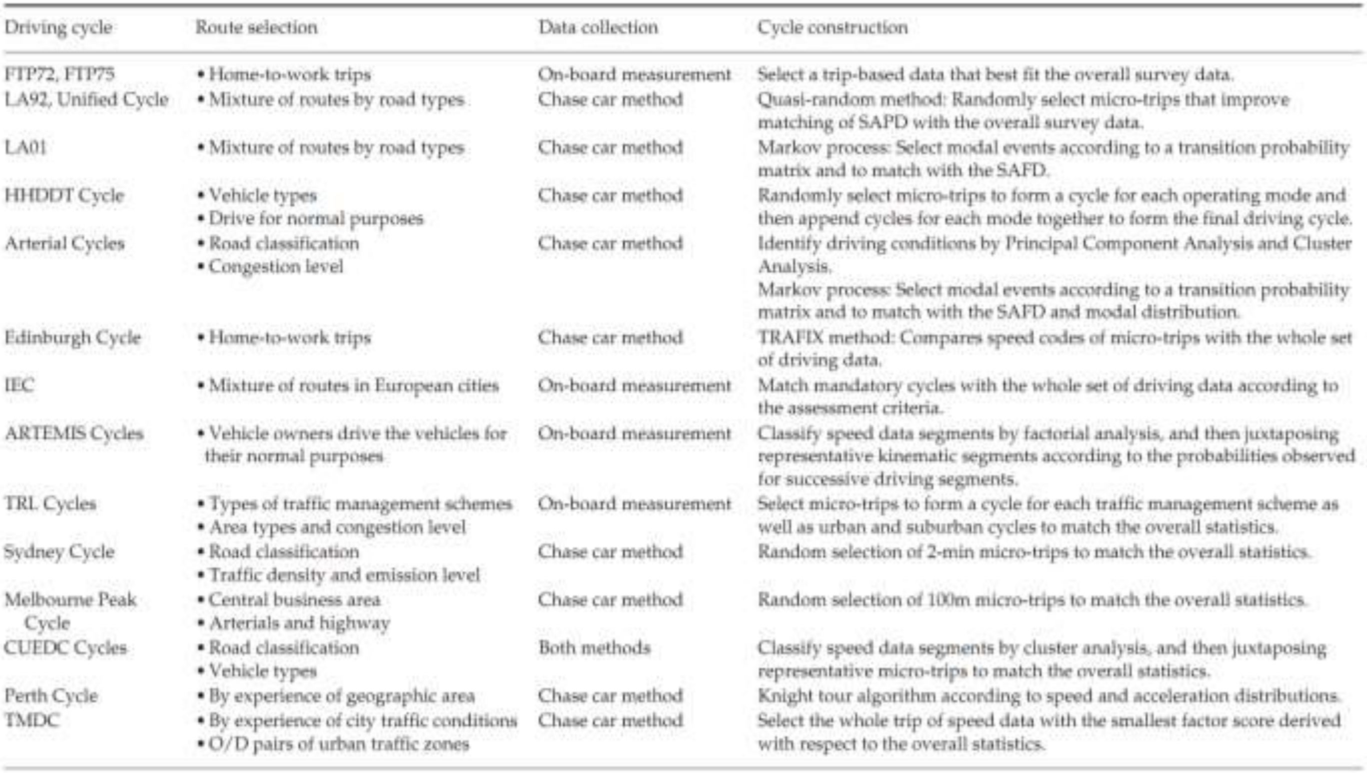

Driving cycle	Route selection	Data collection	Cycle construction
FTP72, FTP75	• Home-to-work trips	On-board measurement	Select a trip-based data that best fit the overall survey data.
LA92, Unified Cycle	• Mixture of routes by road types	Chase car method	Quasi-random method: Randomly select micro-trips that improve matching of SAPD with the overall survey data.
LA01	• Mixture of routes by road types	Chase car method	Markov process: Select modal events according to a transition probability matrix and to match with the SAFD.
HHDDT Cycle	• Vehicle types • Drive for normal purposes	Chase car method	Randomly select micro-trips to form a cycle for each operating mode and then append cycles for each mode together to form the final driving cycle.
Arterial Cycles	• Road classification • Congestion level	Chase car method	Identify driving conditions by Principal Component Analysis and Cluster Analysis. Markov process: Select modal events according to a transition probability matrix and to match with the SAFD and modal distribution.
Edinburgh Cycle	• Home-to-work trips	Chase car method	TRAFIX method: Compares speed codes of micro-trips with the whole set of driving data.
IEC	• Mixture of routes in European cities	On-board measurement	Match mandatory cycles with the whole set of driving data according to the assessment criteria.
ARTEMIS Cycles	• Vehicle owners drive the vehicles for their normal purposes	On-board measurement	Classify speed data segments by factorial analysis, and then juxtaposing representative kinematic segments according to the probabilities observed for successive driving segments.
TRL Cycles	• Types of traffic management schemes • Area types and congestion level	On-board measurement	Select micro-trips to form a cycle for each traffic management scheme as well as urban and suburban cycles to match the overall statistics.
Sydney Cycle	• Road classification • Traffic density and emission level	Chase car method	Random selection of 2-min micro-trips to match the overall statistics.
Melbourne Peak Cycle	• Central business area • Arterials and highway	Chase car method	Random selection of 100m micro-trips to match the overall statistics.
CUEDC Cycles	• Road classification • Vehicle types	Both methods	Classify speed data segments by cluster analysis, and then juxtaposing representative micro-trips to match the overall statistics.
Perth Cycle	• By experience of geographic area	Chase car method	Knight tour algorithm according to speed and acceleration distributions.
TMDC	• By experience of city traffic conditions • O/D pairs of urban traffic zones	Chase car method	Select the whole trip of speed data with the smallest factor score derived with respect to the overall statistics.

Table 24 – Summary of development methodologies for existing driving cycles (from Tong and Hung, 2009). The table continues in next page.

Driving cycle	Route selection	Data collection	Cycle construction
KHM	• Direction of Travel • Road type with and without central divider for cars and motorcycles	Chase car method	Random selection of micro-trips to match the overall statistics
China Cycles	• By experience according to area types and road types:	Chase car method	Random selection of micro-trips to match the overall statistics weighted according to road types.
Beijing Cycles	• Road type • Length and traffic volume	Chase car method	Rank micro-trips according to their differences in activity and emission measures with the whole data set. Randomly select micro-trips to form candidate cycles. The best cycle is selected according to the difference in vehicle specific power distribution with the whole data set.
HK and Zhuhai Cycles	• Average annual daily traffic • Road types and direction of travel	Chase car method	Random selection of micro-trips to match the overall statistics.
Piuie Cycle	• Major roadways • Time periods (peak and off-peak)	Chase car method	Randomly select micro-trips according to speed group and proportion of each operating mode and match with target parameters and speed group distribution.
Metro Manila Cycle	• Tricycle terminals	Chase car method	Markov process: Select modal events according to a transition probability matrix and match with the SAFD.
BDC Cycle	• Selection of road sections with average travel speed closest to the overall average travel speed in the area of interest	Chase car method	Select micro-trips according speed ranges and match with SAFD and target parameters.

4.3.5. The extended use of “driving cycle datasets”

According to those literature works related with development of “smart” vehicle management strategies (e.g. for HEV or PHEV), the importance of the availability of a large set of real world driving data is undoubted. The last trends in driving cycle definition methods show an evolution from the construction of synthetic cycles – that, after that moment, is then “rigid” – to the definition of a set of data which can be manipulated on the base of probabilistic criteria (e.g. Markov chain approaches) for improved vehicle performance simulation, e.g. for optimization of certain performances or for the build up of “predictive control” tecniques (see the works by: Moura et al, 2010; Gong et al., 2012; Montazeri et al., 2012; Souffran et al., 2012; Schwarzer and Gorbani, 2013). Data measured can therefore be used as a whole, as an “historical” dataset of driving situations; a typical use is in Montecarlo applications, such as the execution of a batch of simulations and/or experiments using randomly extracted data from a suitable space. If a database of driving sequences is available for consultation and processing, each simulation can use a newly extracted driving cycle, exploring a larger part of possible driving situations space.

4.3.6. Notes about additional data

Regarding electric vehicles, main additional data needed for the build up of a complete driving cycles are:

- the altitude profile (which could be obtained by GPS), to be associated to the trips performed; associating a slope to a synthetic driving cycle is not usual
- the consumption of auxiliaries, which is related to the external temperature
- the voltage/current of the powertrain (at least at one point of the electric system, e.g. at the battery) in order to associate it with vehicle speed, acceleration and its driving moment (pressure on throttle or brake pedals).

This latter, in particular, can be particularly interesting to examine; since skilled drivers are expected to optimize the driving style in order to obtain high regeneration from the braking system, a predominance of the deceleration values associated with driveline regenerative system is expected. The limits of deceleration values, in fact, are related to the tuning of the system and the characteristics of the vehicle powertrain. Looking at Figure 95, such values are expected to be quite easily recognizable due to the fact that they are comprehended within a specific range of current (that is, braking torque) for each speed.

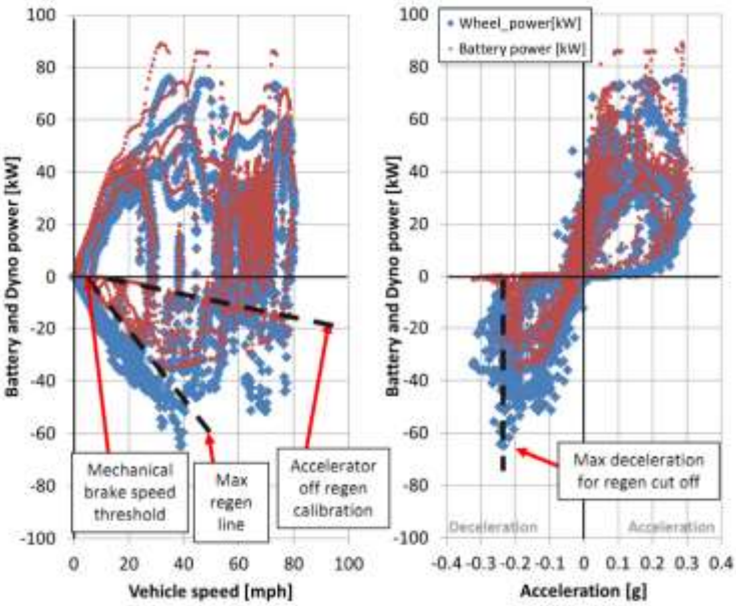

Figure 95 – Regenerative braking power depending on speed and acceleration for Nissan Leaf Vehicle (source: Lohse–Busch et al ., 2012).

5. Real World Data acquisition and processing

The present chapter contains the main results coming from a small campaign of on–road vehicle data acquisition and processing. The study has been integrated in the activities of the already cited ASTERICS research project, in which three different measurements have been performed by different partners in different context:

- large LDV electric van in the context of the city of Turin
- small passenger and LDV electric cars in the context of the city of Florence
- large heavy duty hybrid truck in the context of the city of Lyon.

The measurements activity in the city of Florence has been organized by the author of the present document and is therefore a part of a larger research plan; this has been the most relevant motivation for the development of the study.

Figure 96 – On road vehicle driving (Renault Twizy).

5.1. Driving data acquisition: the case study of the city of Florence

The data acquired in the city of Florence include three main sources:

- GPS data obtained through a commercial GPS–logger using a SirfStar III chipset
- CAN–system signals obtained from vehicle OBD port using a commercial logger, though being subjected to logging limitations, main being:
  - 8 CAN signals as a maximum

  - one subsystem at a time (e.g. “battery management system” or “motor controller”)
  - loss of some events (e.g. vehicle trips) due to misreading of “key on” conditions
- GPS data obtained through a Racelogic Driftbox acquisition device; the device also enabled the simultaneous acquisition of voltage analogic signals. These channels have been used for the acquisition of voltage values and current values on the 12V electric system.

The acquisition took place on vehicles which were used during their normal service; due to this reason, the invasiveness of the acquisitions had to be limited, so that the three main acquisition devices could not be used simultaneously for all vehicles; in addition, some vehicles could not be equipped with GPS devices due to privacy limitations. Therefore, for all the datasets described in this chapter the source of the data and the uncertainties to be considered will be clarified.

The acquisition sessions took place from March 2013 up to November 2013; in order to complete data including those months in which the temperature is lower, further acquisition are planned for January or February 2014. After data selection, the usable data acquired comprehend:

- regarding vehicle speed from OBD, about 1700 km have been acquired
- regarding GPS data about position and speed, about 2300 km have been acquired
- regarding auxiliary consumption data, about 400 km have been acquired
- regarding battery subsystem data, 270 different events (driving or charging activities) were logged; however, it was not possible to assess the total distance run during this phases.

5.1.1. Daily distance run: description of the users and comparison between Florence case study and literature data

The daily distance run by an electric vehicle is particularly important since it characterize the main need of the users and defines the severity of the vehicle mission. Regarding the use case of the city of Florence, it was necessary to distinguish between the different users under examination.

Considering the case of the delivery service, two different type of vehicles owned by a city freight delivery company are used:

- Renault Kangoo ZE, a light delivery vehicle of M1 class (curb mass: 1410 kg; traction power: 44kW; declared range: about 170km on NEDC cycle); 3 different vans of this type are owned by the company
- Renault Twizy, a quadricycle of L7e class (curb mass: 474 kg; traction power: 13kW; declared range: about 100 km on urban cycle); 12 different vehicles of this type are owned by the company.

The company owns a fleet of 15 electric vehicles in total, but, in general, not all the vehicles of the fleet are used every day, since this depends on the workload and on the availability of the drivers.

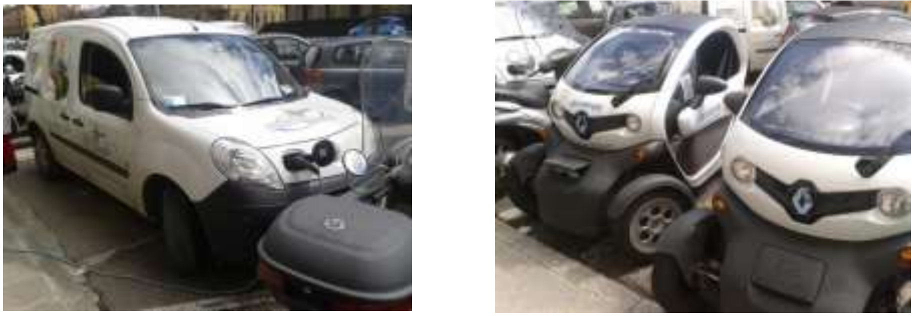

Figure 97 – Renault Kangoo vehicle (left) and Renault Twizy vehicles (right) during service.

The mission of the vehicles are planned according to the differences between vehicle in terms of payload and maximum achievable range; in order to avoid the risk of vehicle stop due to total discharge, the Company suggests to the drivers to try not to exceed the distance of about 120 km/day for the Kangoo van and about 80 km/day for the Twizy quadricycle; these values are significantly lower than the nominal range of the vehicles. In case of necessity, vehicle rotation (e.g. at lunch break) is usually possible: this means that, within the same day, the same vehicle can be used by different drivers. Therefore, it was not possible to identify the total number of drivers using the vehicles, but five of them were asked for their general impressions about the vehicle, even if it was not possible to set up a systematic survey. All of them described the performances of the vehicles as “satisfactory” or “brilliant”; regarding braking regeneration capabilities (that is a peculiarity of EVs and HEVs) in all the cases they said it was “noticeable”.

Due to such intense use, vehicles are charged everyday: charging during night is always performed, while partial recharge during the day is also performed frequently. It is important to note that due to the availability of a charging infrastructure in Florence – even if suitable only for “slow charging” solution due to the presence of single phase plugs, comparable with home plugs – some drivers use the vehicles to go home, then park and charge there. Such kind of trips can be longer than usual delivery trips (e.g. some systematic runs of about 15km in morning and evening hours have been recognized), but it was chosen not to exclude this data from analysis.

Considering the case of passenger transport, two type of vehicles have been used. The first type is the electric passenger vehicle of the PSA group, which comes with different brands: Peugeot iOn or Citroen C–zero; it is a replica of Mitsubishi iMiev vehicle, as described in next chapter. Three different cars of this type have been monitored:

- the first one is used by the members of a family for their daily needs (home – work trips, personal needs, weekend trips – but in this case, only if the expected distance is within about 100 km); two different drivers have been involved for this case
- the second one is owned by a company and is used by the workers for their movements within urban and suburban area, most frequent trip being from the first site of the company (on the center of the city of Florence) to the second site of the company (on the peripheral area of Florence)
- the third one is also owned by a company, but is used by a single person.

Four drivers, in this case, described their impressions on the vehicle, even if not in an organized survey, declaring that braking regeneration capability was “noticeable” and that overall performances where “satisfactory” or “brilliant”.

Figure 98 – Peugeot iOn vehicle.

Another type of passenger vehicle used for testing is, again, the Renault Twizy quadricyle, which has been used for a period of six days by a group of four drivers of the University of Florence. Although this latter data are reliable for driving cycle and style evaluation, daily distances run on these cases are not included in the calculation since they are coming from quite intense testing and are not representative of real use. This group also responded to a questionnaire, which was mainly aimed to understand if the range of the vehicle was considered satisfactory and if the EV typical characteristics (e.g. regenerative braking capabilities, SOC indication, range estimation by trip computer) were fully perceived after a period of use. “Range anxiety” phenomena was not reported by the drivers, but this fact should not be considered relevant due to the conditions of the test and of the group:

- the drivers used the vehicles for a limited period (at least one day each one, but no more than two consecutive days)
- the technical culture of the drivers (all being researchers in an engineering department) implies a consciousness about EV characteristics which cannot be assumed as general.

In order to offer a comparison with other case studies other source have to be considered. Within the context of the area of Florence, a private driver using a conventional ICE vehicle has been monitored for a period of eight days; this case study is different from the previous cases since due to home–work highway trips the daily driven distance is relevant, on average being more than 100 km per day. Looking at literature data, a large amount of information about daily distance driven for private vehicles is available worldwide; a comparison with very recent sources is therefore possible for US case study (source being the work by van Haaren, R., 2011 and the work by Kramm, 2012, both referring to data coming from NHTS, 2011), and for EU countries case studies (source being the work by Pasaoglu et al., 2012, and the related work by Pasaoglu et al., 2013).

N°.	Question	Scale	Driver 1	Driver 2	Driver 3	Driver 4
1	What is your impression about vehicle acceleration?	1: poor 10: brilliant	8	7	8	8
2	Do you think a vehicle effective range of about 80 km would be satisfactory for your transport needs? Expressed the percentage of transport events in which the vehicle could be suitable in comparison with total transports events on a yearly base (e.g. exclude long travels for vacation or business)	0%: yearly transport needs never satisfied 100%: yearly transport needs always satisfied	80%	80%	70%	80%
3	Referring to the percentage of transports events in which the vehicle could be usable, do you think that a vehicle range of 80 km is adequate?	1: insufficient, high risk of discharge in case of any inconvenient or deviation, possibility of "range anxiety" 10: largely overtakes my typical needs	10	8	10	8
4	What is your impression for charging time? (about 3.5 hours in total; range increase during charge from low SOC: about 0.5km/minute)	1: unsatisfactory 10: fully satisfactory	10	7	8	9
5	Do you think that the use of the vehicle with such electric traction system is intuitive?	1: long practice needed 10: immediate confidence and good driveability	9	7	10	9
6	Do you think that the regenerative braking mode is perceptible?	1: not perceptible 10: remarkably advertible, strong	6	8	7	8
7	Do you think that the regenerative braking mode is easy to be exploited? (goodness of implementation and resulting driveability)	1: almost not usable 10: frequently usable	7	6	7	6
8	Do you think that the regenerative braking mode is clearly noticeable from vehicle dashboard display?	1: difficult to understand 10: easy to notice	8	8	10	10
9	Do you think that vehicle instruments (SOC indicator and trip computer) information* are adequate in order to let the user understand the available range?	1: easy to understand 10: remaining range unclear	8	8	10	10
10	How do you consider the driving style you adopted during the test?	1: very smooth 10: very aggressive	6	6	6	8
	* vehicle estimated range is updated during vehicle driving every few minutes, so that wide oscillations can be noticed if driving style or context is changing in the same trip (e.g. due to road slope); the question was aimed to understand if drivers understood this calculation criterion.					

Table 25 – Questionnaire about electric quadricycle and users expectations. A group of four drivers responded; each one used the vehicle for at least one day.

The results of the data coming from the case study of Florence are presented in the box plot of Figure 99, while a short summary of the data and a comparison with the cited sources are presented in Table 26. The results related to the context of Italy (mean daily distance between 50 and 55 km) are coherent with the indications coming from Table 25 (see question n.° 2 and 3), in which all the users declared that a range of 80 km is satisfactory for their most frequent needs and can be suitable for 70–80% of their transport events over a year.

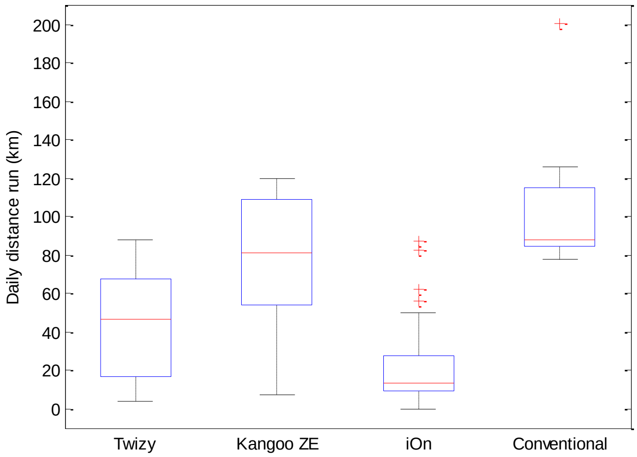

Figure 99 – Box plot representing the daily distances run by city freight delivery electric vehicles (Twizy and Kangoo ZE) and electric passenger vehicles (iOn); the plot also includes the data of a Conventional vehicle frequently used for highway runs.

Data	**Source**	**Mean (km)**	**Standard Deviation (km)**	**95° Percentile (km)**
US Urban	van Haaren, R., 2011	58.7	94.4	–
US Rural	van Haaren, R., 2011	78.2	125.8	–
US Total	van Haaren, R., 2011	63.6	102.4	–
EU France	Pasaoglu et al., 2013	50–60**	–	–
EU Germany	Pasaoglu et al., 2013	50–60**	–	–
EU Italy	Pasaoglu et al., 2013	50–55**	–	–
EU Poland	Pasaoglu et al., 2013	80–90**	–	–
EU Spain	Pasaoglu et al., 2013	70–80**	–	–
EU UK	Pasaoglu et al., 2013	40–45**	–	–
ASTERICS – LDV	Kangoo ZE measurements	74.2	39.8	117.3
ASTERICS – LDV	Kangoo ZE n.1 (average on 14 months)*	89.0	–	–
ASTERICS – LDV	Kangoo ZE n.2 (average on 17 months)*	98.8	–	–
ASTERICS – delivery quadricycle	Twizy measurements	44.8	27.1	87.5
ASTERICS – delivery quadricycle	Twizy odometer (average on 14 months)*	56.3	–	–
ASTERICS – passenger vehicle	iOn measurements	22.7	21.4	74.4
ASTERICS – passenger vehicle	iOn company user (average on 19 months)*	29.9	–	–
ASTERICS – ICE passenger vehicle	ICE vehicle motorway user measurements	106.7	40.8	200.3
* calculated considering odometer total distance, vehicle age and assuming 21 working days for each month				
** data is only available as range (see Figure 100).				

Table 26 – Summary of daily driven distance for the vehicles under study in the city of Florence and for main literature sources.

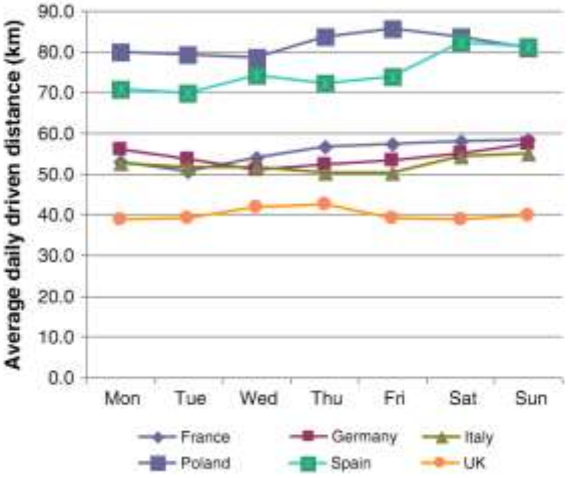

Figure 100 – Average daily travel distance (km) by day of the week and by country (source: Pasaoglu et al., 2013).

Another information that is relevant for the evaluation of EV duty cycle is the length of the trips for which the vehicle is used; also for this case, recent literature data are available. The box plot of Figure 101 represents the main results of the case study, while a summary of the measurements and of relevant literature data is presented in Table 27; it is evident that the mean distance run for each trip (typically 5–6km) both for delivery service vehicles and for passenger vehicles is significantly shorter than literature assessment (15–20km). Multiple reasons can originate this difference, also including the fact that the survey has been based on a reduced number of vehicles and users, though not being representative of the whole Italian/European context but only of the described case studies. A few hypothesis for the reasons determining such values can be formulated:

- the city freight delivery service, by its nature, determines the possibilities of frequent short trips
- the electric passenger vehicles have been used within the city of Florence and, sometimes, through the historical centre of the city: in this context the distances are expected to be short. The owners, when asked, declared that the possibility to access to the historical center of the city (that is subjected to a number of restrictions for conventional vehicles) was one relevant reason that determined the purchase of the electric vehicle.

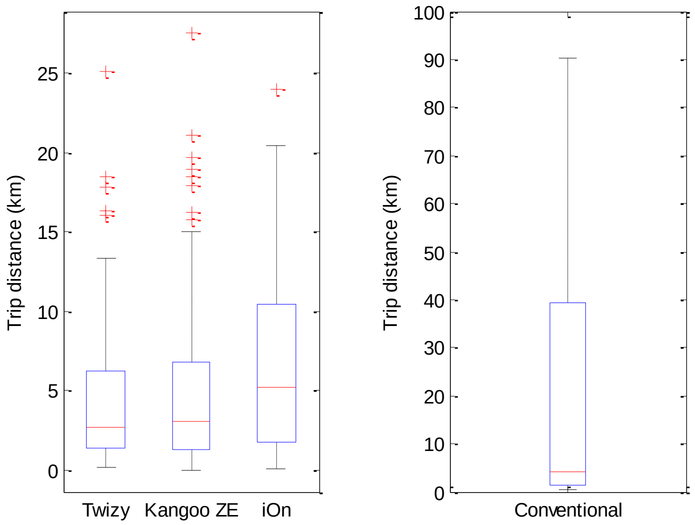

Figure 101 –Box plot representing the trip distances run by city freight delivery electric vehicles (Twizy and Kangoo ZE) and electric passenger vehicles (iOn); the plot also includes the data of a conventional vehicle frequently used for highway runs (represented on a different scale for improved readability).

Data	Source	Mean (km)	Standard Deviation (km)	95° Percentile (km)
US Urban	van Haaren, R., 2011	13.8	22.1	–
US Rural	van Haaren, R., 2011	19.5	31.3	–
US Total	van Haaren, R., 2011	15.1	24.3	–
EU France*	Pasaoglu et al., 2013	17	–	–
EU Germany*	Pasaoglu et al., 2013	17	–	–
EU Italy*	Pasaoglu et al., 2013	16	–	–
EU Poland*	Pasaoglu et al., 2013	22	–	–
EU Spain*	Pasaoglu et al., 2013	34	–	–
EU UK*	Pasaoglu et al., 2013	16	–	–
ASTERICS – LDV	Kangoo ZE measurements	4.8	4.9	15.9
ASTERICS – delivery quadricycle	Twizy measurements	4.7	4.7	16.1
ASTERICS – passenger vehicle	iOn measurements	6.0	4.7	12.3
ASTERICS – ICE passenger vehicle	ICE vehicle motorway user measurements	19.9	24.2	77.7
* data adapted from the case of personal vehicles during weekdays				

Table 27 – Summary of trip distance descriptions for the vehicles under study in the city of Florence and for main literature source.

A final note is necessary regarding the build up of so–called trip chains, that are a sequence of trips describing the movement of a user between main keypoints for its main activities. According to the review by Primerano et al., 2008, a number of different definitions have been proposed in literature, but two commonly accepted definitions arise:

- a sequence of trips segments beginning at “home” activity and continuing until the traveller returns “home”

- a sequence of trip segments between a pair of anchor activities, typically “home” and “work” (or “school”).

It is evident that trip chain definition can be an used for the definition of a number of boundary conditions in vehicle missions. In fact, the knowledge of typical trip chains enables the possibility to evaluate the availability of parking hours for charging and, therefore, the suitability (or not) of an electric vehicles for a daily distance which overpasses its possible range. Due to the limitations of the case study here presented in terms of size of the fleet under study and in terms of GPS data availability (GPS being not used for all vehicles), it could not be possible to offer an analysis about typical trip chains. Again, literature data (Pasaoglu et al., 2013) indicate that in Europe a large number of trip chains for passenger vehicles include just 2 trips (average being 2.5, see Figure 102), that is the typical home–work–home use, and that a significant share of trip chains are below the distance of 50km, well below the typical range of last generation electric vehicles (see Figure 103).

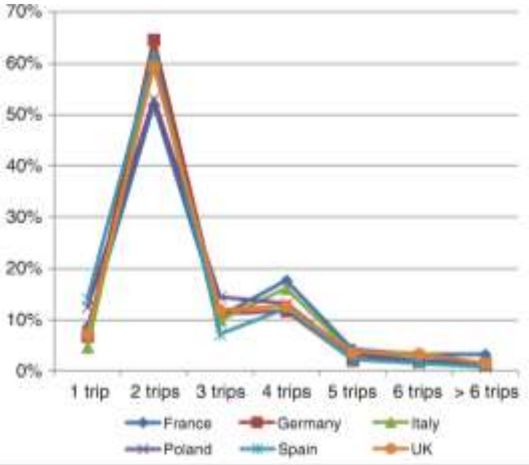

Figure 102 – Distribution of daily car trips by country (source: Pasaouglu et al., 2013)..

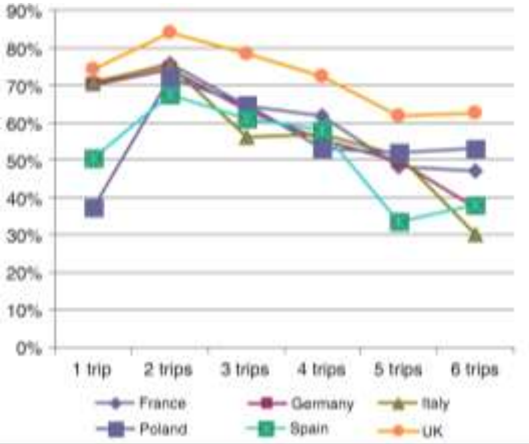

Figure 103 – Share of trips chains with a driven distance <50km by country (source: Pasaouglu et al., 2013).

A few examples of GPS tracks are shown in Figure 104 and Figure 105; increased detail is not possible due to privacy reason. The main information available from such pictures is that light freight delivery vehicles are usually used only in the urban and suburban areas – including the historical center – while passenger vehicles have been used also on rural areas, thus facing significant road slopes. Taking into account this latter data is particularly difficult for a synthetic cycle, and normally longitudinal speed is considered main relevant data. However, when available on motor controller CAN system, estimated motor power – thus taking into account effective traction power on slopes – has also been logged.

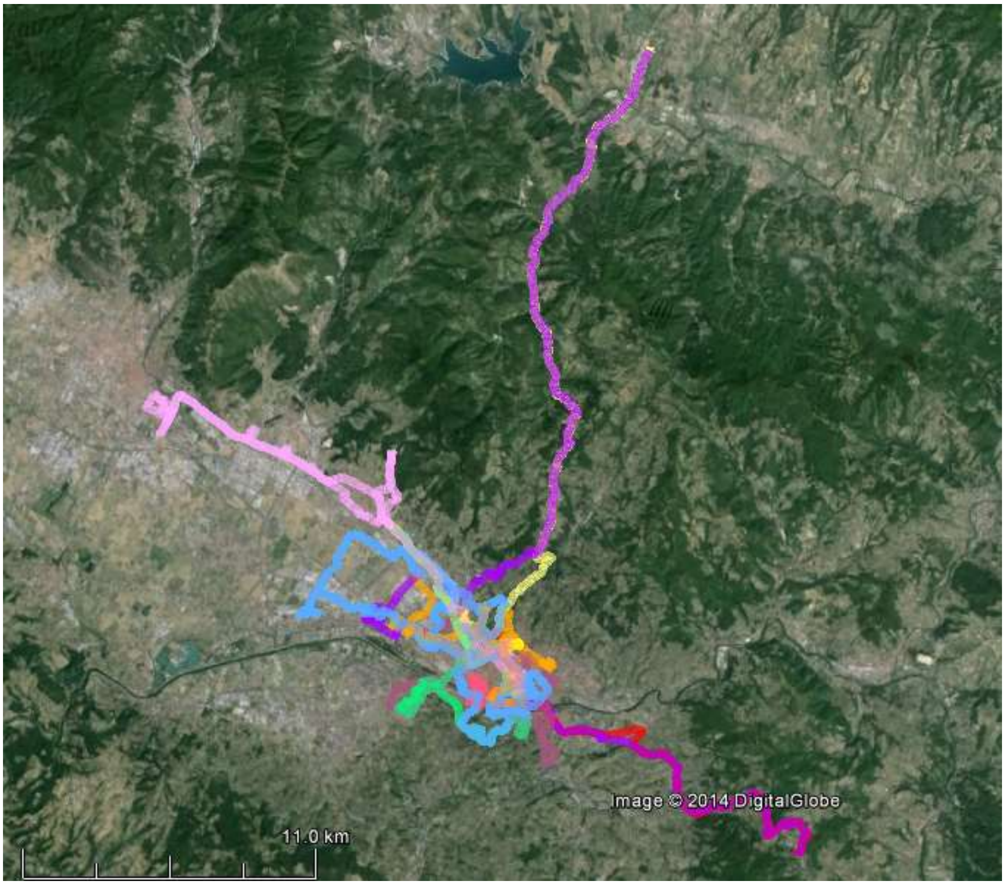

Figure 104 – Electric quadricycle, passenger GPS tracks (one week of use); missions include urban, suburban and rural transports.

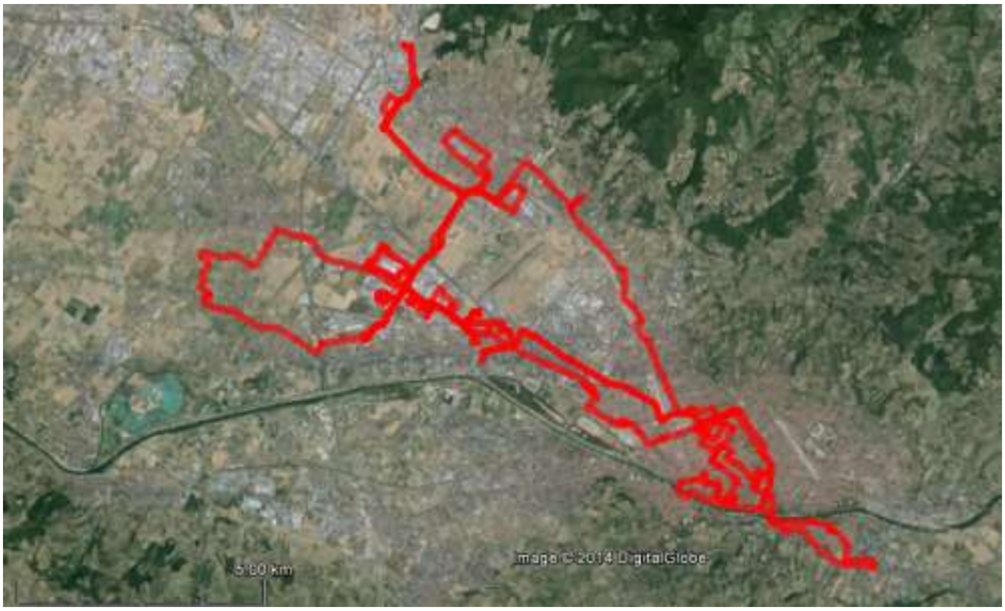

Figure 105 – Light Delivery Vehicle GPS tracks (one day): missions usually include urban and suburban driving, but not highway trips.

5.1.2.Data analysis for driving sequences identification and clustering

The measurements of time–speed sequences from electric vehicle is mainly aimed to develop a “real world” driving cycle specific for kind of vehicles. Even if a very large number of driving cycle is available from worldwide research activities and vehicle regulation standards, a brief literature review highlights that there are still strong reasons pushing for the development of new cycles.

The work by Lin and Niemeier, 2003, demonstrates that significant variation in typical driving patterns parameters (speed and accelerations) can be identified on a regional scale; the present activity can offer a context–related information, thus making available an additional data to be considered during vehicle virtual or real test phases.

The work by Alessandrini and Orecchini, 2003, also highlights that the characteristics of electric vehicles can induce a driving pattern somehow different from those adopted on conventional vehicles by the same users, such as:

- the frequent occurrence of moderately strong accelerations, especially at low speed, even for non–aggressive drivers; this can happen due to human perceptions in terms of reduced noise, that is typical of electric traction systems
- the low peak power, which could be related to the vehicle used in the cited study; for latest N1 or M1 class EVs maximum power is usually comparable with similar conventional vehicle. This observation, however, can still be applied for quadricycles.

Another peculiarity of EVs and HEVs vehicles is the availability of regenerative braking capabilities, which could induce the users to modify their style in order to exploit such characteristic; it has to be said the all the drivers – both professional (using light delivery vehicles) and simple users (using passenger vehicles) – noticed the potential of such deceleration mode in terms of range increase, since all the vehicles highlight regeneration phase on their dashboard instruments and show estimated achievable range on trip computer. In case of the group that responded to the questionnaire shown in Table 25, all of them noticed the occurrence of regeneration phase on the dashboard instruments, and the usability of the system was considered sufficient (question n°. 6,7,8); it is therefore possible that drivers adopted a slightly different style in comparison to what they usually do when driving conventional vehicles. It has to be noted that the implementation of regenerative braking capabilities is not uniform across the producers, main solutions being:

- regeneration on throttle release, sometimes moderate (e.g. Renault Twizy, as stated by drivers' opinion on Table 25), sometimes intense (e.g. described for Iveco Daily EV, that is another ASTERICS case study)
- moderate regeneration in case of throttle release, but intense regeneration if brake pedal is pressed through "blending" of motor torque and mechanical brake torque (e.g. such implementation is adopted on Toyota hybrid systems).

The results in terms of total energy recovery can be different, since the more advanced and intuitive is the implementation, the more energy can be recovered in a similar context. For this reason, the value of motor torque during deceleration (when available on the CAN system) has been logged together with vehicle speed or motor RPM, in order to obtain data about the characteristics of the energy regeneration system and reproduce it on models; data will be shown on next paragraphs.

The first aim of the development of a driving cycle for the Florence case study is to include all these peculiarities in a synthetic time–speed cycle (or a number of them) using only data coming from electric vehicles. A second aim is to make the dataset of acquired data available for processing in other applications as a source of driving data to be used in case of multiple simulation activities, as explained in paragraph 4.3.5. However, a limitations of the present study are that the amount of available data and the dimension of the population of drivers considered are relatively small.

The first step of the analysis included speed data filtering for the elimination of "spikes" or of any irregular data. Data have been acquired at a rate of 4 Hz from vehicle CAN system, than a kernel filter – as described in section 4.3.2 – has been applied, considering a time interval of one second. An example of speed signal smoothing through this method is shown on Figure 106.

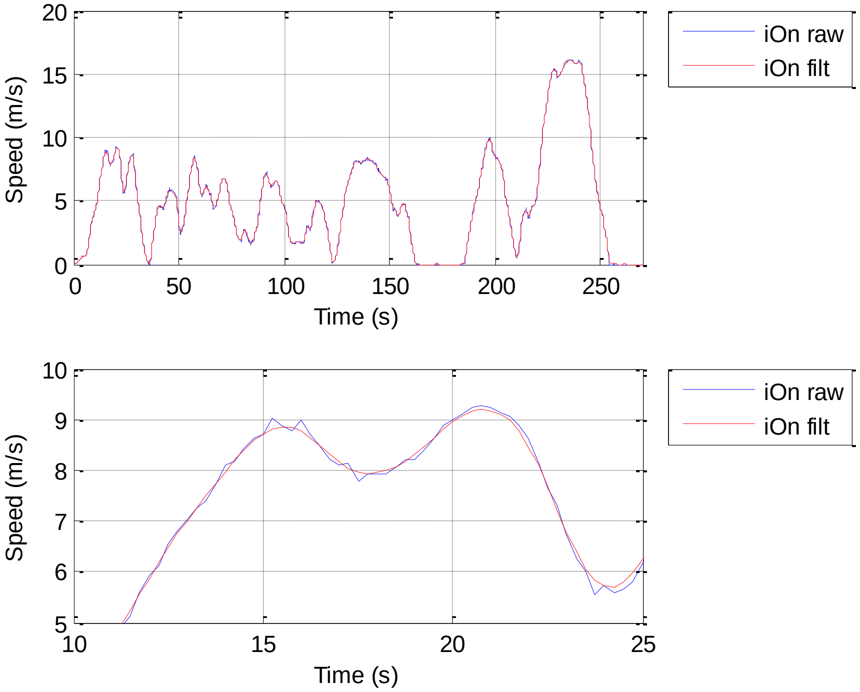

Figure 106 – Upper plot: a portion of speed measurement for iOn passenger vehicle, showing a comparison between raw and filtered data. Lower plot: a detail coming from the same measurement.

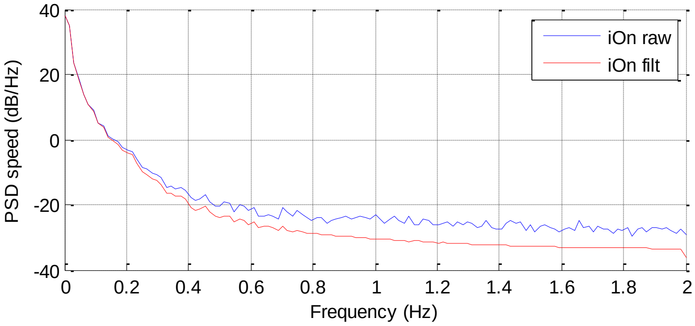

Figure 107 – Power Spectral Density of vehicle speed before and after the application of the filter.

The second step of the analysis included the grouping of the data in different categories. The main strategy adopted is to identify in each mission (or trip) the sequences between two events of speed being equal to zero (microtrips); after that, for each microtrip two different sets of parameters are calculated:

- a vector of indicators, that is a selection of most common indicators adopted in literature
- a speed–acceleration density matrix.

The detail of the indicators and of the thresholds adopted is shown in Table 28. Considering the need to calculate the percentage of driving time spent on idle, cruise, positive and negative acceleration, a threshold for acceleration value has to be introduced; otherwise, cruise time could result zero even in case of almost constant speed phase. Regarding mean positive and negative accelerations, two calculation methods have been adopted:

- the first method calculates these values considering the same threshold used for cruise and acceleration time percentage calculation. In other words, each value of is coherent with the related others (e.g. mean positive acceleration value is calculated for those phases which are considered effective acceleration phases); the values are used also for synthetic cycle selection, as described in next paragraphs
- the second method does not consider any threshold for acceleration, thus the mean acceleration values includes data also coming from cruising phases; the values calculated with this method are used for confrontation with those literature data that are using such parameter.

Regarding the vectors (edges) used for the calculation of SAPD matrix, the limit values have been selected considering the maximum values measured (about 30 m/s for speed and 2.5 m/s^2 for acceleration); the first speed class includes only very low speed (from 0 to 0.1 m/s^2) to identify zero speed phases.

Parameter	Unit	Note	Abbreviation
Duration	s		duration (s)
Distance	m		distance (m)
Percentage of idle time	%	a=0; v=0;	idle %
Percentage of cruise time	%	|a|< 0.05	cruise %
Percentage of positive acceleration time	%	a>0.05	acc %
Percentage of negative acceleration time	%	a<–0.05	dec %
Average speed	m/s		avg speed (m/s)
Average moving speed	m/s	v>0	avg mov speed (m/s)
Mean positive acceleration (a>threshold)	m/s^2	a>0.05	acc+
Mean negative acceleration (a< threshold)	m/s^2	a<–0.05	acc–
RMS	m/s^2		RMS
PKE	m/s^2		PKE
RPA	m/s^3		RPA
Stop rate	–		stops/km
Additional parameters	Unit	Note	
Mean positive acceleraton	m/s^2	a>0	acc+ nth
Mean negative acceleration	m/s^2	a<0	acc– nth
SAPD edges*			
Acceleration classes (51 classes)	m/s^2	from –2.5 to 2.5	
Speed classes (17 classes)	m/s	from 0 to 0.1 and from 0.1 to 30	

Table 28 – Parameters used for cycle characterization and grouping. The numerosity of elements on SAPD matrix used for plots is reduced for better readability.

Main results for each data subset are reported on Table 29, while the representation of SAPD data is presented both as 3D plot and contour plot on Figure 108.

Data	idle	cruise	acc	dec	avg speed (m/s)	avg mov speed (m/s)	acc+ (m/s^2)	acc– (m/s^2)	acc+ nothr (m/s^2)	acc– nothr (m/s^2)	stops/ km
All road data	13.2%	7.5%	41.0%	38.3%	7.4	8.6	0.59	–0.64	0.54	–0.58	1.03
Passenger vehicle (iOn)	7.5%	7.6%	44.7%	40.1%	8.3	9.0	0.59	–0.66	0.53	–0.59	0.85
LDV (Kangoo ZE)	19.3%	6.9%	38.4%	35.4%	6.8	8.4	0.62	–0.67	0.58	–0.62	1.19
Quadricycle (Twizy)	10.4%	8.3%	40.4%	41.0%	7.3	8.2	0.56	–0.55	0.50	–0.50	1.06

Table 29 – Main parameters calculated for each data subset.

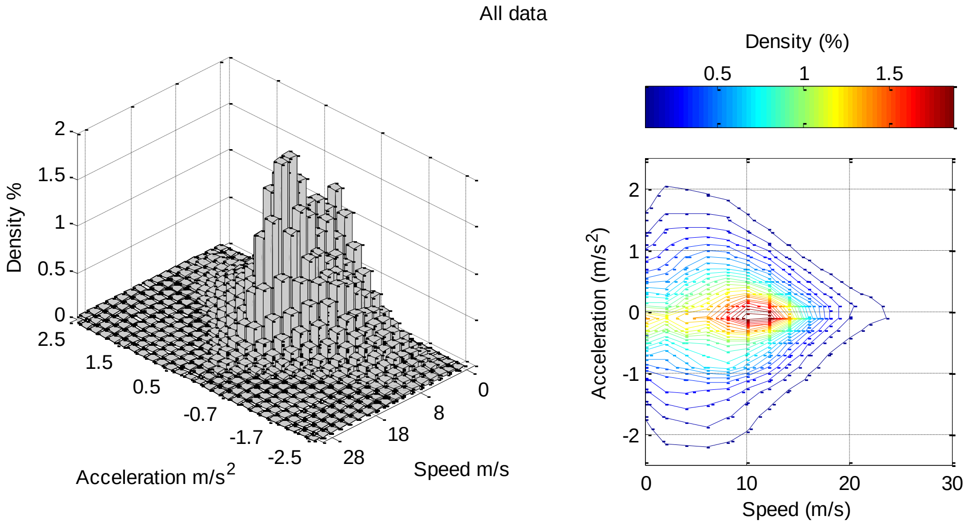

Figure 108 – SAPD matrix 3d plot (left) and contour plot (right) for all the road measurements. The value corresponding to zero speed and zero acceleration has been excluded to avoid distortions due to its dominance.

Before the application of a grouping algorithm on all data, a manual examination has been performed. Short distance microtrips have been identified, since they can include data which are not suitable for general driving cycle generation, such as:

- incomplete microtrips, sometime generated by a delay between vehicle key–on event and logging start
- parking phases
- small movements corresponding to less than 1 meter distance, which seems to be originated both from logging irregularities and from small vehicle displacement (e.g. stop on traffic light without using brake pedal)
- any sequence including reverse gear maneuvers.

Regarding the remaining valid microtrips, those not exceeding the distance of 50 meters can be directly considered as a class of small speed events typical of congested traffic situations or maneuvers outside the road. Since such short sequences represents about 0.5% of total distance run during the survey, it was decided not to include this class into the generated cycles. Such sequences can be used, however, to build up specific driving situations (e.g. queue following).

The examination of total distance run at high speed (exceeding 25 m/s. which has been chosen as threshold) together with the comparison with GPS data (where available) confirms that no continuous highway driving has been measured: the total distance run above such high speed is less than 2% of total data; in particular, about 23 km have been run on a number of 24 different trips.

After manual examination, a number of 1828 microtrips have been subjected to grouping process. Each microtrip is described by the vector of parameters defined in Table

28; considering SAPD elements, each vector can include up to 890 components. The selected algorithm is a k–means procedure – as implemented in Matlab software suite – that is based on the calculation of relative distances (e.g. as square Euclidean distance, or as correlation value) of samples around a number of initially randomly determined centroids. Centroids and points constitute clusters that are iteratively updated; final partitioning is obtained by minimization of the total sum of points–centroid distances. A known limitation of the algorithm is therefore the possibility to individuate only a local minimum, sometimes depending on the initial set of centroids. Through the execution of a number of trial–and–error attempts, the conditions used for partitioning have been chosen:

- each sample is described by SAPD density elements and by RMS, RPA and PKE element, that are all descriptors of microtrip speed and acceleration
- the distance is calculated as correlation between points
- 9 different clusters have been determined.

The results of the grouping algorithms are shown in Table 30, which includes a selection of main parameters describing the microtrips included in the group and some notes describing the most probable driving situation for each cluster. A priori classification (e.g. on vehicle type, since three different have been used) has not been performed, so that each cluster can contain microtrips coming from different vehicles and drivers. Various plots can be used to describe different clusters, starting from the distance – average speed plots (see Figure 110 and subsequents). Centroids indications highlight the degree of separation of the groups, while a certain overlap between the elements of all the clusters is noticeable. Considering SAPD values that have been used for the definition of each group, it is possible to notice significant differences between the "patterns" of each cluster, as is shown in Figure 114.

Number	**Class**	**Stop notes**	**Speed notes**	**Avg mov speed**	**Avg speed**	**Stop duration**	**Stops/km**	**Acc+ nth**	**Acc– nth**
				m/s	**m/s**	**%**	**1/km**	**m/s^2**	**m/s^2**
1	Urban	High stop duration	Unsteady	5.50	1.98	63.9%	3.34	0.57	–0.58
2	Urban	Low stop duration	Very low speed	2.55	2.39	6.2%	4.15	0.32	–0.30
3	Urban	Low stop duration	Low speed	4.19	3.95	5.4%	2.09	0.43	–0.41
4	Urban	Intermediate stop duration	Steady	6.83	4.31	36.7%	2.35	0.58	–0.59
5	Urban	Intermediate stop duration	Unsteady	5.99	4.31	27.8%	3.23	0.65	–0.64
6	Urban	Low stop duration	Unsteady	6.14	5.47	10.6%	2.04	0.65	–0.64
7	Urban	Low Stop duration	Steady	8.26	6.83	17.2%	1.24	0.53	–0.55
8	Urban – Main roads	Flow	Intermediate speed	9.01	8.63	4.0%	0.79	0.60	–0.64
9	Urban – Main roads	Flow, steady	Intermediate speed, steady	11.30	10.92	3.3%	0.44	0.44	–0.52
Manual identified *	Queue, manouvers	high stop duration	Very low speed	1.20	0.50	57.4%	318.00	0.43	–0.37

Table 30 – Summary of main descriptor parameters for each microtrip group. The name of the class and the notes in relation to the speed are assigned after the grouping and are not relevant for analysis.

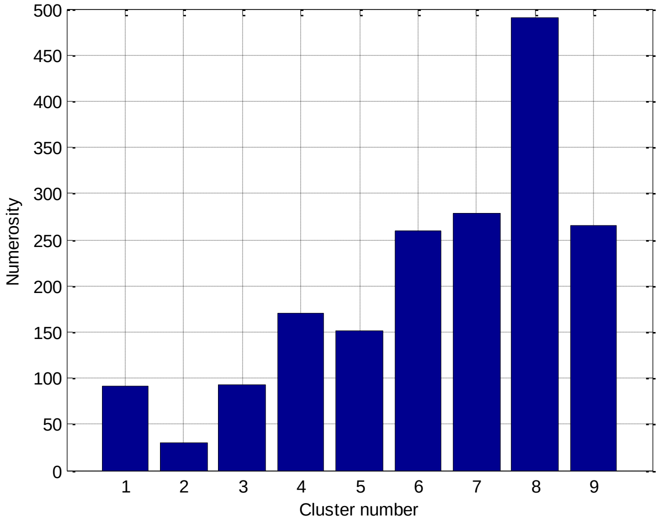

Figure 109 – Number of identified mictrotrips for each cluster.

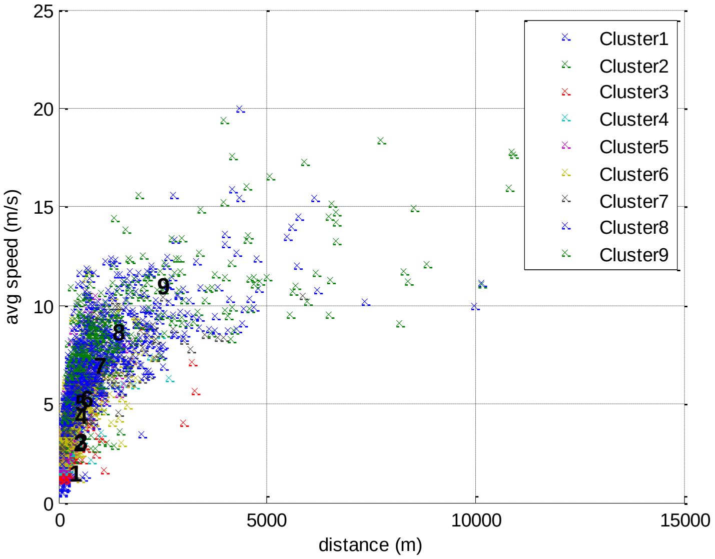

Figure 110 – Scatter plot representing distance and average speed for all cluster elements; centroids are indicated by numbers.

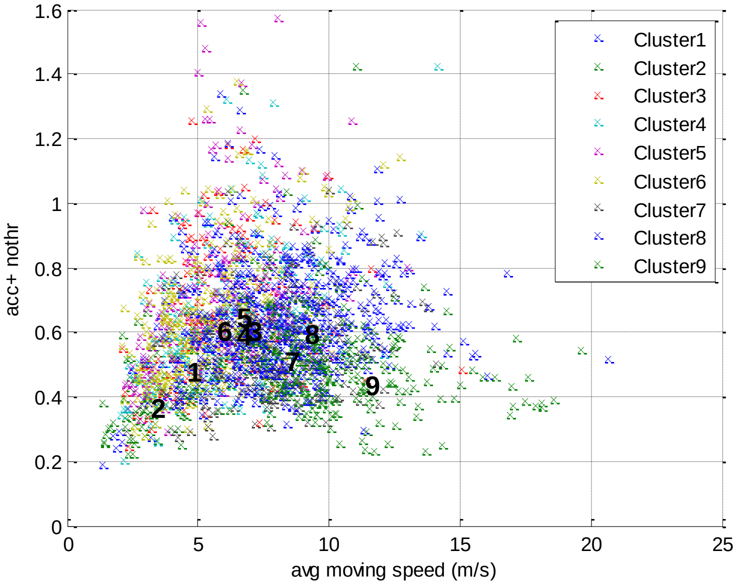

Figure 111 – Scatter plot representing average moving speed and mean positive acceleration for all cluster elements; centroids are indicated by numbers.

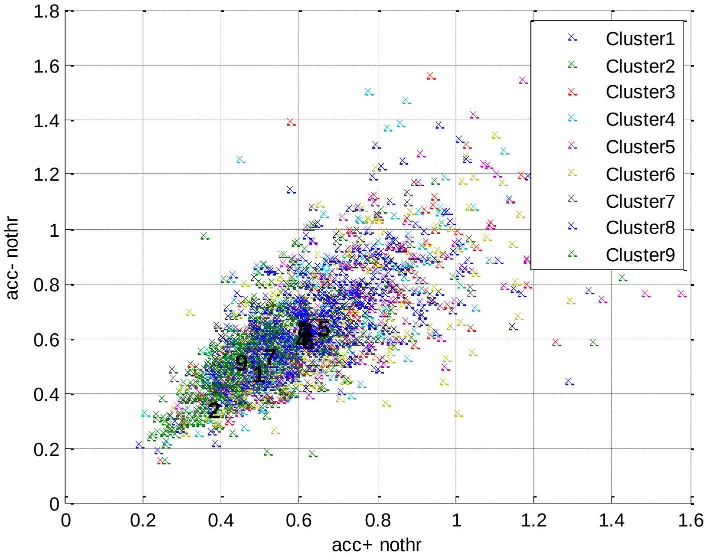

Figure 112 – Scatter plot representing average positive and negative accelerations for all cluster elements; centroids are indicated by numbers.

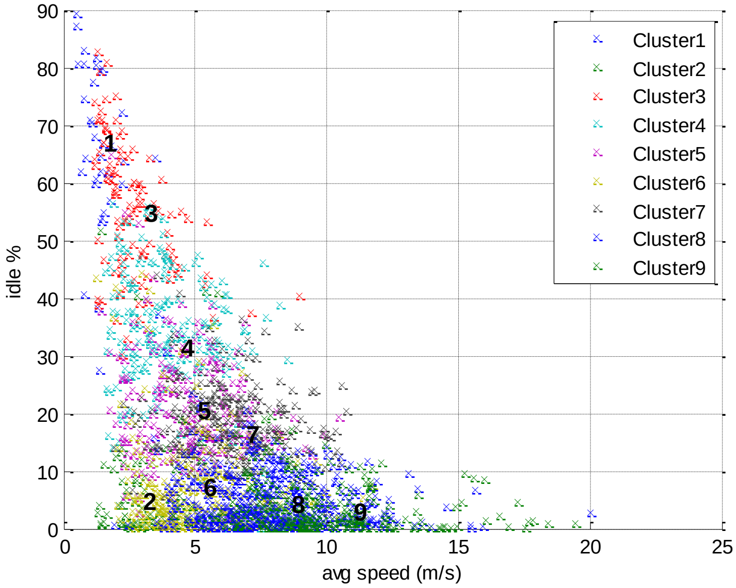

Figure 113 – Scatter plot representing average positive and negative accelerations for all cluster elements; centroids are indicated by numbers.

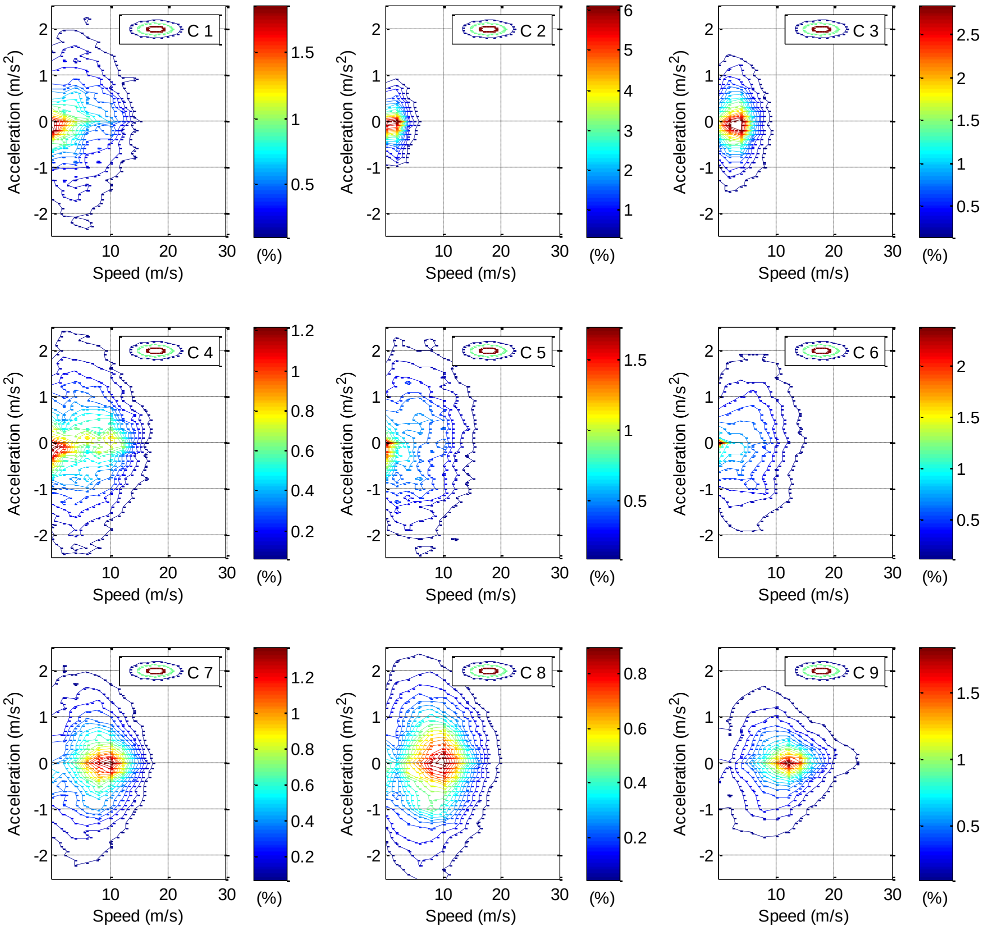

Figure 114 – SAPD contour plot for the microtrip groups described in Table 30; the plots do not include the point corresponding to idle phases (zero speed and acceleration) to avoid distortions due to its predominance.

5.2. Driving data processing: methods and results

5.2.1. Generation process of new driving cycles

After grouping the microtrips, the build up process of a representative cycle consists of a first phase of “generation”:

1. the selection of the main group of microtrips to be used (e.g. only for a certain vehicle, only for a set of clusters)
2. the selection of a target distance for the whole cycle
    a) for each cluster, a target distance is set in order to maintain the same proportion of the original data set

3. random microtrips from each group are selected, until the target distance for that cluster has been reached
    a) if a chosen microtrip causes exceeding of target distance, the microtrip is truncated on a random point and glued together with the final portion of another microtrip, maintaining coherence for speed, acceleration and jerk values (threshold being 0.1); new microtrips are therefore generated
4. all the chosen or generated microtrips are put beside each other, thus generating a cycle
5. the process is repeated for a number of predetermined attempts (e.g. 1000 cycles can be generated in a few minutes of calculation).

After the generation of the attempt cycles, the final proposal cycle is selected on the basis of three main criteria:

1. considering the parameters of Table 28 (from number 3 to number 14), the difference between original dataset values and generated cycles has to be below 5% for at least 11 over 12; about 0.5–1% cycles of the generated ones usually respect this condition for a distance of about 10–15km; the bigger the distance, the more the satisfactory number of generated values due to averaging phenomena
2. for the reduced number of cycle chosen at the former point, those having similar PV are considered as candidate
3. for the remaining candidate cycles, the final one is that having lower SSD between SAPD matrix.

If a satisfactory cycle cannot be found (e.g. it is not possible to find a cycle having both low PV and low SSD in comparison with other cycles), the whole process is repeated generating new values.

Using this procedure, 10 different cycles have been generated, their characteristics being:

- there are 5 categories, depending on the source of the data:
    - all data from all vehicles are used, so that the cycle is representative of “average” electric vehicles; quadricycles data are included since, especially in urban driving, it is assumed that its performances are comparable with those of other vehicles (e.g. chasing is possible in most cases);
    - data from N1 passenger vehicle, so that the cycle is representative of small class passenger vehicle such as Peugeot iOn
    - data from M1 light delivery vehicle, so that the cycle is representative of light delivery vehicle such as Renault Kangoo ZE
    - data from quadricycles, so that the cycle is suitable for low powered vehicles
    - data from N1 and M1 vehicles, trying to choose most “unsteady” sequences
- for each category, two different distances have been used:
    - “long” cycles are based on the 95th percentile trip distance, according to Table 27; all the microtrip clusters are considered (excluding clusters 1, 2, 4 and 7 for unsteady cycle)
    - “mean” cycles are based on mean distance, according to Table 27, but clusters 8 and 9 are not included since their data also include quite “long”

microtrips, by far exceeding the whole target distance; clusters 1, 2 and 4 are excluded for unsteady cycle.

Table 31 summarizes the informations and the assumptions for the driving cycle generation, while Table 32 shows the parameters that determined the selection of final driving cycles amongst all those generated (standard value: 2000 attempts for each class). The final description of the data used for generation is shown in Table 35, while the characteristic of the synthetic cycles and is shown in Table 34; Table 35 shows a comparison between original and synthetic cycles.

Finally, all the cycles and the corresponding SAPD are described on Figure 115 and followings.

N.	**Cycle name**	**Vehicles**	**Groups**	**Target Distance (km)**
1	All long	All	1 to 9	12
2	All mean	All	1 to 7	6
3	Passenger long	N1, Passenger	1 to 9	15
4	Passenger mean	N1, Passenger	1 to 7	6
5	LDV long	M1, LDV	1 to 9	15
6	LDV mean	M1, LDV	1 to 7	4.8
7	Quadricycle long	L7, Quadricycle	1 to 9	15
8	Quadricycle mean	L7, Quadricycle	1 to 7	6
9	Unsteady long	Passenger and LDV	3, 5, 6, 8, 9	12
10	Unsteady mean	Passenger and LDV	3,5,6	6

Table 31 – Information summary for all generated cycles.

N.	**Cycle name**	**Corresponding values**	**PV**	**SSD**	**Distance (m)**
1	All long	12	1.3	12.1	11566
2	All mean	11	1.2	19.2	5837
3	Passenger long	11	1.1	11.6	15675
4	Passenger mean	12	2.3	47.5	6481
5	LDV long	11	2.2	8.3	14017
6	LDV mean	12	2.2	4.9	4755
7	Quadricycle long	11	1.8	7.4	15480
8	Quadricycle mean	11	3.0	14.6	6360
9	Unsteady long	11	0.9	10.1	12854
10	Unsteady mean	12	1.0	7.6	6082

Table 32 – Main parameters regarding synthetical cycles selected after generation.

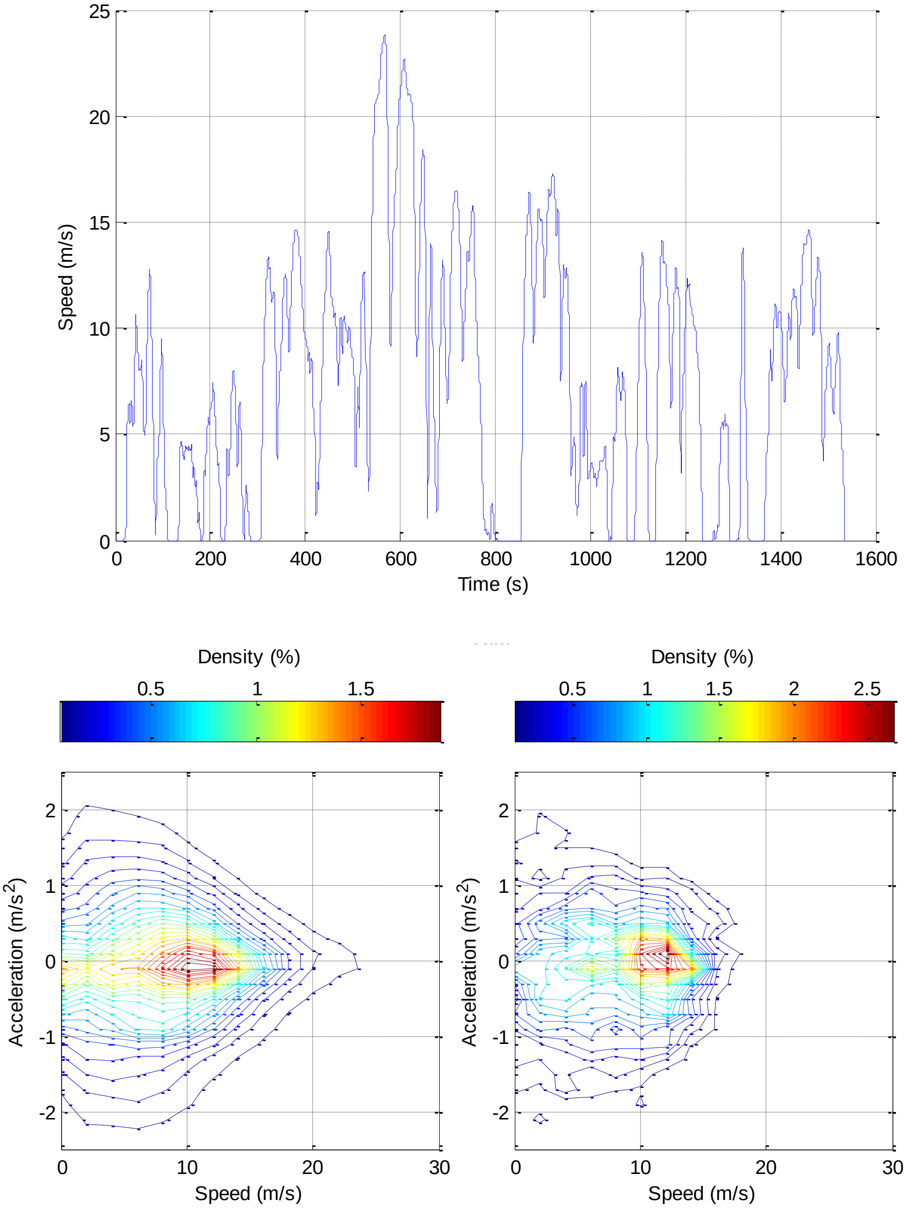

Figure 115 – Upper plot: "All long" cycle. Lower plot: comparison between original SAPD (left) and cycle SAPD (right).

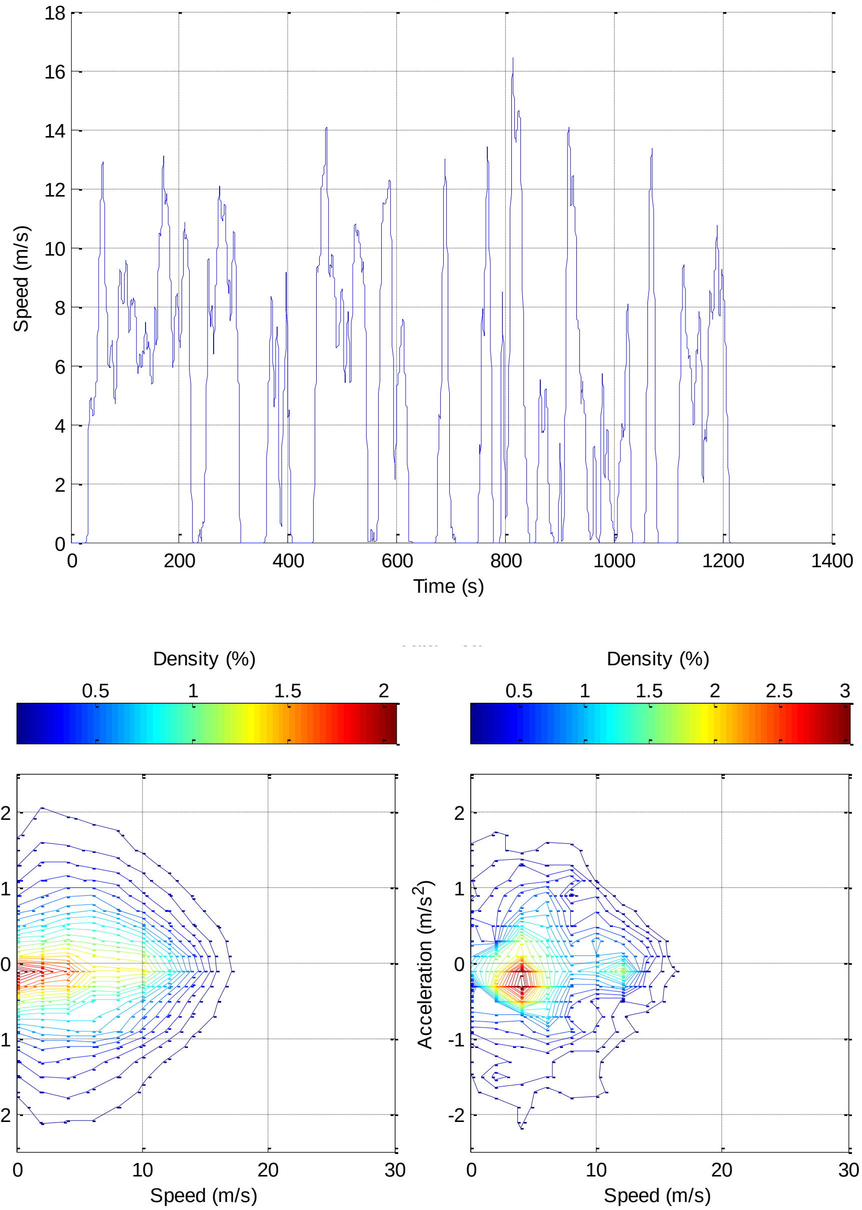

Figure 116 – Upper plot: "All mean" cycle. Lower plot: comparison between original SAPD (left) and cycle SAPD (right).

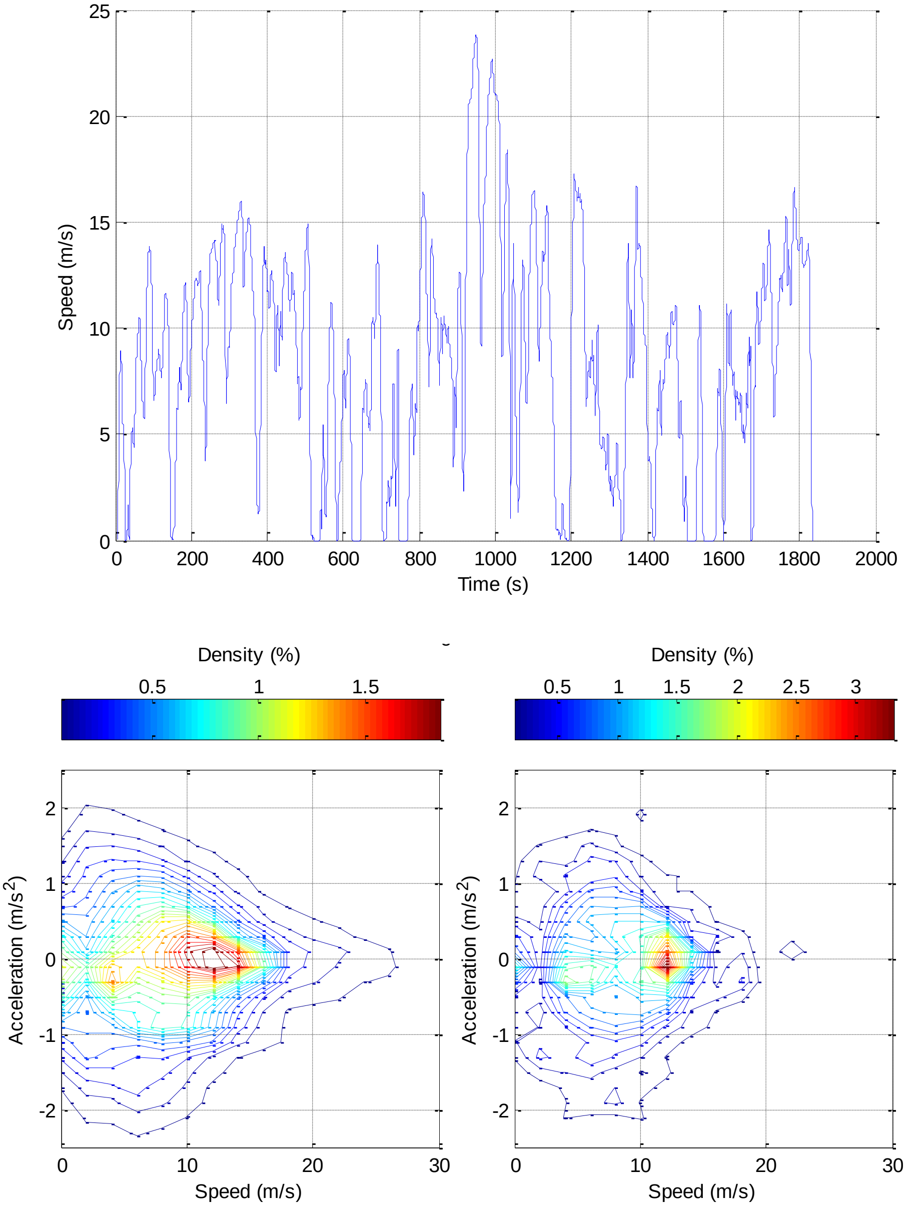

Figure 117 – Upper plot: "Passenger long" cycle. Lower plot: comparison between original SAPD (left) and cycle SAPD (right).

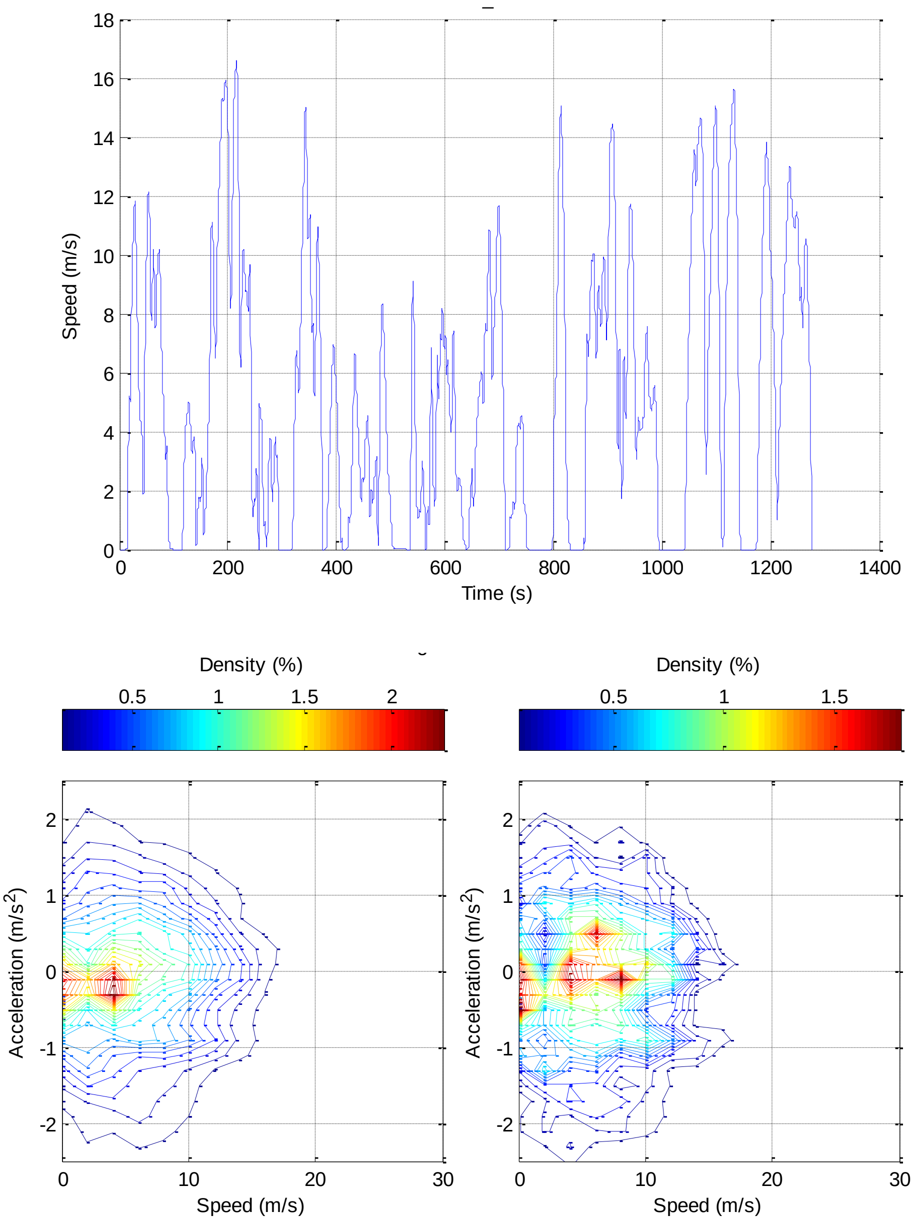

Figure 118 – Upper plot: “Passenger mean” cycle. Lower plot: comparison between original SAPD (left) and cycle SAPD (right).

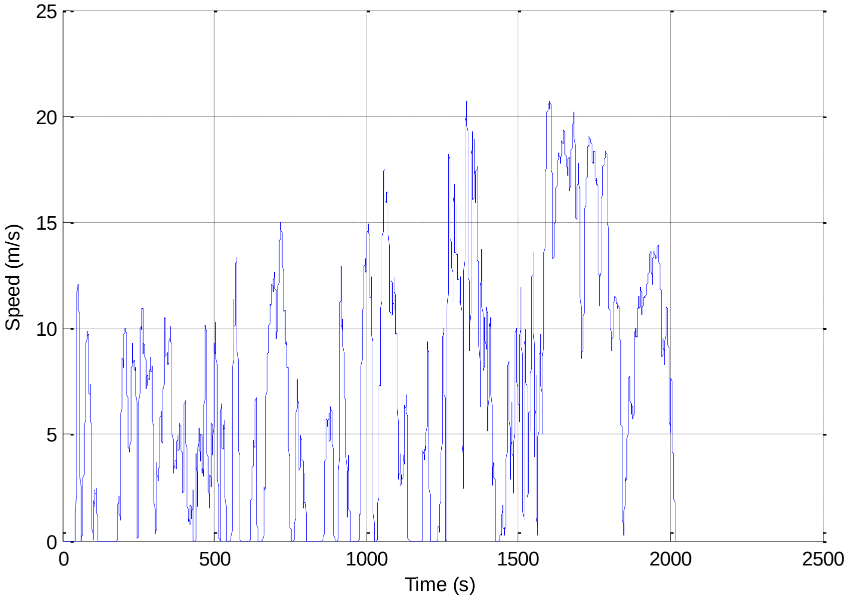

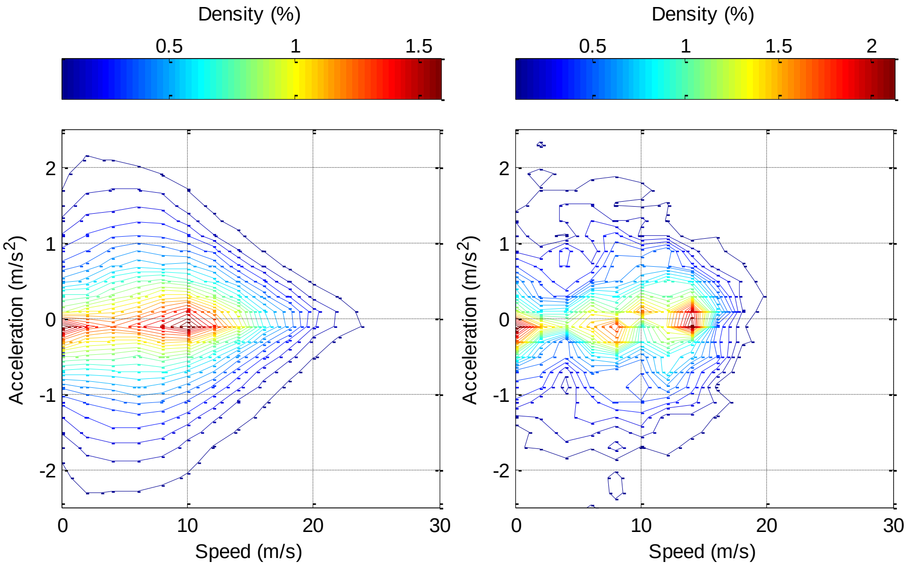

Figure 119 – Upper plot: "LDV long" cycle. Lower plot: comparison between original SAPD (left) and cycle SAPD (right).

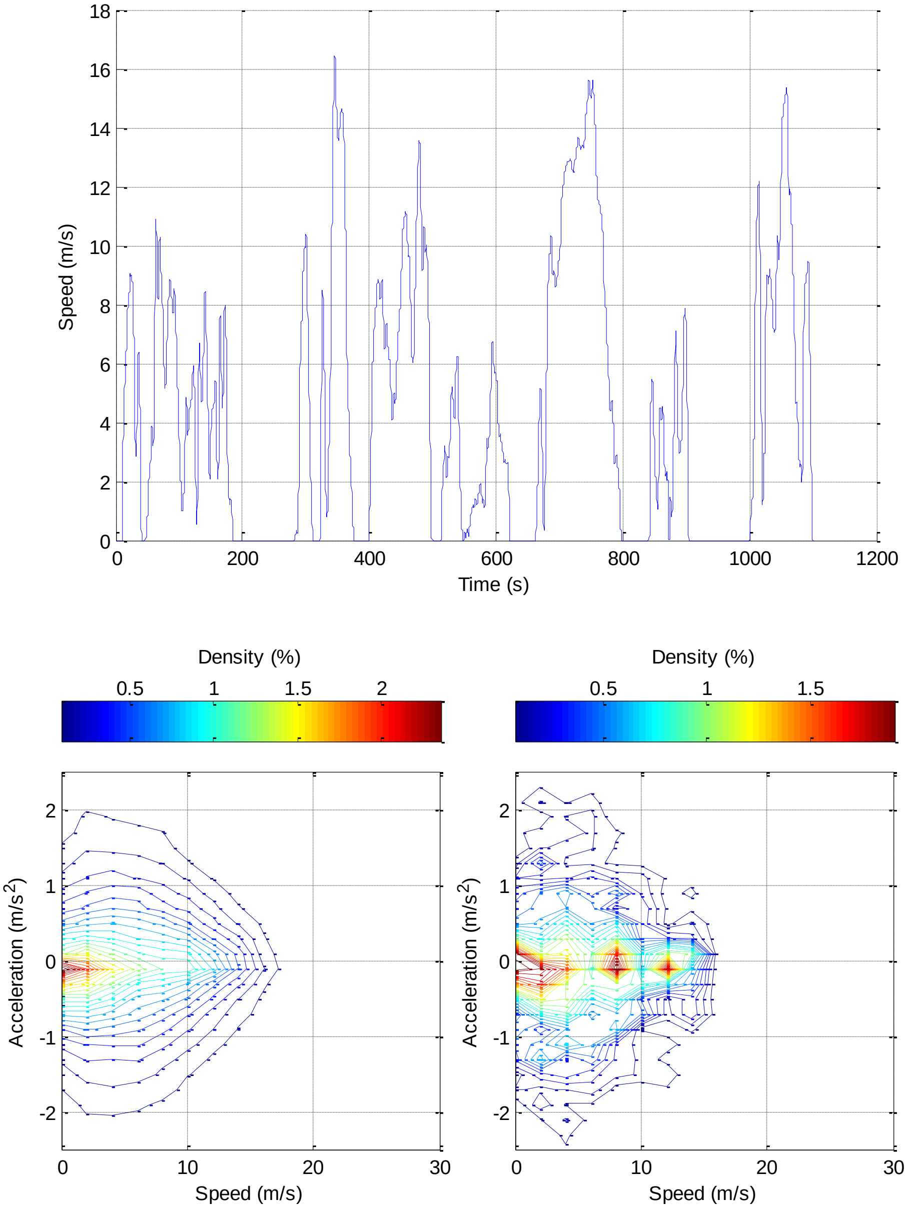

Figure 120 – Upper plot: “LDV mean” cycle. Lower plot: comparison between original SAPD (left) and cycle SAPD (right).

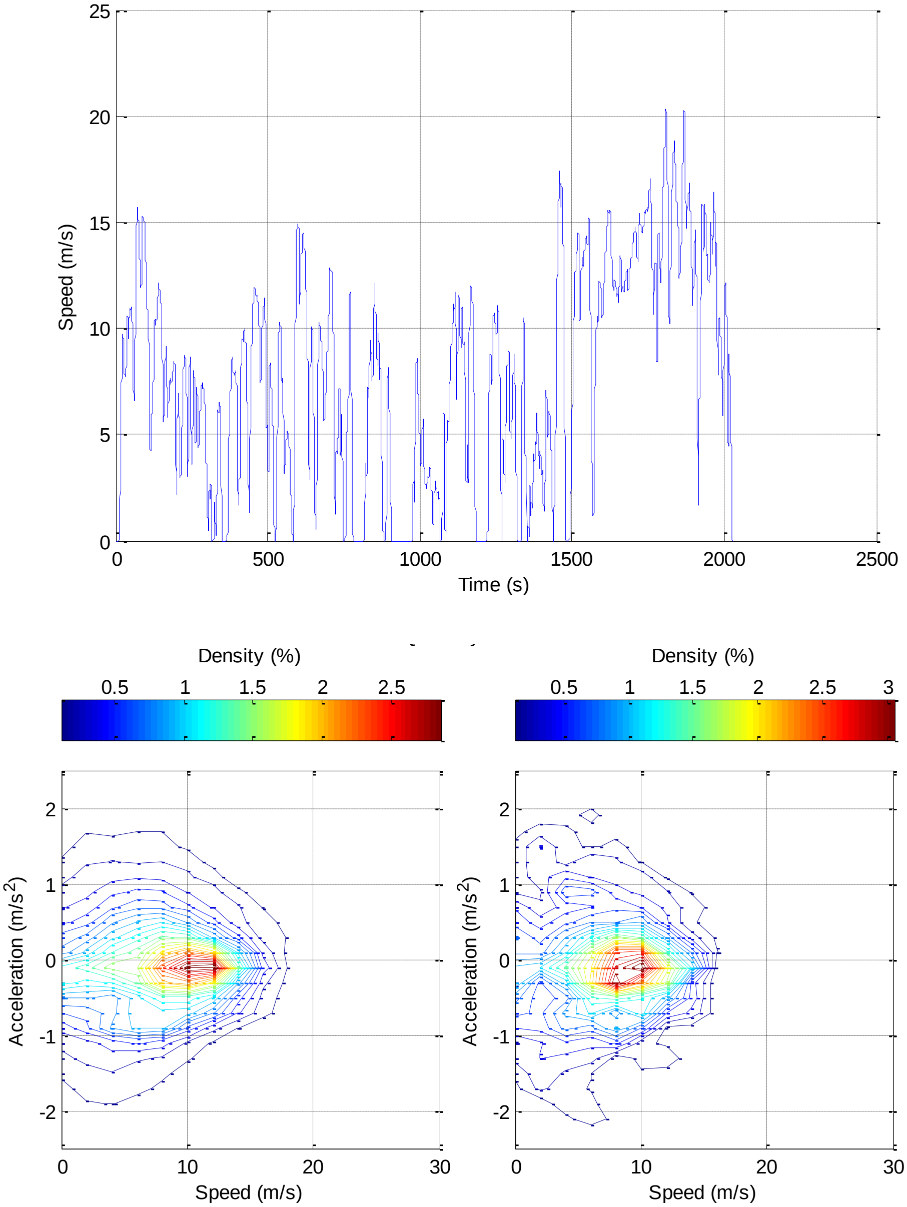

Figure 121 – Upper plot: "Quadricycle long" cycle. Lower plot: comparison between original SAPD (left) and cycle SAPD (right).

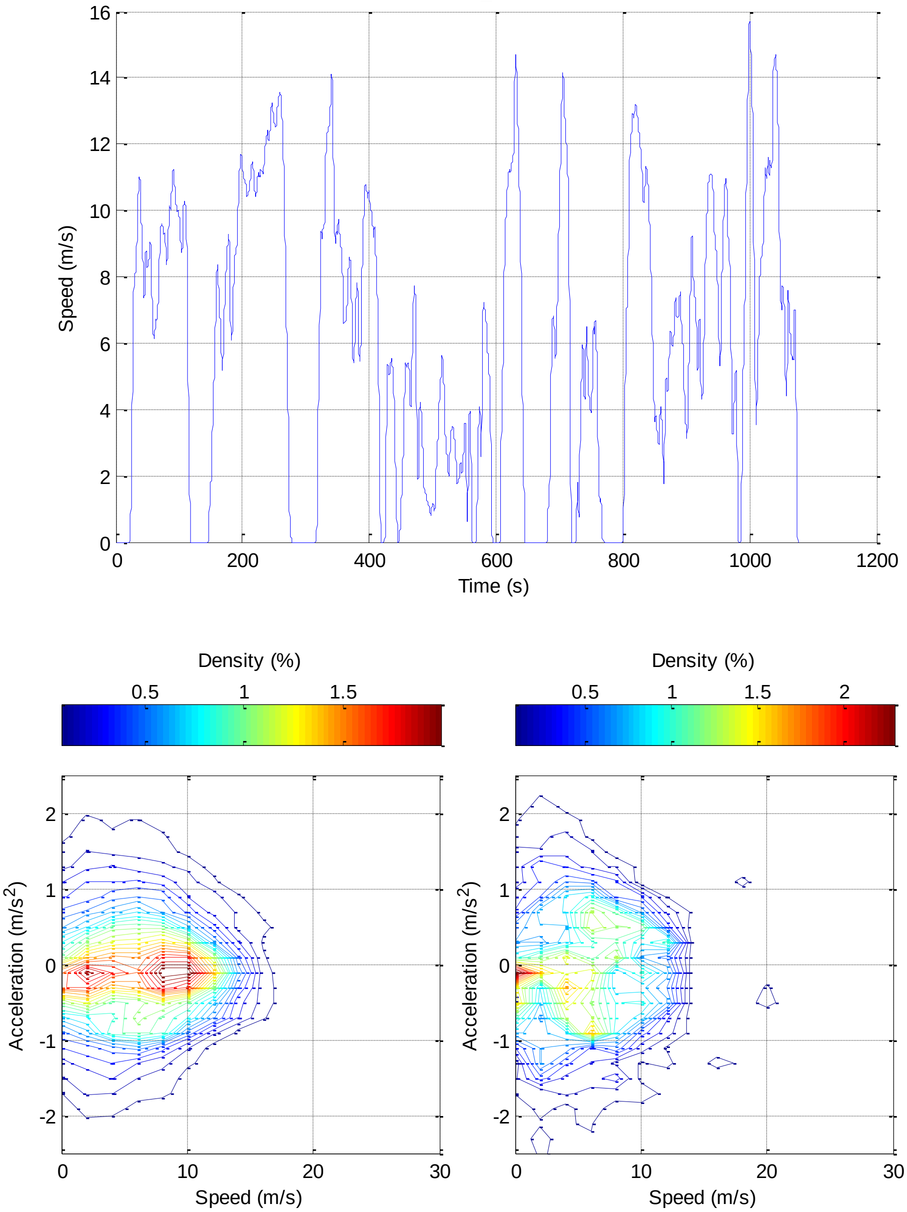

Figure 122 – Upper plot: "Quadricycle mean" cycle. Lower plot: comparison between original SAPD (left) and cycle SAPD (right).

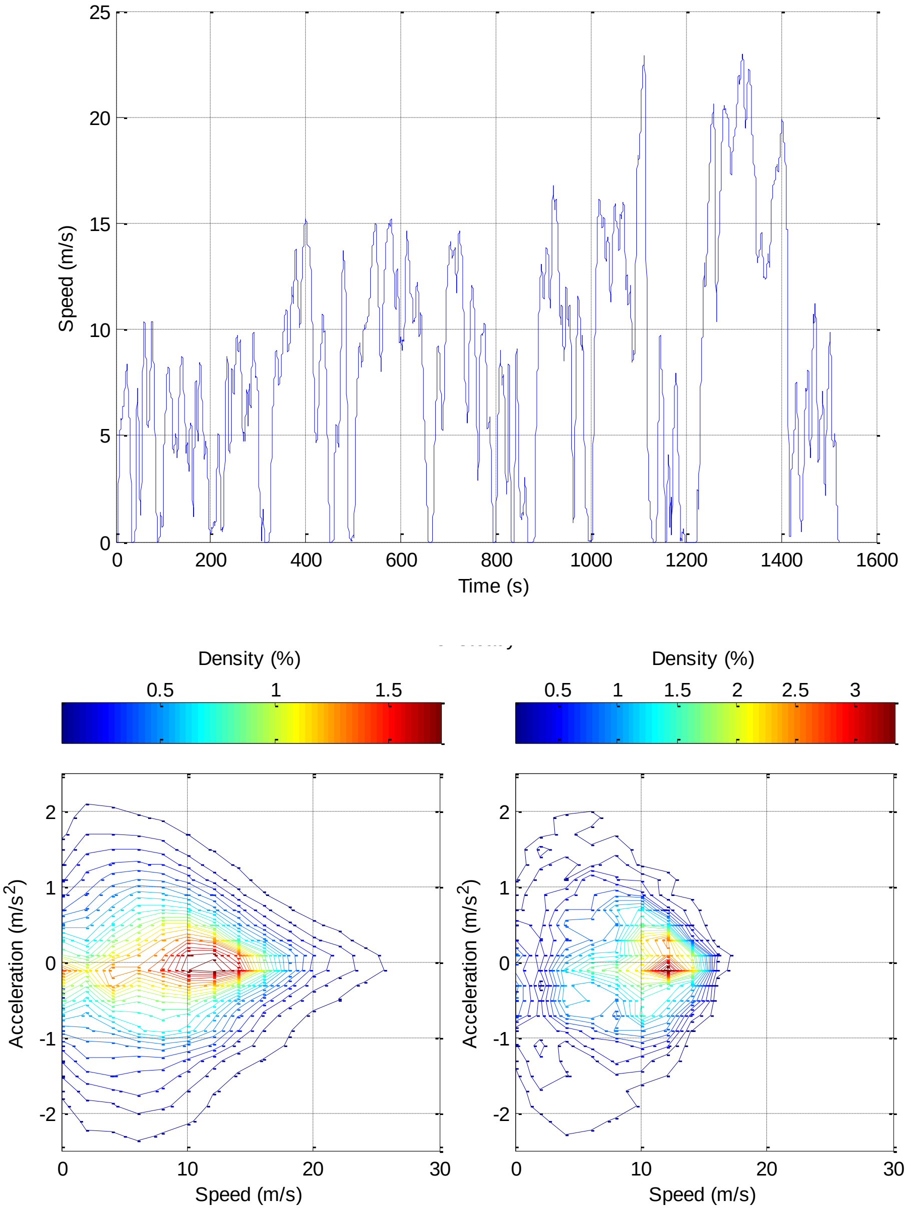

Figure 123 – Upper plot: “Unsteady long” cycle. Lower plot: comparison between original SAPD (left) and cycle SAPD (right).

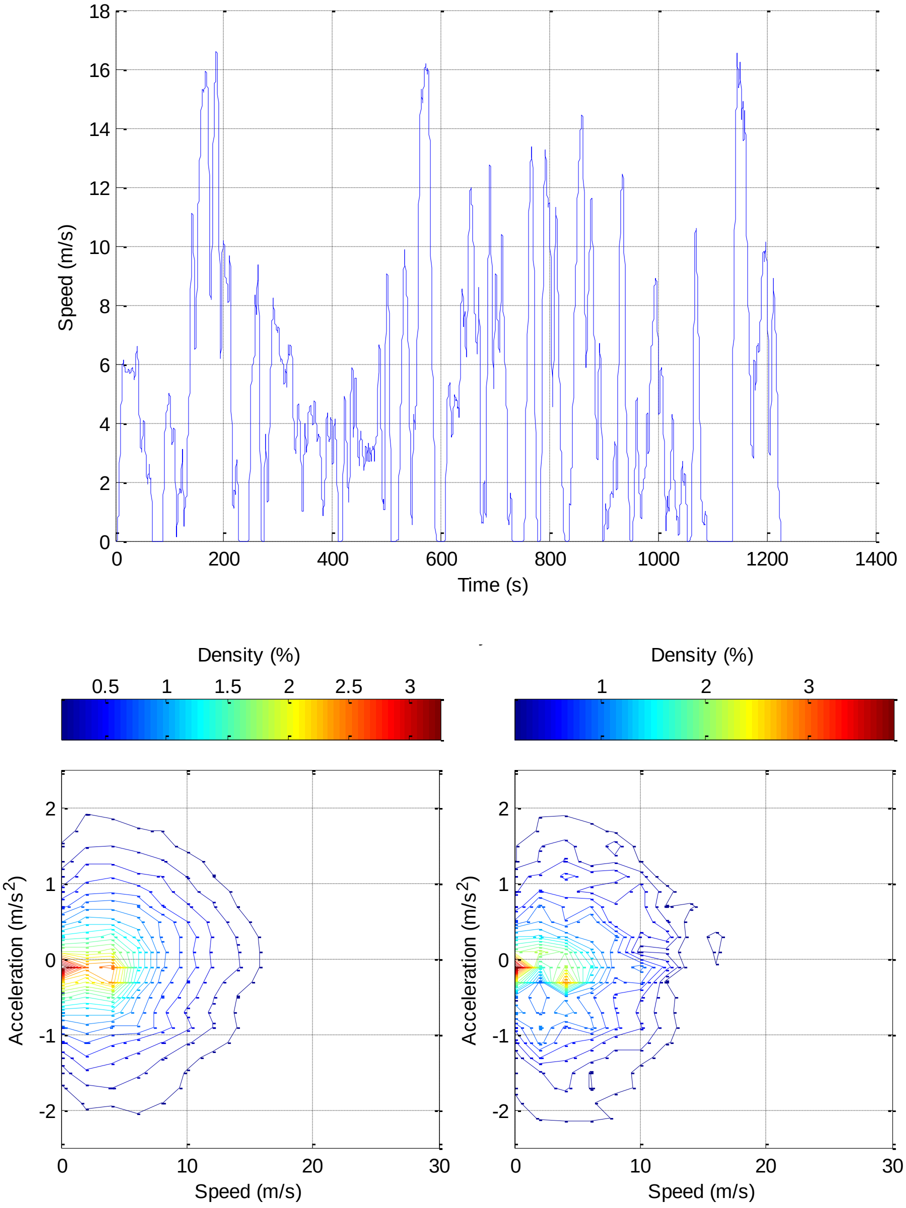

Figure 124 – Upper plot: “Unsteady mean” cycle. Lower plot: comparison between original SAPD (left) and cycle SAPD (right).

N.	Cycle name	idle %	cruise %	acc %	dec %	avg speed (m/s)	avg mov speed (m/s)	acc+ (m/s^2)	acc– (m/s^2)	stop/km	PKE (m/s^2)	acc+ noth (m/s^2)	acc– noth (m/s^2)
1	All long	13.2%	7.5%	41.0%	38.3%	7.4	8.6	0.59	–0.64	0.73	0.52	0.26	1.0
2	All mean	24.0%	6.5%	34.8%	34.6%	4.9	6.5	0.62	–0.62	0.68	0.57	0.29	1.9
3	Passenger long	7.5%	7.6%	44.7%	40.1%	8.3	9.0	0.59	–0.66	0.76	0.53	0.27	0.8
4	Passenger mean	17.3%	6.9%	38.3%	37.4%	5.1	6.2	0.66	–0.68	0.75	0.65	0.33	2.1
5	LDV long	19.3%	6.9%	38.4%	35.4%	6.8	8.4	0.62	–0.67	0.74	0.54	0.28	1.2
6	LDV mean	30.3%	6.2%	32.0%	31.4%	4.4	6.4	0.63	–0.64	0.68	0.58	0.29	2.1
7	Quadricycle long	10.4%	8.3%	40.3%	41.0%	7.3	8.2	0.56	–0.55	0.67	0.45	0.23	1.1
8	Quadricycle mean	16.6%	6.9%	37.6%	38.8%	5.8	6.9	0.56	–0.54	0.63	0.48	0.24	1.6
9	Unsteady long	6.0%	7.8%	45.3%	40.8%	8.5	9.1	0.61	–0.67	0.79	0.54	0.27	0.9
10	Unsteady mean	12.9%	7.6%	39.6%	40.0%	4.9	5.6	0.68	–0.67	0.78	0.68	0.35	2.3

Table 33 – Characteristics of each group of microtrips used as input for cycle generation.

N.	Cycle name	duration (s)	distance (m)	idle %	cruise %	acc %	dec %	avg speed (m/s)	avg mov speed (m/s)	acc+ (m/s^2)	acc– (m/s^2)	stop/km	PKE (m/s^2)	acc+ noth (m/s^2)	acc– noth (m/s^2)
1	All long	1536	11566	13.7%	7.4%	40.6%	38.3%	7.5	8.7	0.60	–0.64	1.0	0.53	0.55	–0.59
2	All mean	1214	5837	24.0%	6.7%	34.6%	34.8%	4.8	6.3	0.63	–0.62	2.2	0.56	0.57	–0.57
3	Passenger long	1835	15675	7.3%	7.6%	45.0%	40.1%	8.5	9.2	0.58	–0.65	0.9	0.51	0.54	–0.59
4	Passenger mean	1277	6481	17.6%	6.7%	39.2%	36.6%	5.1	6.2	0.65	–0.69	2.2	0.64	0.60	–0.63
5	LDV long	2015	14017	19.3%	7.2%	37.6%	35.9%	7.0	8.6	0.64	–0.66	1.3	0.54	0.59	–0.62
6	LDV mean	1100	4755	31.3%	6.1%	31.7%	31.0%	4.3	6.3	0.64	–0.65	2.1	0.55	0.59	–0.61
7	Quadricycle long	2028	15480	10.4%	7.8%	40.8%	41.1%	7.6	8.5	0.57	–0.56	1.0	0.46	0.52	–0.52
8	Quadricycle mean	1076	6360	17.2%	6.9%	38.3%	37.7%	5.9	7.1	0.56	–0.56	1.7	0.46	0.51	–0.52
9	Unsteady long	1521	12854	6.2%	7.7%	45.5%	40.7%	8.5	9.0	0.61	–0.68	1.0	0.53	0.57	–0.63
10	Unsteady mean	1227	6082	12.7%	7.4%	40.0%	39.8%	5.0	5.7	0.67	–0.67	2.3	0.65	0.62	–0.61

Table 34 – Parameters synthetized driving cycles.

N.	Cycle name	idle %	cruise %	acc %	dec %	avg speed (m/s)	avg mov speed (m/s)	acc+ (m/s^2)	acc– (m/s^2)	stop/km	PKE (m/s^2)	acc+ noth (m/s^2)	acc– noth (m/s^2)
1	All long	–3.9%	0.8%	1.0%	0.2%	–1.4%	–1.9%	–1.3%	–0.4%	1.0%	–2.6%	–2.5%	–0.7%
2	All mean	0.2%	–2.2%	0.8%	–0.5%	2.3%	2.5%	–0.7%	0.5%	0.9%	0.9%	0.8%	–14.2%
3	Passenger long	3.1%	0.0%	–0.6%	0.1%	–2.4%	–2.0%	2.6%	2.3%	0.4%	4.0%	4.0%	–5.2%
4	Passenger mean	–1.2%	3.4%	–2.2%	2.2%	1.2%	1.2%	2.1%	–2.2%	–0.2%	1.7%	1.5%	–0.8%
5	LDV long	–0.3%	–4.2%	2.1%	–1.3%	–2.9%	–2.8%	–3.1%	0.5%	–1.4%	1.2%	1.1%	–8.0%
6	LDV mean	–3.1%	1.9%	1.1%	1.5%	2.5%	1.4%	–1.4%	–1.8%	–3.3%	4.2%	3.7%	–1.6%
7	Quadricycle long	–0.1%	6.5%	–1.2%	–0.1%	–4.1%	–3.9%	–2.2%	–2.6%	–1.9%	–1.7%	–1.8%	2.2%
8	Quadricycle mean	–3.3%	0.5%	–1.8%	3.1%	–2.3%	–2.8%	0.7%	–4.0%	0.4%	3.2%	3.3%	–9.1%
9	Unsteady long	–2.0%	1.7%	–0.4%	0.4%	0.8%	0.8%	–0.4%	–0.9%	0.6%	2.1%	2.1%	–18.4%
10	Unsteady mean	1.5%	1.6%	–1.1%	0.3%	–1.0%	–0.5%	1.3%	–0.1%	0.5%	4.1%	4.0%	–1.1%

Table 35 – Percentage difference between the parameters describing the input measurements and the corresponding synthetized driving cycles.

5.2.2. Implementation of driving cycle synthesis methodology for dissemination

The second main product of driving cycle analysis activity is a “package” for data analysis and cycle synthesis. The package implements the same methodology applied for cycle generation (as described in the former paragraph) and is prepared as a Matlab–language product with Graphical Users Interface (GUI). Two “tools” are proposed.

The first tool – named “builder” – is an interpreter of data that can be used to “produce” new cycles and to verify their similarity with original data. The user can set a few parameters (the target distance, the vehicle data to be used, the data “clusters” to be included, the acceptance thresholds), than a number of “attempts” cycles can be generated; if any of the created cycles fits with original dataset, the tools plots the generated “representative” cycle and saves it in a spreadsheet. Saved data include the speed signal, the acceptance results (number of similar parameters, Performance Values – PV – indicator, Sum Square Distance – SSD – of speed–acceleration density matrix – SAPD) and the general describing parameters. The interface of the tool is shown in Figure 7; it is also part of ASTERICS project results and is therefore one of the final deliverables. Its typical output is shown in Figure 8.

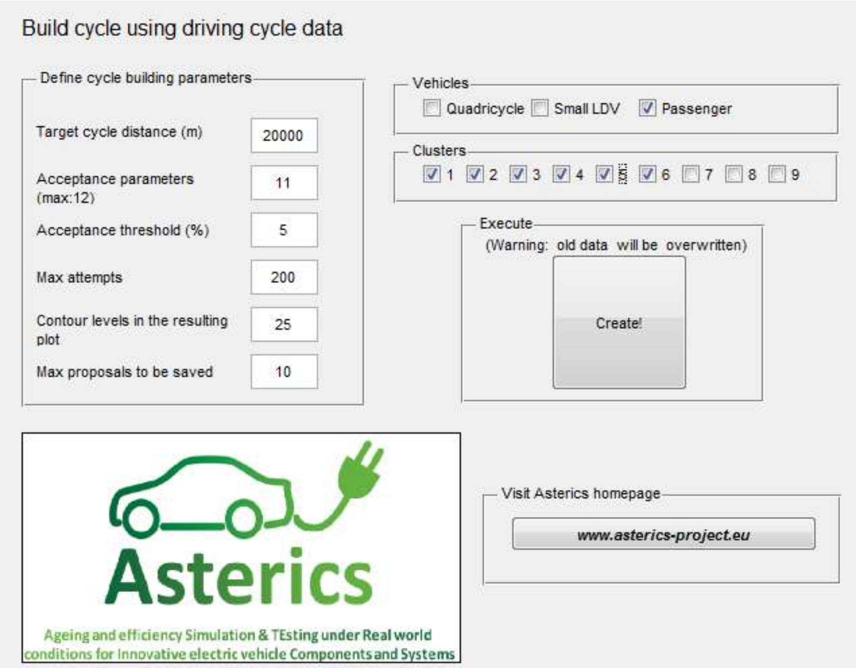

Build cycle using driving cycle data

Define cycle building parameters

Target cycle distance (m): 20000

Acceptance parameters (max:12): 11

Acceptance threshold (%): 5

Max attempts: 200

Contour levels in the resulting plot: 25

Max proposals to be saved: 10

Vehicles: ☐ Quadricycle ☐ Small LDV ☑ Passenger

Clusters: ☑ 1 ☑ 2 ☑ 3 ☑ 4 ☑ 5 ☑ 6 ☐ 7 ☐ 8 ☐ 9

Execute

(Warning: old data will be overwritten)

Create!
Asterics
Ageing and efficiency Simulation & TEsting under Real world conditions for Innovative electric vehicle Components and Systems
Visit Asterics homepage
www.asterics-project.eu

Figure 125 – Driving cycle “builder” tool: main GUI screenshot.

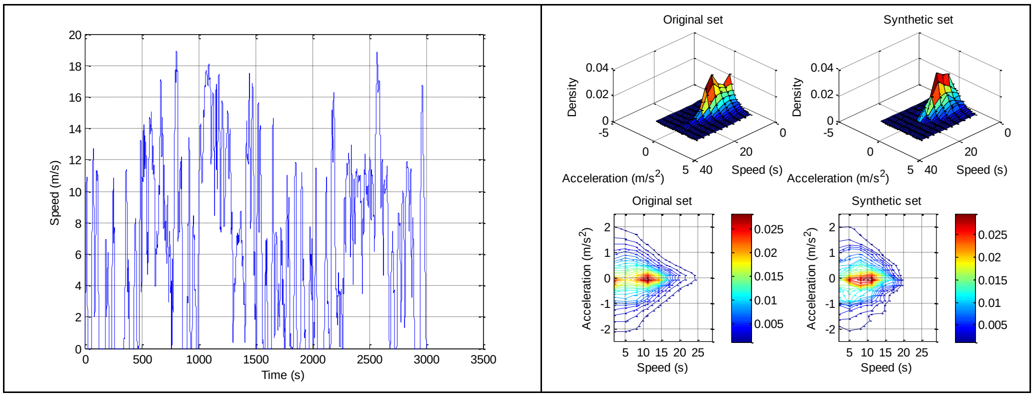

Figure 126 – Output from “builder” tool: cycle plot (left), cycle SAPD plot (right).

The second tool – named “binder” is a cycle explorer, editor and creator.

It can be used to “explore”, plot and save each cycle from a “collection” of data. The sources are:

- ASTERICS cycles and recent relevant driving cycles, e.g. ADAC highway cycles (see Kolke, 2013), WLTP cycles (see Steven, 2013)
- the database created for the former ARTEMIS project, which is still downloadable from project homepage, that includes legislative and research cycles.

As an editor, the tool can be used to “trim” existing cycles and to paste them together, as requested to reproduce some testing procedures described in literature (e.g. “EPA–5” test, ADAC “ECO test”); then, it calculates the energy needed to run the cycle (in kWh) using the pre–calculated results coming from a simplified model; the calculation is therefore almost immediate. This latter consumption estimation is based on a M1, A–class electric vehicle, curb mass being about 1100kg; the results should be considered a “rough” estimation of energy needed for a comparable vehicle, but are not validated for any specific case. The model used for such calculation is an adaptation of the one described in next chapter.

As a creator, the tool can be used to build new cycles using ASTERICS data assembled through the same methodology implemented in the “builder” tool, but, in this case, any cycle is accepted: the product of the randomization has to be considered as an “extraction” from the whole data, rather than a synthetic cycle. The same random recombination of cycles is possible for a selection of highway cycles, so that a single sequence of any length can be obtained. The reason for the use of such function is that highway cycle in literature are usually quite short (usually below 50km) in comparison with real case (e.g. a single run of 200–300 km is possible): the simple “juxtaposition” of highway cycles determines the occurrence of a zero–speed phase between different sequences; using linking criteria, the occurrence of stops is reduced. The interface of the tool is shown in Figure 127. Its typical output is shown in Figure 128. The product is also part of ASTERICS project results and is therefore one of the final deliverables. The tool can be used also directly through Matlab command line; the input, in fact, is a matrix that can be prepared with any text editor or using the binder GUI; command line use is preferable in case that a large number of simulations, each one using a different cycle, is needed. Therefore, the whole dataset is used and its segments are recombinated, so that the virtual test of the vehicle can be based on a large amount of data instead that on a “representative” set of that. The tool is aimed to fit with the needs of latest vehicle applied research, and, in particular, is supposed to be used for the definition of BEVs–HEVs energy management strategies or for “Montecarlo” simulation approaches (see Gong et al., 2012).

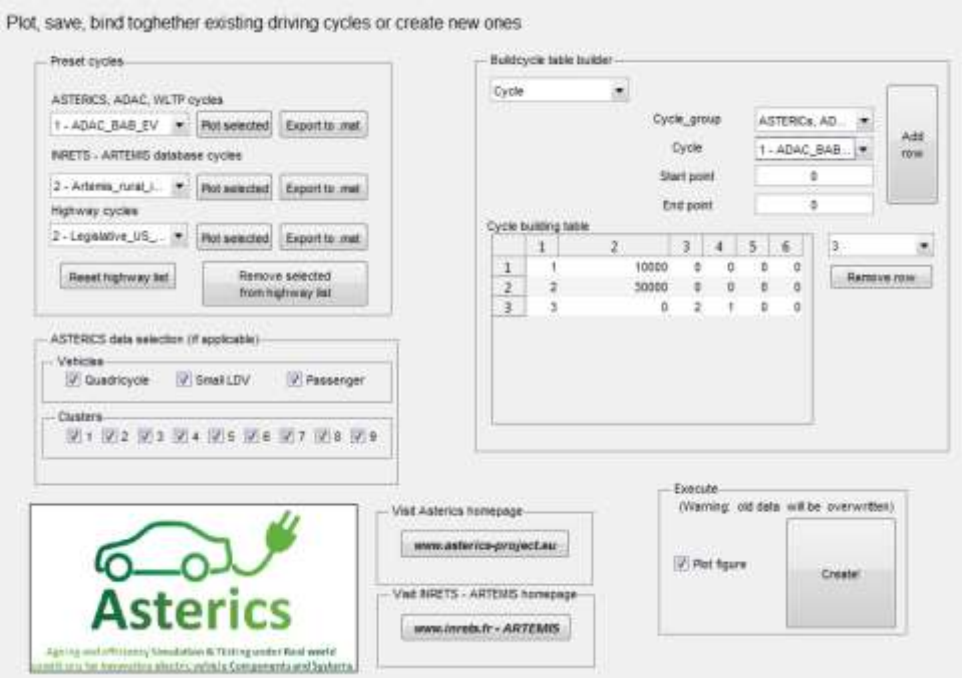

Plot, save, bind toghether existing driving cycles or create new ones

Preset cycles

ASTERICS, ADAC, WLTP cycles: 1 - ADAC_BAB_EV

INRETS - ARTEMIS database cycles: 2 - Artemis_rural_i...

Highway cycles: 2 - Legislative_US_...

ASTERICS data selection (if applicable)

Vehicles: ☑ Quadricycle ☑ Small LDV ☑ Passenger

Clusters: ☑ 1 ☑ 2 ☑ 3 ☑ 4 ☑ 5 ☑ 6 ☑ 7 ☑ 8 ☑ 9

Buildcycle table builder: Cycle

Cycle_group: ASTERICs, AD...

Cycle: 1 - ADAC_BAB...

Start point: 0

End point: 0

Cycle building table

	1	2	3	4	5	6
1	1	10000	0	0	0	0
2	2	30000	0	0	0	0
3	3	0	2	1	0	0

Execute

(Warning: old data will be overwritten)

☑ Plot figure

Plot selected
Export to .mat
Plot selected
Export to .mat
Plot selected
Export to .mat
Reset highway list
Remove selected from highway list
Add row
3
Remove row
Visit Asterics homepage
www.asterics-project.eu
Visit INRETS - ARTEMIS homepage
www.inrets.fr - ARTEMIS
Create!
Asterics

Figure 127 – Driving cycle “binder” tool: main GUI screenshot.

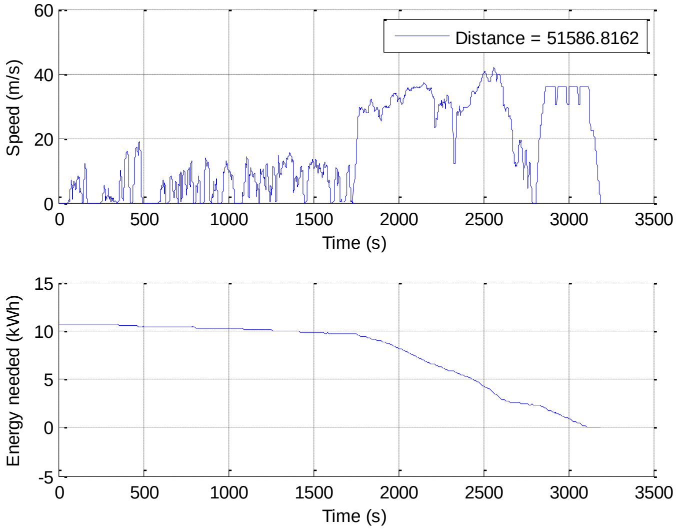

Figure 128 – Typical output from “binder” tool.

5.2.3. Additional results from on–road measurements

The plot in Figure 129 shows the results of the acquisition of motor working points (RPM–Torque) for the iMiev–type vehicle, highlighting the existence area of regenerative braking. Such data is useful to tune the simulation model explained in next chapter in order to have a realistic response during deceleration phase simulation.

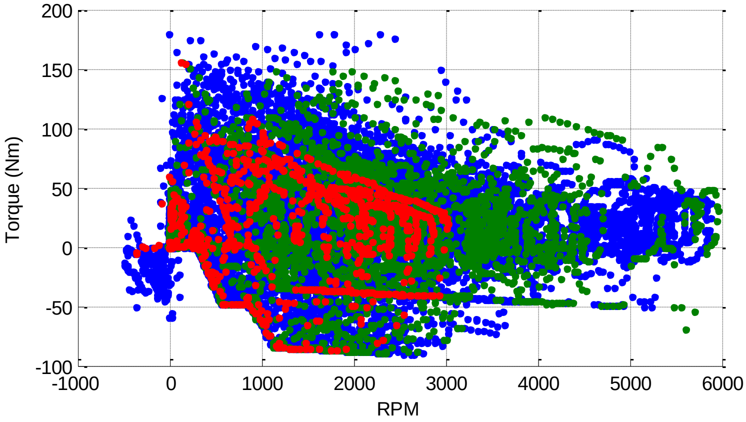

Figure 129 – iMiev motor working points from CAN acquisition; different colours corresponds to different trips.

The Twizy vehicle has been subjected to the measurements of the 12V system during the hiring period, that is about a week and more than 400km driven. The vehicle is a quadricycle, so that in comparison with other higher class cars it is not equipped with optionals as power windows and air conditioning system. Most equipment is similar and include:

- Full–power lighting system
    - indicators, stoplights and projectors etc.
- Windscreen washer
- Windscreen electric heater
- A number of ECUs for vehicle control (airbag system, motor management, carbody management)

In the light of this fact, the acquired power could represent the approximated consumption also for other vehicles; in particular, the prolonged acquisition is useful since it considers the average absorption of vehicle "metabolism" (due to ECUs) and the losses of the charging system from high–voltage to low–voltage system through a DC/DC converter. Main data are shown in Table 36 and Figure 130.

12V load	Power (Watt)
Key on and logger	7.0
Key on	4.2
Position light	43.4
Headlights (low beam)	186.2
Headlights (high beam)	200.2
Headlights (dipped)	336.0
Windshield heater	119.0
Stoplights	70.0
Windscreen cleaner pump	77.0
Windscreen wiper speed 1	47.6
Windscree wiper speed 2	60.2
Indicator	56.0
Hazard Indicator	112.0
Horn	50.4

Table 36 – Adsorbed power for main Twizy 12V components.

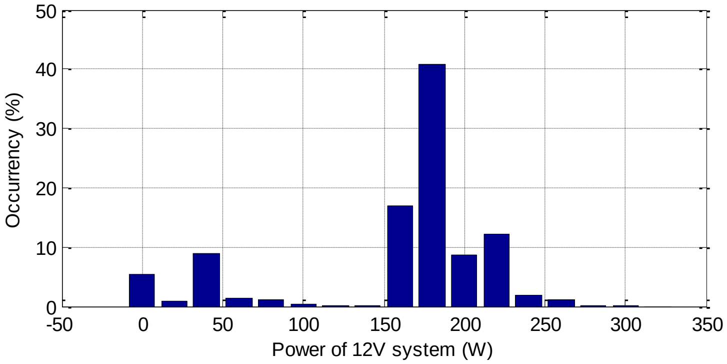

Figure 130 – Frequency of energy consumption for 12V system of Twizy during use.

6. A simulation framework application

This chapter illustrates the development of a model for vehicle simulation and its use for an evaluation of vehicle performances depending on components sizing. The first part of the chapter describes the choices adopted for the definition of each vehicle component; the second part describes the strategy implemented for the energy management of the vehicle in case that a range extender is installed, while the third part analyses vehicle performances over two main scenarios. Different sizing alternatives are also compared in order to study their influence on final vehicle performance indicators. The reference vehicle modeled is the Mistubishi iMiev vehicle, since it was used during the measurements phase and for which are available published articles and data (see Hosokawa et al, 2008; Kamachi et al., 2010; Kamachi and Hosokawa, 2011; Shankar et al, 2012 for general vehicle information).

6.1. Context and motivation for the study

The battery system is certainly the key component for electric and hybrid electric vehicles, both for those using it as main energy storage unit (BEV, EREV, PHEV) and for those using it mainly as “energy buffer”, such as HEV and small range PHEV.

It is undoubted that the characteristics (energy density, energy power, durability) of last generation cells (mainly lithium–based technologies) enabled the possibility to build BEV capable of overall performances comparable of even preferable to those of conventional vehicles within a relevant range. In particular, the achievement of 100–150 km range became possible at reasonable conditions in terms of cost, size, and weight of the installed battery. In this context, a question arise: is it possible to identify the minimal characteristics for a technology “breakthrough”, in order to define a roadmap for applied research? The definition of reference parameters has been discussed in literature and research, as shown on paragraph 3.1.1.

On author’s opinion, even if commercially available BEVs are mainly based on the use of single–type battery cells, it is not possible to state that battery technology is mature. Some alternatives are proposed in research for the enhancement of system performances through the integration of electrochemical cells or even through the complete substitution of cells with other, different technologies. A brief literature analysis shows that “dual” energy systems can comprehend the installation of two types of cells having different characteristics (e.g. as in the “SuperLib” project, see Omar et al., 2012) or the use of supercapacitors elements. In both cases, the use of advanced electronic system for control (e.g. SOC balancing between cells), power supply and management is needed, and the overall results determine if the integration of systems is “useful” (e.g. increase durability, efficiency, or performances) or not; the final cost of the whole system is also one of the main elements determining the choice. Figure 131 shows the results (in terms of energy and power density) of the combination of Li–based battery cells with supercapacitors (see Cericola et al., 2010).

Supercapacitors can be used in a large number of application, such as a power support for fuel–cells vehicles (see Bauman and Kazerani, 2008), in case of high–performance vehicles in which the energy to power ratio is very low (see Frenzel et al., 2011), in case of application with lead batteries (see Lam and Louey, 2006) and also in case of EVs using Li–batteries. However, the success of the application on PHEV/BEV depends on a number of factors, so that each case should be examined in detail (see Burke, 2000, for an introduction on SCs, and the more recent works by Burke, 2007 and by Burke and Miller, 2010 for applicability of technology).

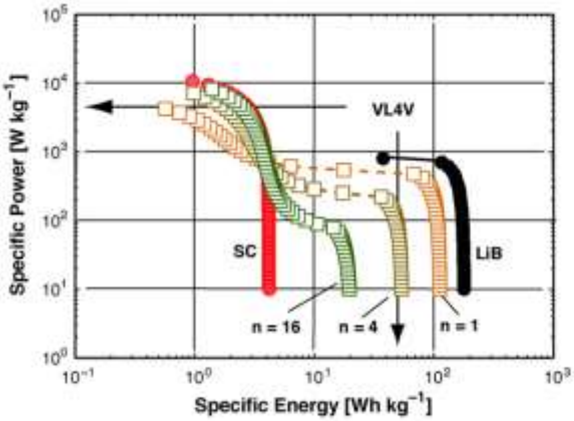

Figure 131 – Simulated Ragone plots for constant power discharge for the battery cells (BU, black), capacitors cells (SC, red) and various combination of both (see n=16, n=4 and n=1 configurations, corresponding to different LiB–SC couples). Source: Cericola et al, 2010.

One of the aims of the simulation activity is to verify if the “downsizing” of battery system is advantageous in case of the presence of a range extender; this means that, for small battery systems (e.g. 25% or 50% of reference vehicle capacity) the C–rate of the cells increases if the maximum power to be supplied remains the same. In case that the C–rate overpasses the capabilities of the cells, two main solutions are possible:

- the technology of the battery system together with its size is modified in order to guarantee that it can supply higher C–rate
- the battery is supported by the generator, so that the maximum C–rate is maintained below that threshold.

The first solution can be actuated through the use of different cells, through the installation of supercapacitors as “power aid” or through both. The second solution implies the frequent use of the generator, so that the fuel consumption could result in a significant increase.

In the present activity, it has been chosen to verify the effectiveness of alternatives comprehending the use of battery and supercapacitors together with generator support or of this latter without using supercapacitors. It has been chosen not to use standalone supercapacitors system (a solution proposed by Solero et al., 2011 for urban vehicles), in order to maintain a relevant pure electric range since this capability allows to access to traffic restricted zone, that is an important driver pushing for EV use for the users monitored within ASTERICS. Also, it has been chosen to study one type of cells, based on the data of a commercially available type, instead of substituting the cells with high power ones.

6.2. Modelling electric vehicle

This paragraph describes the choices adopted for each vehicle component. According to the guidelines defined in previous chapters, the model is intended to be used for general energy management strategy definition and for archetype confrontation. Such activity requires the repetition of simulation execution to represent the variability of use cases; a low calculation effort is preferable. The model is mainly based on simplified components submodels; this detail is coherent with the fact that an accurate model validation has not been possible during the study.

6.2.1. **Simulation environment**

The model is running in Matlab–Simulink environment; co–simulation with external tools is not needed. Three different capabilities of the environment have been used:

1. Data management: the model is interfaced with external sources using Matlab capabilities for data import and export of any kind; in particular, the experience coming from the data acquisition on vehicles is fully available to the model using the “binder” tool, which acts as a bridge between measurements and simulations, and is called directly by command line or scripts.
2. System control and functional logic implementation: such capabilities can be implemented in Simulink using standard blocks library coupled, if necessary, with command–line functions; State–Flow functions (available as a library that is specific for system control definition, graphical visualization and debugging) have not been used.
3. Physical models: depending on the needs, physical components have been built using standard blocks (which define the component equations in explicit, causal form) or Simscape library blocks, for which a different formalism is used. Simscape blocks interacts with the system using “physical” ports instead of “signal ports”, so that an interpreter is needed between the two. As an example, a single mechanical rotational link acts as a “shaft”, so that it is characterized by two variables: rotational velocity (across variable) and torque (through variable); virtual measurements blocks from mechanical links to two distinct signals are therefore needed to make this variables available to conventional Simulink blocks. Physical network elements are defined through acausal equation, so that the solver needs an interpreter for the reformulation and the solution of final ODE equations.

This model structure has been prepared to represent the core of a platform for system development rather than a rigid tool for numerical calculation. It can be said that even if a single software has been used, the structure of the model is composed by an “hub” (the Simulink environment and its solver) interacting with information database, control networks and physical networks; each component can therefore be substituted with an “equivalent” one (e.g. a one having the same function and input/output ports, but capable of increased accuracy) even using an external software if a suitable interface is available.

6.2.2. Vehicle Body Characteristics

The values adopted to represent general vehicle characteristics are critical for the quality of the evaluation of overall vehicle performances. Assuming that the main aim is the calculation of energy consumption, a simplified representation has to include:

- the mass of the vehicle
- the drivetrain rotational inertia
- the aerodynamic characteristics of the body (front section, expressed in m^2, and drag coefficient)
- the tyre rolling resistance factor
- the driveline overall loss factor, related to transmission characteristics due to friction phenomena on bearings, to mechanical seals or due to interaction between lubricant and mechanical elements (e.g.”churning” and “windage” phenomena)

This parameters are sufficient to calculate the forces that are therefore acting on the vehicle, supposed as a single translational mass. Distinction between unsprung and sprung masses, lateral dynamics and load variation between front and rear axles are not considered.

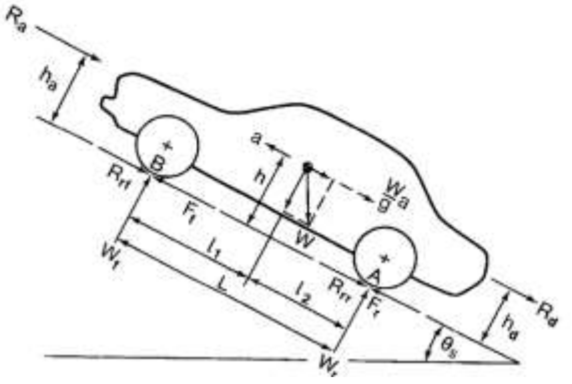

Figure 132 – Forces acting on vehicle body (Wong, 2001).

Considering that the main relevant losses at constant speed are related to roll friction and to aerodynamic drag, a second degree function can be used to represent the resistance force as a function of speed.

It is possible to evaluate general loss factors through coast down test. It consist in measuring vehicle speed during “coasting” deceleration from a predetermined speed; it is therefore possible to obtain the instantaneous deceleration and the forces on the vehicle, assuming that disturbances are not relevant (e.g. wind speed, road slope). Losses parameters can then be obtained through 2nd degree fitting function on the measured acceleration or 3rd degree fitting function on the measured speed (numerical calculation being more stable). As known, the resistance force acting on the vehicle can be expressed as a function of vehicle speed v:

$$F = R_a + R_r + R_d + R_g + R_o + a * M$$

Where F is the total traction force, R_a is the aerodynamic resistance force, R_r is the rolling resistance of wheels, R_d is the drawbar load (not considered in the model), R_g is the grade resistance, a is the longitudinal acceleration and M is the mass. Total resistance is therefore a function of speed:

$$R_v = R_a + R_r + R_d$$
$$R_v(v) = \frac{1}{2} * \rho * C_d * S * (v + v_{wx})^2 + f_r * m * g * sin(\alpha) + m * g * cos(\alpha)$$

Where the terms indicate, respectively:

- for second degree: the air density, the drag coefficient, the vehicle frontal area; speed can be corrected to take into account the component of wind speed parallel to vehicle speed (v_{wx})
- for zero degree: roll factor per vehicle mass per g constant; α is the road slope.

Tyre rolling resistance factor can depend on the speed according to:

$$f_{rt} = f_r + f_{rv} * v^2$$

The work by Wong, 2001, suggests the following values for speed below 150 km/h:

$$f_r = 0.0136$$
$$f_{rv} = 0.4 * 10^{-7}\ [1/(\mathrm{km/h})^2]$$

The values highlight the quite low relevance of the variation for common use speed (e.g. at 130 km/h, the increment is 0.00068, less than 5% on rolling factor, that is not the main loss at such high speed).

However, depending on known vehicle parameters, it is not always possible to disaggregate in detail each loss parameters (e.g. it cannot be possible to distinguish the f_{rv} roll factor from aerodynamic factor since they are both included into 2st degree force fitting term). The indications on how to perform the test are described through international standards (see UNECE R.83, 2011) defining both boundary conditions such as the additional testing mass of the vehicle (100kg), the correction factors for temperature (e.g. air density can vary) and the criteria for the averaging and accept the results as statistically significant after a number of repetitions.

The Mitsubishi iMiev [6] model – which is one of the first “lithium generation” commercially available EV – has been used for various benchmarking studies (see Becker et al., 2013; Eickstein et al., 2013). Table 37 shows the differences between two different coast down characterizations performed on the same model; Surprisingly, the results are significantly different; the value of frontal section, as an example, is not coherent with vehicle declared dimension and suggests that a refuse is present on the text. As exposed on 6.2.10 paragraph, a comparison between preliminary simulations, results shows that data coming from the work by Eickstein et al., 2013, are acceptable.

---

[6] The vehicle has been presented on the EU market also by different brands, assuming the commercial name of Peugeot iOn and Citroen C–zero.

Value	**Eickstein et al., 2013**	**Becker et al., 2013**
Vehicle mass (kg)	1100	1240
Frontal area (m^2)	2.14	2.85
Drag coefficient C_d	0.33	0.35
Roll coefficient f_r	0.011	0.016

Table 37 – Coast down results from literature for the Mitsubishi iMiev EV.

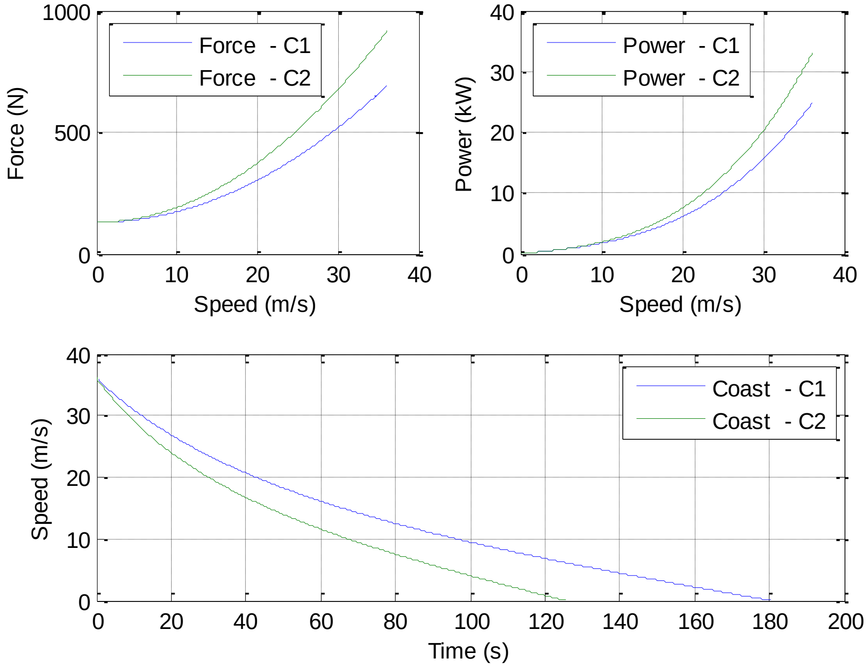

Figure 133 – Calculated traction force, traction power and coast down time from 130 km/h for data on Table 37; C1 refers to Eckstein et al., 2013 source and C2 refers to Becker et al., 2013 source.

Regarding vehicle mass, the curb weight value of about 1100kg has to be added of an amount which takes into account “standard” driving conditions (100kg for drivers and various, according to R101); this value is therefore used for effective weight force calculation. During simulation, the mass used for the calculation of inertia characteristics has been added of an additional value related to the rotational inertia of the driveline. The rotational inertia of main components such as the wheels, the shafts, the differential and the flywheel of a conventional ICEv has been considered comparable to the inertia of the electric powertrain, so that values used in the simulation are similar to those suggested in literature (see Genta and Morello, 2009b). The equation describing the inertial equivalence between rotational wheels and translation masses is, as known:

$$M_{eq} = \frac{J}{r^2}$$

Where M_{eq} is the equivalent translational mass of the rotational element, J is the moment of inertia of the element and r is the radius of the wheel; if the element is on an axis subjected to a ratio τ in comparison with wheel axis, the equivalence become:

$$M_{eq} = \frac{J * \tau^2}{r^2}$$

The estimated inertia are shown in Table 38; the value of 41.5 kg is about 3.8% of total vehicle mass.

Element	Radius (m)	Ratio	Rotational Inertia (kgm^2)	Equivalent mass (kg)
One Wheel (including shaft and differential)	0.3	1	0.75	8.33
Motor rotor	0.3	6.066	0.02	8.18
Total equivalent mass (4 wheels)				41.5

Table 38 – Equivalent mass calculation.

At each simulation time, the model calculates the resistance forces and the traction fort provided by the wheel; therefore, the “car body” block uses a simple integrator to obtain vehicle speed using the very well known equation for acceleration calculation:

$$F_{tot} = M_{eq} * a$$

The model is, therefore, a forward simulation one (see paragraph 3.1.1).

6.2.3. Battery modelling

Regarding battery system, its representation in a model is set up in order to assess the energy throughput of the component and its approximated voltage characteristics, while the modelling of short–time phenomena has not been considered a priority; the scope of the simulation activity, in fact, is mainly the assessment of overall vehicle energy consumption. The general model build within the activity refers to the category of equivalent circuit systems, including only generators, resistors and capacitors. Such category of model is frequently used in literature also due to the fact that it is flexible, since the represented battery impedance can be tuned increasing the number of elements on the circuit (see the works by Van Mierlo et al., 2004; Dubarry and Liaw, 2007; Einhorn et al., 2011; He et al., 2012; Hu et al., 2012). Due to the fact that this family of model is almost a “black box” representation, an analysis of lithium battery characteristics and of electrochemical phenomena at cell level is not included in this study. The model prepared for the activity is based on equivalent circuit structure; the number of capacitor–resistor elements can be modified, obtaining a different response.

The voltage drop at battery terminal due to current supply can be expressed through a transfer function in the frequency domain. Referring to the schemes in Table 39, the voltage drop between OCV source (V_{oc}) and battery terminals (V_{B12}) is:

$$E_L = V_{B12} - V_{OC}$$

If the current I_B is the input and E_L the output, the transfer function *G(s)* is defined as:

$$G(s) = \frac{E_L(s)}{I_B(s)}$$

As shown in He et al, 2013, the general expression for the transfer function of a network composed by a resistor R_s and a number of resistors R_{di} and capacitors C_{di} is:

$$G(s) = R_s + \sum_{i=1}^{N} \frac{R_{di}}{1 + R_{di}C_{di}s}$$

If the model is tuned using the values suggested by Einhorn et al., 2013, and subjected to a current step of 20A, the responses assume the shape shown in Figure 134.

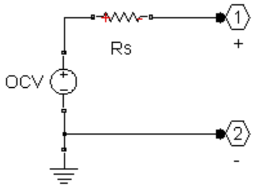

$$G(s) = R_s$$

R_s=3.00 $m\Omega$

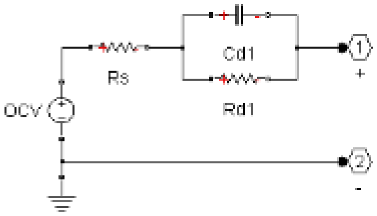

$$G(s) = R_s + \frac{R_{d1}}{1 + R_{d1}C_{d1}s}$$

R_s=1.55 $m\Omega$; R_{d1}=1.46 $m\Omega$; C_{d1}=63 kF

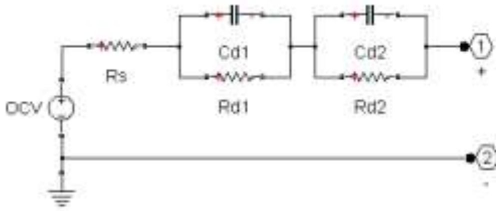

$$G(s) = R_s + \frac{R_{d1}}{1 + R_{d1}C_{d1}s} + \frac{R_{d2}}{1 + R_{d2}C_{d2}s}$$

R_s=1.20 $m\Omega$; R_{d1}=0.50 $m\Omega$; R_{d2}=1.20 $m\Omega$

C_{d1}=25 kF; C_{d2}=85 kF

Table 39 – Equivalent networks alternatives for battery modelling and the related transfer function of order zero, one and two. The parameters suggested come from Einhorn et al., 2013.

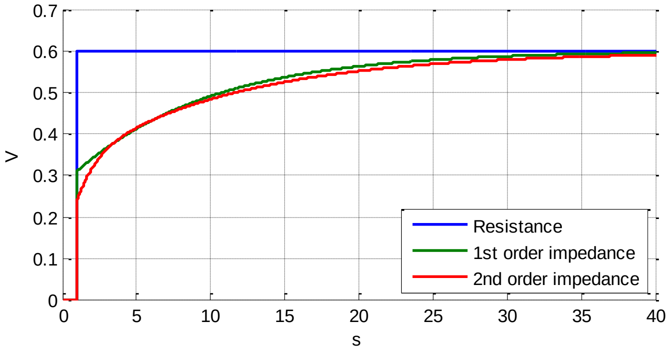

Figure 134 – Voltage drop for cells elements in Table 39 as a response of a current step.

The equivalent electric network is be completed by subsystems including:

- a subset for the estimation of the SOC (e.g. through Coulomb Counting method)
- a subset for the calculation of elements parameters depending on battery state
- a subset for the calculation of the temperature
- a subset for the calculation of the SOH (that is, the current evaluation of battery capabilities in comparison from when it was new) and/or of the accumulated damage of battery depending on its use.

The latter point deals with the critical evaluation of battery degradation and ageing, which mainly depends on battery lifetime, on battery working and storage temperature, on depth of discharge. The analysis of the factors determining ageing and the build up of suitable empirical function for the evaluations of the damage are under debate in literature but will not be considered in the present work. A brief review can include the work by Liaw et al., 2005, that defines an empirical model for capacity fade and resistance increase and propose an application on a lumped parameter; Vetter et al., 2005, which describes ageing phenomena at cell level and is based on a large bibliographic study; Rong and Pedram, 2006 proposing an online prediction model; Marano et al., 2009, proposing a framework for ageing estimation using methods "borrowed" from material fatigue analysis, the study by Smith et al., 2012, that correlates an ageing model to the working condition in which the vehicle is operating. A model adapted from this latter study is:

$$SOH = a_1(T, SOC) * t^{\frac{1}{2}} + a_2(T, SOC, I) * N$$

Where the first term expresses the "storage" ageing (a_1 is a coefficient depending on temperature and state of charge of the battery, while t is the storage time) and the second expresses the "cycling" ageing (a_2 is a coefficient depending on temperature, on state of charge of the battery or on its variation, I is the average current – or the C-rate – and N is the number of cycles performed).

Figure 143 shows a scheme of battery modelling framework.

Considering that detailed measurements for the recognition of battery equivalent system parameters were not available, the model of the battery has been prepared through of a simplified approach, similar to the one explained in the work by Barreras et al., 2012 and Petricca et al., 2013, which is based on cell datasheet information. In this case:

- a model based on an ideal voltage generator (representing “zero load” voltage) and resistor (representing internal resistance) is adopted
- the state of the battery is described by its State Of Charge (SOC) and its temperature (T).

Proper functions have to be defined to express the relation between SOC and components characteristics; in general; the hypothesis assumed is that the voltage is depending only on SOC, while the internal resistance is depending on both:

$$V_{oc} = f(SOC)$$
$$R_{int} = g(T, SOC)$$

Look up tables can be used to express such relation in a general way, thus being able to describe any shape for the two. In the model, a 1D look up table (only depending on SOC) has been used for the voltage generator, while a 2D look up table has been used for the resistor.

The calculation of the SOC, which is critical for the coherence of the model, is based on a so called “Coulomb counting” method, that is the ratio of known battery capacity and the integral of the current on the time of use:

$$SOC = \frac{1}{Q}\int_0^{\tau} I(t)dt$$

where Q is the battery capacity, I(t) is the current ant τ the time of use.

However, since the capacity of the battery can depend on the entity of the current supplied (e.g. expressed as C–rate) and on the temperature at which the component is acting, the accuracy of the estimation can be improved using two weight coefficients which are depending on the two values and that can take into account the described effect:

$$SOC = \frac{1}{Q}\int_0^{\tau} \alpha(I) * \beta(T) * I(t)dt$$

where $\alpha(I)$ and $\beta(T)$ are described by two proper functions (again, look up tables can be used).

Accurate temperature estimation usually requires a detailed model able to represent the heat generation of the cell within its internal structure (e.g. if the cell is obtained by a number of substrates, each point is an heat source, the intensity of the generation depending on the reactions on the surface), its thermal capacity and its heat exchange coefficients, that should be calculated in order to consider:

- the heat exchange from the “core” of the battery to its outer surfaces;
- the heat exchange between the internal part of the battery and the external surface

- the heat exchange between the cell and the battery systems (comprehending other cells, casing, cooling systems, conductors etc.).

In general, the internal temperature of the battery can be significantly different from the external surface especially in case of “unsteady” current supply (e.g. current at a relevant C–rate for a short time). For this application, it was excluded to consider any internal thermal unbalance of the battery and only the overall temperature has been estimated through the use of a simplified, lumped–parameters model comprehending (see Figure 135):

- an heat generation source, the power being calculated by Joule losses on battery equivalent internal resistor
- a thermal mass, representing the thermal capacity of the materials of the cell
- an heat exchange coefficient as single, aggregated value – not distinguishing between irradiation, convection and conduction
- an external “sink” at constant temperature representing the external environmentl
- an heat generation source, representing the cooling system, that is supposed to be sufficient to keep the temperature below a determined threshold at maximum power

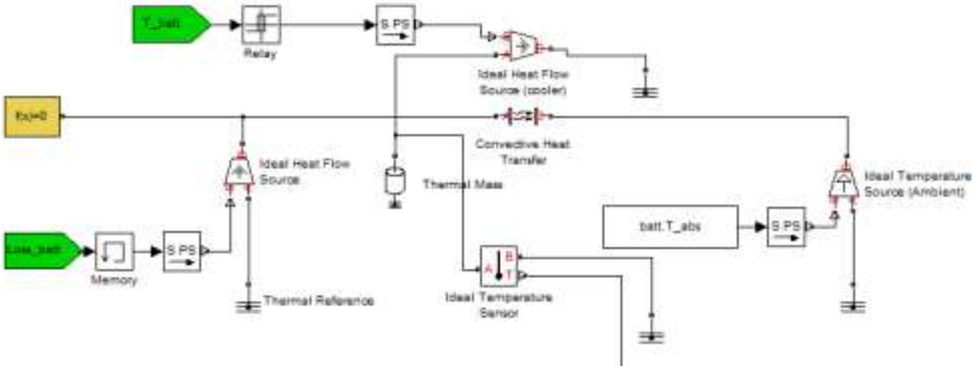

Figure 135 – Thermal section of the battery model.

The aim of such simplified model is not, in any case, to determine the temperature of the cells with accuracy, but to represent the temperature increase of the battery with a conceivable time constant; otherwise, in case of battery start at low temperatures (e.g. 0°C) – a condition in which the internal resistance is estimated to be significantly higher in comparison with temperatures such as 20°C – it would be unrealistic to consider the temperature to remain stable for the whole use time, thus not representing the effective performance of the battery in terms of energy supplied during its whole discharge.

The data related to the battery have been obtained using the datasheet of the cells used on the Mitsubishi iMiev, model Yuasa LEV50 (see Kitano et al, 2008); the battery systems of the vehicles comprehend a series of 88 cells, thus having a nominal voltage of 330V, a nominal capacity of 50Ah and a nominal energy capacity of about 16 kWh. The data describing the battery cells are shown in Table 40.

Attribute	Unit	Value
Nominal capacity	Ah	50
Nominal voltage	V	3.7
Mass	kg	1.7
Specific energy*	Wh/kg	109
Energy density	Wh/l	218
Maximum suggested C-rate**	-	6

* Eickstein et al, 2013, measured 217 kg for the full battery assembly (including casing, cooling system, connectors, sensors, control system etc.), while the mass of the 88 cells on the system is about 150 kg. This means that the specific energy per battery system has to be decreased to about 75 Wh/kg.
** C-rate is the ratio between the current and the value of current that can be supplied for 1 hour.

Table 40 – Specifications of LEV50 lithium ion cell.

The datasheet comprehends the value of the battery voltage depending on different C–rate (from 0.2 to 6, that is the maximum for the battery) and on temperature, at constant C–rate. The values coming from the datasheet are processed to get the values of voltage and resistance on any point of the curve (common value being SOC) by the solution of the simple system:

$$\begin{cases} V_{oc}(SOC) - R_{int}(SOC) * I_k = V_k(SOC) \\ V_{oc}(SOC) - R_{int}(SOC) * I_i = V_i(SOC) \end{cases}$$

Where k and i are two different voltage curves, as represented in fig.. The solution of the system at each SOC is:

$$V_{oc}(SOC) = \frac{V_k(SOC) - V_i(SOC) * \frac{I_k}{I_i}}{1 - \frac{I_k}{I_i}}$$

and for the resistance:

$$R_{int}(SOC) = \frac{V_{oc}(SOC) - V_k(SOC)}{I_k}$$

Voltage and resistance resulted on slight different values depending on the couples of (k ; i) used for the calculation, so that – on the hypothesis that voltage and resistance do not vary with C–rate – an average value on more estimations has been calculated as “final” value; such differences can be also related to the inaccuracy of the plots provided on the datasheets. The values of the resistance depending on Temperature are calculated using:

$$R_{int}(T, SOC) = \frac{V_{oc}(SOC) - V_T(SOC)}{I_T}$$

The final estimated values for the V_{oc} resistance are plot in Figure 137. It is noticeable a certain decrease of the internal resistance from high SOC to intermediate SOC, this shape being similar to that shown on Barreras et al, 2013. Following figures show main parameters calculated.

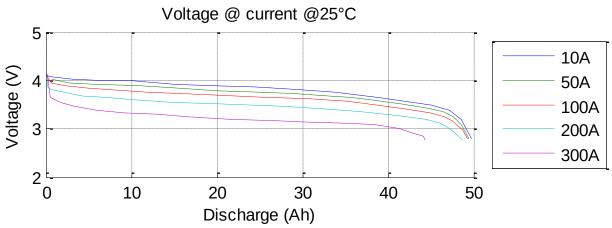

Figure 136 – Battery open circuit voltage V_{oc} according to datasheet.

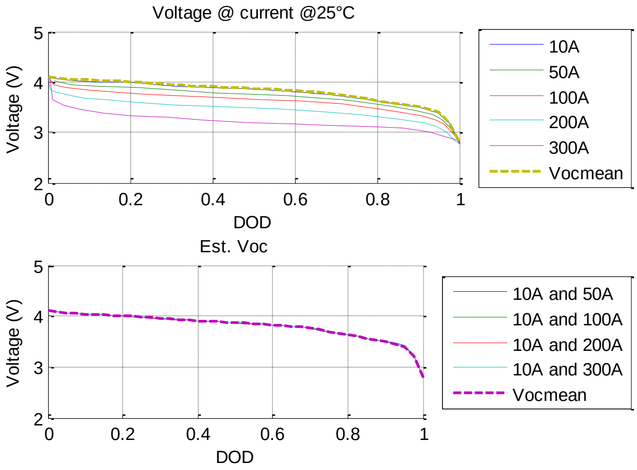

Figure 137 – Battery open circuit voltage V_{oc} using a normalized DOD value and calculated V_{oc} depending on the current couples used.

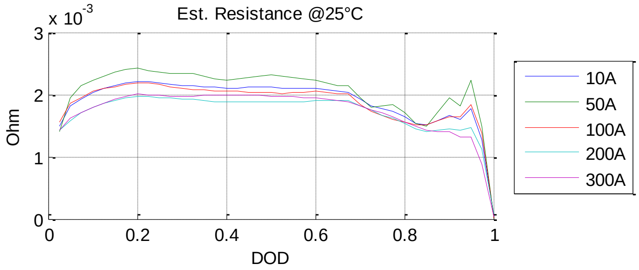

Figure 138 – Estimated resistance depending on the Current plot selected for estimation. The values at the edges (DOD=1 or DOD=0) need manual adjustment due to inaccuracy of the data available on the datasheet. The differences on the estimation depending on C–Rate are probably due to inaccuracy in the datasheet. A mean value has been used.

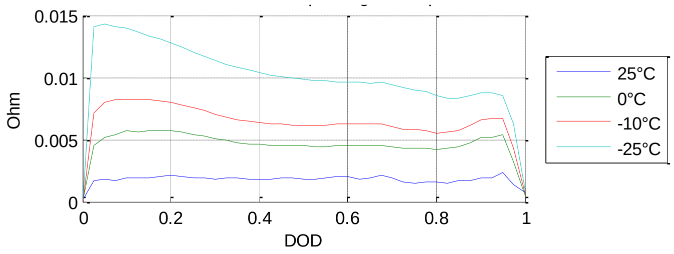

Figure 139 – Estimated resistance depending on temperature at constant current (50A). The values at the edges (DOD=1 or DOD=0) need manual adjustment due to inaccuracy of the data available on the datasheet.

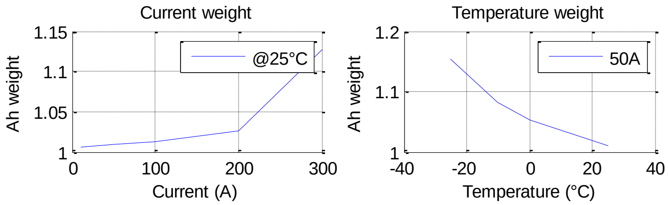

Figure 140 – Coefficients for current emphasis for SOC calculation depending on current and on temperature.

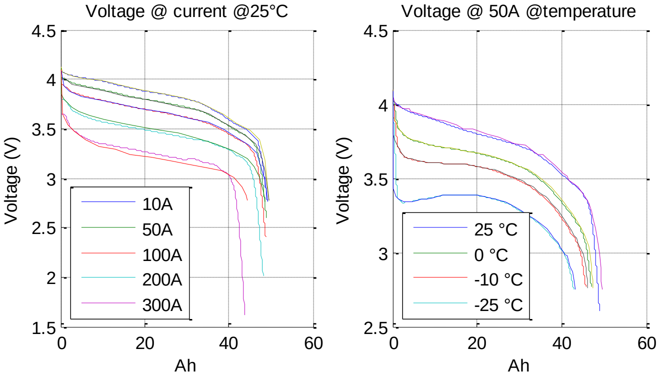

Figure 141 – A comparison between datasheet and simulated voltage.

A final verification has been performed on the basis of the comparison with measured data, comprehending battery current, battery voltage and SOC as estimated by vehicle diagnosis through CAN logging. A direct system recognition through model fitting of model observer has not be performed on the CAN signals due to two main reason:

- since the signal is coming from vehicle self–diagnosis, it is affected by uncertainties in terms of precision and signal processing procedures (e.g. truncation, filtering, sensor accuracy) which are unknown
- the signal is, in general, quite “smooth”, while for a system identification process a signal with a “rich” band of frequency should be preferable (e.g. step, sine sweep).

However, the total error on delivered energy on a discharge from 90% SOC to 40% SOC was about 4%; such value is considered acceptable for the scope of the analysis. The values of the iMiev battery are therefore assumed as a basis for the modelling of a battery system reasonably representative in terms of weight, energy, power and sensitiveness to use conditions. Final model is shown in

Figure 143

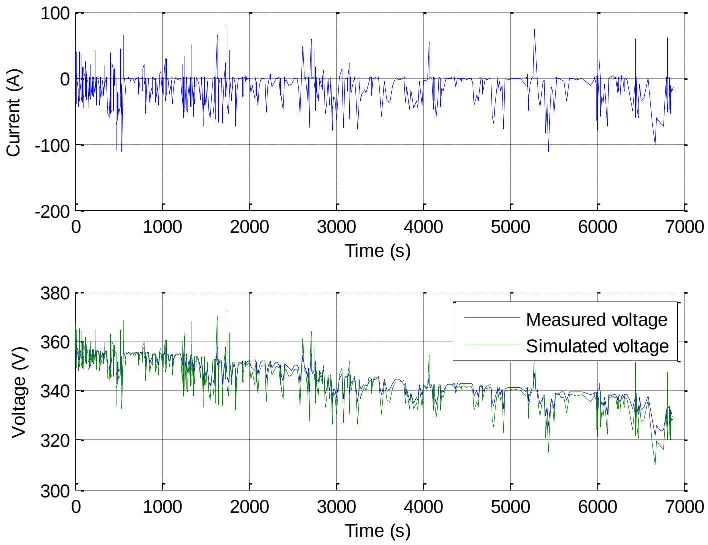

Figure 142 – Voltage “shift” between measured and simulated battery voltage depending on current (negative current corresponds to traction). The SOC is varying from 90% to 40%, while the total error on the supplied energy is 4.3%.

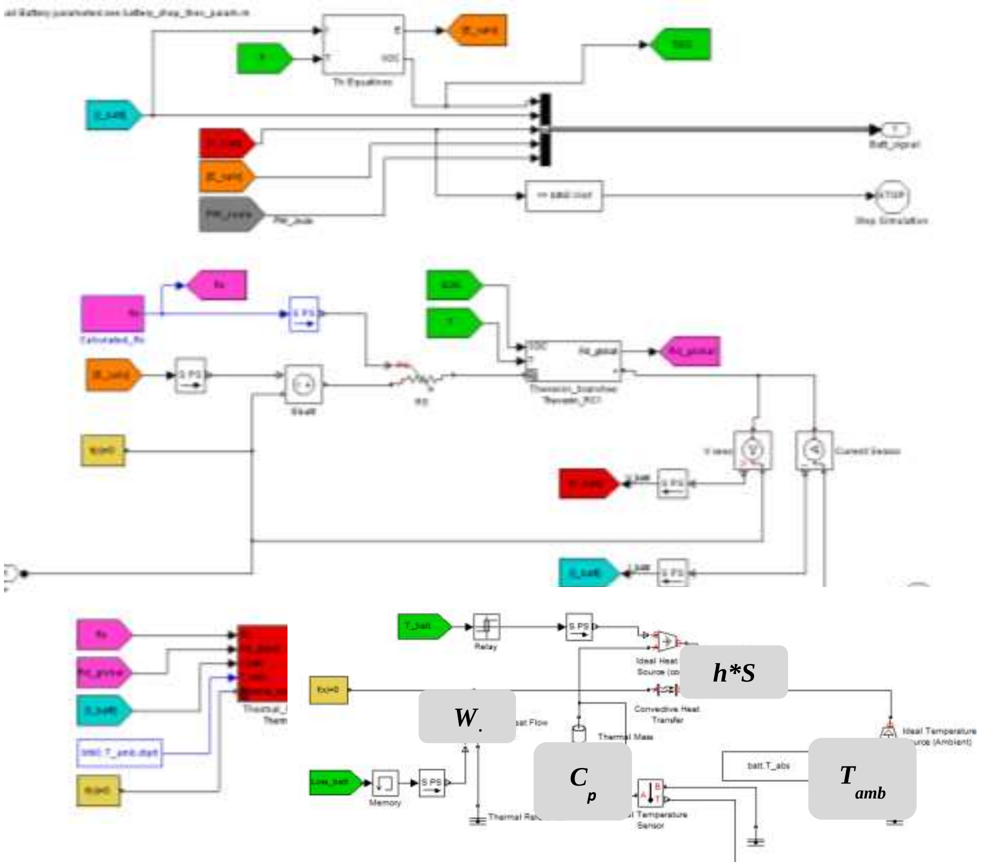
Th Equations
Batt_signal
Stop Simulation
Calculated_Ro
Current Sensor
Relay
Memory
Ideal Heat Source
Convective Heat Transfer
Thermal Mass
Temperature Sensor
Ideal Temperature Source (Ambient)
batt.T_abs
h*S
W
C p
T amb

Coulomb counting section:

$$SOC = \frac{1}{C}\int_0^t a(i)b(T)i\,dt$$

Ageing function(if applied):

$$SOH = a_1(T,SOC) * t^{\frac{1}{2}} + a_2(T,SOC,I) * N$$

t: battery lifetime
N: cycles performed by the battery

Equivalent circuit model section:

$$V_{oc} = f(SOC)$$

$$R_{int} = g(T,SOC)$$

$$G(s) = R_s + \sum_{i=1}^{N} \frac{R_{di}}{1 + R_{di}C_{di}s}$$

Thermal model section:

$$C_p\frac{dT}{dt} = W_j - h * S * \Delta T$$

Figure 143 – Battery model layout.

6.2.4. Supercapacitor system modelling

The model of supercapacitors cells, according to the work by Van Mierlo et al., 2004, has been kept as simple as possible using a lumped element network including a capacitor in series with a resistor representing internal resistance; another small resistor in parallel with capacitor is used to represent self–discharge. The stored energy is calculated as usual for capacitors:

$$E_{sc} = \frac{1}{2} C * V^2$$

The SOC of the supercapacitor is calculated as the available ratio of usable energy, obtained considering the difference between full–charged energy and lower allowed energy; this latter is determined by the cut–off voltage, that has been set as half the value of the maximum voltage, according to the indications of Maxwell technologies application note, 2009:

$$SOC_{sc} = \frac{E_{curr}}{E_{max} - E_{min}} = \frac{V^2}{(V_{max}^2 - V_{min}^2)}$$

Such model is simplified, in particular since it does not take into account the efficiency of the system. In the application, the capacitor is used in a way that the maximum power is always minor than the matched impedance value:

$$P_{max} = \frac{V^2}{4 * R}$$

For a detailed analysis of supercapacitors, see the work by Burke and Miller, 2010; the data used for capacitance, maximum voltage and internal resistance also are provided by this text; the dimensioning of the supercapacitors subsystem will be explained in next paragraphs. The model is shown in Figure 144; the voltage of the supercapacitors unit is converted to the level of the battery block using through a step-up/step-down converter.

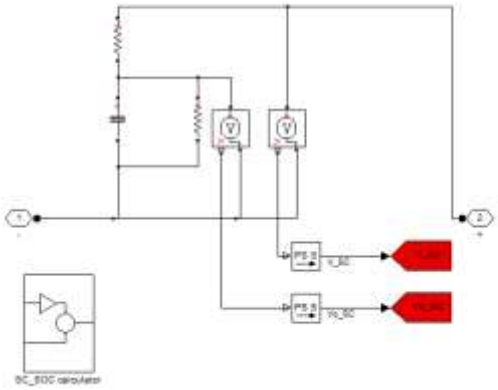

Figure 144 – Capacitor and resistor network for supercapacitor simulation.

6.2.5. **Electric motor modelling**

The motor model uses a look–up table for calculation of efficiency at given rotational speed and torque. Since a detailed map for iMiev vehicle was not available, the data coming from Nissan Leaf electric vehicle (measured by Burress and Campbell, 2013) have been used, since both are synchronous PM machines. The map includes inverter efficiency and is “stretched and scaled” to fit with three known parameters of iMiev motor:

- Base speed
- Maximum torque
- Maximum speed

The power has been set to 47 kW, as shown in Figure 145. Figure 146 and Figure 147 show the comparison between original and adapted map.

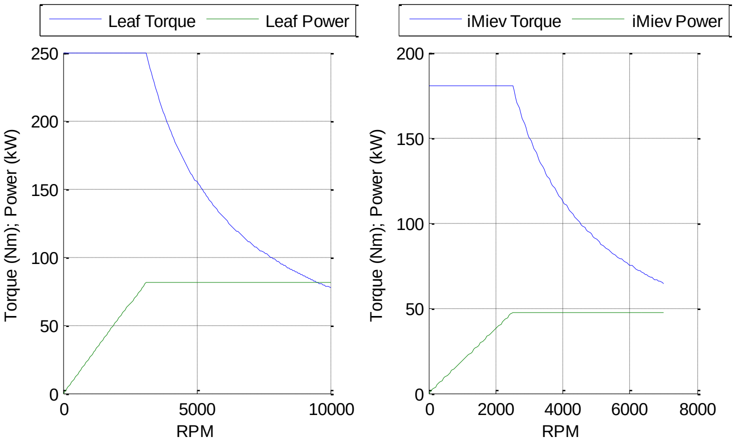

Figure 145 – Torque and Power of Leaf motor (left) and of iMiev motor (right).

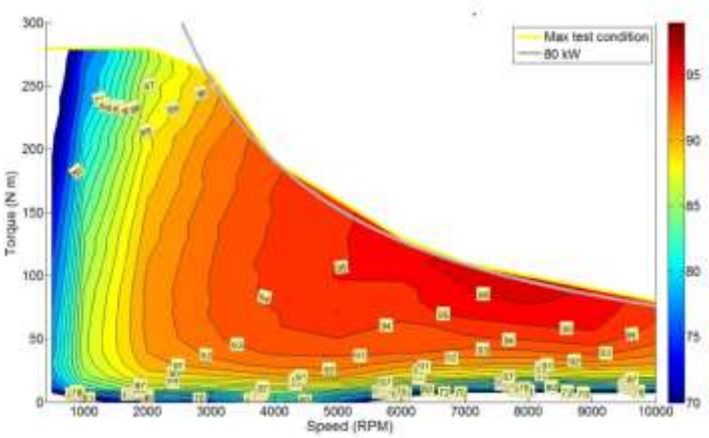

Figure 146 – Efficiency map for Leaf motor (source: Burress and Campbell, 2013).

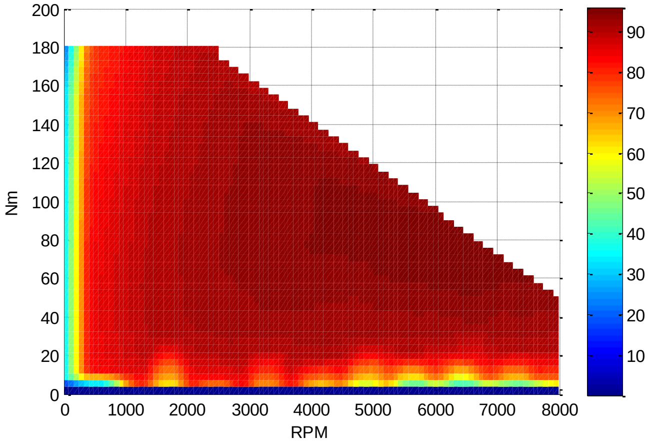

Figure 147 – Adapted efficiency map for iMiev motor.

The model implements the efficiency map using as input for look up table two parameters:

- Motor shaft rotational speed
- Torque requested by the driver.

Torque is calculated considering the maximum value available at the instantaneous RPM multiplied for the request of the user (a value comprehended between 0 and 1); two blocks are used, for regeneration (see Figure 129) and for traction. Electric power is then calculated and communicated to other blocks.

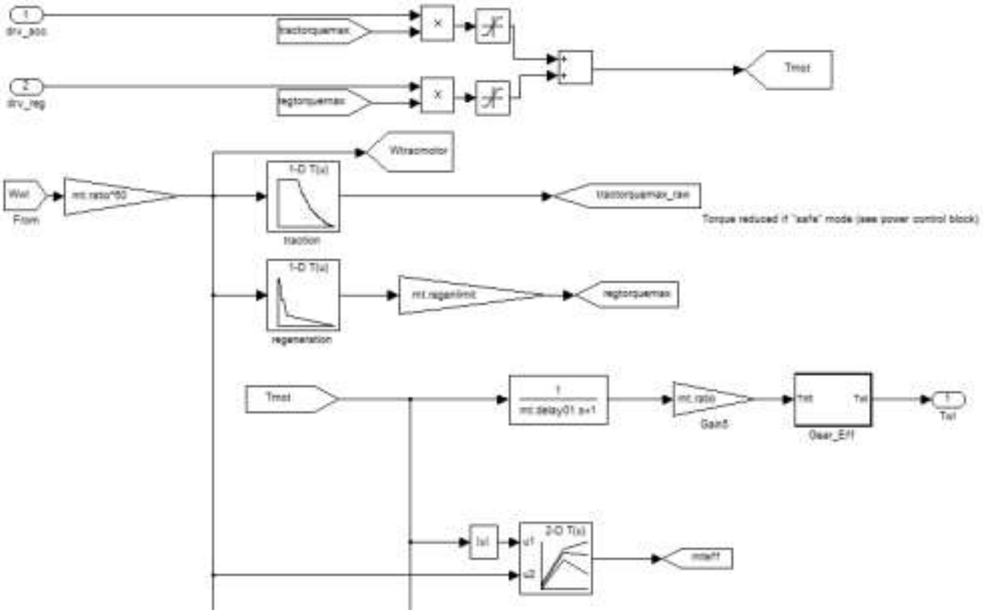
1
drv_acc
2
drv_reg
tractorquemax
regtorquemax
×
×
+
+
Tmot
Wtracmotor
Wwl
From
mt.ratio*60
1-D T(u)
traction
tractorquemax_raw
Torque reduced if "safe" mode (see power control block)
1-D T(u)
regeneration
mt.regenlimit
regtorquemax
Tmot
1
mt.delay01 s+1
mt.ratio
Gain5
Tmt
Twl
Gear_Eff
1
Twl
|u|
2-D T(u)
u1
u2
mteff

Figure 148 – Motor model blocks.

6.2.6.Range extender modelling

In order to provide energy to the vehicle in addition to the amount that can be provided by the battery, a so called “range extender” is added to the model. A “range extender” is a power unit able to convert the energy available from an high–density vector or source (e.g. a liquid or gaseous fuel) into a usable electrical energy; this function can be performed by different components, such as from fuel cell systems, conventional combustion engines and generator assemblies, microturbines and generators assemblies (see Varnaghen et al., 2011; Ribau et al., 2012). In case of an internal combustion engine range extender, the powertrain can be described as a pure series hybrid electric vehicle, and, in general, the acronym “EREV” is used to describe the vehicle. The differences between PHEV and EREV are quite narrow, the first being an hybrid vehicle capable to charge his battery from an external source, the latter being a BEV capable of long range. In practice, a PHEV uses the battery both as an energy storage system and an energy buffer, but the ICE can have a mechanical link to the final drive through “powersplit” or parallel transmissions; an EREV uses the battery as main energy storage, so that it has the capability to run in electric mode at almost full performances for a noticeable range, while the motor being used only in case of need (“sustain” mode) and does not have a mechanical link to the final drive.

Commercial and literature examples show the availability of different alternatives in terms of ratio between ICE/electric motors power and size, transmission architecture, battery capacity; the model Chevrolet Volt (and the similar Opel Ampera), as an example, can act both as a PHEV or as a EREV, since the power–split transmission system – that is the “three way” (usually an epicycloidal gear) link between motor, generator and internal combustion engine – can decouple the engine from the driveline through the use of clutches, while the battery as a “large” nominal capacity (16 kWh) in comparison with other HEV–PHEV and can be externally charged.

The use of a pure series configuration is disadvantageous in comparison with “parallel”, “powersplit” or even conventional powertrains (especially for some operating points, e.g. constant speed) in terms of efficiencies, but enables the possibility to install the engine with a quite large “design freedom” for engineers due to the absence of a mechanical link to final drive system; some examples of this kind of vehicles have been studied on applied research experiences (see FUEREX final report, 2013) and, in very recent times, have been proposed as commercial solutions (BMW i3 model). Proposals for pure series EREV are oriented towards the use of small stroke power units, capable of a relatively small maximum power: less than the main traction motor and less than ICE powertrains for comparable conventional vehicles. The aim is to reduce as much as possible the weight and the size of the unit, aiming to find a compromise between the capability to sustain battery charge (that, as shown on the simulation results chapter of the present work, is not very critical for most urban/rural trips) and the capability to keep the vehicle running at high speed continuously (typical of highway driving), a situation in which the lack of power could significantly limit performances, thus failing to meet customer expectations. The limitations in terms of efficiency and performances can be acceptable if the vehicle is run in range–extender mode in a way that the total balance(in terms of aggregated indicators such as: environmental impact, energy use, cost) over a use period (e.g. a year of use, or total vehicle life) is still favorable in comparison with other solutions, such as conventional vehicles. In addition, it is important to remember that, on the basis of the users’ monitoring activity related to ASTERICS project in Florence, the EV users chose this kind of vehicle for opportunity reasons (e.g. reaching traffic limited areas) that are not directly related to the need to minimize energy consumption or vehicle use cost.

The aim of the simulation activity here presented is to verify the advantages over a large number of different use situation; due to the need of short calculation time, the model applied has a reduced complexity and is based on:

- a look up table for fuel consumption of the ICE unit, expressed as g/kWh depending on RPM and torque
    - since the "map" needed for look up tables are based mainly on steady state measurements, a correction factor depending on torque derivate is used
- a look up table for electric generator efficiency.

In order to use quite realistic data for the size of the vehicle chosen, a recent commercial product (Mahle range extender, gasoline, four stroke, atmospheric two cylinder engine –see Bisordi, 2011) has been taken as reference for mass, power, usable RPM and expected fuel consumption. The specification provided by the manufacturer are quite detailed, but a full consumption map is not provided: only a "best" value for each RPM is available. Considering that the aim of the activity is to model the consumption of an archetype powertrain for a determined size rather than to reproduce in detail a precise vehicle model, another map for gasoline ICE (from Van Basshuysen, R., and Schäfer, F., 2004) has been adapted in order to fit the nominal performances of the data in a few point (maximum power point, best fuel consumption point), while the other points are the results of the adaption and, therefore, are used to reproduce other working points even if not validated. It is also important to note that the declared best value of fuel consumption for MAHLE ice, that is about 250 g/kWh, is not a "state of the art" value for gasoline ICE technology, which can reach the value of 240 g/kWh; thus, the assumed data are quite conservative. The result of the adaptation (that is a scaling on BMEP values) is shown in Figure 149. The efficiency map of the electric generator has the same shape of the one used for the traction motor (thus being derived from Nissan Leaf motor measurements) and comprehends overall efficiency of electric system including inverter losses; an additional, constant 2% loss factor is added to keep the model conservative. The matching is effectuated in the way that:

- maximum power of the engine can be reached by electric machine at the specified RPM;
- the ICE "best" efficiency point falls within the high efficiency area of the generator.

The total mass of the unit is critical for the estimation of energy consumption over a prolonged period of use. A rough estimation of the total mass of the system is 150% the value of the "nude" range extender power unit, in order to include the additional mass of fuel tank (comprehending fuel pump), cooling and exhaust system.

The strategy for the management of the engine in a "charge sustaining" application can be quite simple and can be based on a few rules, starting from the scheme of hysteresis "thermostat control" on SOC battery – minimum and maximum acceptable being below 40% SOC of the battery; respectively 15–20% and 30%–40% is a typical range.

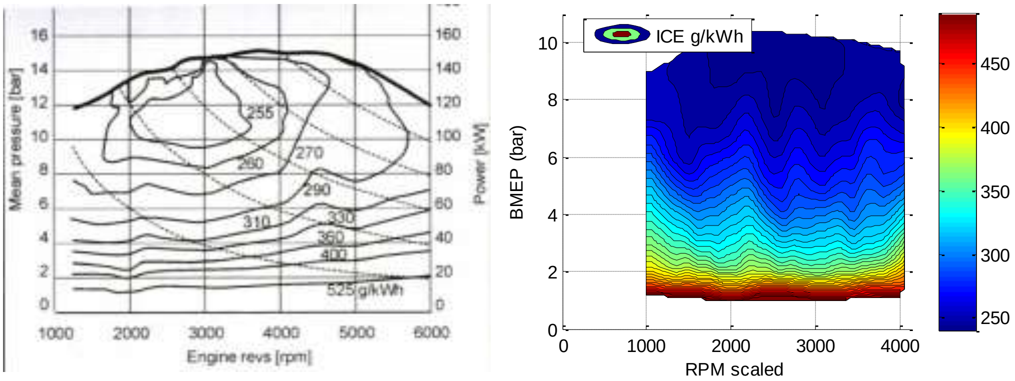

Figure 149 – Original ICE map (left) and adapted ICE map for specific consumption.

Main data describing range extender are shown in Table 41; final performances of Range extender assembly are shown in Figure 150 and Figure 151.

MAHLE ICE powertrain characteristics		
Power (engine)	30 kW@4000RPM	
Mass (including Generator)	65 kg	
Total Mass (including all, guess)	97.5 kg	
Length	416 mm	
Width	327 mm	
Height	481 mm	
Best specific consumption	250 g/kWh	

Table 41 – Main MAHLE ICE for range extender characteristics.

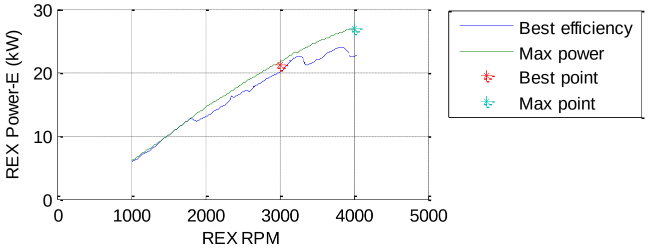

Figure 150 – Final performances of range extender assembly: power power of range extender unit depending on RPM. The first curve shows the points for which the efficiency is best for each RPM; the best point over all is highlighted. The second curve shows maximum power points; the maximum point over all is highlighted.

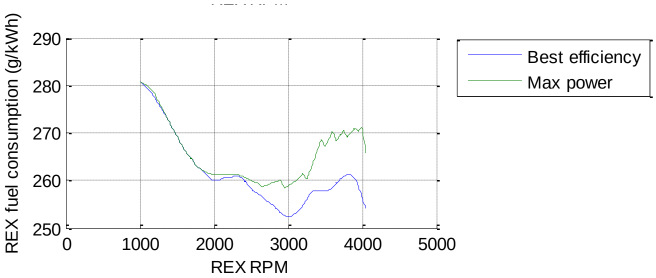

Figure 151 – Final performances of range extender assembly: specific fuel consumption depending on RPM. The first curve shows the points for which the consumption is lower is for each RPM. The second curve shows the consumption at maximum power points.

6.2.7. Virtual driver model

The driver is modeled as a PI controller acting on the error between desired speed (that is, input driving cycle) and the effective vehicle speed. Similarly to the solution used for AMEsim driver, two PIs are acting in parallel, one of the two using an anticipated signal to obtain better acceleration results. To obtain a good stop condition after deceleration, the integral part of the PI is reset when vehicle speed is zero. The driver produces two signals: acceleration and brake, values being between 0 and 1. Another block splits the brake signal in regeneration and mechanical braking request (these latter being used if the calculated torque exceeds regeneration torque, according to the look–up table defined in the motor paragraph). The anticipation factor is 1s; speed signal is also processed with 1pole transfer function having a time constant of 0.05, to reduce the effect of “spikes” in driving cycle (a condition that is possible for trapezoidal signals).

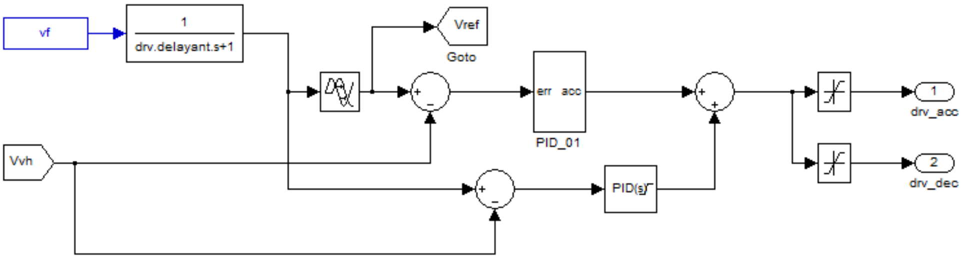

Figure 152 – “Virtual driver” block using two PI. Normal one: P=1.2; I=0.5. Anticipated one: 0.3. Anticipation value: 1s.

6.2.8. Low voltage system, auxiliaries and comfort elements

Low voltage system is not modeled in detail. The power used by these elements is calculated from:

- The signal acquired for Twizy (see paragraph 5.2.3), is used to produce a power consumption with the same statistical distribution

- The heater and air conditioning system is modeled as a pulse signal, having as height the nominal consumption of iMiev system (respectively, 5kW and 4.5kW) and as percentage of "on" time, a value set by the user.

The values are then smoothed with transfer function having 1s time constant to smooth "spikes" which could slow down the solver. The subsystem is shown in Figure 153.

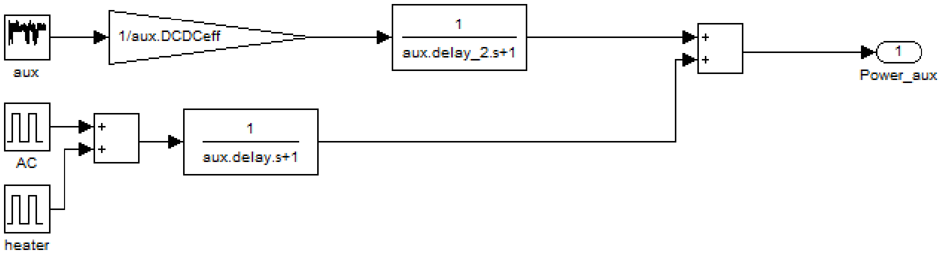

Figure 153 – Simplied model for auxiliaries.

6.2.9. **Full model layout**

The final block model is shown in Figure 154. An explanation for simulation flowchart is (please note the numbers on the list correspond to the blocks on the picture):

1. Virtual driver receives the cycle input and produces acceleration and braking signals
2. A control block splits braking signals into braking and regeneration signals
3. The motor provides the requested torque to the wheels
4. Mechanical brake provides the requested torque to the wheels
5. The wheels transform the torque to a longitudinal force for vehicle acceleration
6. Car body reacts and gives speed as output
7. Additional consumption for auxiliaries is calculated
8. The power control units receives traction and auxiliary power as input and controls battery (9), supercapacitors (10) and range extender (11) to supply the requested power.

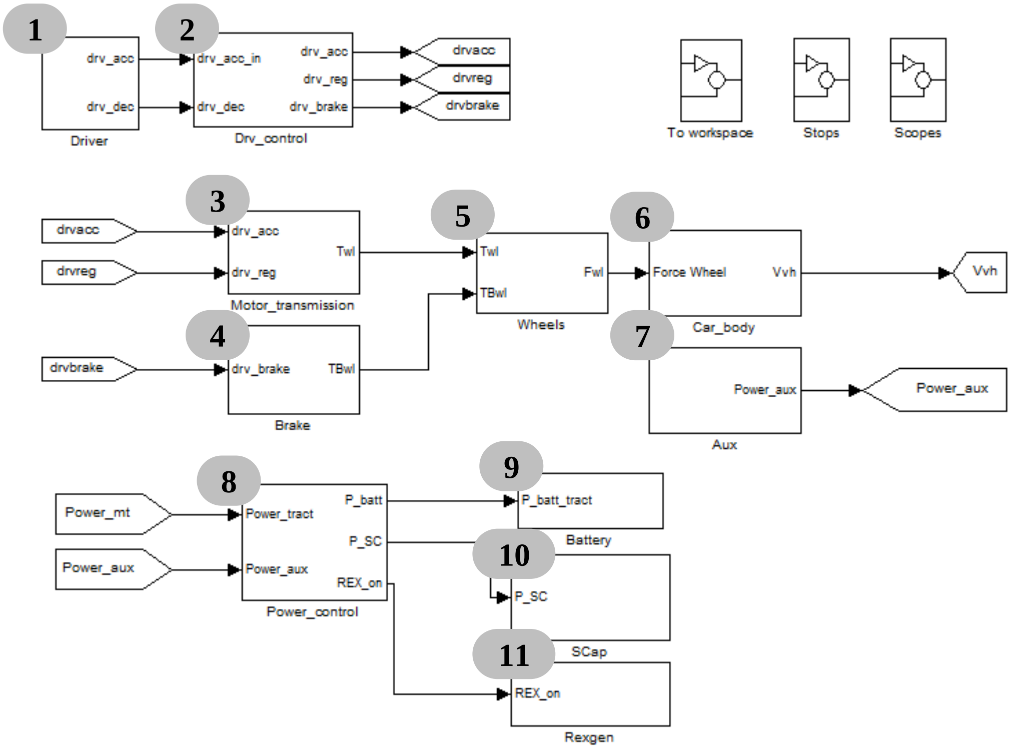
1
2
drv_acc
drv_dec
Driver
drv_acc_in
drv_dec
drv_acc
drv_reg
drv_brake
Drv_control
drvacc
drvreg
drvbrake
To workspace
Stops
Scopes
3
drvacc
drvreg
drv_acc
drv_reg
Twl
Motor_transmission
4
drvbrake
drv_brake
TBwl
Brake
5
Twl
TBwl
Fwl
Wheels
6
Force Wheel
Vvh
Car_body
Vvh
7
Power_aux
Aux
Power_aux
8
Power_mt
Power_aux
Power_tract
Power_aux
P_batt
P_SC
REX_on
Power_control
9
P_batt_tract
Battery
10
P_SC
SCap
11
REX_on
Rexgen

Figure 154 – Full model layout.

6.2.10. Model representativeness verification

Considering the hypothesis used for the definition of powertrain component characteristics and the lack of detailed electric measurements, an accurate validation of the model is not possible. However, due to the fact that its use is limited to an archetype comparison, to general sizing activities and to overall energy strategy definition, the validation of overall consumption characteristics can be considered as a sufficient verification fir first step analysis. For this reason, a reference value for energy consumption is necessary. For the iMiev type vehicle (including the replicas Citroen C–zero and Peugeot iOn) more than one benchmarking study have been published in literature, but the results about energy consumption and effective range are significantly different even if the declared test condition are similar. An assumption is needed: the report by Geringer and Tober, 2013, has been used as main reference since it comprehends a full explanation of boundary conditions and detailed results data tables. In particular, the consumption over different driving sequences and external temperatures is presented:

- urban driving sequences (low speed part of ECE–15, Artemis Urban)
- extra urban driving sequences (moderate/high driving speed: extra–urban part of ECE–15, ARTEMIS extra urban cycle)
- highway driving sequences (according to the cycle defined by ADAC german association)

- ECOTEST sequence, that is the aggregate consumption on all the urban, extra urban and highway driving sequences (see Figure 155)
- constant speed consumption at various speed
  - 30 km/h
  - 50 km/
  - 70 km/h
  - 100 km/h
  - 130 km/h.

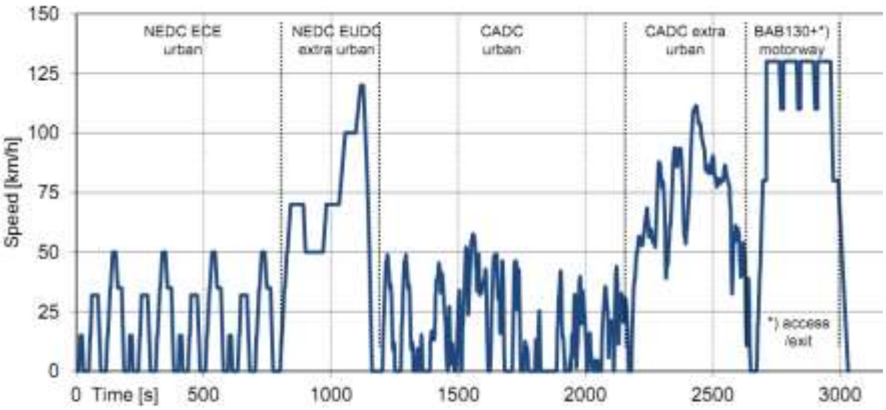

Figure 155 – ECOTEST driving cycle (source: Geringer and Tober, 2012).

The external condition includes temperatures from –20°C to 30 °C (increment being 10°C); in total, 48 independent driving conditions are presented. The results of the study also include the energy consumption of other systems (HVAC system – both heating and air conditioning – and auxiliaries), so that the average power is known. In addition, the net energy supplied by the battery system is also measured, resulting on a total amount varying from 14.1 to 15.3 kWh (respectively at –20°C and at 0°C).

The vehicle model is executed for different cycles and temperatures[7]. The results of raw energy consumption for traction are shown in Table 42: the difference with reference results is acceptable for most driving cycles; however, the consumption on constant driving at low speed (below 70km/h) are not reproduced correctly. Since these latter inaccuracy are related to un–realistic constant speed driving conditions, the results are considered acceptable. Another note is necessary: the overall value for the "Ecotest" cycle, that is a sequence comprehending all the other sequences (urban, extraurban, highway), is affected by a 4% error that is significantly lower than the error on the single sequences; this is not possible, since the error should be the weighted average of other errors, and it suggests that there is an incoherence in the consumption presented in the values of the study. Such impression is confirmed by the calculation of Ecotest values from the partial segments (see last row of Table 42); another inaccuracy is that the distance of the cycle is not coherent with the data used for simulation, which are reliable since come from UNECE reg.101 documents (for ECE15 and EUDC) and directly from ADAC association (for the highway cycles). Table 43 shows the consumption of 12V systems and of HVAC depending on external temperature; the values are used to tune the simplified consumption assessment block for auxiliaries in the model.

---

[7] –20°C is not simulated since battery performances are significantly affected by the low temperature and the results could be excessively approximated without using a detailed thermal model.

Cycle	**Reference Distance (km)**	**Reference consumption (Wh/km)**	**Simulated distance (km)**	**Simulated consumption (Wh/km)**	**Variation on consumption %**
Urban (ECE15 and CADC–u)	8,850	80,0	8,927	94,5	18%
Extra urban (EUDC and CADC ex)	15,886	111,0	15,991	120,3	8%
Highway (ADAC BAB EV)	10,770	177,0	11,381	192,6	9%
Ecotest	35,506	131,0	36,299	136,5	4%
30 km/h		72,0		68,4	–5%
50 km/h		86,0		74,0	–14%
70 km/h		97,0		99,3	2%
100 km/h		152,0		152,6	0%
130 km/h		214,0		218,3	2%
Ecotest (weighted average)	35,506	123,3	36,299	136,6	11%

Table 42 – A comparison between reference data and simulated ones.

External temperature	**HVAC additional power (W)**	**12v system power (W)**
+30°C	299	275
+20°C	0	208
+10°C	1032	208
0°C	2515	312
–10°C	3123	332
–20°C	3833	367

Table 43 – Power used by HVAC and auxiliaries depending on external temperature (adapted from Geringer and Tober, 2012).

Other results are calculated:

- Table 44 shows the expected total range, that is a result depending on all factors such as battery efficiency, energy needed for traction, energy needed for HVAC and auxiliaries.
- Table 45 shows the kWh supplied by the battery depending on Temperature and cycles.

Temperature (°C)	Urban (ECE and CADC–u)	Extra urban (EUDC and CADC ex)	Highway (ADAC BAB EV)	Ecotest	30 km/h	50 km/h	70 km/h	100 km/h	130 km/h
+30°C	141	127	80	110	180	185	148	101	72
+20°C	166	132	82	117	210	202	156	104	73
+10°C	102	116	77	100	144	160	136	97	70
0°C	67	99	72	81	100	124	115	89	67
–10°C	58	94	70	75	89	113	109	86	65

Table 44 – Expected range for the vehicle depending on cycle and on temperature.

Temperature (°C)	ECE15	EUDC	ART urban	ART rural	BAB_EV	30 km/h	50 km/h	70 km/h	100 km/h	130 km/h	ECO TEST
+30°C	15,8	15,5	15,5	15,4	15,1	16,1	16,0	16,0	15,7	15,3	15,3
+20°C	15,5	15,5	15,2	15,4	15,0	16,0	15,9	15,8	15,7	15,3	15,2
+10°C	15,2	15,1	14,9	15,0	14,8	15,6	15,6	15,5	15,3	15,0	14,9
0°C	15,0	14,7	14,7	14,6	14,4	15,2	15,2	15,1	14,9	14,6	14,5
–10°C	14,6	14,2	14,3	14,2	14,0	14,8	14,7	14,7	14,4	14,2	14,1

Table 45 – Energy supplied by the battery (in kWh) depending on cycle and on temperature; for this case, single driving cycles have been considered.

Finally, the acceptable calculation of vehicle consumption suggests that the model can be used to calculate the energy performances of a “typical” vehicle, even if it has not been validated on the whole set of performances of a precise model.

6.2.11. Calculations for all the driving data

The model has been used to calculate the energy consumption over all the available driving data, excluding the consumption of 12V system. Three values are calculated, distinguishing between the energy used for traction, the energy coming from regeneration and the net value of energy provided by the storage system. The data have been stored and are available through the “binder” tool, described in the former chapter.

Table 46 summarizes the results in terms of energy consumption for a list of cycles, while Figure 156 summarizes the results for all the cycles included in binder tool, highlighting the relevance of regeneration capabilities for most cycles.

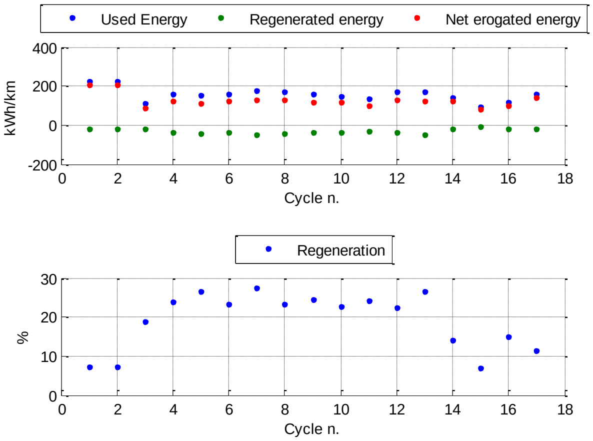

1. ADAC_BAB_EV
2. ADAC_BAB_GAS
3. AST_UNIFI_all_long
4. AST_UNIFI_all_mean
5. AST_UNIFI_ion_long
6. AST_UNIFI_ion_mean
7. AST_UNIFI_kze_long
8. AST_UNIFI_kze_mean
9. AST_UNIFI_tw7_long
10. AST_UNIFI_tw7_mean
11. AST_UNIFI_unsteady_long
12. AST_UNIFI_unsteady_mean
13. WLTCv2_1
14. WLTCv2_2
15. WLTCv2_3

Table 46 – Calculation of energy used and regeneration results for a list of recent driving cycles.

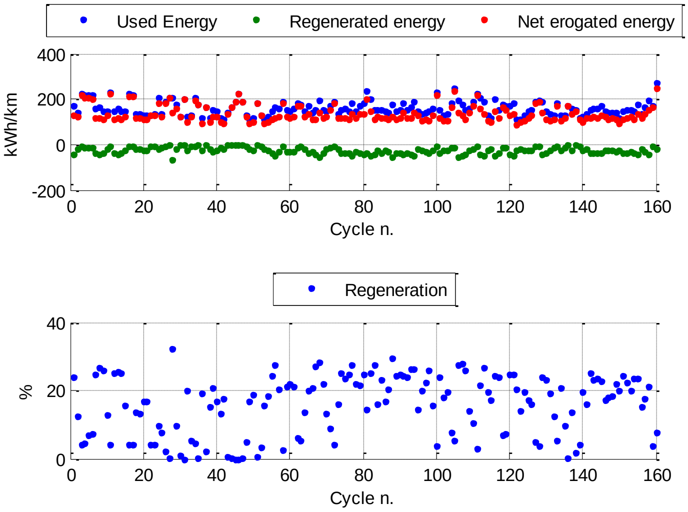

Figure 156 – Calculation of energy used and regeneration results for driving cycles included in the “binder” tool.

6.3. Strategy definition for range extender vehicle

The strategy used to control the ICE in HEV, PHEV and EREV significantly determines the performances of the system in terms of:

- achievable range
- fuel consumption over a same driving cycle

- availability of full traction power in all driving situations, especially at low SOC.

A large number of research are available for the determination of “smart” strategies, mainly in terms of optimization of vehicle overall efficiency through the examination of driving data: past, current and future prevision. The literature studies considered for the set–up of vehicle strategy in the present model include the works by: Guzzella and Amstutz, 1999; Barsali et al., 2004; Liu and Peng, 2005; Sciarretta and Guzzella, 2007; Gong et al., 2008; Wirasingha and Emadi, 2011; Chen et al., 2013. The need for an input to such optimization works also needs “driving cycle” creator tools, as shown in paragraph 4.3.5. Adaptive–tuning capabilities are therefore requested, as well as the effectuation of a large number of simulations. It is also important to note that the parameter to control HEV powertrains having some “degree of freedoms” (e.g. units with power split device) can be tuned to run the same cycle in many different ways, while a pure serial (range extender) powertrain has a simpler architecture. The development of an advanced strategy is not the aim of the present work; however, since the simulation of vehicle performances requires to define at least a simplified strategy, a proposal has been defined and applied on the model. Three alternatives are presented:

- pure “charge sustaining” mode
- “charge sustaining” mode and use of the range extender unit to sustain traction at high power driving situations
- “trip program” mode, which modifies the criteria for charge sustaining depending on a prevision of the energy needed during next time window.

6.3.1. **Strategies for range extender use**

The strategy of “charge sustaining” defines a few rules to maintain the battery SOC over a predefined value. In particular:

- the range extender unit is started if battery SOC falls below a threshold, that in the model has been set to 20%
- the range extender unit is stopped as soon as battery SOC reaches a safe threshold, that in the model has been set to 30%
- the power supplied by the range extender depends on vehicle speed; in the model, a function is used to “link” the two values (see 6.3.2). Therefore range extender RPM is varying, while the torque corresponds to the best efficiency point for that RPM
- in case that it is impossible to sustain battery SOC and that this falls in the range of very low SOC, the power available for traction is reduced, while the range extender is set to its maximum power point in order to ensure that the SOC is getting higher in a short time.

The rules are based on the hypothesis that the vehicle battery is able to supply al the power needed by powertrain and auxiliaries in normal condition, while additional energy is required only at low SOC. Since in this work a confrontation comprehending vehicle equipped with “small” battery (designed for a range of about 25–30 km) has been prepared, it is possible to verify an imbalance between the maximum power needed from vehicle systems and the maximum power that the battery can supply, exceeding the C–rate suggested by the manufacturer of the cells or just working in a low efficiency point.

The rule based strategy is therefore extended with a supplementary rule to be applied in case of needing:

- the range extender is started (even at high SOC) if the power requested exceeds a threshold predefined for the battery at that state (Temperature and SOC can be considered); the range extender keeps running until the power used by the vehicle falls below the threshold
    - in any case, the range extender is kept running for a minimum time interval (e.g. 20–30s) to avoid frequent start–stops events.

In this case, the range extender is used not only as a pure battery sustainer but as a component that is necessary for normal vehicle use. The use of range extender for power support function can be avoided if the battery system, even if using low–capacity cells, is provided with complementary components able to extend its power capabilities, as described in paragraph 6.1.

Considering that in certain driving situation it can be possible to get low SOC together with an high and continuous power demand, the performances of the vehicle could be significantly limited, especially in terms of maximum speed. For this reason, an additional strategy is proposed in order to let the vehicle use the range extender to keep the SOC at a very high level on the basis of the energy and on the power that is expected to be used during the trip. Such estimations can be evaluated through the use of simple Information Technology tools. Any GPS navigation systems, in fact, is able to estimate the average speed on a certain programmed track; by today it is already possible to integrate map data with additional information regarding traffic congestion. The distance, the maximum allowed speed on the track, the average speed expected can therefore be used for a rough estimation of the energy needed; more precise data can be obtained in case that driving data for the same trip are available, as an example from the user itself (former trip can be saved in a private database) or through connection with web–communities of other users; a number of studies based on applications of common devices (e.g. smartphones) are available in literature (see Katsargyri et al., 2009, and Kolmanovsky et al., 2011). The study of the details for similar IT tool is not part of the present study, but, to verify the effectiveness of the strategy, a "generator" of estimated driving data has been built. Using a simplified vehicle model the traction power and the auxiliary power are calculated for each known driving sequence; full power is integrated over the time, so that an "energy" signal is memorized. The sample time is quite long (it has been set to 5s) to contain the size of the data; a detailed signal is not necessary. The created small dataset of driving energy comprehends the full set of ASTERICS binder data (measurements, legislative and literature driving cycle). In case that a trip is programmed, a driving cycle is created: when a time – speed sequence is glued to another, the corresponding time–energy signals are also glued together. In order to take into account the variability of driving conditions, each sequence is multiplied for a random generated factor (using a uniform distribution) in the range of –15;+15%. As a result, the energy consumption on the same sequence (that means, for the same distance and cycle) can be up to 30% different if different cycles are generated. Considering that every new cycle is composed by a chain of existing, pre–calculated microtrips (or parts of that), the calculation effort is very low even in case of "long" driving sequences (e.g. hundreds of kilometers). Using this approach, the expected energy consumption is roughly known at any moment of the trip; the value is used to decide if it is needed start the range extender for a charge–

sustaining mode at high SOC; in the model, such high threshold have been set to 85%, with an hysteresis window up to 99% SOC. The rule is formulated as:

- the range extender is started for high–SOC charge sustaining (e.g. above 80%) if any of the three alternative is verified:
    - “total energy”: the expected energy consumption on the whole expected trip time exceeds battery energy; the range extender is set in order to work on its best efficiency point
    - “next section energy”: the expected energy consumption on a variable time window portion (that, in this case, has been set on 20% of total trip duration) exceeds the available energy, that is the sum of battery energy and of the energy that the range extender can supply on that time if working at its optimal point; the range extender is therefore used at its maximum power
    - “next section energy – fixed time”: the expected energy consumption on a fixed time window portion exceeds the available energy, that is the sum of battery energy and the energy that the range extender can supply on the fixed time if working at its optimal point; the range extender is therefore used at its maximum power. The duration of fixed time window can be set on the basis of battery capacity; in the model, it has been calculated as the time needed to recharge the battery from low SOC (the lower threshold for normal SOC sustain, that was set at 20%) to high SOC (the higher threshold for programmed SOC sustain, e.g. 85%) using maximum range extender power.

Different time windows are needed to ensure that the use maximum range extender power, when necessary, is recognized: in case of intense driving sequence (e.g. highway, high slope roads etc.) followed by low–power driving sequence (e.g. steady rural driving), in fact, the “total energy” criteria could not be able to guarantee that the intense driving sequence is started at maximum possible SOC. All the criteria, however, stop the range extender as soon as the battery SOC is considered sufficient to terminate the programmed trip: it is desirable, in general, to reach the destination with a quite low SOC in order to charge the vehicle from the grid.

The use of the range extender at its maximum power is performed only in case of necessity for two main reasons:

- since the range extender is running at quite high RPM (about 4000 RPM) regardless of vehicle speed, passenger perception could be negatively affected in terms of acoustic comfort and unexpected behavior
- efficiency is quite low both due to non–optimal ICE efficiency and due to charging losses on batteries.

The described strategy has been completed with two additional conditions.

First of all, even if the vehicle has to run for a long distance, it could be inappropriate to maintain the SOC at a very high SOC if a strong energy regeneration is going to be performed, that could happen in case that the vehicle is going to be driven downhill. The high charge sustain threshold for SOC is reduced by a quota that is comparable to the recoverable energy expected on next segments, in order to reduce the probability that the battery cannot be used for regeneration at too high SOC.

A critical data for the successful implementation of the strategy is the implementation of a calculation method to modify the initial estimation of expected energy consumption. The value is adjusted using the ratio calculated between the energy effectively used in the last use period (tunable by the user) and the energy estimated for that period by the IT system. Such value is calculated for every running instant, but can be affected by a number of spikes; therefore, its values is smoothed by the application of two methods:

- a low–pass transfer function (set at 1 pole, 60s time constant) is applied on the calculation of the ratio
- a weighted average is calculated between current ratio (resulting from the calculation since when the vehicle has been started) and the current, filtered value.

An application of the strategy is shown in next plots; Figure 157 shows a cycle for which about 15 kWh are estimated to be needed, overpassing battery capacity (set at 4 kWh). Figure 158 shows how the estimated energy is corrected by the “ratio” factor, while Figure 159 shows a situation in which the range extender is forced to run at his maximum power as soon as the required energy overpasses the available energy.

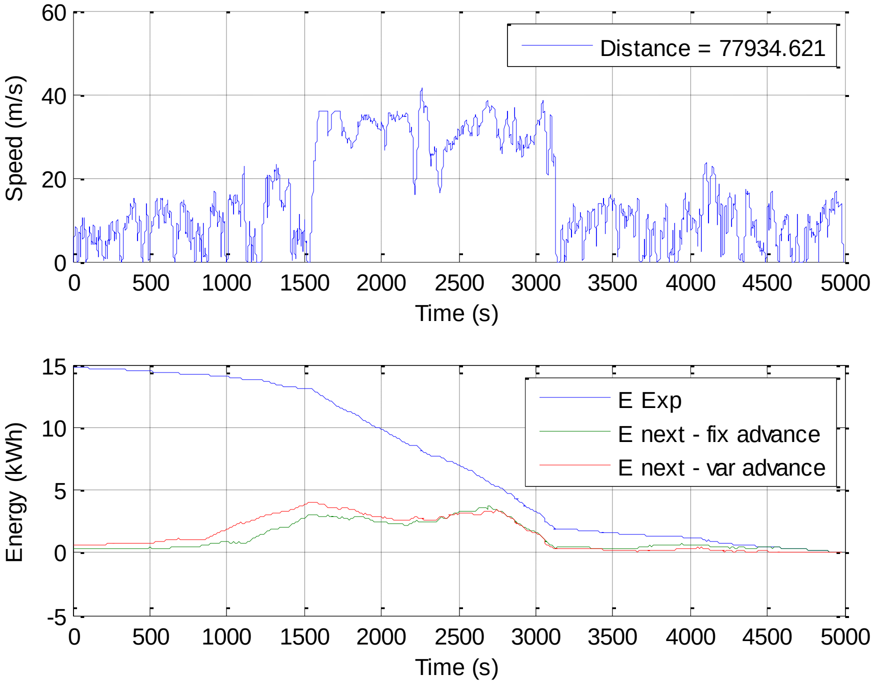

Figure 157 – An example cycle, comprehending an “unsteady” cycle, an highway sequence and a passenger cycle (upper plot). Bottom plot shows the total energy consumption expected and the energy consumption expected on next time portion both for “fixed” and “variable” time advance.

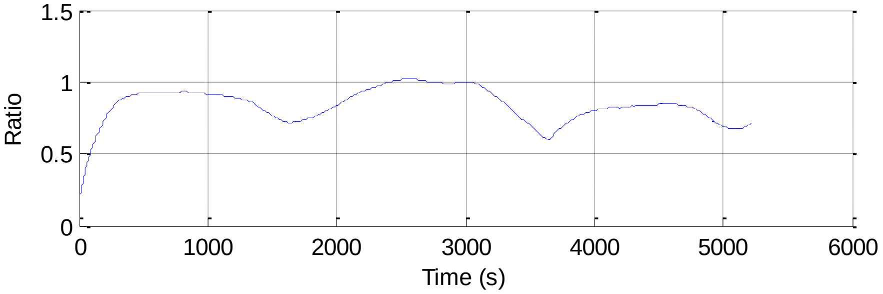

Figure 158 – The ratio between energy used and energy expected to be use during the simulation of the cycle described in the preceding plot.

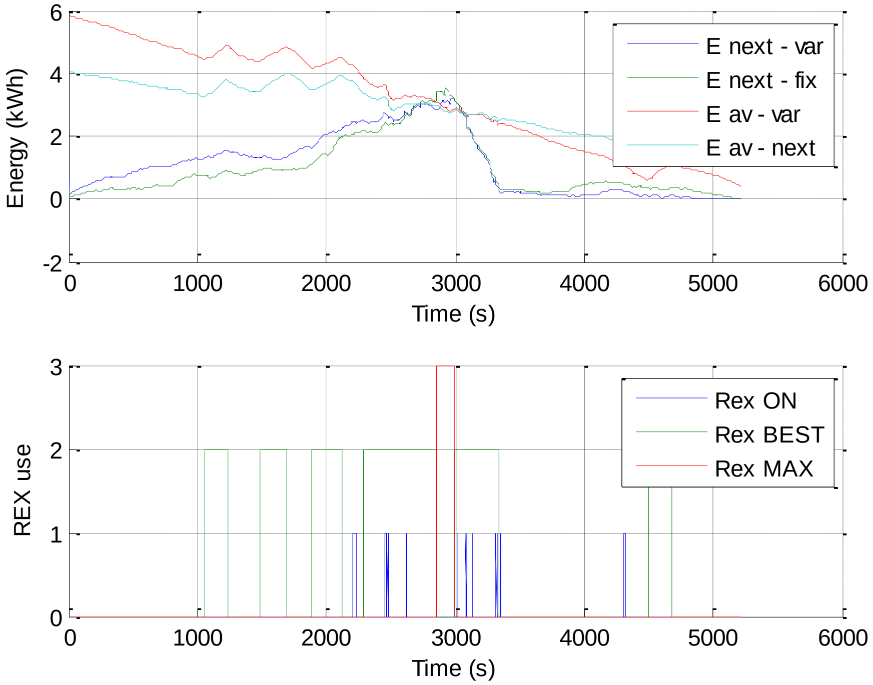

Figure 159 – Upper plot: a comparison between the energy needed to run the cycle as estimated by the scheduling logic ("E next", with variable and fixed time windows) and the energy available on the vehicle (that is, the sum of remaining battery energy and the energy that the range extender can supply in that time windows). As soon as one of the needed energy overpasses the available energy, the range extended is activated at maximum power (bottom plot). The range extender is often operated at his best efficiency point due to the fact that the overall needed energy overpasses the energy of the battery.

6.3.2. Range extender control depending on vehicle speed

Amongst the various possibilities for the use of the range extender unit depending on vehicle speed and on trip characteristics, the proposed strategy implements a rule for which the power supplied by the range extender is related to vehicle speed. The possible working points of the range extender include a number of RPM–torque points, as shown in Figure 149. Considering that the aim of the strategy is to maximize the efficiency of range extender unit, for each RPM the torque for which the specific fuel consumption is the lowest is considered; therefore, a 2D table (RPM–Torque–Power) is restricted to a 1D table (RPM – power). In case of necessity (e.g. very low battery SOC), other points corresponding to maximum possible power can be used (see Figure 150). Two points are highlighted: the value of minimum specific consumption and the value of maximum possible. Such points are used to tune the “travel scheduling” logic.Two functions linking range extender RPM to vehicle speed are implemented (see Figure 160):

- the first sets the RPM as a linear function depending on vehicle speed; max range extender RPM is reached in case of maximum vehicle speed, while the speed that can be maintained without depleting the battery has been set to about 28 m/s; higher values determine battery depletion
- the second uses a function which has the same degree of the function describing the power needed for vehicle traction at constant speed; in this case, the speed that can be maintained for an undetermined time without depleting battery SOC is slightly higher in comparison with other case, being about 30m/s.

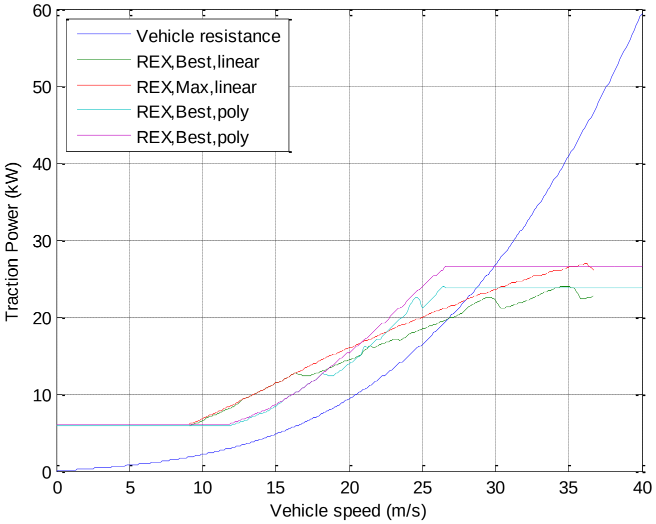

Figure 160 – Traction power of vehicle depending on speed and power supplied by the range extender using a linear link function or 3rd degree polynomial link function.

6.3.3. Supercapacitors control strategy: active filtering

The model includes a configuration in which supercapacitors are used to participate to traction power in order to reduce the load on the battery cells. An “active filtering” strategy is used: it means that a power switch converter is used to interface the supercapacitors system with the DC–link of the motor controller, so that SC system is not acting as a pure low–pass filter but its smoothing effect can be controlled by the active system, almost regardless of the voltage of the battery and supercapacitors at that moment.

In the case study the SC are used in order to provide the “high frequency” part of the traction load, while battery is used for the low–frequency part. Similarly to other literature works (Trovão et al, 2013), the strategy in implemented on the model using of an high–pass filter transfer function applied on traction power; the pre–calculated value high frequency power signal is the power load on the SC system. In real systems, this condition can be obtained using a controller acting on a step–up/step–down power switch which is able to reach the desired SC power controlling its voltage and current value; in the model, the losses of such power elements are considered through a constant loss factor of 6% (a quite pessimisti value). The time constant of the transfer function and the SC capacity needed to satisfy that for a similar time the full power can be supplied by SC are determined by the simple relation:

$$\tau = \frac{E_{SC}}{P_{SC}}$$

In the case of this study, the power has been set to traction power (47kW), while the energy has been determined by a limitation on the mass of SC that is about 15kg; assuming a power density of 5.89 Wh/kg (see Burke and Miller, 2010) a time constant of about 4s can be achieved.

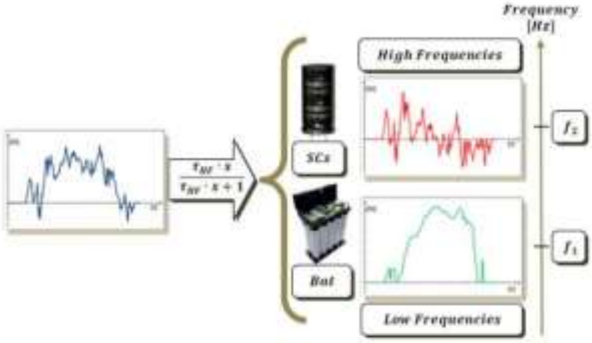

Element mass (kg)	0.057
Energy density (Wh/kg)	5.89
Mass additional factor	1.5
Internal resistance (mOhm)	1.4
Series elements in system	160
System energy	53.7 Wh
Discharge time @47kW (s)	4s
Total mass of SC system	13.7 kg

Table 47 – Power disaggregation through transfer function (Trovão et al, 2013) and simplified dimensioning data for supercapacitor system.

In addition to such control, the SOC of the SC bank is maintained at a predetermined value through a PID controller that commands the power transfer from or to the battery: the first case can occur as a consequence of an intense discharge of SC, while the second can occur in case of prolonged and intense regeneration.

6.3.4.Model applications

The plots from Figure 161 to Figure 166 describe the effect of the vehicle configuration as simulated by the model.

They are shown to demonstrate how the power supplied by the battery can vary; in particular, Figure 165 shows how supercapacitors are supposed to work, especially in “stop and go” phases: regenerative energy is mainly stored and released by them, while the load on the battery is significantly low. In absence of supercapacitors, in case of small batteries (in this case, 25% of iMiev battery has been used), it is necessary to start up the range extender for some acceleration events to obtain full performances, thus increasing fuel consumption. A few results regarding mean (absolute value is considered) value, maximum values and standard deviation of the current supplied by the battery are shown in Table 48, that demonstrate the effectiveness of the solution.

	Pure BEV	**BEV with supercapacitors**	**EREV with support by range extender**
Imean (A)	18.4	12.3	17.4
Imax (A)	147.5	77.3	119.2
Istd (A)	19.4	13.5	17.2

Table 48 – Current supplied by the battery on three different configuration.

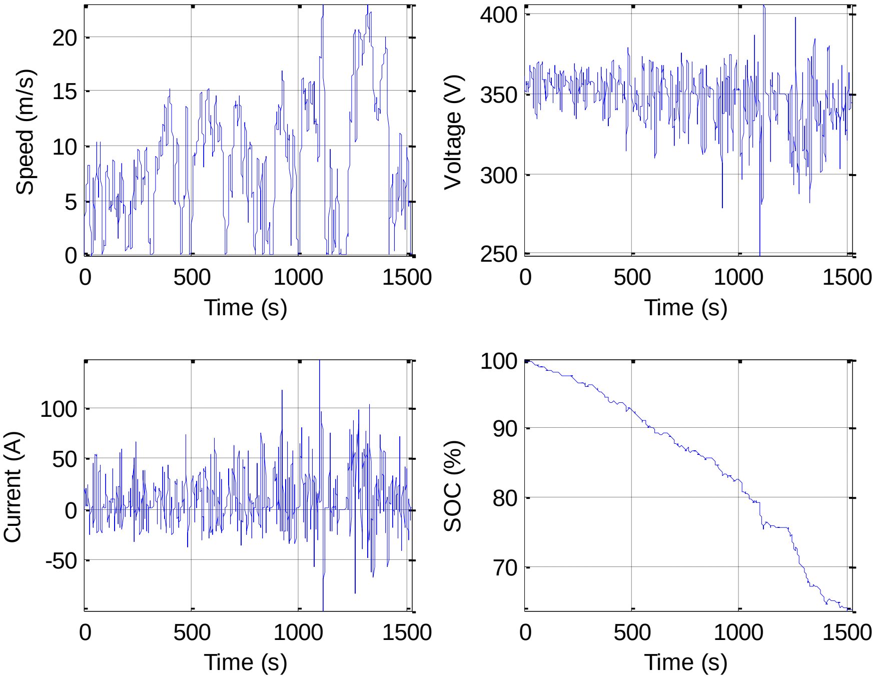

Figure 161 – Various plots coming from the simulation of “unsteady–long” cycle for pure BEV (to emphasize the discharge, a small battery is used – 25% of original size).

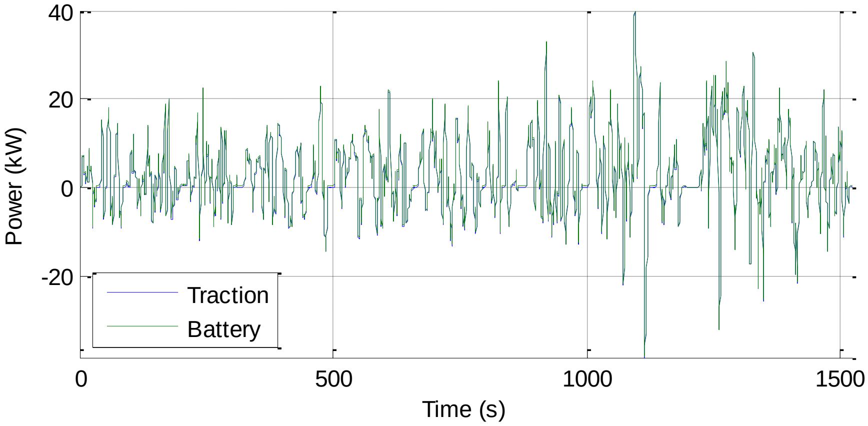

Figure 162 – Traction and battery power the simulation of "unsteady–long" cycle, pure BEV.

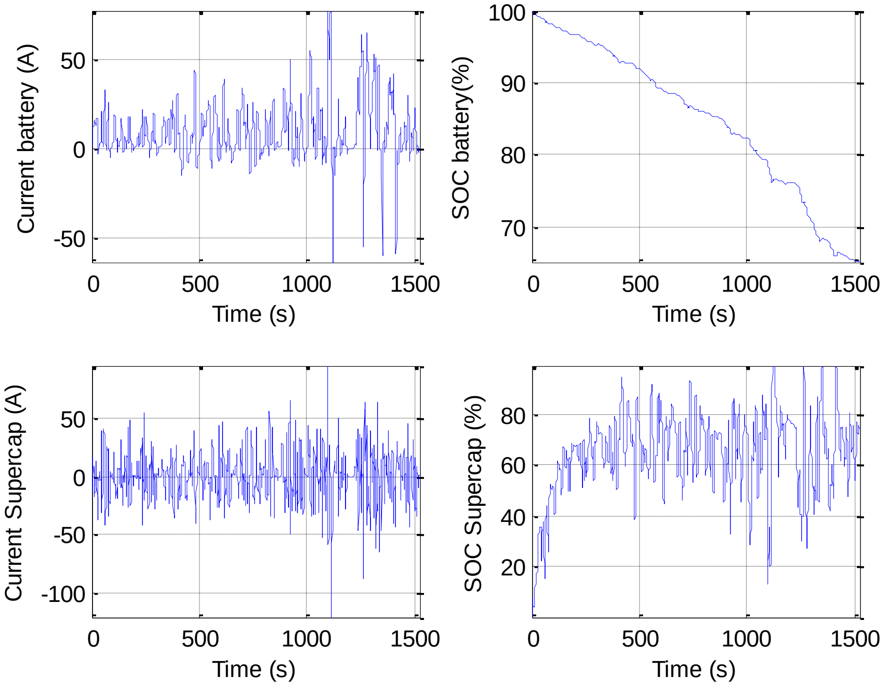

Figure 163 – Various plots coming from the simulation of "unsteady–long" cycle for BEV–supercapacitor (to emphasize the discharge, a small battery is used – 25% of original size).

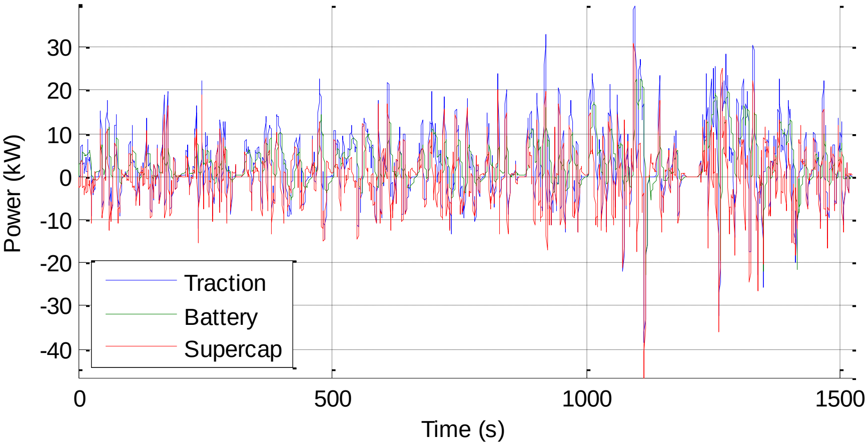

Figure 164 – Traction, battery and SC power the simulation of "unsteady–long" cycle, BEV with supercapacitors.

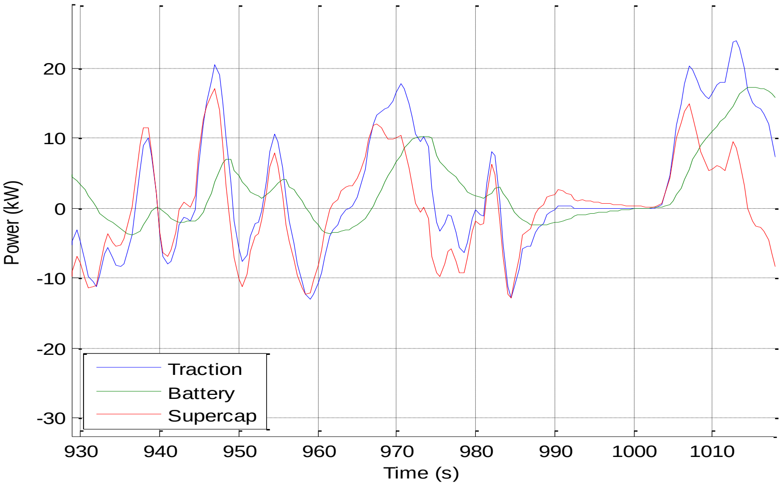

Figure 165 – Traction, battery and SC power the simulation of "unsteady–long" cycle, BEV with supercapacitors (detail).

Figure 167 and Figure 168 show the comparison of vehicle speed and battery SOC in case of application of "trip scheduling" criteria or not; in the first case (total distance being about 150km) the vehicle needs to slow during highway driving, since the desired driving power exceed range extender capabilities, while in the second case the anticipated start of the range extender keeps an higher SOC for the battery, thus full speed can be maintained for a longer time.

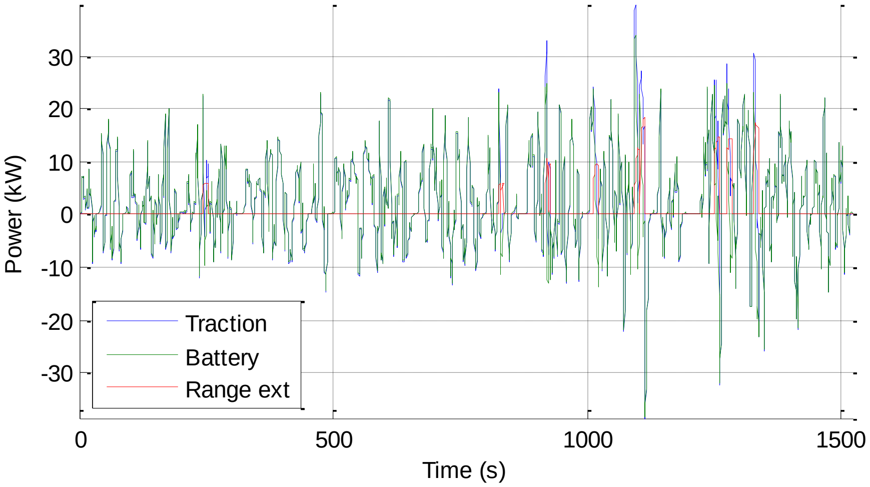

Figure 166 – Traction, battery and range extender power for the simulation of "unsteady–long" cycle, BEV with range extender used as support for higher power.

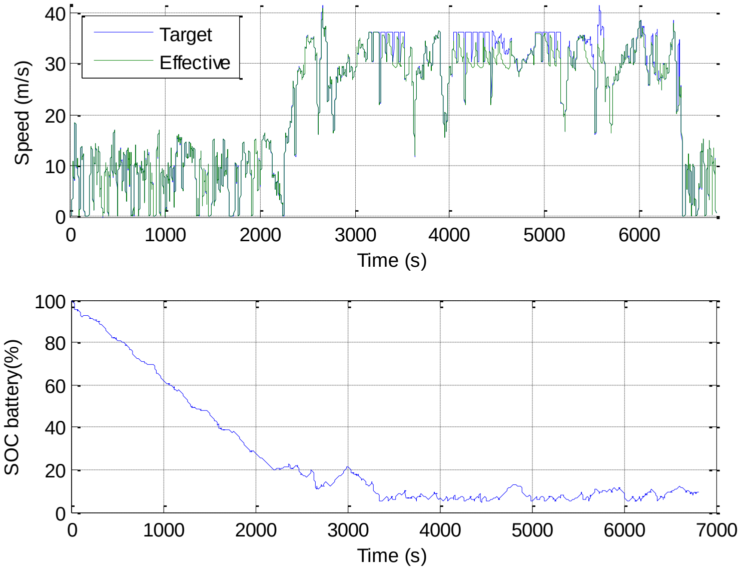

Figure 167 – Upper plot: desired speed and effective speed of the vehicle; in highway driving, since requested power exceeds range extender capability it is possible that the battery SOC falls to low level, determining the occurrence of "safe" mode, highlighted by the distance between target and effective speed.

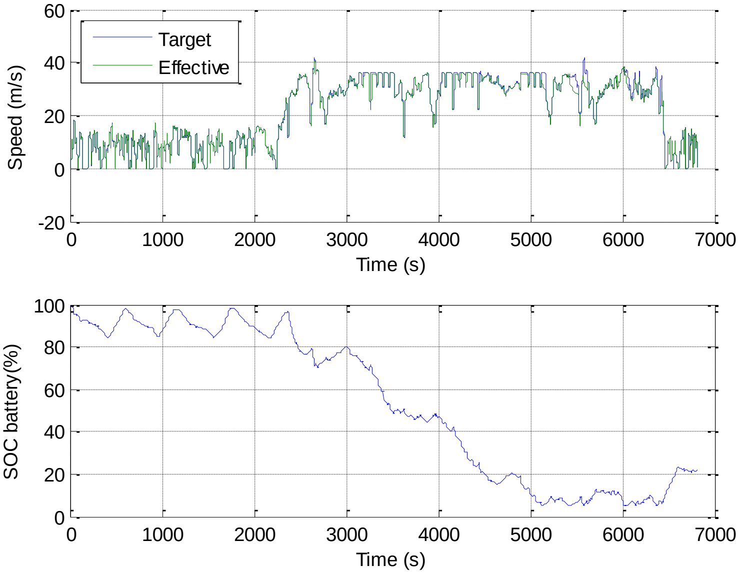

Figure 168 – Upper plot: desired speed and effective speed of the vehicle; bottom plot: corresponding battery SOC in case of application of "trip scheduling" strategy.

6.4. Preparing use–case scenarios

The last part of the chapter deals with the application of the model defined. The aim of the activity is to verify which configuration is best suitable for a realistic use case built using the data acquired on real–world situations. Due to the large variability of the data, a number of hypothesis to reduce the wideness of the field of study are introduced. Some alternatives for vehicle configuration are proposed as main representative examples. For each scenario, many events (at least one year of used) are simulated, varying the boundary conditions through randomization of data using suitable stochastic alternatives; such approach is sometimes described as “Montecarlo” simulation. Figure 169 synthetize the steps to be performed.

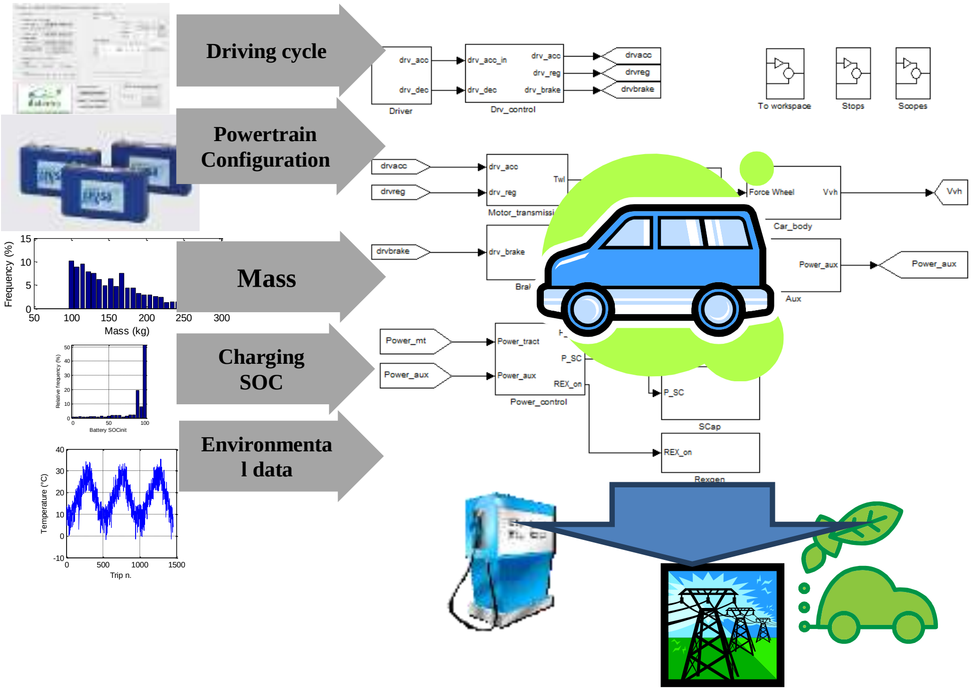
Driving cycle
Powertrain Configuration
Mass
Charging SOC
Environmenta l data
Frequency (%)
Mass (kg)
Battery SOCinit
Temperature (°C)
Trip n.
drv_acc
drv_dec
Driver
drv_acc_in
drv_reg
drv_brake
Drv_control
drvacc
drvreg
drvbrake
To workspace
Stops
Scopes
Motor_transmissi
Force Wheel
Vvh
Car_body
Power_aux
Aux
Power_mt
Power_tract
P_SC
REX_on
Power_control
SCap
Rexgen

Figure 169 – The approach adopted for the simulation: the model receives boundary condition at input, which are varying according to their distribution over the year, and the output are calculated in terms of energy and fuel consumption as well as GHG emissions. The model is adapted on the input conditions depending on their influence on vehicle data (e.g. varying powertrain configuration varies mass and energy management strategy).

Next paragraphs describe the set–up of the case study and the verification of results.

6.4.1. A scenario for a Light Delivery Vehicle

A first case study for the comparison of energy performances of different vehicle alternatives has been prepared using ASTERICs data. The aim is to verify which configuration should be preferable for a Light Delivery Vehicle of small size[8] used predominantly in an urban–suburban context for small freight – postal delivery; the time period under analysis covers a period of a full year of use, thus the schedules for a large number of days and events has been defined. Assuming a yearly distance of about 20.000km (comparable with the value registered by vehicle odometers for the ASTERICs LDV case study), daily trips have to be planned in terms of distance and of additional conditions: charging strategy, mass transported, external temperature.

Regarding the daily distance, a value of 230 working days per year is assumed; the mean daily distance is therefore 86 km. A normal distribution is assumed, its standard deviation (also coming from ASTERICs) being 40 km. A maximum of 200km/day is used, since – according to typical urban average speed (below 30km/h) – this value saturates the typical daily working time of eight hours.

The charging strategy adopted for LDV is particularly simple: one full charge per day (up to 100% battery SOC) is performed. For this application it is assumed that intermediate charging is undesirable, since it corresponds to vehicle unavailability time. In current use, since the number of vehicles in the fleet currently exceeds the number of drivers, it is possible to switch vehicle when it is supposed to exceed the available range, and this typically happen after “lunch break”. The company currently performs intermediate charging only in case of risk of vehicle stop before reaching home destination, using public charging stations (about 100 low power charging point, installed in the late ‘90s, are available in the city of Florence).

The transported mass is varied for every day (but not for every trip of the day) assuming a “basic vehicle mass” (curb weight plus 100 kg, comprehending the drivers and standard load) plus a variable mass – corresponding to the load – having and average mass of 170 kg and a standard deviation of 40 kg.

The external temperature affects the energy consumption of the HVAC system and determines the starting temperature of the battery system; for every single day, a value is generated through random extraction from a temperature database. The measurements coming from the city of Rome (an adaptation of data available at ECA, 2013) over a period of five years are used; two temperatures are available for each day: the mean value of “hot hours” (daytime, 7am–7pm) and the mean value of “cold hours” (7pm–7am). For this scenario, only daytime temperatures are considered (see Figure 170).

Finally, for one year (365 days), a schedule is calculated:

- 230 working days are extracted considering systematic exclusion (Saturday – Sundays) and random exclusions;
- for each working day a distance, a mass and a Temperature are extracted, coherently with the period of the year
- for each distance, a driving cycle data is generated using ASTERICs data; (quadricycle data are excluded and all the clusters are used).

---

[8] Such vehicles are frequently used in the context of Italy; the LDV models are originated by simple adaptations of corresponding passenger car, including “sub–compact” european models (e.g. Fiat Panda Van; Peugeot Bipper).

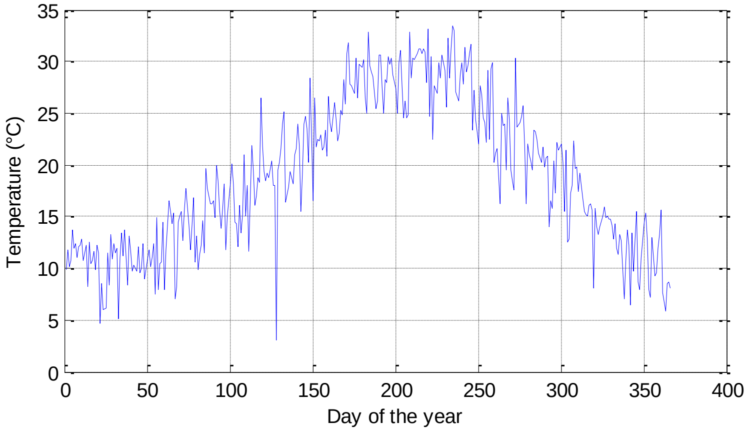

Figure 170 – Daily external temperature for the simulations of LDV scenarios.

The generated driving cycle is, in general, different for each day; no highway cycles are introduced. The configuration used for the LDV is varied modifying battery size, installation of supercapacitors (or not), installation of range extender and, in case, the configuration that has been used (e.g. using or not trip scheduling, supporting or not vehicle traction depending on supercapacity availability); a scheme is reported in the Table 49.

The range extender RPM is set in order to follow a third degree function (see Figure 160).

LDV configuration	1	2	3	4	5	6	7	8	9	10	11	12
Battery size	32	24	16	8	8	8	4	5,28	5,28	5,28	5,28	5,28
Supercapacitors						X			X		X	X
Range extender			X	X	X	X	X	X	X	X	X	X
Range extender support					X	X	X	X		X	X	X
Range extender "trip programming"										X		X

Table 49 – Configurations tested for “LDV” case study.

6.4.2. A scenario for a Passenger Vehicle

A second use case scenario for passenger vehicle has also been prepared. In this case, the input data needed regarding driven distance have been set using also literature data, since ASTERICs data regarding private users were obtained from a small number of vehicles. First of all, a distribution for daily distance is needed; even if Pasaouglu et al., 2012, study is very recent, the publication does not specify some important details: only average distance per country (in the context of Europe) is declared. Very complete data coming from US (see NTHS, 2011; Krumm, 2012, and Smart et al., 2013) can be suitable, but a source focused on Europe is preferable. The report by Enerdata, 2012 (using results coming from research project Odyssee) shows that the yearly driven distance for passenger cars can vary from a minimum of 8000 km to a maximum of 18000km, the average value between 12000km and 13000 km.

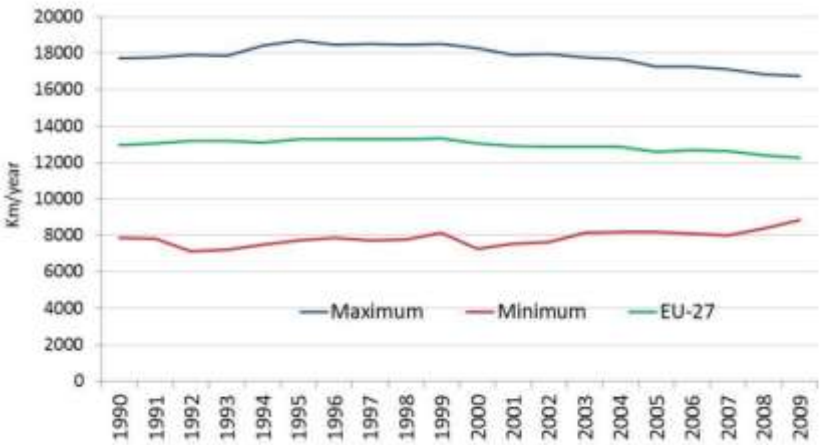

Figure 171 – Trends in the average annual distance travelled by car (source: Enerdata/Odyssee consortium, 2012).

Considering that the model used for the analysis is based on iMiev vehicle (small size vehicle), mainly suitable for urban context, the maximum value of 18000 km is excluded. Regarding the distribution of distances per day, the work by Marker et al., 2013, proposes the results of a measurement campaign on Berlin, Germany, and can therefore considered as a suitable choice for a European city context. The probability density of daily driven distance does not corresponds to commonly used distributions, so that it has been reproduced using a spline (see Figure 172).

The obtained function, if used to generate the travels of a year of use (365 random generations), results in a distance in the range of 12.000–14.000 km; if it used to generate a large number of distances (10^5 generation, corresponding to about 28 years), the resulting yearly average value is 12700 km: this value (confirmed repeating the random generation with different seeds) is coherent with cited Odyssee study. Due to the fact that private users can experience a less systematic use in comparison with LDV operated by a freight delivery company, the number of charging events can vary day by day both in terms of number and in terms of final SOC. Therefore, for each day a number of different trips separated by charging events has to be generated.

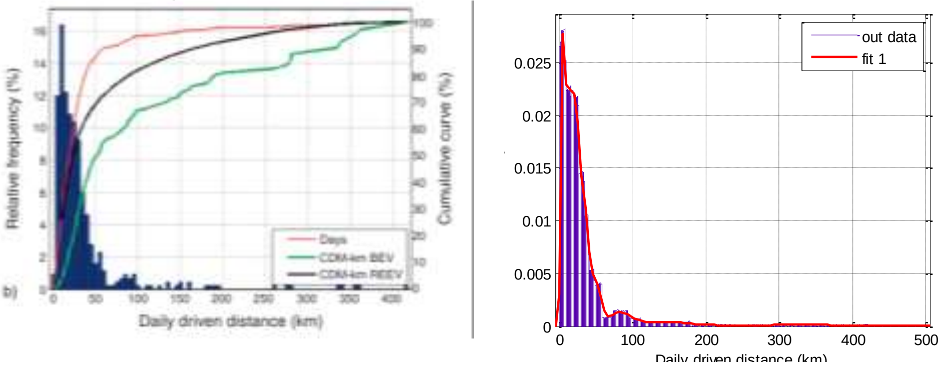

Figure 172 – Daily driven distance distribution from original source (Marker et al, 2013) and fitted function.

Vehicle experimentation results on use cases are available in literature; information regarding mean driven distance between charging events, typical SOC at the beginning of a trips and similar useful information have been recently published by Smart et al., 2013.; the data presented in the study, even if obtained in the US context, have been used since this study is one of the most detailed within those currently available (e.g. the work by Marker et al. is using a starting SOC of 100% as simplified hypothesis). The available data have been used to define:

- the number of charging events for each day; two simplifications are applied:
  - for distance of the day <mean daily distance, max 2 charging events (that means, 1 intermediate charge) are supposed (see Figure 173)
  - for distance of the day >mean daily distance, the max possible value of charging events is 4
- the battery SOC at the beginning of the trips, that is coming from Smart et al., 2013 data assuming that
  - the first trip of the day starts from “home” location
  - other trips start from “away” location
  - effective SOC init is the maximum between the randomly generated value and the value corresponding to SOC final of the former trip.

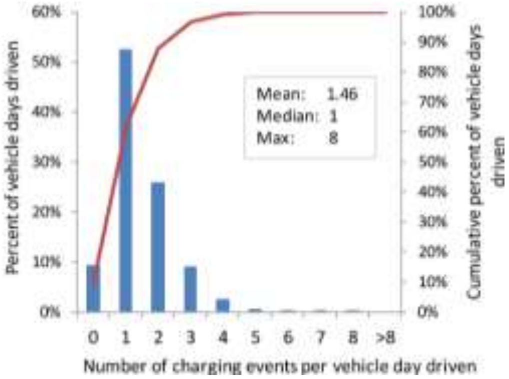

Figure 173 – Charging events per vehicle day driven (source: Smart et al., 2013).

Regarding temperature, the same criteria used for the generation of random values from Rome data on scenario LDV are used; in this case, also “cold” temperatures are used, assuming that 25% of trips are run on the 7p.m.–7a.m. time range.

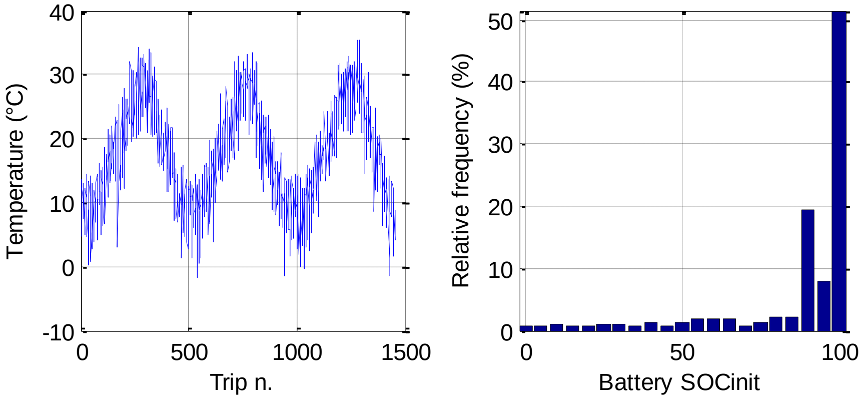

Figure 174 – Boundary condition for each driving event temperature and battery initial SOC (here represented as a distribution).

The mass of the vehicle includes a standard additional value of 100kg plus a value generated by a distribution having mean zero and standard deviation 75kg; max value is limited at 200kg and min at –20 (so that at least 80kg, corresponding to the driver, are considered). A value is generated for each trip.

The daily distance distribution is quite concentrated on values below 50km (average being 35km), so that events above 100–200km are quite rare and distances exceeding 300–400km are occasional (2–3 events per year); such unbalance can determine the risk that the random generation of a small number of events is not representative of the distribution, e.g. none of this long distance events can occur in one year, while changing the seed of the random generation can provide 5–6 of them: in other words, high per–year variation can occur. For this reason, trips are scheduled for a long simulation period (3 years) to reduce the occurrence of such non–representative generation events. In total, in a period of 1098 days, 1453 driving events have been generated, each one representing a "trip chain" between two charging events; the mean value of a trip chain is 26.3 km.

Once that a daily distance and its subdivision in one or more events has been scheduled, the driving cycle for each trip is generated. Some arbitrary hypothesis are adopted:

- if the distance is below 6km, all the cycle is generated from ASTERICs data using all vehicle measurements, and clusters from 1 to 7 (pure urban cycle);
- if the distance is within 6–35 km, all the cycle is generated from ASTERICs data using all vehicle measurements and all clusters (mixed urban–suburban cycle);
- if the distance is above 35 km, an high–speed cycle corresponding at least to 65% of total distance is generated; two segments generated from ASTERICs driving cycles are generated and put before and after the high speed phase, their total distance being 35% of trip distances or 30km as a maximum.

Two observations are necessary.

- such hypothesis are aimed to represent typical vehicle use on the basis of common experiences and qualitative knowledge; in case that detailed use data will be available in future, the driving cycle can be generated according to any kind of dataset

- it has been decided to generate new highway driving cycles instead of using the repetition of existing ones since, in this latter case, vehicle stops to zero speed would have been unavoidable. The generator, on the contrary, can produce highway driving cycle comprehending a maximum of 200–250 km without stops, thus being more general.

The configuration tested are shown in the Table 50.

Passenger configuration	1	2	3	4	5	6	7	8	9	10	11	12	13	14
Battery size (kWh)	32	24	16	16	8	8	8	8	8	4	4	4	4	4
Supercapacitors					X		X		X		X		X	X
Range extender	X	X	X	X	X	X	X	X	X	X	X	X	X	X
Range extender support					X		X		X	X		X	X	X
Range extender "trip programming"			X			X		X	X			X		X

Table 50 – Configurations tested for “Passenger vehicle” case study.

6.5. Simulation results

A first observation is needed about the model. According to the reduced complexity, the simulation of one vehicle configuration (that is, the repetition for about 20000 in a year) can be performed in an acceptable time – about 12–15 hours depending on the generated driving cycles, using a “rapid accelerator” Matlab solver on a desktop machine of low–standard calculation performances (an AMD Phenom X4, 3.40 GHz processor, 8Gb ram running Windows 7 professional; Matlab version is 2013a, compiler is Microsoft SDK 7.1). The simulation time of all the alternatives can be shortened significantly considering that more configurations can be run on parallel solvers (up to 4, in the considered machine, can be run maintaining system stability) and that the recompilation of the model (which consumes a significant time) is not needed for similar configuration. In total, about 24 hours are needed for the simulation of LDV use case and about 36 hours for the simulation passenger vehicle use case; such effort is considered acceptable.

The final evaluation of the results of the simulation has to be based on aggregated parameters able to identify the quality of the performances of the vehicle.

The first one is the ability of the vehicle to achieve the distance needed in the schedule. In case of the LDV, the target cycle distance has not been reached in some situation by the pure BEV configurations, while range extender vehicles are always able to reach the required range, even if, in case of very low SOC, performance limitation can occur. For passenger case study, all the configurations include the use of the range extender. The total time spent in “safe” mode should be as low as possible.

The second one is the energy consumption of the vehicle, which should be as low as possible. Electriciy and fuel consumption are expressed separately but, in order to compare the environmental impact of different vehicle configurations, an aggregation criterion is necessary; specific GHG emission (gCO_2/km), as described in 1.1.3 paragraph, is a suitable one. The GHG emission for the electric energy consumption for each cycle is calculated from battery SOC variation and battery energy capacity product; charging losses also have to be included:

$$G_{ee} = \frac{\Delta SOC * E_{batt}}{\eta_{ch}} * S_{ee}$$

E_{batt} being battery energy (in kWh), η_{ch} being charging efficiency (0.94, according to Geringer and Tober, 2012) and S_{ee} being specific electric energy GHG emission (gCO_2/kWh). Since supercapacitors are supposed to start at zero SOC at each trip, their energy is considered wasted after vehicle turn off and therefore is not taken into account.

The GHG emission for the fuel is calculated using:

$$G_{gf} = M_{gf} * \rho_{gf} * S_{gf}$$

Where the three factors are the mass of gasoline fuel consumed, the density of the gasoline fuel (usually varying between 720–780 g/l; an average value of 750 g/l is assumed), and the specific emission factor for electricity production (described in 1.1.3 paragraph).

6.5.1. Results for LDV scenario solution

Table 51 shows the results of the simulation for the LDV scenario. The data that for such configuration a pure BEV battery is a suitable solution, since it is supposed that a range of more than 200km will not be overpassed in any time. The dimensioning of the battery should be at least 32 kWh (a value that is double than current iMiev vehicle), since the second column of the table shows that a 50% increase of battery capacity is not enough: it could lead to the impossibility to reach the yearly schedule. All range–extender solution, however, are able to reach the distance, and in none of the cases the vehicle met the “safe” condition. “Safe condition” can occur in case that range extender cannot support battery due to continuous driving at high power, that is not the typical use of LDV moving within urban/suburban context. For this application, using a battery having half the capacity of standard vehicle (8 kWh) leads to a fuel consumption that, even if acceptable (about 4–5 l/100km in overall), causes an increase in GHG emissions so that the vehicle cannot reach values below 120gCO_2/km in current European average carbon intensity .

The use of supercapacitors, as expected, reduces the fuel consumption but – probably due to the low efficiency selected of the step–up/step–down converter – slightly increases the GHG emissions (see columns 5–6). However, the opportunity for the use of supercapacitors should also depend on the estimation of battery ageing, a topic that is not addressed in the present study; the positive effect on the reduction of battery C-rate is clear from the table.

The use of range extender scheduling, however, significantly reduces emissions even in case of a fuel consumption increase (see columns 11–12).

As a conclusion, for a vehicle running an average daily distance above 80km as this, it is suggested that battery capacity is not reduced below the value that can satisfy the achievement of typical driving range.

6.5.2. Results for Passenger scenario solution

Table 52 includes the result for the passenger vehicle scenario, that is supposed to be used on a short daily distance. The first comparison is related to the implementation of the function linking range extender power and vehicle speed; the linear solution clearly leads to a relevant occurrence of “safe” condition (especially for low battery), thus being unsatisfactory. The solution using a third degree function significantly reduces the occurrence of “safe” condition; the effectiveness of the trip scheduling proposal, however, is shown by the comparison of columns 13 and 14. Thus, a range extender having limited performances is still suitable for a vehicle of this size since even in case of very small battery.

The specific GHG emission has been calculated only for this latter solution. For this application, battery capacity reduction negatively affects the GHG impact, but the sensitiveness is reduced in comparison with former case. The overall fuel consumption (not taking into account electric energy) is below 4 l/100km for a small 4kWh battery (25% of current iMiev battery, thus leading to about 30km range); the vehicle in this configuration is acting more as an HEV rather than an EREV. In addition, it can be noted that for electricity production from “carbon intense” sources (above 600gCO_2/kWh), the solution using the larger battery does not achieve the best results on overall emissions. As a conclusion, the proposal of this kind of vehicle having a “downsized” battery and a small range extender could reach the environmental target of recent normatives; the case study application is hypothesizing a daily driven distance within 35km.

In an author’s opinion, such solution could also be suitable for those users looking for a vehicle that is able to reach the limited traffic zone of the cities and to be used also on the weekends and consider secondarily relevant the economical factor or environmental factor: these users also corresponds to the profile of the private drivers that participated to data measurements.

A final observation is necessary. The scenario here presented is not aimed at offer a final answer about the vehicle solution that is preferable for the mission considered, but it represents an example on how the method and the data proposed can be combined to obtain the performances not only on the basis of “one” or “a few cycles” but over a complex scenario. The case studies proposed are two example of applications which do not pretend to be exhaustive of the large variability of use cases in which a vehicle can be enrolled..

LDV configuration		1	2	3	4	5	6	7	8	9	10	11	12
Battery size (kWh)		32	24	16	8	8	8	4	5.28	5.28	5.28	5.28	5.28
Supercapacitors							X			X		X	X
Range extender				X	X	X	X	X	X	X	X	X	X
Range extender support						X	X	X	X		X	X	X
Range extender "trip scheduling"											X		X
Distance (km)		20019	19857.0	20096.4	20092.0	20092.0	20092.5	20089.8	20090.5	20090.9	20090.6	20091.1	20091.1
Safe time (h)		0	0	0	0	0	0	0	0	0	0	0	0
Electric energy used (kWh)		3263.5	3032.8	2369.4	1125.6	1075.7	1149.0	227.7	532.2	729.8	242.9	706.7	374.5
Gasoline used (l)		0.0	0.0	237.7	869.4	886.8	905.3	1145.9	1052.0	1028.5	1064.7	1035.7	1059.9
Fuel consumption (l/100km)		0.0	0.0	1.2	4.3	4.4	4.5	5.7	5.2	5.1	5.3	5.2	5.3
Charging efficiency		0.94	0.94	0.94	0.94	0.94	0.94	0.94	0.94	0.94	0.94	0.94	0.94
Gasoline emission gCO2/l		2360	2360	2360	2360	2360	2360	2360	2360	2360	2360	2360	2360
C-rate mean		0.11	0.14	0.22	0.46	0.46	0.34	0.88	0.68	0.49	0.81	0.49	0.71
		Emission CO2/km											
Electricity specific emission	100 gCO2/kWh	17.3	16.2	40.5	108.1	109.9	112.4	135.8	126.4	124.7	126.3	125.4	126.5
	200 gCO2/kWh	34.7	32.5	53.0	114.0	115.6	118.5	137.0	129.2	128.5	127.6	129.1	128.5
	300 gCO2/kWh	52.0	48.7	65.5	120.0	121.2	124.6	138.2	132.0	132.4	128.9	132.9	130.5
	400 gCO2/kWh	69.4	65.0	78.1	126.0	126.9	130.7	139.4	134.9	136.3	130.2	136.6	132.4
	500 gCO2/kWh	86.7	81.2	90.6	131.9	132.6	136.8	140.6	137.7	140.1	131.5	140.4	134.4
	600 gCO2/kWh	104.1	97.5	103.2	137.9	138.3	142.8	141.8	140.5	144.0	132.8	144.1	136.4
	700 gCO2/kWh	121.4	113.7	115.7	143.8	144.0	148.9	143.1	143.3	147.9	134.1	147.8	138.4
	800 gCO2/kWh	138.7	130.0	128.3	149.8	149.7	155.0	144.3	146.1	151.7	135.4	151.6	140.4
	900 gCO2/kWh	156.1	146.2	140.8	155.8	155.4	161.1	145.5	148.9	155.6	136.6	155.3	142.3

Table 51 – Results for the simulation of LDV case study over a year of driving. Note for the vehicle configuration: "X" means "in use".

Passenger vehicle		1	2	3	4	5	6	7	8	9	10	11	12	13	14
Battery size		32	24	16	16	8	8	8	8	8	4	4	4	4	4
Supercapacitors						X		X		X		X		X	X
Range extender		X	X	X	X	X	X	X	X	X	X	X	X	X	X
Range extender support						X		X		X	X		X	X	X
Range extender "trip scheduling"				X			X		X	X			X		X
Linear REX use	Distance (km)	38201.9	38200.5	38221.6	38195.7	38174.9	38178.7	38165.9	38223.8	38223.5	38097.6	38037.4	38218.7	38066.3	38216.2
	Safe time (h)	0.7	1.0	0.0	1.2	2.7	2.5	3.3	0.0	0.0	8.9	13.2	0.4	11.3	0.6
	Electric energy used (kWh)	6112.2	5445.0	3845.5	4616.9	3321.8	3311.3	3497.0	2691.5	2838.7	1800.0	2391.4	1206.3	2150.5	1512.6
	C-rate mean	0.20	0.25	0.40	0.36	0.68	0.67	0.55	0.74	0.62	1.26	1.04	1.39	1.01	1.17
	Gasoline used (l)	315.7	443.9	872.8	630.0	979.4	982.2	995.5	1164.9	1192.6	1446.2	1400.0	1627.4	1399.7	1589.8
	Overall fuel consumpt. (l/100km)	0.8	1.2	2.3	1.6	2.6	2.6	2.6	3.0	3.1	3.8	3.7	4.3	3.7	4.2
Third degree REX use	Distance (km)	38216.9	38219.2	38221.6	38221.6	38220.3	38220.7	38216.1	38223.8	38223.5	38193.6	38166.4	38218.6	38178.7	38216.2
	Safe time (h)	0.0	0.0	0.0	0.0	0.2	0.2	0.5	0.0	0.0	2.5	4.8	0.4	3.8	0.6
	Electric energy used (kWh)	6094.7	5429.6	3836.5	4631.5	3306.3	3302.0	3486.1	2691.0	2824.3	1843.8	2380.7	1235.7	2143.4	1513.5
	C-rate mean	0.20	0.25	0.40	0.36	0.68	0.67	0.55	0.74	0.62	1.25	1.04	1.39	1.01	1.17
	Gasoline used (l)	312.2	436.0	840.8	606.1	956.8	956.5	969.4	1118.5	1149.0	1398.5	1373.7	1554.6	1369.6	1526.2
	Overall fuel consumpt.(l/100km)	0.8	1.1	2.2	1.6	2.5	2.5	2.5	2.9	3.0	3.7	3.6	4.1	3.6	4.0
	Charging eff	0.94	0.94	0.94	0.94	0.94	0.94	0.94	0.94	0.94	0.94	0.94	0.94	0.94	0.94
	Gasoline emission gCO2/l	2360	2360	2360	2360	2360	2360	2360	2360	2360	2360	2360	2360	2360	2360
		Emission CO2/km													
Electricity specific emission	100 gCO2/kWh	36.3	42.1	62.6	50.3	68.4	68.3	69.7	76.5	78.8	91.8	91.9	99.4	90.9	98.5
	200 gCO2/kWh	53.2	57.2	73.3	63.2	77.6	77.5	79.4	84.0	86.7	96.9	98.5	102.9	96.9	102.7
	300 gCO2/kWh	70.2	72.3	84.0	76.1	86.8	86.7	89.1	91.5	94.5	102.1	105.2	106.3	102.9	106.9
	400 gCO2/kWh	87.2	87.4	94.6	89.0	96.0	95.9	98.8	99.0	102.4	107.2	111.9	109.8	108.9	111.1
	500 gCO2/kWh	104.1	102.5	105.3	101.9	105.2	105.1	108.5	106.5	110.2	112.4	118.5	113.2	114.9	115.3
	600 gCO2/kWh	121.1	117.7	116.0	114.8	114.4	114.3	118.2	114.0	118.1	117.5	125.2	116.6	120.9	119.5
	700 gCO2/kWh	138.1	132.8	126.7	127.7	123.6	123.5	128.0	121.5	126.0	122.7	131.8	120.1	126.8	123.7
	800 gCO2/kWh	155.1	147.9	137.3	140.6	132.9	132.7	137.7	129.0	133.8	127.8	138.5	123.5	132.8	128.0
	900 gCO2/kWh	172.0	163.0	148.0	153.5	142.1	141.9	147.4	136.5	141.7	133.0	145.2	127.0	138.8	132.2

Table 52 – Results for the simulation of a passenger vehicle in various configuration for a three–year period of use. Note for the vehicle configuration: "X" means "in use".

Conclusions and final remarks

The activity presented in this thesis deals with the development of electric vehicles aiming at defining a methodology for the efficient use of the tools needed for their design.

First of all, the reasons determining a demand for new generation vehicle on the market have been analyzed, focusing on the potential for environmental impact reduction. Greenhouse gas emission, in particular, is a parameters that can be used for the overall evaluation of vehicle performance and for the ranking of the powertrain alternatives.

The analysis has then been focused on the vehicle design process: engineers are facing a surprisingly number of alternatives in terms of software, methods, data, approaches and problems to be solved, as demonstrated by a wide scientific and technical literature on automotive research. Therefore, the aim has been to find a general point of view to coordinate the resources involved in the challenging process of designing vehicles and, more in general, of mechatronics systems. Since vehicles are complex mechatronics products, a feature requested to simulation environment is the possibility to solve problems defined in multiple physical domains: thermal, mechanical, electrical. The objective of a modelling activity is to represent component and system performances; however, there is not a unique way to satisfy such needing and each model has to be built taking into account both the need for accuracy and the need for low computation effort, sometimes complying with low data availability (especially during early design phase). For this reason, it could be not correct to define a model as “better” than another one, since each design phase has different priorities to deal with. This study has been developed and exploited within an international research project, since it was needed to provide a general strategy for the integration and the valorization of different experiences related to system simulation and to data sharing. In other words, the elements for the definition of a “structured approach” were needed. Therefore, a general model categorization is provided, aiming to highlight the advantages and the disadvantages of each approach, using a few literature references as examples. The activity highlighted that modelling tools have the potential to be used as guiding framework for product development instead of being mere aid for “single” simulation activities. However, a few conditions have to be respected during model design to guarantee the exploitation of such capabilities: flexibility is the main one. The results include guidelines for model definition and for integration of different tools, which are aimed to guarantee the upgradeability of the models over the time and the possibility to include in a unique software environment all the information available for the system.

Following these premises, two main topics have been analyzed and developed in detail.

Use cycles represents one of the main input in any design activity, and within automotive design strong efforts are spent for the creation and the continuous upgrading of so called “driving cycles”. Vehicle driving cycle measurement, characterization and analysis has been a topic under discussion and research over the last thirty years, since it is a key activity both from an Authority point of view (for legislative compliance verification) and from an Industrial or applied research point of view. Considering the innovative characteristics of EV vehicles, the demand for tailored cycles arises. A framework for driving data analysis and for representative sequences definition has been developed through the review and the selection of known literature experiences, having as a goal the application on a real case study. A small–scale measurements campaign in the city of Florence has been conducted by the candidate and the method defined for data treatment has been implemented in a calculation environment: it includes preprocessing capabilities (e.g. data filtering), analysis (e.g. microtrips clustering) and synthesis functions; these latter demonstrated the capability to generate new cycles that are acceptable as representative of input data, according to the criteria used in literature. The main product of the activity consists of a set of representative driving cycles for which only data coming from EVs were used. The examined vehicle include quadricycles, Light Delivery Vehicles and passenger vehicles; the cycles produced from the data are differentiated on the basis of the characteristics of the use verified for each type of vehicle. An interpreter tool for further valorization of the whole dataset has also been prepared and distributed to other users. The method used for cycle synthesis is based on general statistical tools and competencies, so that the experience can be applied on other fields of industrial and applied research.

The availability of such data has been the driver for the preparation of a case study, in which a vehicle model and the driving data are used for a “randomized” scenario analysis. The activity is a subsequent output for the modelling framework proposed on the first phase of the study. The model is based on the characteristics of the existing iMiev vehicle, but an accurate validation has not been possible; however, it has been used for vehicle sizing and preliminary comparison analysis. Two solutions for which the future on the market is still uncertain, such as supercapacitors and range extenders components, are included. The energy management strategies for the use of a power unit comprehending battery, supercapacitors and range extender are proposed using common rule-based approaches. In particular, the driving cycle generator tool has been used for the preparation of a “trip scheduling” strategy for vehicle energy management, which lead to an improvement on the usability of the vehicle in case of continuous driving at high speed, that is a critical condition for those range extenders having limited power. Two different scenario are then simulated, the first one representing the use of a LDV, the second one representing the use of a passenger vehicle. In both cases, a long period (at least one year of use) is considered. The vehicle is then configured in different alternatives and its performances are compared. One indicator based on the greenhouse gas emissions on air has been used as aggregated parameter for the estimation of the environmental compatibility of the solution. For the selected case studies, the result is that LDV is sensitive to battery size and that “large” battery, able to cover the most part of the driven distance, would be preferable; for passenger vehicle, the solution depends on the context in which the energy is provided but the use of “small” battery together with a frequently operated range extender is still able to maintain the GHG emissions below current target values. However, the applications shown do not offer an exhaustive analysis of vehicle sizing alternatives but should be intended as “demonstrator” of the method proposed.

The achievements of the study do not represent the conclusion of the process of modelling design investigation; all the topics addressed within this thesis can be deepened in detail. Regarding modeling activities, main key points to be considered for future development are the possibility to increase the detail in modelling strategy and framework definition (proposing model alternatives compatible with current environment and input/output ports) and the need for increased detail on the model itself.

Regarding topics related to driving cycles, it would be useful to expand the driving cycle database using data coming from the same users or from new ones, comparing BEVs, HEVs and ICEVs for similar users if possible. Randomized driving cycle data have been used for the preparation of a rule-based strategy for vehicle powertrain management, but their potential can be best exploited within structured optimization activities of vehicle performance, cost and consumption.

A topic which has not been analyzed in detail in the present work is the battery ageing: the attention on this latter topic, in particular, is greatly increasing due to its relevance for users' acceptance of new generation vehicles. The study of the boundary conditions such as the "duty cycle" is the first step to be satisfied for the analysis of ageing phenomena that can occur during real-world use; therefore, the use of a method to quantify the ageing on each scenario could offer another relevant indicator for the selection of suitable vehicle alternatives.

Acknowledgements

The present thesis work was carried out in the Department of Industrial Engineering of the University of Florence. Foremost, I would like to express my sincere gratitude to all the people working in this Department, starting from my Supervisors, Dr. Eng. Massimo Delogu and Prof. Eng. Marco Pierini. During these years, I appreciated the motivation, the suggestions and the useful criticism they communicated to me in the context of a relation based on mutual respect and trust. They also gave me the impulse to participate to relevant and interesting project activities. I am grateful to the members of the internal PhD Board for the interest they had on my work, to the Students that prepared their degree thesis collaborating with me for the things I learned from them, and to my colleagues for the friendship, the participation and the familiarity that I experienced. A special dedication to Filippo.

My acknowledgement goes to the people of the Fraunhofer Institute LBF of Darmstadt, in which I spent six stimulating months within the VECOM[9] project. I would like to thank Dr. Eng. Thomas Bruder and Dr. Eng. Riccardo Möller for the useful support I received from them. I would like to cite Riccardo Bartolozzi, for countless reasons, and my office-mate Björn Haffke for his precious presence. I remember all the colleagues and the friends I met in Darmstadt for making that period not only a professional opportunity, but also, or even mainly, an important human experience.

A Special thank goes to the whole ASTERICS[10] Consortium, starting from Dr. Eng Horst Pfuegl (AVL) as project coordinator. Amongst many colleagues, I would like to cite. Annica van Rij, Carolien Mazal (Uniresearch), Claudia Keinrath (AVL) for their efficient support in coordination; Pacôme Magnin, Franck Sellier (LMS–Imagine), Franz Diwoky, Stephen Jones, Christoph Kügele (AVL) for their valuable contribution to model analysis; Laura Borgarello, Claudio Ricci, David Storer (CRF), Hellal Benzaoui, Philippe Dutal, Magnus Larsson, Florian Pereyron (VOLVO) for the constructive cooperation and, in particular, for the suggestions I got during the development of real–world driving cycles. Many thanks also to those companies and those volunteers that provided their time and their vehicles for the measurement activity.

---

[9] VECOM – http://www.vecom.org/, EU FP7 Marie Curie Initial Training Network (ITN) Grant Agreement 213543.

[10] ASTERICS – http://www.asterics–project.eu/. The project is co–funded by the 7th Framework Programme of the EC.

From a personal point of view, the first thoughts are for my family, for letting me achieve my personal goals and for the continuous support I received not only for my PhD study, but during the whole path that conducted me at the end of this phase.

I am grateful to my friends for being with me in these years. Each one of us had to find and to follow his opportunities and we have been together in facts and in thoughts, regardless of the physical distance that separated us.

I can’t even try to describe my gratitude to Elisabetta, that shared with me both the good moments and the most demanding ones of this experience.

Bibliography

Alessandrini, A., Orecchini, F., 2003. A driving cycle for electrically–driven vehicles in Rome. Proceedings of the Institution of Mechanical Engineers, Part D: Journal of Automobile Engineering 217, 781–789.

Alessandrini, A., Filippi, F., Orecchini, F., Ortenzi, F., 2006. A new method for collecting vehicle behaviour in daily use for energy and environmental analysis. Proceedings of the Institution of Mechanical Engineers, Part D: Journal of Automobile Engineering 220, 1527–1537.

Alessandrini, A., Orecchini, F., Ortenzi, F., Campbell, F.V., 2009. Drive–style emissions testing on the latest two Honda hybrid technologies. Eur. Transp. Res. Rev. 1, 57–66.

André, M., 2004. The ARTEMIS European driving cycles for measuring car pollutant emissions. Science of The Total Environment 334–335, 73–84.

André, M., Rapone, M., Joumard, R., 2006a, Analysis of the cars pollutant emissions as regards driving cycles and kinematic parameters.

André, M., Joumard, R., Vidon, R., Tassel, P., Perret, P., 2006b. Real–world European driving cycles, for measuring pollutant emissions from high– and low–powered cars. Atmospheric Environment 40, 5944–5953.

Axsen, J, Burke, A., Kurani, K., Are batteries ready for Plug–in Hybrid Electric buyers? Transport Policy , 17, pp.173–182, 2010.

Barlow, T.J., Latham, S., McCrae, I.S., Boulter, P.G., 2009. A reference book of driving cycles for use in the measurement of road vehicle emissions.

Barkenbus, J., 2009. Our electric automotive future: CO2 savings through a disruptive technology. Policy and Society 27, 399–410. doi:10.1016/j.polsoc.2009.01.005

Barreras, J.V., Schaltz, E., Andreasen, S.J., Minko, T., 2012. Datasheet–based modelling of Li–Ion batteries, in: 2012 IEEE Vehicle Power and Propulsion Conference (VPPC). Presented at the 2012 IEEE Vehicle Power and Propulsion Conference (VPPC), pp. 830–835. doi:10.1109/VPPC.2012.6422730.

Barsali, S., Miulli, C., Possenti, A., 2004. A control strategy to minimize fuel consumption of series hybrid electric vehicles. IEEE Transactions on Energy Conversion 19, 187–195. doi:10.1109/TEC.2003.821862

Bauman, J., Kazerani, M., 2008. A Comparative Study of Fuel–Cell –Battery, Fuel–Cell–Ultracapacitor, and Fuel–Cell–Battery–Ultracapacitor Vehicles. Vehicular Technology, IEEE Transactions on 57, 760 –769. doi:10.1109/TVT.2007.906379

Bayar, K., Wang, J., Rizzoni, G., 2012. Development of a vehicle stability control strategy for a hybrid electric vehicle equipped with axle motors. Proceedings of the Institution of Mechanical Engineers, Part D: Journal of Automobile Engineering.

Becker, M.C., Salvatore, P., Zirpoli, F., 2005. The impact of virtual simulation tools on problem–solving and new product development organization. Research Policy 34, 1305–1321.

Benders, B., Winther, K., Kolf, C., 2013, Methodology of EV measurements – Deliverable 6.1 for Greene–Motion fp7 project, http://www.greenemotion–project.eu/dissemination/deliverables.php, last seen 01/2014.

Bilgin, B., Emadi, A., Krishnamurthy, M., 2012. Comprehensive Evaluation of the Dynamic Performance of a 6/10 SRM for Traction Application in PHEVs. IEEE Transactions on Industrial Electronics PP, 1.

Bisordi, A., 2011, Range Extender Engine Development using GT–Suite, GT users' conference 2011, Frankfurt.

Borgarello, L., Fontana, R., Fortunato, A., Mina, L., 2001. Identification of driving cycles and emissions in the traffic of Bologna, in: Proceeding of the 7th International Conference ATA 2001. Presented at the the 7th international conference ATA 2001, Firenze.

Bringmann, E., Kramer, A., 2008. Model–Based Testing of Automotive Systems, in: 2008 1st International Conference on Software Testing, Verification, and Validation. Presented at the 2008 1st International Conference on Software Testing, Verification, and Validation, pp. 485–493.

Butler, K.L., Ehsani, M., Kamath, P., 1999. A Matlab–based modelling and simulation package for electric and hybrid electric vehicle design. IEEE Transactions on Vehicular Technology 48, 1770 –1778.

Burke, A., 2000. Ultracapacitors: why, how, and where is the technology. Journal of Power Sources 91, 37–50. doi:10.1016/S0378–7753(00)00485–7.

Burke, A.F., 2007. Batteries and Ultracapacitors for Electric, Hybrid, and Fuel Cell Vehicles. Proceedings of the IEEE 95, 806–820. doi:10.1109/JPROC.2007.892490

Burke, A., Miller, M., 2011. The power capability of ultracapacitors and lithium batteries for electric and hybrid vehicle applications. Journal of Power Sources 196, 514–522. doi:10.1016/j.jpowsour.2010.06.092.

Burress, T., Campbell, S., 2013. Benchmarking EV and HEV power electronics and electric machines, in: 2013 IEEE Transportation Electrification Conference and Expo (ITEC). Presented at the 2013 IEEE Transportation Electrification Conference and Expo (ITEC), pp. 1–6. doi:10.1109/ITEC.2013.6574498

Campanari, S., Manzolini, G., Garcia de la Iglesia, F., 2009. Energy analysis of electric vehicles using batteries or fuel cells through well–to–wheel driving cycle simulations. Journal of Power Sources 186, 464–477.

Camuffo I. , Caudano M., Pascali L. : MB–SHARC©: an integrated environment for suspension, handling and ride–comfort simulation based on Adams. 2002, MSC.ADAMS Conference – London.

Cericola, D., Ruch, P.W., Kötz, R., Novák, P., Wokaun, A., 2010. Simulation of a supercapacitor/Li–ion battery hybrid for pulsed applications. Journal of Power Sources 195, 2731–2736. doi:10.1016/j.jpowsour.2009.10.104.

Chen, K., Bouscayrol, A., Berthon, A., Delarue, P., Hissel, D., Trigui, R., 2008. Global modelling of different vehicles using Energetic Macroscopic Representation, in: IEEE Vehicle Power and Propulsion Conference, 2008. VPPC '08. Presented at the IEEE Vehicle Power and Propulsion Conference, 2008. VPPC '08, pp. 1–7.

Chen, K., Bouscayrol, A., Lhomme, W., 2008b. Energetic Macroscopic Representation and Inversion–based Control. Journal of Asian Electric Vehicles 6, 1097–1102.

Chen, B.–C., Wu, Y.–Y., Tsai, H.–C., 2014. Design and analysis of power management strategy for range extended electric vehicle using dynamic programming. Applied Energy 113, 1764–1774. doi:10.1016/j.apenergy.2013.08.018

Cocron, P., Bühler, F., Neumann, I., Franke, T., Krems, J.F., Schwalm, M., Keinath, A., June. Methods of evaluating electric vehicles from a user's perspective – The MINI E field trial in Berlin. IET Intelligent Transport Systems 5, 127–133. doi:10.1049/iet–its.2010.0126

Corti, A., Manzoni, V., Savaresi, S.M., 2012. Vehicle's energy estimation using low frequency speed signal, in: 2012 15th International IEEE Conference on Intelligent Transportation Systems (ITSC). Presented at the 2012 15th International IEEE Conference on Intelligent Transportation Systems (ITSC), pp. 626–631.

Dong–xu, Z., Xiao–hua, Z., Peng–yu, W., Qing–nian, W., 2009. Co–simulation with AMESim and MATLAB for differential dynamic coupling of Hybrid Electric Vehicle, in: 2009 IEEE Intelligent Vehicles Symposium. Presented at the 2009 IEEE Intelligent Vehicles Symposium, pp. 761 –765.

Doucette, R.T., McCulloch, M.D., 2011. Modelling the CO2 emissions from battery electric vehicles given the power generation mixes of different countries. Energy Policy 39, 803–811.

Dubarry, M., Liaw, B.Y., 2007. Development of a universal modelling tool for rechargeable lithium batteries. Journal of Power Sources 174, 856–860. doi:10.1016/j.jpowsour.2007.06.157

Duflou, J.R., De Moor, J., Verpoest, I., Dewulf, W., 2009. Environmental impact analysis of composite use in car manufacturing. CIRP Annals – Manufacturing Technology 58, 9–12.

EC – European Commission Report, 2009, EU Energy trends to 2030 – update 2009, downloaded from: http://ec.europa.eu/energy/observatory/trends_2030/index_en.htm, last seen 02/2013.

EC – European Commission Report, 2013, EU Energy, transport and GHG emissions trends to 2050 – Reference scenario 2013, downloaded from: http://ec.europa.eu/energy/observatory/trends_2030/index_en.htm, last seen 02/2013.

ECA, 2013, European Climate Assessment & Dataset, http://eca.knmi.nl/dailydata/predefinedseries.php (last seen 01/2014).

Eckstein, U.–P.D.–I.L., Göbbels, D.–I.R., Wohlecker, D.–I.D.–W.I.R., 2013. Benchmarking des Elektrofahrzeugs Mitsubishi i–MiEV, in: Siebenpfeiffer, W. (Ed.), Energieeffiziente Antriebstechnologien, ATZ / MTZ–Fachbuch. Springer Fachmedien Wiesbaden, pp. 22–29.

Einhorn, M., Conte, V., Kral, C., Fleig, J., 2011. Comparison of electrical battery models using a numerically optimized parameterization method, in: Vehicle Power and Propulsion Conference (VPPC), 2011 IEEE. pp. 1 –7. doi:10.1109/VPPC.2011.6043060

Enerdata, 2012, Energy Efficiency Trends in the Transport sector in the EU – Lessons from the ODYSSEE MURE project.

Eurostat, 2013, Supply, transformation, consumption – electricity – annual data, http://epp.eurostat.ec.europa.eu/portal/page/portal/energy/data/database, last seen 02/2013.

Forgez, C., Vinh Do, D., Friedrich, G., Morcrette, M., Delacourt, C., 2010. Thermal modelling of a cylindrical LiFePO4/graphite lithium–ion battery. Journal of Power Sources 195, 2961–2968.

Frenzel, B., Kurzweil, P., Rönnebeck, H., 2011. Electromobility concept for racing cars based on lithium–ion batteries and supercapacitors. Journal of Power Sources 196, 5364–5376.

FUEREX final report, 2013, Multi–fuel Range Extender with high efficiency and ultra low emissions, http://www.fuerex.eu/ (last seen 01/2014).

Gao, W., Porandla, S.K., 2005. Design optimization of a parallel hybrid electric powertrain, in: Vehicle Power and Propulsion, 2005 IEEE Conference. Presented at the Vehicle Power and Propulsion, 2005 IEEE Conference.

Gao, D.W., Mi, C., Emadi, A., 2007. Modelling and Simulation of Electric and Hybrid Vehicles. Proceedings of the IEEE 95, 729–745.

Genta, G. and Morello, L. 2009a, The Automotive Chassis: Volume 1: Components Design (Mechanical Engineering Series), Springer, Berlin.

Genta, G. and Morello, L. 2009b, The Automotive Chassis: Volume 2: System Design (Mechanical Engineering Series), Springer, Berlin.

Geringer, B., Tober, W.K., 2012, Battery Electric Vehicles in Practice, Costs, Range, Environment, Convenience, 2nd extended and corrected edition, Vienna University of Technology.

Gong, Q., Li, Y., Peng, Z.–R., 2008. Trip–Based Optimal Power Management of Plug–in Hybrid Electric Vehicles. IEEE Transactions on Vehicular Technology 57, 3393–3401. doi:10.1109/TVT.2008.921622

Gong, Q., Midlam–Mohler, S., Marano, V., Rizzoni, G., 2012. Virtual PHEV fleet study based on Monte Carlo simulation. International Journal of Vehicle Design 58, 266–290. doi:10.1504/IJVD.2012.047388

Graham–Rowe, E., Gardner, B., Abraham, C., Skippon, S., Dittmar, H., Hutchins, R., Stannard, J., 2012. Mainstream consumers driving plug–in battery–electric and plug–in hybrid electric cars: A qualitative analysis of responses and evaluations. Transportation Research Part A: Policy and Practice 46, 140–153. doi:10.1016/j.tra.2011.09.008

Guzzella, L., Amstutz, A., 1999. CAE tools for quasi–static modelling and optimization of hybrid powertrains. IEEE Transactions on Vehicular Technology 48, 1762 – 1769. doi:10.1109/25.806768

Guzzella, L., 2009. Automobiles of the future and the role of automatic control in those systems. Annual Reviews in Control 33, 1–10.

Haan, P.D. and M. Keller. 2001. Real–world driving cycles for emission measurement: ARTEMIS and Swiss cycles, INFRAS Final Report, Bern.

Hawkins, T.R., Singh, B., Majeau–Bettez, G., Strømman, A.H., 2012. Comparative Environmental Life Cycle Assessment of Conventional and Electric Vehicles. Journal of Industrial Ecology no–no. doi:10.1111/j.1530–9290.2012.00532.x

He, H., Zhang, X., Xiong, R., Xu, Y., Guo, H., 2012. Online model–based estimation of state–of–charge and open–circuit voltage of lithium–ion batteries in electric vehicles. Energy 39, 310–318.

Hosokawa, Takashi, Koji Tanihata, and Hiroaki Miyamoto. "Development of i MiEV next–generation electric vehicle (second report)." Mitsubishi Motors Technical Review 20 (2008): 53–60.

Hu, X., Li, S., Peng, H., 2012. A comparative study of equivalent circuit models for Li–ion batteries. Journal of Power Sources 198, 359–367. doi:10.1016/j.jpowsour.2011.10.013.

Hung, W.T., Tong, H.Y., Lee, C.P., Ha, K., Pao, L.Y., 2007. Development of a practical driving cycle construction methodology: A case study in Hong Kong. Transportation Research Part D: Transport and Environment 12, 115–128.

ISPRA, 2011, Produzione termoelettrica ed emissione di CO_2, Roma, downloaded from: http://www.isprambiente.gov.it/it/pubblicazioni/rapporti/produzione–termoelettrica–ed–emissioni–di–co2, last visualization: 01/2014.

Jobson, J.D., Applied Multivariate Data Analysis – volume II: Categorical and Multivariate Methods, 1992 Springer–Verlag New York, pages 345–431.

Jun, J., Guensler, R., Ogle, J., 2006. Smoothing Methods to Minimize Impact of Global Positioning System Random Error on Travel Distance, Speed, and Acceleration Profile Estimates. Transportation Research Record: Journal of the Transportation Research Board 1972, 141–150.

Kalhammer, F.R., Kopf, B., Swan, D., Roan, V., Walsh, M., 2007. Status and Prospects for Zero Emissions Vehicle Technology: Report of the ARB Independent Expert Panel 2007. Prepared for State of California Air Resources Board, Sacramento, California, April 2007 (http://www.arb.ca.gov/msprog/zevprog/zevreview/zev_panel_report.pdf).

Kamachi, M., Miyamoto, H., Sano, Y., 2010. Development of power management system for electric vehicle i–MiEV, in: Power Electronics Conference (IPEC), 2010 International. Presented at the Power Electronics Conference (IPEC), 2010 International, pp. 2949–2955. doi:10.1109/IPEC.2010.5542016

Kamachi, M., Hosokawa, T., 2011. Study on Practicality of Electric Vehicle “i–MiEV” under Severe Weather (SAE Technical Paper No. 2011–39–7241). SAE International, Warrendale, PA.

Katsargyri, G.–E., Kolmanovsky, I.V., Michelini, J., Kuang, M.L., Phillips, A.M., Rinehart, M., Dahleh, M.A., 2009. Optimally controlling Hybrid Electric Vehicles using path forecasting, in: American Control Conference, 2009. ACC ’09. Presented at the American Control Conference, 2009. ACC ’09., pp. 4613–4617. doi:10.1109/ACC.2009.5160504.

Khaligh, A., Li, Z., 2010. Battery, Ultracapacitor, Fuel Cell, and Hybrid Energy Storage Systems for Electric, Hybrid Electric, Fuel Cell, and Plug–In Hybrid Electric Vehicles: State of the Art. IEEE Transactions on Vehicular Technology 59, 2806–2814.

Kiyota, K., Chiba, A., 2011. Design of switched reluctance motor competitive to 60 kW IPMSM in third generation hybrid electric vehicle, in: 2011 IEEE Energy Conversion Congress and Exposition (ECCE). Presented at the 2011 IEEE Energy Conversion Congress and Exposition (ECCE), pp. 3562 –3567.

Kitano, S., Nishiyama, K., Toriyama, J., Sonoda, T., 2008. Development of large–sized Lithium–ion Cell “LEV50” and its battery module “LEV50–4” for Electric vehicle. GS Yuasa Corporation Technical Report.

Kolke, R., Cycle beating: How are OEM’s optimising the vehicle to test cycles?, GFEI – Green Global NCAP labelling / green scoring workshop, 30th April 2013, http://www.iea.org/media/workshops/2013/gfeilabelling/09.ieaworkshop_adac_greenscoring_en.pdf, last seen February 2013.

Kolmanovsky, I., McDonough, K., Gusikhin, O., 2011. Estimation of fuel flow for telematics–enabled adaptive fuel and time efficient vehicle routing, in: 2011 11th International Conference on ITS Telecommunications (ITST). Presented at the 2011 11th International Conference on ITS Telecommunications (ITST), pp. 139–144. doi:10.1109/ITST.2011.6060041.

Krumm, J., 2012. How People Use Their Vehicles: Statistics from the 2009 National Household Travel Survey (SAE Technical Paper No. 2012–01–0489). SAE International, Warrendale, PA.

Krzanowski, W.J. Principles of Multivariate Analysis, 1988 Clanderon Press Oxford, pages 49–85, 254–258, 477–503.

Kumar, R., Parida, P., Saleh, W., Gupta, K., Durai, B.K., 2012. Driving Cycle for Motorcycle Using Micro–Simulation Model. Journal of Environmental Protection 03, 1268–1273.

Lam, L.T., Louey, R., 2006. Development of ultra–battery for hybrid–electric vehicle applications. Journal of Power Sources 158, 1140–1148. doi:10.1016/j.jpowsour.2006.03.022.

Lee, T.–K., Filipi, Z.S., 2011. Synthesis of real–world driving cycles using stochastic process and statistical methodology. International Journal of Vehicle Design 57, 17–36.

Liaw, B.Y., Jungst, R.G., Nagasubramanian, G., Case, H.L., Doughty, D.H., 2005. Modelling capacity fade in lithium–ion cells. Journal of Power Sources 140, 157–161. doi:10.1016/j.jpowsour.2004.08.017

Lieven, T., Mühlmeier, S., Henkel, S., Waller, J.F., 2011. Who will buy electric cars? An empirical study in Germany. Transportation Research Part D: Transport and Environment 16, 236–243. doi:10.1016/j.trd.2010.12.001.

Lin, J., Niemeier, D.A., 2003. Regional driving characteristics, regional driving cycles. Transportation Research Part D: Transport and Environment 8, 361–381.

Liu, J., Peng, H., Filipi, Z., 2005. Modelling and Control Analysis of Toyota Hybrid System, in: Proceedings, 2005 IEEE/ASME International Conference on Advanced Intelligent Mechatronics. Presented at the Proceedings, 2005 IEEE/ASME International Conference on Advanced Intelligent Mechatronics, pp. 134–139. doi:10.1109/AIM.2005.1500979.

Lhomme, W., Bouscayrol, A., Barrade, P., 2004. Simulation of a series hybrid electric vehicle based on energetic macroscopic representation, in: 2004 IEEE International Symposium on Industrial Electronics. Presented at the 2004 IEEE International Symposium on Industrial Electronics, pp. 1525–1530 vol. 2.

Lohse–Busch, H., et al., 2012, Nissan Leaf testing and analysis, http://www.transportation.anl.gov/D3/index.html (visualized September 2013).

Lyons, T.J., Kenworthy, J.R., Austin, P.I., Newman, P.W.G., 1986. The development of a driving cycle for fuel consumption and emissions evaluation. Transportation Research Part A: General 20, 447–462.

Marano, V., Onori, S., Guezennec, Y., Rizzoni, G., Madella, N., 2009. Lithium–ion batteries life estimation for plug–in hybrid electric vehicles, in: Vehicle Power and Propulsion Conference, 2009. VPPC '09. IEEE. pp. 536 –543. doi:10.1109/VPPC.2009.5289803.

Marker, S., Rippel, B., Waldowski, P., Schulz, A., Schindler, V., 2013. Battery Electric Vehicle (BEV) or Range Extended Electric Vehicle (REEV)? —Deciding Between Different Alternative Drives Based on Measured Individual Operational Profiles. Oil & Gas Science and Technology – Revue d'IFP Energies nouvelles 68, 65–77. doi:10.2516/ogst/2012103.

Maxwell Technologies, 2009, Maxwell Technologies' Test Procedures for Capacitance, ESR, Leakage Current and Self–Discharge Characterizations

of Ultracapacitors, Application note.

Miller, T.J.E., Glinka, M., McGilp, M., Cossar, C., Gallegos–Lopez, G., Ionel, D., Olaru, M., 1998. Ultra–fast model of the switched reluctance motor, in: The 1998 IEEE Industry Applications Conference, 1998. Thirty–Third IAS Annual Meeting. Presented at the The 1998 IEEE Industry Applications Conference, 1998. Thirty–Third IAS Annual Meeting, pp. 319 –326 vol.1.

Montazeri, M., Fotouhi, A., Naderpour, A., 2012. Driving segment simulation for determination of the most effective driving features for HEV intelligent control. Vehicle System Dynamics 50, 229–246.

Monti, F., Hybrid and electric vehicles – Powertrain architecture and sizing design, PhD thesis, Turin, 2010.

Moradi, H., Afjei, E., 2011. Analysis of brushless DC generator incorporating an axial field coil. Energy Conversion and Management 52, 2712–2723.

Moura, S.J., Callaway, D.S., Fathy, H.K., Stein, J.L., 2010. Tradeoffs between battery energy capacity and stochastic optimal power management in plug–in hybrid electric vehicles. Journal of Power Sources 195, 2979–2988.

Nagpure, S.C., Dinwiddie, R., Babu, S.S., Rizzoni, G., Bhushan, B., Frech, T., 2010. Thermal diffusivity study of aged Li–ion batteries using flash method. Journal of Power Sources 195, 872–876.

Notter, D.A., Gauch, M., Widmer, R., Wäger, P., Stamp, A., Zah, R., Althaus, H.–J., 2010. Contribution of Li–Ion Batteries to the Environmental Impact of Electric Vehicles. Environ. Sci. Technol. 44, 6550–6556. doi:10.1021/es903729a.

NTHS – National Households Travel Survey – NTHS data center, 2011, http://nhts.ornl.gov/download.shtml, last seen December 2013.

Omar, N., Coosemans, T., Martin, J., Sauvant–Moynot, V., Salminen, J., Kortschak, B., Hennige, V., Van Mierlo, J., Van den Bossche, P., 2012. SuperLib Project: Advanced Dual–Cell Battery Concept for Battery Electric Vehicles, Proceedings of EVS26 International Battery, Hybrid and Fuel Cell Electric Vehicle Symposium, Los Angeles.

Orofino L., Amante F., Mola S., Rostagno M., Villosio G., Piu A. : An integrated approach for Air Conditioning and Electrical system impact on vehicle fuel consumption and performances analysis: DrivEM 1.0. 2007, SAE2007 World Conference – Detroit.

Ozaki, R., Sevastyanova, K., 2011. Going hybrid: An analysis of consumer purchase motivations. Energy Policy 39, 2217–2227. doi:10.1016/j.enpol.2010.04.024

Pasaoglu, G., Fiorello, D., Martino, A., Scarcella, G., Alemanno, A., Zubaryeva, A., Thiel, C., 2012. Driving and parking patterns of European car drivers – a mobility survey.

Pasaoglu, G., Fiorello, D., Martino, A., Zani, L., Zubaryeva, A., Thiel, C., n.d. Travel patterns and the potential use of electric cars – Results from a direct survey in six European countries. Technological Forecasting and Social Change (IN PRESS at December 2013).

Pesaran A.A., Thermal Management Studies and Modelling, DOE Hydrogen Program and Vehicle Technologies, Cristal City, May 18–22, 2009.

Petricca, M., Shin, D., Bocca, A., Macii, A., Macii, E., Poncino, M., 2013. An automated framework for generating variable–accuracy battery models from datasheet information, in: 2013 IEEE International Symposium on Low Power Electronics and Design (ISLPED). Presented at the 2013 IEEE International Symposium on Low Power Electronics and Design (ISLPED), pp. 365–370. doi:10.1109/ISLPED.2013.6629324.

Primerano, F., Taylor, M.A.P., Pitaksringkarn, L., Tisato, P., 2008. Defining and understanding trip chaining behaviour. Transportation 35, 55–72.

Propfe, B., Kreyenberg, D., Wind, J., Schmid, S., 2013. Market penetration analysis of electric vehicles in the German passenger car market towards 2030. International Journal of Hydrogen Energy 38, 5201–5208. doi:10.1016/j.ijhydene.2013.02.049

Ribau, J., Silva, C., Brito, F.P., Martins, J., 2012. Analysis of four–stroke, Wankel, and microturbine based range extenders for electric vehicles. Energy Conversion and Management 58, 120–133. doi:10.1016/j.enconman.2012.01.011

Rong, P., Pedram, M., 2006. An analytical model for predicting the remaining battery capacity of lithium–ion batteries. Very Large Scale Integration (VLSI) Systems, IEEE Transactions on 14, 441 –451. doi:10.1109/TVLSI.2006.876094

Roscher, M.A., Leidholdt, W., Trepte, J., 2012. High efficiency energy management in BEV applications. International Journal of Electrical Power & Energy Systems 37, 126–130.

Ross, S., Evans, D., Webber, M., 2002. How LCA studies deal with uncertainty. Int J LCA 7, 47–52.

Sadeghi, S., Sadeghi, R., Sadeghi, M., 2006. Dynamic performance of a switched reluctance motor for propulsion systems, in: International Symposium on Power Electronics, Electrical Drives, Automation and Motion, 2006. SPEEDAM 2006. Presented at the International Symposium on Power Electronics, Electrical Drives, Automation and Motion, 2006. SPEEDAM 2006, pp. 1419 –1424.

Saleh, W., Kumar, R., Kirby, H., Kumar, P., 2009. Real world driving cycle for motorcycles in Edinburgh. Transportation Research Part D: Transport and Environment 14, 326–333.

Schmidt, W.–P., Dahlqvist, E., Finkbeiner, M., Krinke, S., Lazzari, S., Oschmann, D., Pichon, S., Thiel, C., 2004. Life cycle assessment of lightweight and end–of–life scenarios for generic compact class passenger vehicles. Int J LCA 9, 405–416.

Schuitema, G., Anable, J., Skippon, S., Kinnear, N., 2013. The role of instrumental, hedonic and symbolic attributes in the intention to adopt electric vehicles. Transportation Research Part A: Policy and Practice 48, 39–49. doi:10.1016/j.tra.2012.10.004

Schwarzer, V., Ghorbani, R., 2013. Drive Cycle Generation for Design Optimization of Electric Vehicles. IEEE Transactions on Vehicular Technology 62, 89–97.

Sciarretta, A., Guzzella, L., 2007. Control of hybrid electric vehicles. IEEE Control Systems 27, 60–70. doi:10.1109/MCS.2007.338280.

Shankar, R., Marco, J., Assadian, F., 2012. A methodology to determine drivetrain efficiency based on external environment, in: Electric Vehicle Conference (IEVC), 2012 IEEE International. Presented at the Electric Vehicle Conference (IEVC), 2012 IEEE International, pp. 1–6. doi:10.1109/IEVC.2012.6183192.

Smart, J., Powell, W., Schey, S., 2013. Extended Range Electric Vehicle Driving and Charging Behavior Observed Early in the EV Project (SAE Technical Paper No. 2013–01–1441). SAE International, Warrendale, PA.

Smith, K., Earleywine, M., Wood, E., Neubauer, J., Pesaran, A., 2012. Comparison of Plug–In Hybrid Electric Vehicle Battery Life Across Geographies and Drive Cycles (SAE Technical Paper No. 2012–01–0666). SAE International, Warrendale, PA.

Solero, L., Lidozzi, A., Serrao, V., Martellucci, L., Rossi, E., 2011. Ultracapacitors for fuel saving in small size hybrid vehicles. Journal of Power Sources 196, 587–595. doi:10.1016/j.jpowsour.2009.07.041

Souffran, G., Miegeville, L., Guerin, P., 2012. Simulation of Real–World Vehicle Missions Using a Stochastic Markov Model for Optimal Powertrain Sizing. IEEE Transactions on Vehicular Technology 61, 3454–3465.

Steven, H., Homologation test cycles worldwide – Status of the WLTP. IEA Green Global NCAP labeling/green scoring Workshop, 30.04.2013, Paris. http://www.iea.org/media/workshops/2013/gfeilabelling/07.08.Homologationtestcyclesworldwide.pdf (last seen September 2013).

Sullivan, J.L., Baker, R.E., Boyer, B.A., Hammerle, R.H., Kenney, T.E., Muniz, L., Wallington, T.J., 2004. CO2 Emission Benefit of Diesel (versus Gasoline) Powered Vehicles. Environ. Sci. Technol. 38, 3217–3223. doi:10.1021/es034928d.

Thomas, C.E., 2009. Fuel cell and battery electric vehicles compared. International Journal of Hydrogen Energy 34, 6005–6020.

Tong, H.Y., Hung, W.T., 2010. A Framework for Developing Driving Cycles with On-Road Driving Data. Transport Reviews 30, 589–615. Published Project Report PPR354. Source: http://www.trl.co.uk (last seen September 2013).

Tran, M., Banister, D., Bishop, J.D.K., McCulloch, M.D., 2013. Simulating early adoption of alternative fuel vehicles for sustainability. Technological Forecasting and Social Change. doi:10.1016/j.techfore.2012.09.009

Transport & Environment – TE, 2013, How clean are Europe’s cars? An analysis of carmaker progress towards EU CO_2 target in 2012, downloaded from www.transportsandenvironment.com, last visualization 01/2014.

Trovão, T., Santos, V.D.N., Pereirinha, P.G., Jorge, H.M., Antunes, C.H., 2013. Comparative Study of Different Energy Management Strategies for Dual–Source Electric Vehicles, in: EVS27 International Battery, Hybrid and Fuel Cell Electric Vehicle Symposium. Barcelona, Spain.

Tutuianu, M., Marotta A., Steven, H., Ericsson, E., Haniu., T., Ichikawa, N., Ishii, H., Development of a World–wide Worldwide harmonized Light duty driving Test Cycle (WLTC) – Draft Technical Report. WLTP–DHC–18–06, 2013.

Tutunji, T., Molhim, M., Turki, E., 2007. Mechatronic systems identification using an impulse response recursive algorithm. Simulation Modelling Practice and Theory 15, 970–988.

UNECE, 2005, Regulation No. 101, Uniform provision concerning the approval of passenger cars powered by an internal combustion only or powered by a hybrid electric powertrain [..],E/ECE/324 – E/ECE/TRANS/505, http://www.unece.org/fileadmin/DAM/trans/main/wp29/wp29regs/r101r2e.pdf (last seen 12/2013).

UNECE, 2011, Regulation No. 83, Uniform provisions concerning the approval of vehicles with regard to the emission of pollutants according to engine fuel requirements, E/ECE/324/Rev.1/Add.82/Rev.4, 26 April 2011, http://www.unece.org/fileadmin/DAM/trans/main/wp29/wp29regs/r083r4e.pdf (last seen September 2013).

UNECE, 2013. Worldwide harmonized Light vehicles Test Procedure (WLTP). https://www2.unece.org/wiki/pages/viewpage.action?pageId=2523179 (last seen September 2013).

Valera, J.J., Iglesias, I., Peña, A., 2009. Integrated Modelling Approach for Highly electrified HEV. Virtual Design and Simulation Methodology for Advanced Powertrain Prototyping., in: Proceedings of International Battery, Hybrid and Fuel Cell Electric Vehicle Symposium (EVS 24).

Van Basshuysen, R., and Schäfer, F. (2004). Internal combustion engine handbook–basics, components, systems and perspectives (Vol. 345).

Van Haaren, R., 2011. Assessment of Electric Cars Range Requirements and Usage Patterns based on Driving Behavior recorded in the National Household Travel Survey of 2009. Solar Journey USA 1–56.

Van Mierlo, J., Van den Bossche, P., Maggetto, G., 2004. Models of energy sources for EV and HEV: fuel cells, batteries, ultracapacitors, flywheels and engine–generators. Journal of Power Sources 128, 76–89.

Varnhagen, S., Same, A., Remillard, J., Park, J.W., 2011. A numerical investigation on the efficiency of range extending systems using Advanced Vehicle Simulator. Journal of Power Sources 196, 3360–3370. doi:10.1016/j.jpowsour.2010.10.086

Vetter, J., Novák, P., Wagner, M.R., Veit, C., Möller, K.–C., Besenhard, J.O., Winter, M., Wohlfahrt–Mehrens, M., Vogler, C., Hammouche, A., 2005. Ageing mechanisms in lithium–ion batteries. Journal of Power Sources 147, 269–281. doi:10.1016/j.jpowsour.2005.01.006

Wang, Q., Huo, H., He, K., Yao, Z., Zhang, Q., 2008. Characterization of vehicle driving patterns and development of driving cycles in Chinese cities. Transportation Research Part D: Transport and Environment 13, 289–297.

WBCSD – World Business Council for Sustainable development, 2004, Mobility 2030: Meeting the Challenges to Sustainability, downloaded from: http://www.wbcsd.org/, visualized 01/2014.

WCED – World Commission on Environment and Development, 1987, Our Common Future, Report of the World Commission on Environment and Development, published as Annex to General Assembly document A/42/427, Development and International Co–operation: Environment.

Weiss, M., Bonnel, P., Hummel, R., Provenza, A., Manfredi, U., 2011. On–Road Emissions of Light–Duty Vehicles in Europe. Environ. Sci. Technol. 45, 8575–8581.

Williamson, S.S., Emadi, A., Rajashekara, K., 2007. Comprehensive Efficiency Modelling of Electric Traction Motor Drives for Hybrid Electric Vehicle Propulsion Applications. IEEE Transactions on Vehicular Technology 56, 1561 –1572.

Wipke, K.B., Cuddy, M.R., Burch, S.D., 1999. ADVISOR 2.1: a user–friendly advanced powertrain simulation using a combined backward/forward approach. IEEE Transactions on Vehicular Technology 48, 1751–1761.

Wirasingha, S.G., Emadi, A., 2011. Classification and Review of Control Strategies for Plug–In Hybrid Electric Vehicles. IEEE Transactions on Vehicular Technology 60, 111–122. doi:10.1109/TVT.2010.2090178.

Wong, Y., 2001, Theory of Ground Vehicles – Third edition, John Wiley & Sons. Inc..

Yi, J., Kim, U.S., Shin, C.B., Han, T., Park, S., 2013. Modelling the temperature dependence of the discharge behavior of a lithium–ion battery in low environmental temperature. Journal of Power Sources.

Yoo, H., Sul, S.–K., Park, Y., Jeong, J., 2008. System Integration and Power–Flow Management for a Series Hybrid Electric Vehicle Using Supercapacitors and Batteries. IEEE Transactions on Industry Applications 44, 108–114. doi:10.1109/TIA.2007.912749

Yoon, Y.–H., Kim, J.–M., Won, C.–Y., Lee, B.–K., 2009. New approach to SRM drive with six–switch converter. Mechatronics 19, 1321–1333 (in press).

Yuan, X., Gao, Y., Ehsani, M., 2008. Study on the performance and control of SR machine for vehicle regenerative braking, in: IEEE Vehicle Power and Propulsion Conference, 2008. VPPC ’08. Presented at the IEEE Vehicle Power and Propulsion Conference, 2008. VPPC ’08, pp. 1 –5.

Zubaryeva, A., Thiel, C., Barbone, E., Mercier, A., 2012. Assessing factors for the identification of potential lead markets for electrified vehicles in Europe: expert opinion elicitation. Technological Forecasting and Social Change 79, 1622–1637. doi:10.1016/j.techfore.2012.06.004.